Cognitive function in mice with segmental trisomy of human chromosome 21 Down Syndrome genes

Tara Canonica

Cardiff University

Submitted for the degree of Doctor of Philosophy at Cardiff University

2019

Acknowledgements

First of all, I would like to thank my supervisor, Mark Good, who has been an incredible support over the past four years. Thank you Mark, for always making a priority the time to see me a and for always providing me with renewed motivation and enthusiasm during hard times. You can't imagine how much it meant to me to know that I could always count on you.

A big thank you also to Emma Kidd. Thanks Emma, for welcoming me in your laboratory and for always being interested in my work. I'm very grateful for all your precious inputs on my western blots and your precious words of encouragement.

Next, I would like to thank Elizabeth Fisher and Victor Tybulewicz for generously providing the three mouse lines that were studied in this thesis and enabling a very smooth collaboration. Thank you for all your aid and guidance, having the chance to visit you in London was a fantastic experience.

I would also like to thank Rhys Perry and the JBIOS staff for taking such good care of my animals. Thank you Rhys for all your help with the mice and for always being in the mood for a chat along the BNL corridors, you have made the long working days (and weekends) a lot more enjoyable.

To Charles Evans, a massive thank you. Thank you for always finding the time and the patience to answer my never-ending questions and clearing all my doubts, while also making lab work a lot more amusing. You have taught me so much and I'm extremely grateful.

A big thank you to Adam and Tommy. We have always had each other's backs over the past years, which really helped lighten the load and keep the morale high during stressful times, thank you.

Finally, thanks to Federico. It has been an intense four years, especially during the write-up period, but somehow you always make everything better. You continuously provided me with much needed doses of motivation, endless understanding and emotional support (in addition to fantastic home cooked food supplies), I'll never thank you enough. You have no idea the difference it made to know that you were always believing in me, from day one.

And last, thanks to my family. You have all taught me so much and I wouldn't be the person I am today if it weren't for you. Thanks to my sister Petra, for teaching me to believe in myself. Thanks to my sister Chantal, for teaching me that things can always be done a little better. Thanks to my sister Claudia, for teaching me to be ambitious. Thanks to my dad, for teaching me to appreciate a job well done. And thanks to my mom, for teaching me to never give up.

I would need a "control Tara" to prove this scientifically but I think it's only fair to say that I could not have accomplished this work without you all. Thank you.

Thesis summary

Down Syndrome (DS) is a complex genetic disorder characterised by learning and memory impairments and age-related early-onset Alzheimer's Disease. Sixty years ago, Lejeune et al. (1959) discovered that DS is caused by an extra copy of chromosome 21 (Hsa21). Despite a large body of research dedicated to the study of DS pathophysiology, the complex relationship between gene over-dosage, cognitive function and decline is still unclear.

Genes on Hsa21 share synteny with orthologous regions on three mouse chromosomes (Mmu): Mmu16, Mmu17 and Mmu10. The primary aim of this thesis was to evaluate the contribution of the three orthologous regions to memory function in DS by studying genetically engineered mouse models, trisomic entirely and exclusively for one of the three regions: the Dp1Tyb, Dp3Yey and Dp2Yey. A battery of object-recognition memory tasks was used to assess different attributes and retention-spans of recognition memory in adult (12-13 months) and aged (18-20 months) mice of the three models. Performance in these tasks has been demonstrated to require glutamatergic activity within a network of medial temporal lobe structures, including the hippocampus. Dp1Tyb mice displayed age-independent impairments in recognition memory affecting selectively short-term memory processes. Dp3Yey mice displayed intact recognition memory. Dp2Yey mice displayed age-dependent impairments in recognition memory processes.

At cellular level, the acquisition of new memories is proposed to rely on the regulation of synaptic transmission via changes in glutamate receptor expression. The secondary aim of this thesis was to identify biochemical mechanisms possibly associated to the pattern of memory performance of the three models. Glutamate receptor expression was thus assessed with western blots of hippocampal synaptosomes from the three models. Dp1Tyb mice displayed a downregulation of the postsynaptic scaffold protein PSD95 and an upregulation of the GluA1 AMPA receptor subunit, which has been previously implicated in short-term memory processes. Protein expression was unaltered in Dp3Yey mice. The Dp2Yey displayed an age-dependent downregulation of PSD95 and of the GluK5 kainate receptor subunit.

This thesis studied for the first time the separate contribution of Hsa21 orthologues to recognition memory function and to glutamate receptor expression. Genes located on Mmu16 and 10 were found to be differentially important for memory processes, whereas no changes were observed with trisomy of genes on Mmu17. Potential candidate genes contributing to the behavioural and synaptic changes are considered and the contribution of these findings to understanding the complex genetic and functional changes observed in DS are discussed.

Table of contents

Abbreviations

A1 – Primary active state

A2 – Secondary active state

Aβ – Amyloid-β peptide

AD – Alzheimer's disease

AMPA – α-amino-3-hydroxy-5-methyl-4-isoxazolepropionic acid

ANOVA – Analysis of Variance

APP – Amyloid Precursor Protein

BCA – Bicinchoninic Acid Assay

BSA – Bovine Serum Albumin

CFC – Contextual Fear Conditioning

CBS – Cystathionine-β-Synthase

DNA – Deoxyribonucleic Acid

DS – Down Syndrome

DSCR – Down Syndrome Critical Region

DYRK1A – Dual specificity tyrosine-phosphorylation-regulated kinase 1A

EPM – Elevated Plus Maze

ES – Embryonic Stem cells

GABA – γ-aminobutyric acid

GluA1 – AMPA glutamate receptor 1

GluK5 – Kainate glutamate receptor 5

GluN1 – NMDA glutamate receptor 1

GluN2A/B – NMDA glutamate receptor 2A/B

GRIK1 – Glutamate Receptor Ionotropic Kainate 1

H0 – Null hypothesis

H1 – Alternative hypothesis

HPC – Hippocampus

HRP – Horseradish Peroxidase

Hsa21 – Homo sapiens autosome 21

I – Inactive state

KAR – Kainate Receptors

Loc – Object Location

LTD – Long Term Depression

LTM – Long-Term Memory

LTP – Long Term Potentiation

MA – Mental Age

Mmu – Mus musculus chromosome

mPFC – medial Prefrontal cortex

MRI – Magnetic Resonance Imaging

MWM – Morris Water Maze

NMDA - N-methyl-D-aspartate

NOR – Novel Object Recognition

OiP – Object-in-Place

PCR – Polymerase Chain Reaction

pGluA1(S845) – GluA1 phosphorylated at serine 845

pGluN2B(Y1472) – GluN2B phosphorylated at tyrosine 1472

PRH – Perirhinal

PSD – Post Synaptic Density

PSD95 – Post Synaptic Density scaffolding protein 95

RCAN1 – Regulator of Calcineurin 1

S1 – Sample phase 1

S2 – Sample phase 2

S100B – S100 calcium-binding protein B

SOP – Sometimes Opponent Process

STM – Short-Term Memory

Syn-Per – Synaptic Protein Extraction Reagent

TBS-T – Tris-buffered saline with Tween

TG - Transgenic

TRPM2 – Transient Receptor Potential Melastatin 2

TOr – Temporal Order

TTS – Triple Trisomic Strain

WT – Wildtype

List of tables

List of figures

Chapter 1: Introduction

Overview

This chapter outlines the background to the thesis, providing a general introduction to Down Syndrome and to mouse models of Down Syndrome. Aims and hypotheses of the thesis are then presented.

1.1. Thesis overview

Down Syndrome (DS) is the most frequent form of intellectual disability and is caused by trisomy of chromosome 21 (Dierssen, 2012). Based on the conserved synteny between chromosome 21 and mouse chromosomes, different mouse models of DS have been developed over the past decades. Nevertheless, the complex relationship between gene over-dosage and memory impairments in DS is still unclear.

The present chapter will outline the background to the thesis. The following sections will provide a general introduction to DS, reviewing genetic cause and clinical presentation of the syndrome. Particular attention will be dedicated to cognition and memory function in DS individuals. Subsequently, transgenic mouse lines modelling DS will be presented, reviewing physical and behavioural phenotypes of the different models. In the final section, aims and hypotheses of the thesis will be presented.

In this thesis, three novel mouse models of segmental DS were used to study the contribution of different chromosome 21 orthologues to memory dysfunction in DS. The general methods employed will be described in chapter 2. In chapter 3, background information on memory systems and their neural substrates will be presented, followed by a series of behavioural experiments on the three mouse models. In brief, the animals were tested on a battery of object-recognition memory tests assessing memory for novel objects (NOR), novel locations (Loc), object-in-place associations (OiP) and temporal order of object presentation (TOr). In chapter 4, background information on synaptic plasticity mechanisms and glutamate receptors will be presented, followed by a series of western blotting experiments. In brief, hippocampal samples were collected from the three mouse models and the expression ionotropic glutamate receptors was assessed. In the last chapter, behavioural and biochemical findings are merged together, discussing how they can inform our understanding of DS in humans.

1.2. Down Syndrome

Down Syndrome was first described by John Langdon Down in 1866 and was later linked to the presence of an extra copy of chromosome 21 (Lejeune, Gautier, & Turpin, 1959). For this reason, DS is also known as “trisomy 21”. Besides significantly impaired cognitive abilities, individuals with DS are also affected by a number of physical conditions, such as cardiac, respiratory and gastrointestinal defects (Weijerman & de Winter, 2010). Within Europe, the prevalence of DS has been estimated at 11.2 every 10’000 live births (Loane et al., 2013). Estimates vary however between countries, depending on the availability of prenatal screening tests and pregnancy termination. In 2011, approximately 40’000 people with DS were estimated to live in the UK (Wu & Morris, 2011). Over the past decades, the DS survival rate has largely increased, owing to modern medical care and interventions. For example, the life expectancy of the DS population was approximately 10 years in year 1970 and now has reached 50 years (Presson et al., 2013).

1.2.1. Genetic cause

In healthy individuals, cells contain 23 pairs of chromosomes. Chromosomes are structures composed of a deoxyribonucleic acid (DNA) molecule. DNA contains the entire genetic material of the organism, assembled into a series of the nucleotides cytosine, guanine, adenine, and thymine. Within the cell nucleus, genetic information is transcripted into ribonucleic acid (RNA) and subsequently expressed in the cytoplasm. Portions of DNA that code for the synthesis of a specific protein are called genes. Genes determine all biochemical and physiological properties of an organism, ultimately resulting in their physical form and functional capability. Different genes are located on different chromosomes and imbalances in genetic material can severely impact development (Alberts et al., 2002).

Cells of individuals with DS contain an extra copy of human chromosome 21 (*Homo sapiens autosome 21*; Hsa 21). Hsa21 is the smallest human chromosome and makes approximately 1.5% of the entire human genome (Hattori et al., 2000). The long arm of Hsa21 was completely sequenced in year 2000 (Hattori et al., 2000). Currently, 233 protein-coding genes, 404 non-coding RNA genes and 188 pseudogenes have been identified on Hsa21 (www.ensembl.org/Homo_sapiens/Location/Chromosome?r=21:1-46709983; Ensembl release 62).

In 97% of the cases, DS is due to incorrect cell division during the formation of reproductive cells (egg cells or sperm cells) in one of the parents. During meiosis (I or II), chromosome 21 is unequally split between the two daughter cells, generating a cell containing two copies of the chromosome. Since fertilisation adds a set of chromosomes to

the cell, the fertilised cell will carry three full copies of chromosome 21 (Morris, Alberman, Mutton, & Jacobs, 2012). In the majority of the cases, meiotic nondisjunction errors occur in egg cells, whereby advanced maternal age is the most important risk factor for DS. Allen et al. (2009) found that 92% of meiotic nondisjunction errors were of maternal origin, associated to increased maternal age (≥ 40 years). Although rare, DS can also be caused by partial trisomy 21. In this case, the affected individual carries a trisomy of only a portion of Hsa21 (Delabar et al., 1993; Korbel et al., 2009).

Trisomy 21 can also be caused by nondisjunction errors occurring after fertilisation, during mitotic cell division of the zygote. This type of error results in a fraction of cells carrying trisomy 21, while the remaining cells contain the correct number of chromosomes, a pattern known as mosaicism (as reviewed in Papavassiliou, Charalsawadi, Rafferty, & Jackson-Cook, 2004). Mosaic DS occurs only in 1% of the trisomy 21 cases, has less severe phenotypes, and is not associated with either parental origin or maternal age (Allen et al., 2009; Morris et al., 2012).

Finally, chromosomal translocations, usually Robertsonian translocations, can also result in DS (Robinson et al., 1994). During meiotic cell division, part of chromosome 21 can become attached to another chromosome, frequently chromosome 14. Fertilisation of a daughter cell containing both a copy of chromosome 21 and the translocated chromosome results in translocation DS. Translocations account for around 3% of DS cases and can also occur between Hsa21 and chromosome 13, 15 or 21 (Morris et al., 2012).

The molecular and cellular events linking the surplus genetic information to abnormal development and DS phenotypes are not entirely clear. Initially, the study of cases of partial trisomy 21 led to the identification of a specific segment on Hsa21 that if duplicated, seemed sufficient for the pathogenesis of DS. This region contains approximately 50 genes and was called “Down Syndrome critical region” (DSCR) (Delabar et al., 1993). It was proposed that over-dosage of one or a few genes within the DSCR produced many of the physical and cognitive features of DS. More recently however, larger studies of partial trisomy 21 revealed that several Hsa21 regions contribute to DS, contradicting the hypothesis of a single critical region (Korbel et al., 2009). Nonetheless, animal studies proved that some DSCR-genes (e.g. Down Syndrome Cell Adhesion Molecule - *DSCAM*, or the Dual specificity tyrosine-phosphorylation-regulated kinase 1A - *DYRK1A*) are indeed crucial for the expression of DS-like phenotypes (as reviewed in Lana-Elola, Watson-Scales, Fisher, & Tybulewicz, 2011).

Over the years, two main hypotheses have been advanced in an attempt to explain how the extra chromosomal material can give rise to DS. The “developmental instability hypothesis” proposes that over-dosage of Hsa21 genes leads to a non-specific, generalised imbalance in gene expression, disrupting cellular homeostasis and thus normal

development (Hall, 1964). The “gene dosage hypothesis” proposes that over-dosage of Hsa21 genes causes the overexpression of critical Hsa21 genes, resulting directly in the abnormal phenotypes (Antonarakis, Lyle, Chrast, & Scott, 2001). Although increased gene copy number has been related to increased amount of gene product expressed by a cell, it is important to bear in mind that gene transcription is a highly regulated process. A wide range of cellular mechanisms operates to increase or reduce the expression of specific genes, involving gene products coded from chromosomes other than Hsa21 (Dierssen, 2012). A review by Gardiner (2004) reported in fact that in both human and mouse models of DS, only the product of some and not all duplicated genes was overexpressed (typically by ~ 1.5 fold), as measured by RNA levels. Interestingly, gene overexpression varied between tissue types and between subjects, and altered gene expression (increase or decrease) was observed also in a number of non-trisomic genes form different chromosomes.

Both hypotheses provide helpful perspectives on the pathogenesis of DS. Over-dosage of Hsa21 genes is likely to disrupt normal development by influencing numerous molecular processes, including the overexpression of dosage-sensitive Hsa21 genes, compensatory regulatory mechanisms of gene transcription involving non-Hsa21 genes and inter-individual epigenetic variations (Dierssen, 2012). A better understanding of the gene-phenotype relationship comes from the generation of mouse models of DS, enabling us to study the consequences of over-dosage of specific Hsa21 genes or segments. Before considering animal models in more detail, the next section will summarise the main phenotypes of DS.

1.2.2. Clinical presentation

Down Syndrome is characterised by a widespread range of physical and cognitive features, whereby symptom manifestation and severity vary between individuals. In general, DS results in a number of dysmorphic features along with increased risk of concomitant disorders and delayed cognitive development. At birth, the presence of a series of DS characteristic features, such as flat facial profile, slanted eyes, and low muscle tone, can direct genetic testing to confirm the diagnosis of DS (Weijerman & de Winter, 2010).

1.2.2.1. Physical features

The physical problems occurring in DS concern a wide range of body systems, as briefly reviewed below.

Craniofacial dysmorphia

The skull of DS individuals is atypically short, resulting in a relatively flat head (brachycephaly). Additional craniofacial manifestations include ear anomalies, increased interocular distance (hypertelorism) and a flat nasal bridge (Arumugam et al., 2016).

Oral disorders

Oral dysmorphic features include an enlarged tongue (macroglossia), abnormal tongue positioning (glossoptosis), maloccusion, abnormal teeth development and enlarged tonsils (Weijerman & de Winter, 2010).

Orthopaedic disorders

The tone of the skeletal system is diminished (hypotonia), resulting in general weakness and floppiness. Motor development is significantly delayed and DS individuals require physical therapy as they display difficulties in postural control, craniocervical instability and abnormal motor patterns. Joint hypermobility is also observed and spontaneous hip dislocations occur frequently (Weijerman & de Winter, 2010).

Vision disorders

The prevalence of ocular abnormalities in DS ranges from 38-80% (Weijerman & de Winter, 2010). Frequent abnormal anatomical features of the visual system include narrowed or slanted palpebral fissures, skin folds covering the inner corner of the eye (epicanthal folds) and small spots on the iris (brushfield spots). Individuals with DS are often affected by vision disorders such as strabismus, nystagmus, cataract, refractive errors and glaucoma.

Hearing disorders

Malformations of the inner ear and of the nasopharynx are frequent in DS and can result in chronic otitis media and hearing disorders. The prevalence of hearing disorders has been estimated at 38-78% and early implementation of hearing aids is particularly important to aid the speech development (Weijerman & de Winter, 2010).

Cardiovascular disorders

Approximately half of DS neonates are born with cardiovascular defects, most frequently atrioventricular and ventricular septal defects (Weijerman & de Winter, 2010). The major complication associated to cardiac anomalies is pulmonary arterial hypertension,

increasing the risk of heart failure and death. Cardiac defects are usually surgically corrected at 2-4 months of age.

Respiratory disorders

Anatomical anomalies of the upper and lower airways can give rise to respiratory problems, especially in the presence of heart defects and hypotonia. Around one third of DS individuals report recurrent wheezing. Obstructive sleep apnoea is observed in over half of the cases in conjunction to oral malformations. (Weijerman & de Winter, 2010).

Gastrointestinal tract disorders

Congenital defects of the gastrointestinal tract are relatively rare (4-10% of cases) but have a much higher incidence in DS compared to the general population. Usually, anatomical defects can be treated surgically and include the absence or narrowing of gastrointestinal cavities, such as duodenal or anal stenosis/atresia. Celiac disease and constipation problems also occur more frequently in the DS population (Weijerman & de Winter, 2010).

Hematological and immunological disorders

Individuals with DS often report anomalies in the production and counts of white blood cells (T- and B- lymphocytes). Down Syndrome is in fact associated to a 10-fold increased risk of developing blood cancer, primarily acute myeloid leukemia or acute lymphocytic leukemia (Hickey, Hickey, & Summar, 2012). A small portion of newborns with DS (10%) presents a form of preleukemia that develops in utero, known as transient myeloproliferative disease. This preleukemia may disappear spontaneously, but in some cases precedes the development of myeloid leukemia (Weijerman & de Winter, 2010).

Endocrine disorders

The prevalence of thyroid disorders (primarily hypo- or hyperthyroidism) in the DS population is estimated at 28-40% and increases with age (Weijerman & de Winter, 2010). Thyroid hormones are essential in the regulation of energy use and body growth. Children with DS follow a DS-specific growth pattern and are predisposed to overweight. Diabetes mellitus also occurs at a higher incidence in DS.

Seizures

Compared to the general population, individual with DS are at higher risk of seizures, although the risk is lower compared to other forms of intellectual disability (Hickey et al., 2012). Typically, the onset of seizures occurs either in the first year of life or around 30 years of age, whereby late seizure onset of seizures is associated to the emergence of dementia (Lott & Dierssen, 2010).

1.2.2.2. Cognitive features

The main characteristic of DS is intellectual disability, along with general learning and memory impairments (Lott & Dierssen, 2010). The extent of the impairments varies between cognitive domains and between individuals, whereby several factors such as early interventions and physical health modulate cognitive function (Lott & Dierssen, 2010). Individuals with DS show delayed language development and language deficits persist through life. Intelligence tests indicate that intellectual disability ranges from moderate to severe. Consequently, cognitive performance of DS individuals is often compared against younger control subjects, matched on intelligence scores (IQ), verbal measures or a combination of variables corresponding to mental age (MA). The matching procedure allows assessment of the impact of DS in addition to baseline intellectual dysfunction. Analogously, cognitive studies also often compare performance between DS individuals and individuals affected by other types of intellectual disability, to reveal cognitive phenotypes specifically associated to trisomy of Hsa21 genes (Godfrey & Lee, 2018).

Poorer cognitive skills in DS have been associated with the presence of comorbidities (Lott & Dierssen, 2010). For example, DS individuals affected by sleep apnoea, thyroid disorders or seizures, generally report more severe deficits than unaffected DS subjects. Additionally, hearing and vision disorders can negatively affect performance in cognitive tests. All these factors need to be carefully considered when assessing cognitive phenotypes in DS.

The cognitive impairments observed in DS are thought to result from the important structural anomalies found in DS brains. Before considering cognition in detail, it is important to understand how trisomy 21 impacts brain development.

Brain development

The brain begins developing during gestation and continues after birth, growing and maturing until adulthood. Neurogenesis takes place primarily between the 10-25 week of gestation, following the formation of the neural tube. During this period, neural stem cells proliferate in large numbers, migrate to specific cellular sites and differentiate into neurons or astrocytes (Purves et al. 2012). In the hippocampus (HPC), neurogenesis has been shown to continue during the first postnatal years and possibly in adulthood, although to a lesser extent (Sorrells et al., 2018). After birth, the connections between neurons expand greatly, increasing dendritic branching and synapse number. This increase is accompanied by synaptic pruning, whereby surplus synapses and neurons are eliminated (Purves et al. 2012).

Anatomical studies report significant structural anomalies in DS brains and are already visible prenatally. In general, people with DS have smaller brains (Guidi et al., 2008;

Pinter et al., 2001a; Pinter, Eliez, Schmitt, Capone, & Reiss, 2001b). Reduced brain volume is particularly prominent in frontal areas, temporal areas, HPC and cerebellum (Pinter et al., 2001a; Pinter et al., 2001b). Significantly reduced volumes in the HPC and surrounding cortices are already present in DS foetuses between the 17-21 gestational week (Guidi et al., 2008). Postnatally, an MRI study of DS children and adolescents found that on average, total brain volume was reduced by ~18% and hippocampal volume by ~30% compared to typically developing subjects (Pinter et al., 2001a).

Importantly, smaller brain volumes are observed in conjunction with hypocellularity, suggesting a defect in the production of neural stem cells during gestation. In fact, reduced cell numbers are already observed in DS foetuses and low grey matter levels persist postnatally (Guidi et al., 2008; Pinter et al., 2001b). A number of trisomic genes has been proposed to interfere with early brain development, primarily affecting cell cycle during mitotic division. As reviewed in Stagni, Giacomini, Emili, Guidi and Bartesaghi (2018), the overexpression of certain dosage-sensitive Hsa21 genes is thought to alter complex signalling cascades, resulting in an elongation of the cell cycle duration and thus decreasing the rate of cell production. Candidate genes are *DYRK1A*, the Amyloid Precursor Protein (*APP*), the Regulator of Calcineurin 1 (*RCAN1*) and Oligodendrocyte transcription factor 1 and 2 (*OLIG1*, *OLIG 2*). Overexpression of these gene products has been associated to reduced cell numbers in DS foetuses, DS-derived stem cell cultures and mouse models of DS (Stagni et al., 2018). Additionally, studies have shown that the hypocellularity observed in DS is specifically related to a reduced number of neurons, while astrocyte levels are increased (Griffin et al., 1998; Guidi et al., 2008). Prenatal neurodevelopment in DS is thus characterised by defects in cell proliferation and cell differentiation.

At cellular level, DS brains also exhibit reduced dendritic length, dendritic branching and spine density, both in HPC and cortex (Becker, Armstrong, & Chan, 1986; Ferrer & Gullotta, 1990; Takashima, Iida, Mito, & Arima, 1994; Vuksić, Petanjek, Rasin, & Kostović, 2002). Interestingly, cortical dendritic branching was found to be normal in foetuses and in 2.5 months old newborns, but significantly reduced in children older than 2 years (Becker et al., 1986; Vuksić et al., 2002). Reduced branching thus seems to result from poor dendritic growth and synaptogenesis during postnatal development. Aberrant synaptic pruning also contributes to reduced branching, as dendritic degeneration rapidly progresses with aging (Takashima et al., 1994). Decreased levels of excitatory neurotransmitters, including glutamate, have also been observed in temporal and frontal cortices of DS adults (Risser, Lubec, Cairns, & Herrera-Marschitz, 1997). Given the fundamental role of the HPC and of neuronal connections in memory function (as will be discussed in chapter 3 and 4), it can be reasonably assumed that reduced dendritic branching, neurochemical alterations and reduced neuronal cell numbers, underpin cognitive impairments in DS.

Intelligence

The degree of intellectual disability is highly variable. Intelligence tests report quotients ranging from 40 to 70 points in adults, denoting severe to moderate impairment (Dierssen, 2012; Nelson et al., 2005). Intelligence scores increase with age in DS children, indicating that learning processes take place during development, although to a lesser degree compared to typically developing children. Intelligence scores reach plateau in adolescence and start to decline in adulthood (Dierssen, 2012).

Language

Although pre-language behaviour such as babbling emerges within the expected age-range, language development is significantly delayed (Grieco, Pulsifer, Seligsohn, Skotko, & Schwartz, 2015). First words and multi-word phrases emerge late in DS children. As they grow, DS children display deficits in pronunciation and morphosyntax, whereby the use of verbs, nouns and pronouns is often incorrect. Besides abnormal speech production, speech comprehension is also limited and worsens with aging.

Executive functions

Executive functions summarise higher order cognitive processes such as attention, inhibition, flexibility, planning, and working memory. They are primarily associated with activity in frontal and prefrontal cortices (Purves et al., 2012). Working memory is distinguished from explicit and implicit memory as it involves the mental manipulation of information, in addition to memory retrieval. As reviewed in Grieco et al. (2015), both children and adults with DS present poor executive functions, in particular concerning sustained attention and planning skills. People with DS report deficits in working memory tasks employing verbal material, while they are relatively unimpaired with visuospatial material (Grieco et al., 2015). The evidence suggests however a generally reduced working memory capacity, with performance decreasing as the amount of information to be processed increases (Grieco et al., 2015).

Implicit memory

Research on implicit memory is rather limited but suggests that the implicit acquisition of new memories is relatively preserved in DS. For example, DS individuals were found able to acquire a motor sequence to a similar extent as MA-matched typically developing children (Vicari, Verucci, & Carlesimo, 2007). Individuals with DS have also been shown to be as susceptible as controls to visual and verbal priming in picture completion and word completion tasks (Vicari, Bellucci, & Carlesimo, 2000; Vicari et al., 2007).

Short-term explicit memory

Studies assessing short-term memory (STM) in DS generally test memory performance after very brief time intervals. Given the profound language impairments characteristic of DS, most studies investigated performance in verbal versus non-verbal (primarily visuospatial) memory tasks (Godfrey & Lee, 2018). Typically, participants are presented with either a series of words or of spatial locations and asked to immediately reproduce the series. An incremental procedure is often used, measuring memory performance as the longest series of items correctly recalled.

A clear dissociation pattern emerged from the numerous STM studies (Godfrey & Lee, 2018). Generally, memory performance of DS individuals in verbal tasks is severely impaired, in comparison to both typically developing children and subjects affected by other intellectual disabilities. Instead, STM performance in visuospatial tasks is often unimpaired and visuospatial skills are considered a relative strength in DS. For example, Jarrold, Baddeley and Phillips (2002) assessed verbal and visuospatial STM in DS individuals, typically developing children and individuals with learning impairments, matched on their vocabulary level. In the verbal task, a list of numbers was presented either acoustically or acoustically with simultaneous visual support on a computer screen. In the visuospatial task, participants watched the experimenter tap a sequence of spatial locations on a board made of different blocks. Individuals with DS performed worse than typically developing children and individuals with learning impairments in the verbal task, both in the acoustic and the acoustic-visual mode. By contrast, performance of DS individuals in the visuospatial task was no different from the two control groups. Verbal STM deficits thus are not strictly a result of defective processing of auditory information but reflect a generalised impairment in the retention of linguistic information.

Indeed, the short-term retention of verbal material has been found impaired also when assessed with entirely visual tasks (Duarte, Covre, Braga, & de Macedo, 2011). In one study, participants were presented with a sequence of images depicting common words (e.g. cat, ball, house) and asked to reproduce the sequence using the images. The memory-span of DS individuals was significantly reduced compared to MA-matched control children, indicating poorer short-term retention of visually presented verbal information. Interestingly, performance could be rescued by the implementation of visuospatial support: in another experimental condition, the sequence of words was presented by the experimenter pointing to images on a board. In this case, DS individuals could correctly reproduce the sequence. Although it is possible that DS subjects merely retained locations irrespective of the depicted words, the study highlights the strength of visuospatial skills.

Verbal STM deficits observed in visual tasks do not necessarily imply that STM for visual material is impaired. A failure to implement verbal codes in support of the retention

of visual material can in principle underlie poorer performance in DS, especially in comparison to typically developing children whose performance can better profit from verbal skills. In fact, when visual STM was tested with random visual patterns or with non-focal colours, individuals with DS performed no different to controls, suggesting intact visual STM performance (Carretti, Lanfranchi, & Mammarella, 2013; Laws, 2002).

The dissociation between verbal and visuospatial STM has been observed at different developmental stages, from pre-school children to adults (Godfrey & Lee, 2018). A cross-sectional study reported that both verbal and visuospatial memory-span increase with age, indicating that progress indeed takes place during development in DS (Frenkel & Bourdin, 2009). The memory-span for visuospatial material increased however at a much higher rate compared to the verbal memory-span. Interestingly, individuals with Williams syndrome, a neurodevelopmental disorder caused by a mutation in chromosome 7, show the opposite STM dissociation pattern, implicating different genes in the retention of different types of information. For example, individuals with Williams syndrome showed better verbal STM than an IQ-matched DS group, while the DS group outperformed individuals with Williams syndrome in a visuospatial STM task (Edgin, Pennington, & Mervis, 2010).

Several studies have attempted to uncover the reason behind poor verbal STM in DS. According to one study, individuals with DS performed significantly worse than controls when asked to recognise previously listened non-words and their performance decreased as syllable-length increased (Raitano Lee, Pennington, & Keenan, 2010). Consequently, difficulties in phoneme-discrimination were proposed to underlie verbal STM deficits. Support for this hypothesis was however not found in a study by Vicari, Marotta and Carlesimo (2004).

While it is understandable that human DS memory research concentrated on the retention of verbal information, such tasks do not find a direct parallel in animal research. A few studies have attempted to align human and animal STM research. For example, Kogan et al. (2009) tested individuals with DS on a delayed non-match to sample task and a delayed non-match to position task, with a 5 second delay. In the first task, participants were rewarded with nickels for selecting a novel object over a familiar one. In the second task, participants were rewarded for selecting a familiar object in a novel spatial location over an identical object in a familiar location. Individuals with DS performed as well as MA-matched control children on both tasks.

These results were confirmed by a recent study that used a novel battery of object-recognition memory tasks especially developed from rodent studies, the Arizona Memory Assessment for Preschoolers and Special Populations (A-MAP) (Clark, Fernandez, Sakhon, Spanò, & Edgin, 2017). In the study, participants briefly interacted with different three-dimensional objects and were then asked to recognise a previously handled object

(NOR-equivalent). Participants were also presented with a series of identical (Loc-equivalent) or different (OiP-equivalent) objects placed on a board and were then asked to replicate the spatial configuration. Finally, participants also had to judge which of two objects from a pair appeared first in a sequence of previously presented objects (TOr-equivalent). In line with Kogan et al. (2009), DS individuals reported intact recognition memory for single objects (NOR) and locations (Loc). They were however impaired in the retention of specific positions associated to different objects (OiP) and in temporal order judgments (TOr).

The majority of STM studies has concentrated on verbal memory, reporting deficits beyond MA-expectations. Given the severe language delay in DS, it is possible that verbal STM deficits are tightly linked to general language impairments, rather than representing a specific STM-defect per se. Instead, STM for non-verbal material (e.g. objects, locations) is relatively preserved. These studies tested however immediate recall and evidence from patient studies and lesion studies in rodents indicates that such brief intervals are largely independent of the HPC (e.g. Clark et al., 2001; see chapter 3). Hippocampal involvement is instead noted for longer retention intervals, such as when assessing long-term memory (LTM).

Long-term explicit memory

As will be presented in chapter 3, long-term storage of information involves activity within the medial temporal lobe system, in particular on the HPC. Similarly to STM resarch, studies assessing LTM tested the delayed recall of verbal versus non-verbal (primarily visuospatial) material. Overall, the literature points to severely impaired LTM, with deficits concerning both verbal and nonverbal information, emerging at pre-school age and worsening with age (Godfrey & Lee, 2018). While visuospatial skills are relatively preserved in immediate recall tests, they are not when assessed after a retention interval. For example, individuals with DS performed worse than MA-matched children in the delayed reproduction of a previously learned visuospatial sequence (Vicari et al., 2000).

Whether LTM performance of DS individuals is different compared to individuals affected by other forms of intellectual disability is unclear. In one study, DS participants scored significantly higher than individuals with William syndrome both on a verbal and a visuospatial task (Edgin et al., 2010). In another study, DS subjects scored lower than controls in the reproduction of a complex geometrical figure studied 15-min earlier, but similarly to individuals with other types of intellectual disability (Carlesimo, Marotta, & Vicari, 1997). The same DS subjects however, recalled a significantly lower number of words after a 15-min retention interval, in comparison to both control and intellectually disabled subjects.

Verbal LTM deficits have also been observed in entirely visual tasks. For example, individuals with DS recognised a significantly lower number of previously studied images than MA-matched subjects (Vicari et al., 2000). Unlike STM, however, impairments in the long-term retention of visual information did not seem related to a reduced ability to code visual information verbally, because DS subjects were impaired even when tested with random visual patterns (Pennington, Moon, Edgin, Stedron, & Nadel, 2003). In fact, visual memory seems generally impaired at long-term level. In a visual recognition task, individuals were presented with different versions of the same image (e.g. different types of trees) and were asked to recognise the version they studied at an earlier time point. Individuals with DS recognised a significantly lower number of images in comparison to MA-matched children (Vicari, Bellucci, & Carlesimo, 2005).

A possible explanation for the pervasive LTM impairments observed in DS, is the dependency of explicit LTM on the HPC. As described in the “Brain development” section, the HPC presents with several structural anomalies in the DS population. To investigate this hypothesis, Pennington et al. (2003) tested a group of DS and of MA-matched children on a series of verbal and non-verbal LTM tasks known to rely on the HPC and a series of verbal and non-verbal working memory tasks requiring the prefrontal (PFC) cortex. Individuals with DS performed worse than controls on all HPC-dependent LTM tasks, including a test similar to the OiP task, in which participants had to recall the spatial location of distinct, random patterns. By contrast, no significant differences were observed between the groups in the PFC-dependent working memory tasks.

To confirm the pattern of hippocampal dysfunction in the DS population, several studies investigated performance in visuospatial navigation memory tasks which rely on the HPC (Courbois et al., 2013; Lavenex et al., 2015; Purser et al., 2015). In one study (Courbois et al., 2013), participants were instructed to navigate through a virtual environment featuring a variety of landmarks (e.g. tree, dog, bicycle) to reach a particular building (e.g. railway station). After a familiarisation phase in which participants were shown the right path, spatial memory was tested, and participants had a maximum of 10 trials to reach the building without making mistakes. Although DS participants improved their performance across the trials, they required more trials to learn the correct pathway than controls. In a second test phase, participants were asked to find a shortcut to reach the building. Only 2 out of 10 DS participants were able to find the shortcut, in comparison to 5 out of 10 participants from a MA-matched group and all 10 participants from a chronological age-matched group. Additionally, in a subsequent visual recognition memory test, participants with DS recognised a significantly lower number of landmarks that appeared in the virtual environment, compared to both control groups.

Since computerised experiments tend to assess spatial memory from an egocentric perspective, Lavenex et al. (2015) wanted to assess viewpoint-independent, allocentric spatial memory in DS. In the study, participants were asked to locate three rewards (i.e. sweet treats) hidden underneath a number of white plastic cups placed over a test room. The rewards were always located in the same three spatial positions. In one condition, the three cups covering the rewards were red, serving as local cues. In the allocentric condition, all cups were white and distal spatial cues present in the test room served as reference points to navigate the environment and memorise the position of the rewards. Each condition was repeated for 10 trials, over two days. Individuals with DS displayed normal learning in the local cue condition, consistently locating the rewards under the red cups. In the allocentric condition however, the DS group performed only at chance level while a MA-matched group progressively improved performance across the trials.

In sum, the evidence suggests that triplication of Hsa21 genes results in a generalised LTM impairment, affecting the retrieval of verbal, visual and visuospatial information. Behavioural findings, together with anatomical findings reporting aberrant hippocampal anatomy, converge to support a major role of hippocampal dysfunction in the cognitive symptoms of DS.

Early-onset cognitive decline

The LTM impairments observed in DS worsen with increasing age (Godfrey & Lee, 2018). Cognitive abilities in general begin to deteriorate when DS individuals reach middle age. For example, younger DS individuals (22-38 years) performed significantly better than older DS individuals (41-61 years) in a memory task that required participants to recall in which of three boxes and object was hidden, both after a 10-second and a 2-minute delay (Alexander et al., 1997). The cognitive decline observed in DS appears to be more severe compared to other forms of intellectual disability. Individuals with DS are in fact at higher risk of developing early-onset dementia, frequently Alzheimer's type (Lott & Head, 2001). Alzheimer's disease (AD) is a neurodegenerative disorder that progressively impairs memory and other cognitive domains, such as language and executive functions. The disease is initially characterised by impairments in the retention of new episodic memories, in conjunction with hippocampal atrophy. As the disease progresses, neurodegeneration extends to the neocortex and remote memories become affected.

In the general population, the onset of sporadic AD usually occurs at advanced age, with a prevalence of ~10% in individuals of 70 years and older (Plassman et al., 2007). In the DS population however, AD symptoms can emerge as early as the age of 40, with incidence rates increasing dramatically later in life. Prevalences are highly variable, ranging from 15 to 77% in DS individuals over 60 years (Head, Powell, Gold, & Schmitt, 2012).

The brains of AD patients are characterised by an accumulation of neurofibrillary tangles of tau protein aggregates and an accumulation of neuritic plaques made of insoluble amyloid-beta (Aβ) peptides (Lott & Head, 2001). Neurofibrillary tangles and Aβ-plaques interfere with normal cell functioning, leading to synaptic loss and neuronal death. Insoluble Aβ peptides are generated from the incorrect cleavage of the transmembrane amyloid precursor protein (APP). The gene encoding APP is located on Hsa21, implicating that individuals with DS carry three *APP* copies. Consequently, overexpression of APP has been suggested to underlie the elevated AD incidence observed in the DS population (Lott & Head, 2001). In fact, by the age of 40, virtually all DS brains show signs of atrophy and widespread accumulation of Aβ-plaques in hippocampal and neocortical areas (Wisniewski, Wisniewski, & Wen, 1985). However, despite presenting the neuropathological hallmarks of AD, only a portion of DS individuals over 40 years report symptoms of AD (Head et al., 2012).

1.3. Mouse models of Down Syndrome

Down Syndrome is a complex genetic disorder. Important advances in understanding how triplication of Hsa21 genes results in the typical features of DS have been made possible by the generation of genetically modified mice that model trisomy 21. The genetic content of the long arm of Hsa21 is evolutionarily conserved in the mouse genome, sharing synteny with orthologous regions on three mouse chromosomes (*Mus musculus, Mmu)*: Mmu16, Mmu17 and Mmu10 (fig. 1.1) (Lana-Elola et al., 2011). The largest syntenic portion is located on Mmu16, containing approximately 115 genes. The Mmu17 and Mmu10 syntenic portions are smaller, with an estimated number of 19 and 41 genes respectively. Based on the conserved synteny between the human and the mouse genomes, several mouse models of segmental DS duplicating distinct syntenic portions have been generated over the past decades and made commercially available. The majority of the models were generated via Cre/loxP recombination, a novel, highly controlled chromosomal engineering technique (see section 2.1.1) (Herault et al., 2017). Mouse models are of great value to DS research as they provide the unique advantage of studying the consequences of over-dosage of specific Hsa21 segments. Indeed, DS models successfully recreate a number of physical and cognitive phenotypes analogous to human DS. Nonetheless, the role of Hsa21 genes in brain development and in the regulation of memory processes has not yet been fully understood.

To better understand memory function in DS, the current research used three novel mouse models of segmental DS, each carrying an exact duplication of one of the three orthologous regions: the Dp1Tyb for Mmu16, the Dp3Yey for Mmu17 and the Dp2Yey for Mmu10 (also known as Ts1Yey / Dp(16)1Yey, Ts3Yey / Dp(17)1Yey, Ts2Yey / Dp(10)Yey) (Lana-Elola et al., 2011; Yu et al., 2010b). These models represent a unique tool to assess the distinct contribution of the Mmu16, Mmu17 and Mmu10 syntenic regions to DS-like phenotypes. In contrast, as reviewed in the following sections, less recently created models also duplicate non-syntenic genes in addition to the intended Mmu-mutation and/or lack duplication of some syntenic genes, undermining their validity as DS models. Nevertheless, comparison of findings obtained with different models can help the identification of dosage-sensitive genetic portions or single genes directly linked to specific DS phenotypes. To this purpose, mutant mouse lines deficient of specific syntenic genes and crosses between distinct trisomic lines have also been created (Duchon et al., 2011a; Zhang et al., 2014; Yu et al., 2010a).

Because of hippocampal dysfunction observed in individuals with DS, animal studies have concentrated on hippocampal anatomy and physiology, and HPC-dependent memory tasks. Phenotypes of trisomic animals are generally compared against euploid animals, that is, wildtype mice carrying two copies of each chromosome. A schematic representation of

the most frequently employed DS mouse models in the study of memory is shown in fig. 1.1. Phenotypes of the different Mmu16, Mmu17 and Mmu10 trisomy models are described in the following sections and summarised in table 1.1, focusing on brain morphology and memory deficits.

Figure 1.1: Hsa21 orthologous regions in mice and mouse models of DS. Mouse models of DS carry duplications of orthologous portions, except for the Tc1 model that carries a transchromosomic copy of Hsa21 with three deletions. Estimated numbers of duplicated genes are within brackets (Lana-Elola, et al., 2011). TTS: Yu et al., 2010a. Dp1Tyb, Dp3Yey, Dp2Yey: Yu et al., 2010b. Ts65Dn: Reeves et al., 1995. Ts1Cje: Sago et al., 1998. Ts1Rhr: Olson et al., 2004a. Dp1Yah: Pereira et al., 2009. Tc1: O'Doherty et al., 2005.

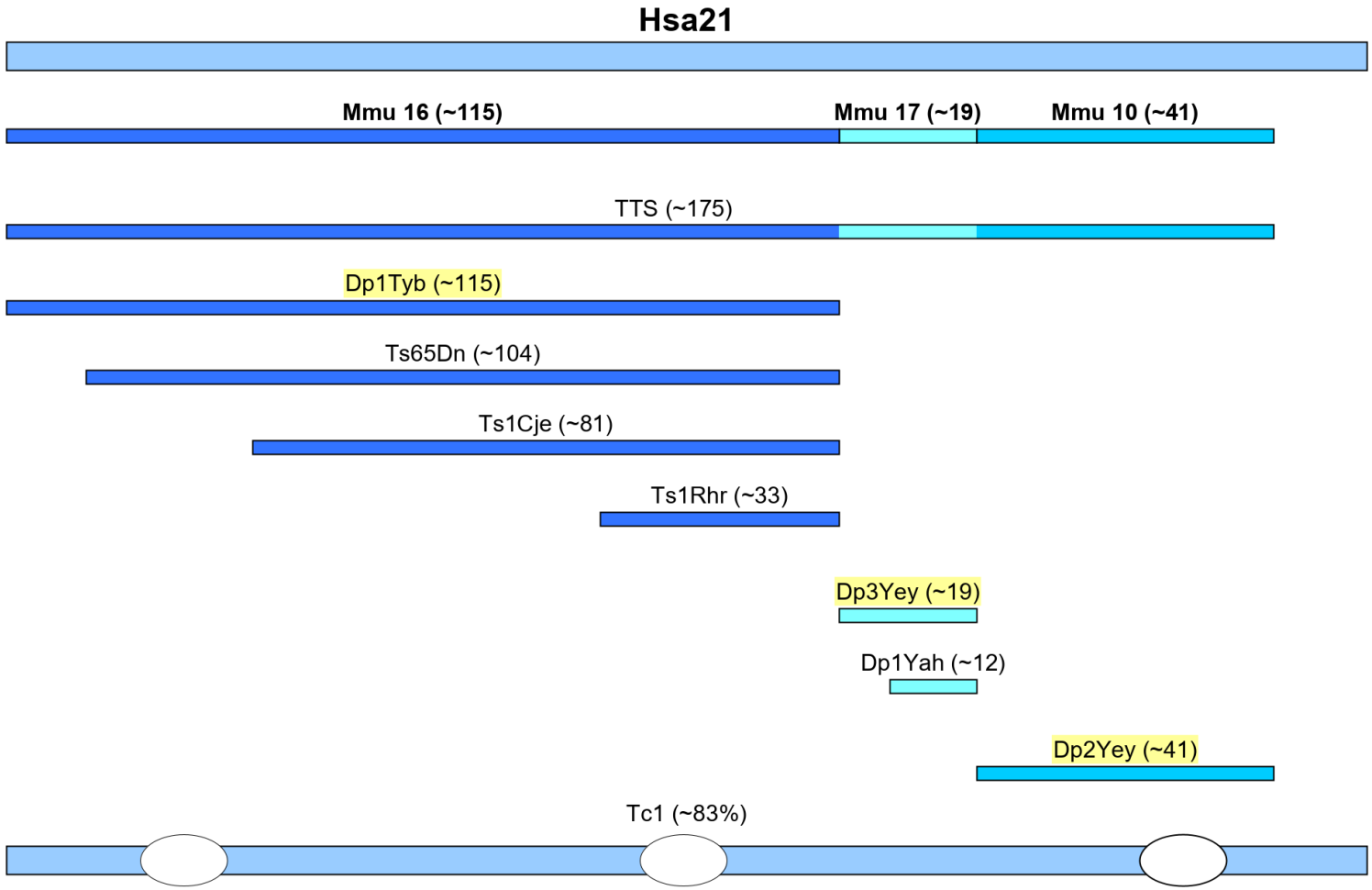

1.3.1. The Dp1Tyb and Mmu16 models

The majority of DS mouse models carry a partial duplication of the Mmu16 syntenic region. The first and most extensively studied model is the Ts65Dn (Reeves et al., 1995). This model is the result of a translocation between Mmu16 and Mmu17, following X-ray irradiation. Ts65Dn mice are trisomic for a large portion but not the entirety, of the Mmu16 conserved region (*Mrpl39* – *Zbtb21*) and for 60 genes on Mmu17 that are not syntenic to Hsa21 (Duchon et al., 2011b). As a consequence, phenotypes observed in the Ts65Dn strain cannot be directly linked to only genes syntenic to human DS and are frequently more severe compared to other models (Belichenko et al., 2009a). Another widely employed model is the Ts1Cje, resulting from a translocation between Mmu16 and Mmu12 (Sago et al., 1998). Ts1Cje mice are trisomic for an overlapping, yet shorter Mmu16 segment (*Sod1* – *Zbtb21*) and monosomic for 7 genes on Mmu12, limiting their validity as DS model (Duchon et al., 2011b). The Ts1Rhr model was instead generated to study DSCR genes and these mice are trisomic for an even shorter Mmu16 portion, corresponding exactly to the DSCR (*Cbr1* - *Mx2*) (Olson, Richtsmeier, Leszl, & Reeves, 2004a). The most recently created model is the Dp1Tyb (also known as Ts1Yey or Dp(16)1Yey). The Dp1Tyb is the only model trisomic entirely and exclusively for the Mmu16 conserved region (*Lipi* – *Zbtb21*) (Yu et al., 2010b). Containing the largest number of triplicated Mmu16 syntenic genes and lacking perturbations of unrelated genes, the Dp1Tyb is the most representative model to study the relationship between DS phenotypes and Hsa21 homologs on Mmu16. Several syntenic genes on Mmu16 have been previously implicated in memory function, such as *Dyrk1A*, *App*, and *Rcan1* (Lana-Elola et al., 2011).

Despite their genetic limitations, classical Mmu16 models reproduce a number of DS-like phenotypes. Concerning physical features, craniofacial anomalies such as a shorter skull and flattened face were observed in Ts65Dn and Ts1Cje, but not Ts1Rhr mice (Olson et al., 2004a; Richtsmeier, Baxter, & Reeves, 2000; Richtsmeier, Zumwalt, Carlson, Epstein, & Reeves, 2002). This type of findings allows one to conclude that genes causing the DS craniofacial phenotypes are located on the Mmu16 segment duplicated in the Ts1Cje model, but do not arise from trisomy of the DSCR alone. Further physical conditions such as heart defects, anomalies in blood cells production, motor dysfunction and delayed body growth have been observed in the Ts65Dn (Costa, Walsh, & Davisson, 1999; Holtzman et al., 1996; Kirsammer et al., 2008). Recent evidence suggests that similar physical phenotypes are also present in the Dp1Tyb strain. Dp1Tyb animals show altered craniofacial morphology, resembling Ts65Dn more than Ts1Cje anomalies (Starbuck, Dutka, Ratliff, Reeves, & Richtsmeier, 2014). Approximately one third of Dp1Tyb embryos have cardiovascular and gastrointestinal malformations (Li et al., 2007). Postnatally, body growth is delayed, along with the acquisition of developmental milestones such as

neurological reflexes (Goodliffe et al., 2016). At 2-3 months of age, Dp1Tyb mice show signs of motor dysfunction, as measured by poorer nest building skills, reduced motor strength, balance and coordination on the rotarod and the hanging wire test (Goodliffe et al., 2016; Watson-Scales et al., 2018). Sensory function seems instead unaltered, with Dp1Tyb mice showing normal nocifensive responses to cold, heat and mechanical stimuli (Watson-Scales et al., 2018).

Naturally, Mmu16 trisomies affect brain structure as well. While brain volume and brain weight are reduced in human DS, these measures are generally normal in mouse models, albeit gross anatomical differences can be observed during embryonic life (Belichenko, Kleschevnikov, Salehi, Epstein, & Mobley, 2007; Chakrabarti, Galdzicki, & Haydar, 2007; Holtzman et al., 1996). For example, brain size is significantly reduced in Ts65Dn embryos, but reaches euploid levels shortly before birth (Chakrabarti et al., 2007). Neocortical and hippocampal growth are also reduced in Ts65Dn embryos (Chakrabarti et al., 2007). These reductions were associated to longer cell cycle duration and reduced neurogenesis, two mechanisms found to be defective in human DS brain development as well. Surprisingly, such neurodevelopmental changes are not observed in prenatal Dp1Tyb mice. Throughout embryonic life, brain size, neocortical and hippocampal growth, and rate of neurogenesis, are no different from euploid controls (Goodliffe et al., 2016). Consequently, genetic differences between the Dp1Tyb and the Ts65Dn models seem to determine the presence of prenatal brain defects. Indeed, despite having the larger number of trisomic genes, only 19 of the Mmu16 homologs were found differentially expressed in Dp1Tyb embryonic brains, in comparison to 46 in the Ts65Dn (Goodliffe et al., 2016).

Further neuromorphological anomalies typical of DS are visible postnatally. Adult Ts65Dn, Ts1Cje and Ts1Rhr all show reduced volume and reduced neuronal cell density in the cerebellum (Olson et al., 2004b; Olson et al., 2007). Dp1Tyb mice show instead unaltered cerebellar anatomy (Watson-Scales et al., 2018). Neonatal and adult Ts65Dn mice also show reduced neuronal cell density in the HPC (Kurt, Kafa, Dierssen, & Davies, 2004). More specifically, the Ts65Dn HPC exhibits decreased levels of excitatory neurons and increased levels of inhibitory neurons (Chakrabarti et al., 2010). This pattern was however not observed in the Dp1Tyb model. As a matter of fact, numbers of inhibitory neurons were found significantly reduced in the neocortex of neonatal Dp1Tyb mice (Goodliffe et al., 2016).

In addition to neuronal cell populations, synapse number and structure are also altered. In Ts65Dn newborns, synaptogenesis was found decreased in both neocortex and HPC, as indicated by reduced levels of the postsynaptic density protein PSD95 (Chakrabarti et al., 2007). Electron microscopy studies confirmed the finding in adult Ts65Dn mice and linked the reduction to a specific decrease in the number of excitatory synapses (Kurt et al.,

2004). Reductions in dendritic spine density were also observed in Ts1Cje and Ts1Rhr mice, along with abnormal spine morphology and abnormal arborisation (Belichenko et al., 2004; Belichenko et al., 2007; Belichenko et al., 2009a). A statistical comparison revealed that dendritic anomalies were more severe in Ts65Dn than in Ts1Cje or Ts1Rhr animals (Belichenko et al., 2009a). While synapse number and structure have not been studied yet in the Dp1Tyb model, research by Souchet et al. (2014) reports alterations in the levels of several synaptic markers, including reduced hippocampal levels of glutamate receptors.

Synaptic plasticity mechanisms, such as long-term potentiation (LTP) and long-term depression (LTD) have been proposed to represent the physiological substrate for HPC-dependent learning and memory (e.g. Morris, Anderson, Lynch, & Baudry, 1986; see chapter 4). These changes alter synaptic transmission efficacy and rely primarily on expression and activity of glutamate receptors. Given the synaptic anomalies described above, plasticity mechanisms are likely to be compromised in Mmu16 trisomy models. Indeed, LTP induction was impaired in hippocampal slices of Ts65Dn, Ts1Cje and Ts1Rhr brains (Belichenko et al., 2007; Belichenko et al., 2009a; Kleschevnikov et al., 2004; Siarey, Villar, Epstein, & Galdzicki, 2005). In the Dp1Tyb, in vitro hippocampal LTP induction was also found significantly decreased (Jiang et al., 2015; Yu et al., 2010b; Zhang et al., 2014). Additionally, Ts65Dn and Ts1Cje slices also showed increased LTD (Siarey et al., 1999; Siarey et al., 2005).

Together, electrophysiological and neuroanatomical observations point to a state of decreased excitatory and increased inhibitory synaptic transmission in Mmu16 trisomies. In fact, application of antagonists blocking inhibitory γ-aminobutyric (GABA) receptors was found to restore LTP in the Ts65Dn, Ts1Cje and Ts1Rhr models (Belichenko et al., 2007; Belichenko et al., 2009a; Kleschevnikov et al., 2004). Such findings led to the formulation of the “GABAergic over-inhibition hypothesis”, whereby altered inhibitory signalling is postulated to affect neural excitability and result in memory impairments (as reviewed in Contestabile, Magara, & Cancedda, 2017). Indeed, although no gene on Mmu16 has yet been directly associated to excitatory or inhibitory neurotransmission, several gene products have been demonstrated to regulate synaptic transmission and plasticity, such as *DYRK1A* or *RCAN 1* (Grau et al., 2014; Martin et al., 2012).

Unsurprisingly, given the number of hippocampal anomalies observed, all Mmu16 models report memory impairments. A frequently employed test to assess hippocampal integrity in rodents is the spontaneous alternation T-maze (Deacon, Bannerman, Kirby, Croucher, & Rawlins, 2002). In this test, mice are placed in the stem of a T-shaped maze and allowed to explore either of the two arms for a period of time. Based on their innate preference for novelty (Ennaceur & Delacour, 1988), rodents show a tendency to alternate entry between the two arms. As shown by a series of studies by Belichenko et al. (2007;

2009a), Ts65Dn, Ts1Cje and Ts1Rhr animals all performed significantly worse than euploid controls on the T-maze test, displaying near chance alternation rates. These findings suggest a degree of hippocampal dysfunction in all three models and that DSCR trisomy alone is sufficient to produce the phenotype. Findings regarding the Dp1Tyb model are instead contradictory, with some studies reporting normal and others impaired performance on the spontaneous alternation T-maze test (Goodliffe et al., 2016; Jiang et al., 2015; Souchet et al., 2019).

Another common paradigm used to assess hippocampal integrity is the Morris water maze (MWM) (Morris, Garrud, Rawlins, & O'Keefe, 1982). In this task, the mouse is placed in a circular pool filled with water and trained to locate a floating platform. The platform can either be clearly visible (e.g. marked by a flag) or hidden. In the cued platform test, spatial information is irrelevant and the test is used as a measure of swimming ability, vision and motivation to escape the water. By contrast, the hidden platform test is sensitive to hippocampal dysfunction because it requires the use of information about the spatial organisation of room cues to locate the platform. Over repeated trials, animals learn the position of the platform, significantly reducing swimming time and distance. Following the learning phase, memory is also assessed by removing the platform and examining the amount of time the animal spends searching for the platform in the correct area. When tested on the MWM, both Ts65Dn and Ts1Cje animals performed normally in the visible platform test but were impaired on a number of measures on the hidden platform test (Sago et al., 2000). Impairments were more severe in the Ts65Dn, as some degree of spatial learning was preserved in Ts1Cje but not Ts65Dn animals (Sago et al., 2000). Surprisingly, despite the T-maze impairment, Ts1Rhr animals were found to perform normally in both the visible and the hidden platform test, implicating that trisomy of the DSCR does not affect hippocampal function in the MWM (Olson et al., 2007). This discrepancy may suggest that performance on the T-maze test and on the MWM may rely on different hippocampal networks (Sanderson & Bannerman, 2012). Indeed, the two tests assess very different retention spans, with the T-maze assessing brief time intervals and the MWM extending over several training days. In line with the longer Mmu16 trisomies, Dp1Tyb performed normally in the MWM with the visible platform but were impaired on the hidden platform test (Goodliffe et al., 2016; Yu et al., 2010b; Zhang et al., 2014). Partial visuospatial learning was however preserved, since Dp1Tyb animals decreased their escape latency and path length over trials, and searched for the platform in the target area, although to a lesser extent compared to wildtype mice.

The contextual fear conditioning task is also frequently used to test hippocampal function. The animal is placed in a conditioning chamber and its ability to associate a given context (e.g. olfactory and visual cues) to the delivery of a foot shock is tested. Memory

performance is quantified as the amount of time spent by the animal freezing when re-placed in the conditioning chamber after a time interval. Ts65Dn animals showed significantly reduced freezing times when tested after 48-h, indicating a weaker memory trace (Kleschevnikov et al., 2012). Interestingly, treatment with GABA receptor antagonists rescued the deficit. Dp1Tyb animals also showed impaired memory on the fear conditioning task, both after 24-h and 72-h (Yu et al., 2010b).

Memory in mouse models of DS is also frequently assessed with Object-recognition memory tasks. In the Ts65Dn model, recognition memory for novel spatial locations (Loc) following a 10-min delay was impaired (Kleschevnikov et al., 2012). In an OiP task, Ts1Cje mice failed to recognise novel object-in-place associations after a 2-min delay (Fernandez & Garner, 2007). Indeed, recognition memory relying on spatial/contextual information has been demonstrated to depend on the HPC (see chapter 3), suggesting once again HPC-dysfunction in Mmu16 trisomy models. Most studies on DS mouse models investigated however recognition memory for novel objects, a feature of recognition memory that is largely independent of HPC-function (e.g. Barker & Warburton, 2011; see chapter 3). A large number of lesion studies indicates that processing of object-information depends primarily on the perirhinal (PRH) cortex. In a NOR task, Ts65Dn mice were found able to discriminate between a familiar and a novel object after a 10-min delay but were impaired with a 24-h delay (Kleschevnikov et al., 2012). Similarly, Ts1Rhr animals performed normally after 1-h but were impaired after 24-h (Belichenko et al., 2009a). Novel object recognition was instead intact in the Ts1Cje after 24-h (Fernandez & Garner, 2007). In general, visual recognition memory for objects seems to be relatively preserved after brief intervals but impaired after longer delays. Moreover, performance of Ts65Dn mice on both the Loc and the NOR task could be rescued by treatment with GABA receptor antagonists (Kleschevnikov et al., 2012). In line with these models, Dp1Tyb animals were found unable to recognise a novel object after a 24-h delay (Nguyen et al., 2018; Souchet et al., 2019). Shorter retention intervals or other types of object-recognition memory tasks have not been tested yet in the Dp1Tyb model. Impairments in novel object recognition suggest that the Mmu16 trisomy does not exclusively affect hippocampal activity but possibly PRH activity as well. Moreover, the duration of the retention interval and activity levels of glutamate receptors seem to represent crucial variables affecting recollection.

Overall, likewise classical Mmu16 trisomy models, the Dp1Tyb strain recreates a number of physical and cognitive features analogous to human DS. The Dp1Tyb strain is however characterised by important neuromorphological differences, especially in comparison to the Ts65Dn strain. Despite carrying the largest Mmu16 duplication, brain development and neurogenesis appear to be normal in Dp1Tyb embryos. However, both Dp1Tyb and Ts65Dn mice show behavioural delays already shortly after birth. Dp1Tyb mice

report motor dysfunction like other Mmu16 models, but their cerebellar anatomy is normal. Nevertheless, structural and functional alterations in the HPC along with deficits in HPC-mediated memory, seem to characterise all Mmu16 trisomy models – including the Dp1Tyb – regardless of the size of the genetic duplication. The presence of motor dysfunction in Mmu16 models highlights the necessity to disambiguate possible confounding effects of motor impairments from cognitive performance.

1.3.2. The Dp3Yey and Mmu17 models

Given the relatively small size of the Mmu17 conserved region, research on DS has primarily focused on the contribution of Hsa21 homologs located on Mmu16. Currently, over-dosage of Mmu17 syntenic genes has been modelled in only two mouse lines. The Dp1Yah model (also known as Ts1Yah) is trisomic for a large portion, but not the entirety, of the Mmu17 conserved region (from *Abcg1* to *Cbs*) (Pereira et al., 2009). This model was created via Cre/loxP engineering and does not carry perturbations of other genetic segments. The Dp3Yey model (also known as Ts3Yey or Dp(17)1Yey), is trisomic entirely and exclusively for the Mmu17 conserved region (from *Abcg1* to *Rrp1b*) (Yu et al., 2010b). Dp1Yah and Dp3Yey mice are trisomic for ~12 and ~19 protein-coding genes respectively. Carrying the complete Mmu17 trisomy, the Dp3Yey represents the most valid model to investigate the contribution of Mmu17 syntenic genes to DS phenotypes. Currently, only one gene on the conserved Mmu17 segment, the Cystathionine-β-Synthase (*CBS*) gene, has been implicated in memory function. The *CBS* gene encodes an enzyme involved in the production of cystathionine, whose deficiency has been associated to intellectual disability (Almuqbil, Waisbren, Levy, & Picker, 2019).

Research on the Dp1Yah and the Dp3Yey is very limited. With respect to the physical features of DS, no study has investigated craniofacial dysmorphia, cardiac or gastrointestinal defects, body growth and development in either of the two Mmu17 models. Some evidence is available concerning motor function in the Dp1Yah. Balance and coordination were assessed with the rotarod test, measuring the animal's ability to walk on a rapidly rotating rod. Dp1Yah adult mice performed similarly to euploid controls, suggesting that motor dysfunction phenotypes are not linked to trisomy of Mmu17 (Marechal et al., 2019; Pereira et al., 2009).

Similarly, neuromorphological alterations have not been investigated in either the Dp1Yah or the Dp3Yey, at any age. The limited available evidence has examined hippocampal LTP. Surprisingly, although baseline hippocampal excitatory activity was normal, LTP was found significantly increased in both Dp1Yah (*in vivo*) and Dp3Yey (*in vitro*) brains, resulting in enhanced and longer lasting potentiation (Pereira et al., 2009; Yu et al., 2010b). Hippocampal synaptic plasticity appears thus to be facilitated in animals

trisomic for Mmu17 syntenic genes, in strong contrast to Mmu16 trisomy models. The reason for this enhancement is unclear, especially since no gene on the Mmu17 portion has yet been directly implicated in synaptic neurotransmission.

Evidence concerning the cognitive phenotypes of Mmu17 models is more abundant. On the spontaneous alternation T-maze test, one study reported reduced alternation rates in Dp1Yah mice (Pereira et al., 2009), while a second study found no impairments (Marechal et al., 2019). These contradictory findings are puzzling, as animals of roughly the same age were tested, with the same methodology. The same two studies were however concordant in reporting intact visuospatial memory in Dp1Yah animals on the MWM hidden platform test, suggesting normal hippocampal function despite abnormal hippocampal LTP (Marechal et al., 2019; Pereira et al., 2009). Memory impairments arose instead when Dp1Yah animals were tested on a NOR task, with Dp1Yah mice unable to discriminate between a familiar object explored 1-h earlier and a novel object, possibly implicating abnormal PRH cortex function (Marechal et al., 2019; Pereira et al., 2009). In Dp3Yey mice, memory function was assessed only by one study. In line with the Dp1Yah, Dp3Yey mice performed normally on the MWM hidden platform test and also showed no deficit in the contextual fear conditioning task (Yu et al., 2010b).

Although the available evidence is rather limited, models of Mmu17 trisomy emerge as very different from Mmu16 models. Behavioural results seem to suggest that the Mmu17 trisomy does not affect HPC-dependent memory. However, electrophysiological evidence reports that hippocampal plasticity is in fact altered, with the Mmu17 trisomy promoting LTP. Theoretically, abnormal plasticity mechanisms in the HPC should have an impact on HPC-dependent memory function (e.g. Morris et al., 1986). Further studies are necessary to investigate this relationship in Mmu17 trisomy models. Nevertheless, impairments in visual object recognition suggest that Mmu17 genes may alter PRH cortex function.

1.3.3. The Dp2Yey and Mmu10 models

Only one mouse line has been created to model trisomy of the Mmu10 conserved region, the Dp2Yey model. The Dp2Yey strain is trisomic entirely and exclusively for the Mmu10 conserved genetic portion (from *Prmt2* to *Pdxk*) (Yu et al., 2010b). Few genes on the Mmu10 conserved region have been implicated in memory. Nevertheless, these include the S100 calcium-binding protein B (*S100B*), a gene encoding a calcium-binding protein expressed by glial cells, and adenosine deaminase 2 (*ADAR2*), a gene encoding an enzyme responsible for the pre-mRNA editing of glutamate receptors (Block, Ahmed, Dhanasekaran, Tong, & Gardiner, 2015).

Research on the Dp2Yey model is however extremely limited. To the author's knowledge, there is currently no data on DS-like physical features or brain pathology in the

Dp2Yey, at any age. Nevertheless, one study measured the expression levels of proteins implicated in memory and synaptic plasticity in the brains of male and female adult Dp2Yey mice (Block et al., 2015). Out of 102 proteins measured, the levels of 68 proteins were altered in the male Dp2Yey brain. The highest perturbation was observed in the HPC, affecting levels of 50 proteins, the majority being overexpressed. Interestingly, female Dp2Yey mice showed the highest perturbation in the cerebellum, with a total of 62 altered proteins. Importantly, of the 102 proteins assessed, only 3 were encoded by genes trisomic in the Dp2Yey, highlighting the fact that segmental trisomies can induce considerable downstream changes in the expression of non-trisomic genes. Out of all the 102 proteins measured, only one protein was consistently altered in all brain regions and both sexes, S100B, with a 25-30% increase. S100B has been implicated in neuronal growth and AD-pathology (Block et al., 2015). Indeed, APP expression was found increased in the HPC of male Dp2Yey, in conjunction with altered expression levels of glutamate receptors (Block et al., 2015). Despite these protein perturbations, LTP induction was found to be normal in Dp2Yey hippocampal slices (Yu et al., 2010b).

Cognitive phenotypes in Dp2Yey mice were investigated only by one study. When tested on the MWM, adult Dp2Yey mice performed normally on both the visible and the hidden platform test (Yu et al., 2010b). Dp2Yey also performed similarly to euploid controls in the contextual fear conditioning task (Yu et al., 2010b). Although the available evidence is extremely scarce, findings seem to suggest that Hsa21 homologs located on Mmu10 do not affect hippocampal function in so far as changing memory processes. However, assessment in this regard has been limited and there are no published data regarding the effects of the mutation on object-recognition memory task.

1.3.4. Non-segmental models

In addition to models of segmental DS duplicating portions of the three conserved regions, mouse models carrying (near) complete Hsa21 trisomy have also been generated, in an attempt to recreate the full complexity of human DS. One of these models is the Tc1 line (O'Doherty et al., 2005). Tc1 mice carry a freely segregating copy of Hsa21 and are thus a "trans-species" model. The Hsa21 copy is, however, incomplete, with Tc1 mice trisomic for ~83% of Hsa21 genes (Lana-Elola et al., 2011). Among the not functionally triplicated genes is the *App* gene, making the Tc1 a useful model to assess the contribution of Hsa21 genes other than *App* to AD-pathology (Wiseman et al., 2018). Additionally, the Hsa21 copy is not retained by all cells, making the Tc1 a model of mosaic DS. In the brain, approximately 66% of nuclei (neuronal and glial cells) retain Hsa21 (O'Doherty et al., 2005). This suggests that phenotypes observed in Tc1 animals may be less severe relative to human DS or other mouse models, since the trisomy affects only a portion of the cells.

Despite its limitations, the Tc1 model has been widely studied. Indeed, Tc1 animals present several DS-like physical features. These include craniofacial anomalies such as a smaller mandible size, frequent cardiac malformations in embryos and suppressed immune responses (O'Doherty et al., 2005). Body weight is also significantly reduced in adult Tc1 mice (Galante et al., 2009). Analogously to DS individuals and models of Mmu16 trisomy, motor function is impaired in the Tc1, with animals displaying deficits in motor coordination and balance on different motor tasks (Duchon et al., 2011; Galante et al., 2009). Subtle abnormalities have also been noticed in the Tc1 gait pattern (Galante et al., 2009).

With regards to brain morphology, Tc1 mice exhibit some features typical of DS and some atypical features. For example, total brain volume is increased in the Tc1 (Powell et al., 2016). Total hippocampal volume is also enlarged, although some sub-regions (e.g. CA3) present reduced volume (Powell et al., 2016). In line with DS features, the Tc1 cerebellum shows reduced total volume and neuronal cell density (O'Doherty et al., 2005; Powell et al., 2016). Although neuronal cell density was found unaltered in the HPC, dendritic spine density was reduced, along with abnormal spine morphology (Witton et al., 2015). Levels of glutamate receptors were also found to be reduced in the HPC (Morice et al., 2008). Unsurprisingly, several studies have found that the *in vivo* induction of hippocampal LTP is impaired in Tc1 brains (Morice et al., 2008; O'Doherty et al., 2005; Witton et al., 2015). Interestingly, detailed investigations showed that impairments were present only shortly after LTP induction while LTP maintenance the following 24 - 48 hours was normal (Morice et al., 2008; Witton et al., 2015).

Although Tc1 mice show altered hippocampal structure and plasticity as observed in other models, the cognitive profile of Tc1 mice is atypical to some degree. In the spontaneous alternation T-maze, Tc1 mice performed no different than euploid controls, alternating significantly above chance between the two arms of the maze (O'Doherty et al., 2005). When tested on the hidden platform MWM, Tc1 animals were once again unimpaired, showing normal improvement in locating the hidden platform over the training days (Morice et al., 2008). Interestingly, memory impairments appeared in Tc1 mice when performance on the MWM was tested with a protocol assessing shorter retention intervals. In this version, animals were trained to locate the hidden platform over consecutive trials separated by brief intervals on the same day. Tc1 mice were impaired, showing delayed acquisition of the platform position and near chance preference for the target area (Duchon et al., 2011; Morice et al., 2008). MWM findings thus seem to reflect decreased early-phase LTP but intact late-phase LTP in the Tc1. Since arm choices on the spontaneous alternation T-maze test are usually separated by brief time intervals, it is surprising that Tc1 mice performed normally on this test.

Further evidence supporting a delay-dependent memory performance in Tc1 mice comes from object-recognition memory tasks. When visual object recognition memory was assessed after a 10-min delay on the NOR task, Tc1 mice were unable to discriminate between novel and familiar objects (Hall et al., 2015; Morice et al., 2008; O'Doherty et al., 2005). However, when the test phase was administered 24-h after the acquisition phase, Tc1 animals successfully recognised the novel object (Hall et al., 2016; Morice et al., 2008). One possible interpretation was that Tc1 mice might have a generalised impairment in the retention of relatively recently formed memories. However, Hall et al. (2016) demonstrated that Tc1 mice were indeed able to form memories during short time intervals, as Tc1 mice were able to recognise familiar objects occupying a previously vacant spatial location after a 10-min delay (Hall et al., 2016). This implicates that short-term memory deficits observed in the Tc1 are not pervasive but specifically affect visual object recognition. Instead, in contrast to findings on DS individuals, memory assessed after longer retention intervals seems generally spared, as Tc1 mice were also able to recognise novel OiP-associations after a 24-h delay (Hall et al., 2016).

A more recently generated mouse line, the Triple Trisomic Strain (TTS), provides a less problematic model of Hsa21 trisomy compared to the incomplete and mosaic Hsa21 trisomy of Tc1 mice (Yu et al., 2010a). Through precise Cre/loxP engineering, TTS animals are trisomic entirely and exclusively for all of the three conserved regions on Mmu16, Mmu17, and Mmu10 (Yu et al., 2010b). Although the TTS model does not allow one to segregate influences originating from distinct genetic portions, the model provides the most complete and accurate representation of Hsa21 trisomy, accounting for functional interactions between all syntenic genes.

Only limited published work is available on the TTS model. TTS animals have reduced body weight and length at young and older age (Belichenko et al., 2015; Yu et al., 2010a). Although most TTS pups have normal appearance, a small portion (~6.5%) exhibit hydrocephalus due to abnormally dilated brain ventricles (Yu et al., 2010a). These animals generally do not survive beyond 2.5 months of age. Although hydrocephalus has not been reported in other DS mouse models, the condition has a higher incidence in the DS population (Yu et al., 2010a).

Decreased hippocampal LTP was also observed in hippocampal slices of TTS animals 15-60 min after stimulation and application of GABA receptor antagonists restored normal LTP (Belichenko et al., 2015; Yu et al., 2010a). On the spontaneous alternation T-maze test, TTS mice performed significantly worse than controls, alternating only at chance levels (Belichenko et al., 2015). TTS animals also showed significantly reduced learning on the MWM and reduced freezing levels in a contextual fear conditioning task after a 24 and

48 hours retention interval (Yu et al., 2010a). Novel object recognition was also impaired after 24-h, as observed in Mmu16 trisomy models (Belichenko et al., 2015).

Overall, mouse models of complete DS recreate aberrant hippocampal function, in line with human DS and Mmu16 trisomy models. Abnormal PRH function is also implicated from the behavioural evidence reporting impairments in object recognition memory. The Tc1 model exhibits however unusual cognitive features, whereby impairments arise exclusively after short retention intervals.

Table 1.1: Overview of LTP and memory phenotypes in mouse models of DS. Downward arrows indicate decreased LTP; upward arrows indicate increased LTP; equals sign indicates normal LTP. Red crosses indicate impaired performance; green ticks indicate intact performance. For NOR task performance, different retention intervals are reported. CFC = Contextual Fear Conditioning task. SA = Spontaneous Alternation. Ts65Dn: Belichenko et al., 2007; Kleschevnikov et al., 2004; Kleschevnikov et al., 2012; Sago et al., 2000. Ts1Cje: Belichenko et al., 2007; Fernandez & Garner, 2007; Sago et al., 2000; Siarey et al., 2005. Ts1Rhr: Belichenko et al., 2009a; Olson et al., 2007. Dp1Tyb: Goodliffe et al., 2016; Jiang et al, 2015; Ngueyen et al., 2018; Souchet et al., 2019; Yu et al., 2010b; Zhang et al., 2014. Dp1Yah: Marechal et al., 2019; Pereira et al., 2009. Dp3Yey: Yu et al., 2010b. Dp2Yey: Yu et al., 2010b. Tc1: Hall et al., 2016; Morice et al., 2008; O'Doherty et al., 2005; Witton et al., 2015. TTS: Belichenko et al., 2015; Yu et al., 2010a.

Mouse line	Trisomy	LTP	MWM	CFC	T-maze SA	NOR	
						≤ 1h	24h
Ts65Dn	incomplete Mmu16	↓	✗	✗	✗	✓	✗
Ts1Cje	incomplete Mmu16	↓	✗		✗		✓
Ts1Rhr	incomplete Mmu16	↓	✓		✗	✓	✗
Dp1Tyb	complete Mmu16	↓	✗	✗	✗ ✓		✗
Dp1Yah	incomplete Mmu17	↑	✓		✗ ✓	✗	
Dp3Yey	complete Mmu17	↑	✓	✓			
Dp2Yey	complete Mmu10	=	✓	✓			
Tc1	incomplete Hsa21	↓	✓		✓	✗	✓
TTS	complete Mmu16, Mmu17, Mmu10	↓	✗	✗	✗		✗

1.4. Research aims and hypotheses

While individuals with DS are relative unimpaired in immediate non-verbal recall tests, severe memory impairments arise in delayed recall tests, concerning all sorts of material. Memory for visual objects and for visuospatial information is equally affected when tested after intervals exceeding a handful of seconds. In conjunction with aberrant hippocampal morphology, the behavioural evidence indicates abnormal HPC-function as the primary cause of LTM impairments in the DS population. The mechanisms through which over-dosage of Hsa21 genes affects hippocampal activity and memory processes, are poorly understood.

By studying the Dp1Tyb, Dp3Yey and Dp2Yey mouse models of segmental DS, the main aim of the current research was to determine the impact of over-dosage of distinct Hsa21 gene orthologous regions on recognition memory function (see chapter 3). The animals were tested on a battery of object-recognition memory tasks known to rely on a network of medial temporal lobe structures that includes the HPC and PRH cortex, in an attempt to link the trisomies to aberrant function of specific subregions. Additionally, since ageing in DS is characterised by a dramatic increase in AD-like pathology, animals were tested both at adult and advanced age, to uncover whether specific orthologous regions contributed to age-related cognitive decline. To better characterise behavioural phenotypes associated to the three trisomies and to control for possible confounding effects of motor function on memory performance, the animals also underwent the Elevated Plus Maze (EPM) test to assess anxiety and locomotor activity levels.

The secondary aim of this research was to study whether patterns of memory performance delineated with object-recognition memory tasks were associated with biochemical alterations in the HPC (chapter 4). Glutamate receptors are fundamental for the synaptic plasticity changes postulated to underpin memory function. Thus, expression of a series of glutamate receptors was measured with western blots in hippocampal synaptosomes collected from the three trisomy models.

Individuals with DS and mouse models of DS report memory impairments that depend on the retention interval and that implicate aberrant function of both the HPC and the PRH cortex. Based on the presence of known relevant genes and on previous studies on mouse models of the Mmu16, Mmu17 and Mmu10 trisomy, the three mouse lines were expected to reproduce these impairments in object-recognition memory tasks, revealing trisomy-dependent memory profiles. This thesis tested the hypothesis that the Mmu16 trisomy would be associated with hippocampal dysfunction, the Mmu17 trisomy with PRH cortex dysfunction and the Mmu16 and Mmu10 trisomies with age-related cognitive decline. Additionally, impairments observed in HPC-dependent memory tasks – OiP, TOr, Loc – were expected to be associated with altered levels of glutamate receptors in the HPC. More

detailed hypotheses on each mouse line will be presented in the experimental chapters 3 and 4.

In comparison to less recently generated DS mouse models, the Dp1Tyb, Dp3Yey and Dp2Yey provide the most accurate representation of the Mmu16, Mmu17 and Mmu10 trisomy. A comprehensive memory profile of the three models has never been carried out before and only very limited research is available concerning the expression of glutamate receptors. The impact of ageing on behavioural and biochemical phenotypes has also never been assessed before in these models. The findings of this thesis are thus anticipated to contribute to the understanding of the complex genotype-phenotype relationship underlying memory impairments in DS and more generally, to the understanding of the neural substrates of recognition memory.

Chapter 2: Methods

Overview

Cohorts of Dp1Tyb, Dp3Yey and Dp2Yey animals were tested on a battery of object-recognition memory tasks and on the elevated plus maze test. Hippocampal and frontal cortex samples were subsequently collected for biochemical analyses assessing expression of glutamate receptors in synaptosome preparations. Information on the cohorts, general procedures, materials and statistical analyses employed in the behavioural and biochemical assays is described in this chapter. Variations from the protocols are described in the specific experimental chapters 3 and 4.

2.1. Animal subjects

All animals were genetically engineered at the Francis Crick Institute (Mill Hill, UK) and bred from the mating with C57BL/6JNIMR. At approximately 3 months of age, the animals were sent to Cardiff University (Cardiff, UK), where all experiments took place. Transgenic animals carried an exact duplication of one of the three Hsa21 orthologous regions on Mmu 16, 17 or 10 (see fig.1.1). Dp1Tyb animals carried a duplication of Mmu16 orthologs (*Lipi* - *Zbtb21*), Dp3Yey animals of Mmu17 orthologs (*Abcg1* - *Rrp1b*) and Dp2Yey animals of Mmu10 orthologs (*Prmt2* - *Pdxk*). Detailed information on the generation of the mouse lines is provided in the following section.

Cohorts

All animals were male. To determine the impact of ageing in the three mutations, cohorts of different age were used (young: 4 months old; adult: 8-12 months old; aged: 20 months old). All cohorts consisted of a roughly equal number of age-matched wildtype (WT) and transgenic (TG) animals. Table 2.1 reports a summary of the tested cohorts.

Housing conditions

The animals were housed in opaque plastic cages (L 48 cm x W 15 cm x H 13 cm) and held in a purpose built holding room with a 12-h light/dark cycle. The room temperature was maintained at a stable 21 ± 2 °C with humidity levels of 60 ± 10%. All cages were lined with sawdust bedding and provided with two cardboard tunnels, a wooden chew stick and cotton for nesting. The animals were housed in groups of 2-5 per cage and had *ad libitum* access to water and grain-based food pellets.

Body weight

The animals were weighed weekly and average body weights are shown in table 2.1. Body weight was consistently reduced in Dp1Tyb mice, deteriorating with ageing. Independent samples Student's t-tests (section 2.2.3 for details on statistical methods) found that weight differences were not significant at 4 months of age ($t_{(21)}$=1.735; p=0.097), but at 8-12 months ($t_{(21)}$=2.339; p=0.029) and at 20 months ($t_{(14)}$=4.189; p<0.001) Dp1Tyb weighed significantly less compared to age-matched wildtypes. No statistically significant weight difference was observed in the Dp3Yey or Dp2Yey cohorts, at any age (data not shown).

Health

Health and wellbeing of the animals were checked weekly along with cage changes. Throughout the housing period, no increase in mortality rates or incidence of physical conditions was observed for trisomic animals of either the three mouse lines.

Ethics

All experiments were conducted in accordance with the Animals Scientific Procedures Act (1986) of the UK and the European Union directive 2010/63/EU. Previous studies from our laboratory indicated that a sample size of 10-12 animals per genotype provided sufficient statistical power while minimising the use of animals and balancing costs.

Table 2.1: Sample size and average weight of the cohorts. [a] denotes significant group difference at $p<0.05$; [b] denotes significant group difference at $p<0.001$.

		4 months			8-12 months			20 months		
	cohort	**WT**	**TG**	**total**	**WT**	**TG**	**total**	**WT**	**TG**	**total**
Dp1Tyb	1				11 (35g)[a]	12 (32g)[a]	23	9 (41g)[b]	7 (33g)[b]	17
	2	11 (31g)	12 (29g)	23						
Dp3Yey	1				12 (37g)	12 (38g)	24			
	2							9 (36g)	12 (37g)	21
Dp2Yey	1				12 (37g)	12 (35g)	24			
	2							9 (38g)	12 (40g)	21

2.1.1. Genetic engineering of the mouse lines

For all three mouse lines, embryonic stem cells (ES) carrying a duplication of one of the three Hsa21 orthologous regions were generated via Cre/loxP engineering. Cre recombinase is an enzyme that recognises loxP sites and recombines genes flanked within loxP sites. Vectors targeting specific gene sequences were transfected to ES cells to insert loxP sites into the endpoints of the respective orthologous region on Mmu16, 17 or 10. Detailed information on the vectors used for each mouse line is reported below. A Cre-expression vector was then transfected into targeted ES cells to induce recombination and thus duplication of the given genetic portion labelled within the loxP sites. The duplication was then confirmed by Southern blot analysis. Successfully recombined ES cells were injected into blastocysts isolated from female C57BL/6J to generate chimeric mice. Chimeric mice were then bred with C57BL/6J to produce a colony of the respective mouse line, with TG animals carrying the genetic duplication. Weaning took place at 4-5 weeks of age. All animals used in this research were backcrossed for at least 5 generations.

Dp1Tyb

Cre-mediated Mmu16 recombination between loxP sites proximal to Lipi and distal to Zbtb21 injecting the MHPP352i17-targeting and the MHPN352i16-targeting vector respectively, in HM-1 mouse ES cells. The recombination duplicated a 23 Mb region syntenic to Hsa21 from q 11.2 to q22.3, corresponding to ~115 genes. The average litter size was 4, with a 30% transmission rate of the mutation. Increased mortality was observed prior to weaning, mainly due to hydrocephalous.

Dp3Yey

Cre-mediated Mmu17 recombination between loxP sites proximal to Abcg1 and distal to Rrp1b injecting the pTV(17)1EP1-targeting and the pTV(17)1EP2-targeting vector respectively, in AB2.2 mouse ES cells. The recombination duplicated a 1.1 Mb region syntenic to the proximal part of q22.3 on Hsa21, corresponding to ~19 genes. The average litter size was 6-8, with a 50% transmission rate of the mutation.

Dp2Yey

Cre-mediated Mmu10 recombination between loxP sites proximal to Prmt2 and distal to Pdxk injecting the pTV(10)1EP1-targeting and the pTV(10)1EP2-targeting vector respectively, in AB2.2 mouse ES cells. The recombination duplicated a 2.3 Mb region syntenic to the distal part of q22.3 on Hsa21, corresponding to ~41 genes. The average litter size was 6-8, with a 50% transmission rate of the mutation.

2.1.1.1. Genotyping

The colonies were genotyped by the molecular diagnostics company Transnetyx (Cordova, Tennessee, USA) using a robotic, fully automated genotyping system. Real-time quantitative polymerase chain reaction (real-time qPCR) was used to determine whether animals were transgenic or wildtype. In real-time qPCR, lysed samples are subjected to repeated heating and cooling cycles to induce a polymerase to synthesise new DNA for a region of interest labelled by oligonucleotide primers bound to specific genetic sequences. DNA synthesis leads to the activation of a fluorescent reporter molecule and fluorescence intensity is then used to quantify the accumulation of newly synthesised target-DNA in a given sample. The amount of newly synthesised target-DNA is proportional to the amount of target-DNA present in the sample before the start of the PCR. Real-time qPCR monitors in real time the amount of target-DNA as PCR cycles are carried out.

Ear biopsies were collected at the Francis Crick Institute (Mill Hill, UK) and then shipped to Transnetyx (Cambridge, UK) in a sealed well plate. Samples were incubated into a caustic lysing buffer (NaOH) for two hours at 55°C to extract DNA and then neutralised in a neutralising buffer. DNA was isolated with a magnetic beads-based nucleic acid purification. Lysed sample solutions were combined with MagneSil paramagnetic particles (Promega) to capture and isolate the extracted DNA. Sample solutions were then washed with EtOH and DNA was eluted with dH2O. Applied Biosystems custom TaqMan assays (ThermoFisher) were designed to test affinity to the three genetic mutations. The primer sequences used in each TaqMan assay are listed in table 2.2. For each mouse line, a specific PCR mastermix solution containing primers (900nM) and a TaqMan probe bound to a fluorescent dye label (250nM) was added to the isolated DNA. The well plate was then loaded onto a Viia7 system (ThermoFisher) and the PCR process initiated. Firstly, sample solutions were subjected to a single cycle of initial DNA denaturation (2 minutes at 50°C and 10 minutes at 95°C). This was followed by a cycle consisting of 15 seconds at 95°C for further denaturation and 1 minute at 60°C for primers' annealing and DNA extension by Taq polymerase. This cycle was repeated 40 times. An automated results review system assessed fluorescence intensity over number of PCR cycles and determined whether samples were positive or negative for a given TaqMan assay. Figure 2.1 shows an example of a real-time qPCR plot obtained from probing Dp3Yey samples.

Table 2.2: Forward and reverse primer sequences for TaqMan assays. These sequences were used to genotype the three mouse lines.

	Target	Forward primer	Reverse primer
Dp1Tyb	Mmu16 - 3'	CGGGCCTCTTCGCTATTACG	CTCTCTCCCTGAGTGCATTCTC
	Mmu16 - 5'	CCCTAAGTCCTTGTCCCTCACA	GCAGTTGTTTAAACTTCTAGAGAATGAGTTC
Dp3Yey	Mmu17	AGCATCAGGGACTCTGGAAGT	CGTTGGCCGATTCATTAATGCA
Dp2Yey	Mmu10	CGGGCCTCTTCGCTATTACG	ACTGCTGCCTTCTGTTTTGGTA

Figure 2.1: Real-time qPCR plot of Dp3Yey samples. The plot shows fluorescence intensity (y-axis) over number of PCR cycles (x-axis), where each line represents a different sample. Lines that peaked and reached plateau at earlier PCR cycles were classified as positive for the Dp3Yey TaqMan assay (TG animals) while lines that peaked only at later PCR cycles were classified as negative (WT animals).

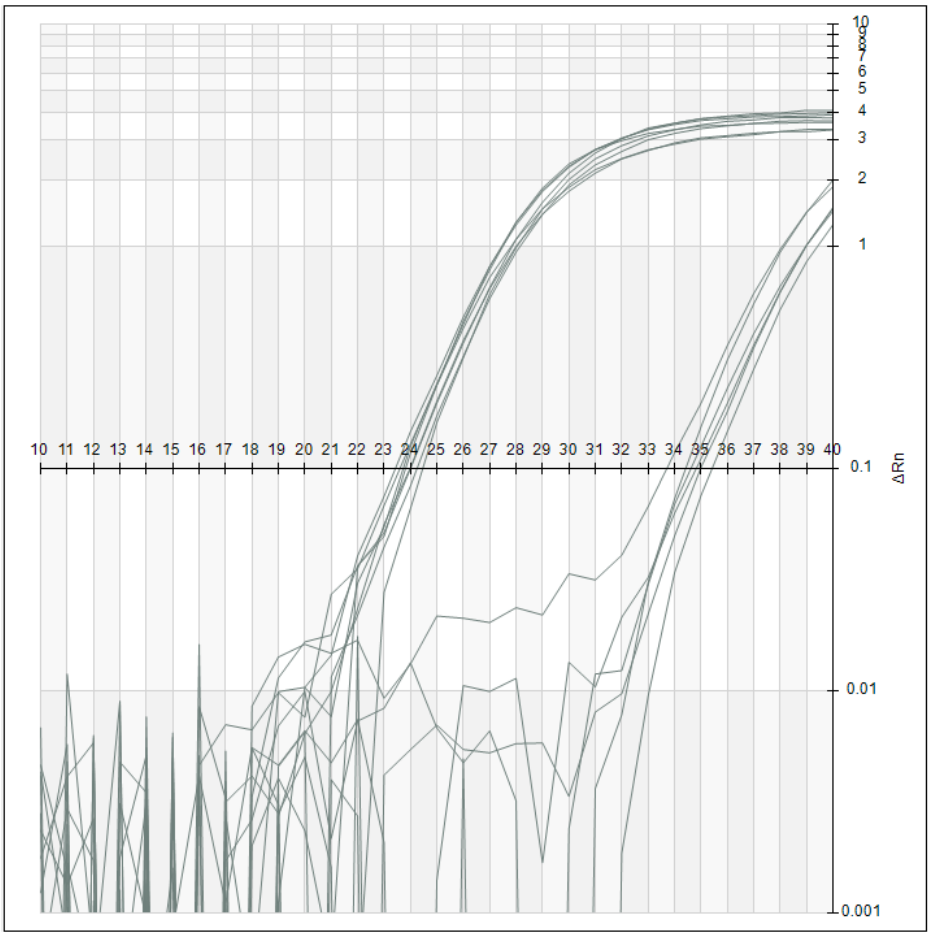

2.2. Behavioural assays

The main aim of this research was to assess learning and memory processes in the three models of segmental Down Syndrome. All animals underwent behavioural assays to test memory, namely different versions of object-recognition memory tasks (2.2.1). As willingness to explore novel environments is a key element of these cognitive tasks, all animals also underwent the Elevated plus maze test of anxiety (2.2.2). For each assay, identification numbers were generated and the experimenter remained blind to genotype throughout the entire experimental period.

2.2.1. Object-recognition memory tasks

All cohorts underwent memory tasks using objects to assess different features of recognition memory that rely on a well-characterised circuit involving the perirhinal cortex, hippocampus and prefrontal cortex. The tasks were also designed to test short-term and long-term memory for object identity, object-in-place associations, object location and temporal order associations. An overview of the different types of object-recognition memory tasks used is provided in figure 2.4. Briefly, the animal was placed in an arena containing different objects and after a relatively short or a longer retention interval, the mouse was re-placed in the same arena now containing familiar and novel object arrays. Contact times with the objects were recorded and intact memory processes were predicted to produce higher contact times with target objects.

2.2.1.1. Materials

Object-recognition memory tasks were run in a 60 cm (L) x 60 cm (W) x 40 cm (H) open field arena made of transparent Plexiglas (fig. 2.2a). The floor of the arena was white and the exterior walls were covered with white paper. Distinct high-contrast visual cues were taped to the walls of the test room and were visible from within the arena, serving as distal, extramaze reference points (fig. 2.2b). The objects used in the tasks were everyday objects of different shape, colours and materials. Black or white adhesive tape was attached to some objects to create high-contrast distinctive patterns and maximise differences between objects (fig. 2.2c). Common features of the selected objects were that they were of sufficient weight not to be displaced by the animals and sufficient height to prevent climbing. The objects were positioned 10cm away from the corners of the arena and always in the same orientation. The objects and the arena were cleaned with 70% ethanol wipes before and between each experimental phase to eliminate odour cues. The experiments were recorded with an overhead camera, a Philips DVD-R recorder and an Hitachi

television. Two Karrimor run stopwatches were used to record contact times with the objects.

Figure 2.2: Materials used in object-recognition memory tasks. a) Plexiglas arena. b) Example of distal spatial cues taped to the walls of the test room. c) Example of objects used.

a)

b)

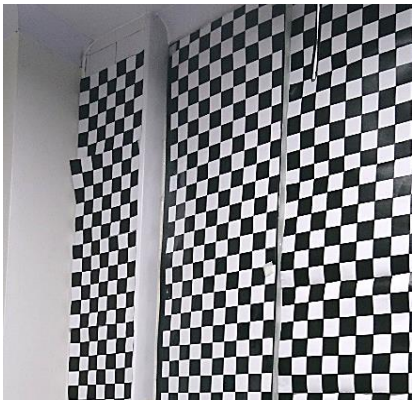

c)

2.2.1.2. Procedure

Habituation

Before the experimental period, the animals were handled in the test room by the experimenter for approximately 5 minutes, for five consecutive days. Two habituation sessions of 10 minutes were then carried out with each animal on two separate days. In the first session, the animal was placed in the empty arena while in the second session, an object was located in the centre of the arena. The aim of the two sessions was to habituate the animal to the new environment and to the presence of objects, respectively. In the second session, contact times with the object were recorded and used as an indicative measure to determine whether the animal was ready to start the experiment. Animals with low contact times (< 7 sec) were given a further habituation session with the object the following day.

Design

All object-recognition memory tasks consisted of two sample phases followed by a test phase (fig. 2.4). Each phase lasted 10 minutes. In all phases, the mouse was placed in the centre of the arena and allowed to freely explore the objects in the arena. In between the phases, the animal was returned to its home cage for a predetermined time interval. The delay between the last sample phase and the test phase was varied to assess different memory spans, testing shorter or longer retention intervals. In the test phase, a feature of the object array was changed (e.g. a new object or an object in a new location), which resulted in familiar and novel target objects.

In tasks where more than one delay between sample and test phases was used, the animals underwent the two delays in counterbalanced order. Testing times were also counterbalanced in respect to morning and afternoon experimental sessions. Position of the objects in the arena and selection of novel objects were counterbalanced amongst the mice, employing as many as possible different setups (fig. 2.3). Testing with different delays or tasks was separated by at least a 24-hour rest period in the home cage.

The animals were run by an experimenter who was blind to the condition of the animals. The mice were run in pairs consisting of a WT and a TG animal. The experimenter was not blind in respect to which objects were novel and which familiar targets in the test phase. Table 2.3 shows an example of how the pairs were allocated to delays and testing times.

Scoring

Contact times with the objects during the sample phases were scored manually with one stopwatch, yielding one score for all objects in the arena. Contact times during the test phase were scored manually with two stopwatches, yielding one score for all familiar objects

and one score for all novel objects. Contact behaviour with the objects was defined as the animal exploring the object (touching the object with the forepaws and/or active, inquisitive sniffing) from a distance not greater than 1cm and facing the object. Passive sitting or grooming in front of the object were not considered explorative behaviour and were not scored. Similarly, attempts to climb onto an object or to chew parts of an object were not scored. Subjects with a total contact time < 3 seconds in the sample phase or test phase of an object-recognition memory task were considered to be exploring the objects insufficiently and were excluded from the analysis of that task.

Mean contact times with the objects during sample and test phases were calculated. The data were further divided to obtain mean contact times with one object in sample phases (total object contact time divided by number of objects) and test phases (total contact time with familiar resp. target objects divided by number of familiar resp. target objects). The main output of object-recognition memory tasks was preference for novel over the familiar targets. To obtain a preference for the novel target independent of overall contact time during the test phase, a discrimination ratio of contact with novel objects over total object contact time was calculated. This resulted in a ratio ranging from 0 to 1, where ratios over 0.5 indicated a preference for novel objects and suggested intact recognition memory processes. In general, discrimination ratios were calculated as follows:

$$\frac{\frac{contact\ time\ with\ target\ objects}{number\ of\ target\ objects}}{\frac{contact\ time\ with\ target\ objects}{number\ of\ target\ objects} + \frac{contact\ time\ with\ familiar\ objects}{number\ of\ familiar\ objects}}$$

Table 2.3: Counterbalancing of testing time and delay. Animals were run blindly, in pairs of one WT and one TG animal.

Pair	Blind ID	Genotype	Delay 1	Testing time	Delay 2	Time of day
1	1	WT	10 min	AM	24 h	PM
	2	TG	10 min	AM	24 h	PM
2	3	TG	10 min	PM	24 h	AM
	4	WT	10 min	PM	24 h	AM
3	5	TG	24 h	AM	10 min	PM
	6	WT	24 h	AM	10 min	PM
4	7	WT	24 h	PM	10 min	AM
	8	TG	24 h	PM	10 min	AM

Figure 2.3: Counterbalancing of object array. Different symbols represent different objects. The position of the objects was continuously rotated clockwise and the selection of the novel object (circled in red) was continuously alternated. An analogous counterbalancing logic was used in all types of object-recognition memory tasks.

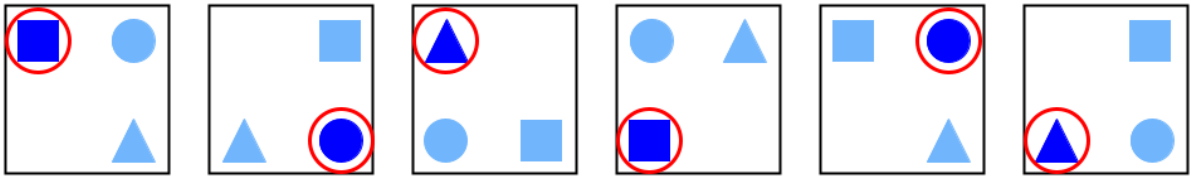

2.2.1.3. Tasks

To assess different features of recognition memory, the Novel object recognition task, the Object-in-Place task, the Object location task and the Temporal order task were used (fig. 2.4). The number and type of object-recognition memory tasks ran with a given cohort was contingent upon intact memory for object identity as tested with the Novel object recognition task. Successful performance in this task was a requirement for further testing with the Object-in-place task and Temporal order task but not the Object Location task, as intact processing of object-information is essential in the first two, but not the latter task (Barker & Warburton, 2011b).

Novel Object Recognition task (NOR)

Three different objects were used in two identical 10-min sample phases, 10 minutes apart. In the 10-min test phase, one of the objects was replaced with a novel object. The side on which the novel object was presented was counterbalanced. The animal was expected to discriminate between objects encountered in the sample phases and the novel object, indicating intact memory for object identity (fig. 2.4a).

Object-in-Place task (OiP)

Three different objects were used in two identical sample phases as described above, 10 minutes apart. The same objects were used in the test phase, however two of the objects exchanged place, in counterbalanced fashion. The animal was expected to discriminate between stationary and displaced objects, indicating intact memory for object-in-place associations (fig. 2.4b). As this task utilised different objects, it depended on intact memory for object identity (Barker & Warburton, 2011b).

Object Location task (Loc)

Three identical objects were used in two identical sample phases as described above, 10 minutes apart. The same objects were used in the test phase, where one object moved to a previously vacant location, in counterbalanced fashion. The animal was expected to discriminate between stationary and displaced objects, indicating intact recognition memory for spatial locations (fig. 2.4c). As this task utilised identical objects, it did not depend on memory for object identity (Barker & Warburton, 2011b).

Temporal order task (TOr)

Two different pairs of identical objects were used in two sample phases, which were separated by one hour. In the test phase, one object from each pair was presented. The animal was expected to discriminate between the more recently and the less recently presented object, indicating intact memory for temporal order associations (fig. 2.4d). As this task utilised different objects, it depended on intact memory for object identity (Barker & Warburton, 2011b). The order in which the pairs of objects were presented in the sample phases was counterbalanced.

Figure 2.4: Design of the object-recognition memory tasks. a) Novel Object Recognition task. b) Object-in-Place task. c) Object Location task. d) Temporal Order task. Different symbols represent different objects and novel objects are in dark blue. The delay between sample and test phase was varied depending on the experiment. S = sample phase; T = test phase.

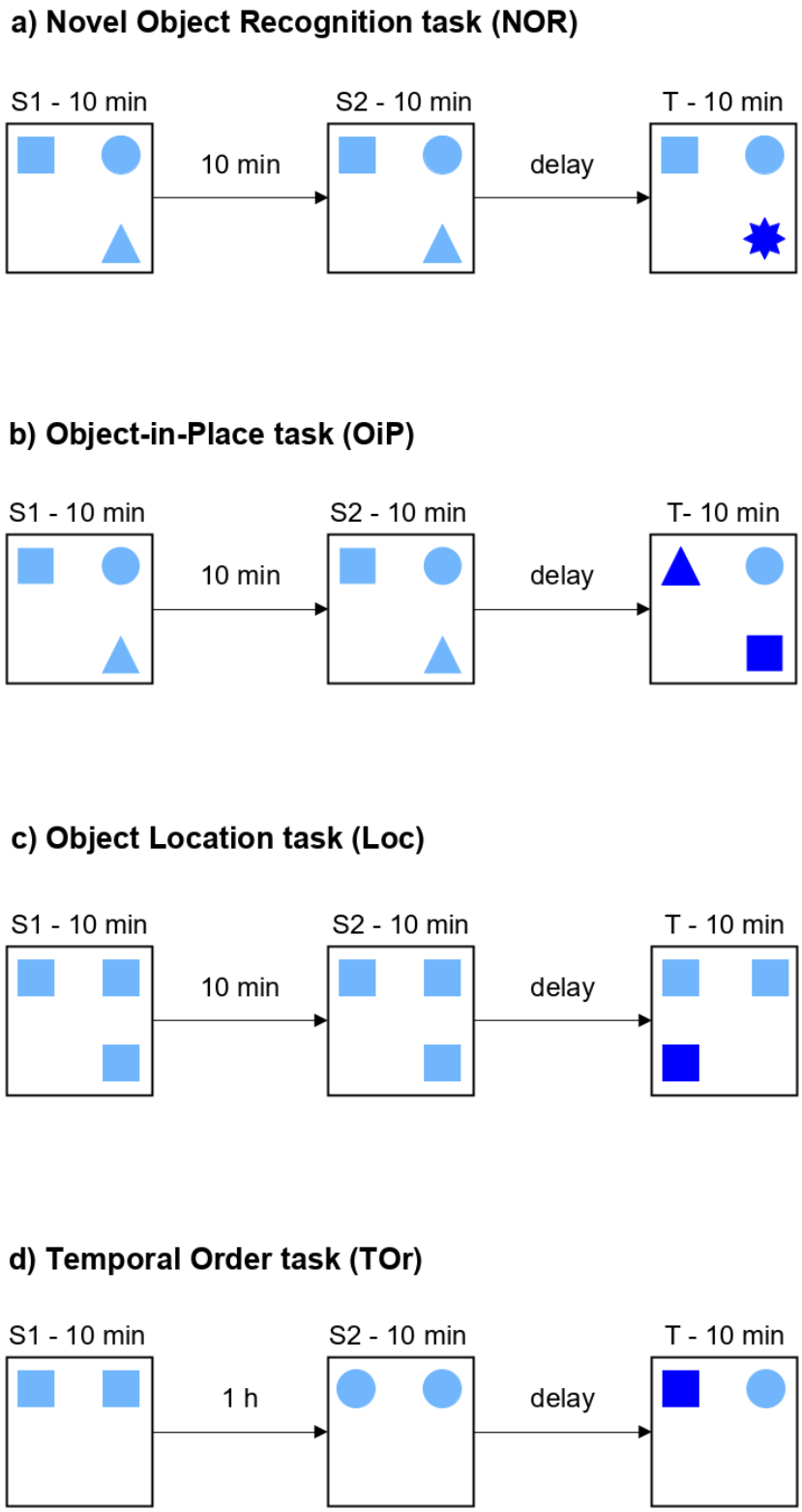

2.2.2. Elevated plus maze test

To determine the impact of the three genetic mutations on affective phenotypes potentially relevant to memory tasks that rely on exploration of novelty, cohorts of the Dp1Tyb, Dp3Yey and Dp2Yey were tested with the Elevated Plus Maze to measure anxiety. Briefly, the animal was placed in a plus-shaped maze made of two enclosed arms and two open arms. The amount of time spent in closed versus open arms was used to determine anxiety.

2.2.2.1. Materials

The test was run in an 86 cm (L) x 86 cm (W) x 74 cm (H) x 6 cm (internal W) plus-shaped wooden maze (fig. 2.5). The plus-shape consisted of two closed arms and two open arms, with a small, neutral, centre area (6x6 cm^2). The closed arms were enclosed within 17 cm-high black walls, while the open arms were surrounded by a 1 cm-high rim of transparent Plexiglas. The floor of the maze was white. The maze was cleaned with 70% ethanol wipes before each tested animal to eliminate odour cues. The experiments were recorded with an overhead camera connected to a Sony VAIO laptop using the open-source Open Broadcaster Software (OBS Studio 20.1.3). The videos were recorded in .avi format (640x480, 30 fps).

Figure 2.5: Elevated plus maze. Closed arms were safe and sheltered in contrast to the exposed open arms of the maze.

2.2.2.2. Procedure

Habituation

Since the Elevated Plus Maze test assessed anxiety levels, the animals were not habituated, either to the test room nor to the maze. The animals were nonetheless already accustomed to being handled by the experimenter due to previous behavioural experiments.

Design

Each animal underwent one trial on the Elevated Plus Maze. The animal was placed in the centre of the maze and explored the area for 5 minutes. Testing was carried out across the day and the groups (WT and TG) were distributed equally across morning and afternoon sessions.

Scoring with EthoVision XT 13

The explorative behaviour of the animal in the maze was scored with the tracking software Ethovision XT 13 (Noldus Information Technology). The recorded video clips were fed to EthoVision and the animal's trail in the maze was tracked throughout the 5-minute trial. Firstly, an image of the maze was used to calibrate the centimetres-to-pixels conversion and to divide the maze into three different zones: closed arms, open arms, and centre. Automated settings were used to recognise and track the animal within the maze. This yielded three different tracked points: nose-point, body-centre-point, and tail-base-point. Zone entry was defined as all three points being located within a given zone. To correct for involuntary movements (e.g. tail jitter) a zone exit threshold of 1.50 cm was used for all three zones. The precision of the tracking was verified by hand for each video clip and tracking errors were corrected manually. Figure 2.6 shows a graphical representation of the setup.

The tracking generated time scores for each zone. The main output of the Elevated Plus Maze was the amount of time spent in closed and open arms. The following mean scores were also generated with EthoVision: arm entry (frequency and latency to first entry), distance walked in the arms [cm] (body-center-point), velocity in the arms [cm/sec] (body-center-point). Head dipping behaviour in the open arms was scored manually with EthoVision (frequency and latency to first dip). Head dipping represented risk assessing behaviour (Cruz, Frei, & Graeff, 1994) and was defined as a clear downward movement of the head towards the floor. The centre of the maze was considered as a neutral, transition zone and behaviour in the centre was not scored. Heat maps of the maze were also generated by merging mean time scores of WT and TG animals in each zone.

Figure 2.6: Elevated plus maze in EthoVision. The maze was divided into three zones: centre (blue), closed arms (orange), open arms (pink). Three points were tracked for each animal: nose-point (yellow triangle), body-center-point (red dot), tail-base-point (blue square).

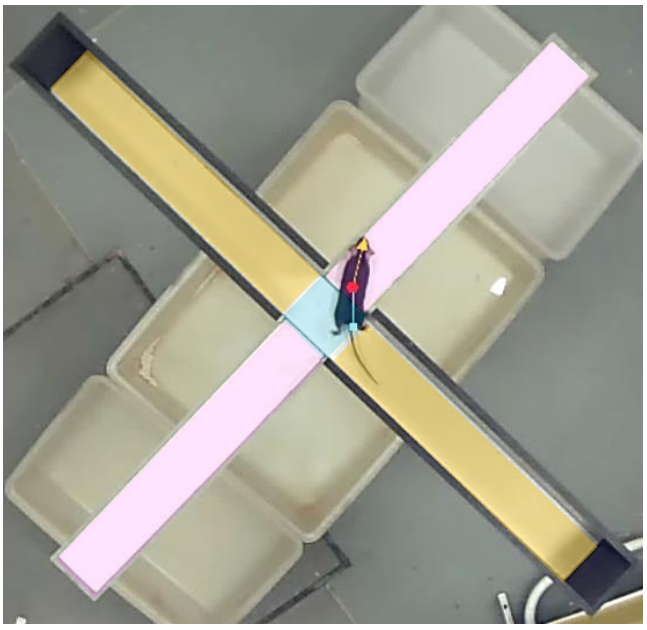

2.2.3. Data analyses

The data were mainly analysed using parametric statistics. Under certain circumstances, the data were further analysed with Bayesian statistical analyses for the reasons outlined below.

For a given dataset, frequentist statistical inference generates a test value which is compared against a critical value representing the theoretical sampling distribution of the test value if the null hypothesis were true. If the test value is more extreme than the critical value, the null hypothesis (H0) is rejected and the alternative hypothesis (H1) is accepted. The result is said to be significant at a predetermined type I error (α-level). This mechanism implies that H0 can only be rejected but never verified, one of the major shortcomings of frequentist statistics. For the cognitive processes investigated in this study, the interpretation of non-significant results was however fundamental, as lack of significant differences between the WT and TG group suggests intact, normal memory processes.

Bayesian factor analysis doesn't rely on significance thresholds but directly reports the strength of the evidence in favour of H0 (B_{01}) and H1 (B_{10}) respectively. The prior distributions of H0 and H1 are compared to the observed dataset (posterior distribution) to calculate its probability under each hypothesis. These probabilities are then used to generate Bayesian factors. Larger Bayesian factors indicate more evidence in favour of a given hypothesis, meaning that the hypothesis postulates the observed data as more probable. Since Bayesian statistics allows one to quantify evidence in favour of H0, non-significant results that carried theoretical relevance were further analysed with Bayesian analyses, making the absence of group differences a testable hypothesis. Detailed information on the data analyses is provided below.

Frequentist statistical analyses

Statistical analyses were conducted using IBM SPSS Statistics 23. For all variables, normal distribution was evaluated with Shapiro-Wilk tests ($p>0.05$), skewness, kurtosis, histograms, and Q-Q plots. Data were checked for outliers by evaluating boxplots (values outside the lower and the upper quartile by 3 times the interquartile range) and standard z-scores, whereby z-scores smaller / greater than ± 3 were labelled as outliers. This is a widely accepted criterion, although it has been criticised (Iglewicz & Hoaglin, 1993). Homogeneity of variance was tested with Levene's tests ($p>0.05$). Data that met the assumptions of parametric statistics were analysed with repeated measures two-way analyses of variance (ANOVAs). If the assumption of sphericity was violated (<0.05), then Greenhouse-Geisser corrected results were reported. Interactions were analysed with LSD adjusted tests of simple main effects. If tests of simple main effects violated Levene's test of homogeneity of variance ($p<0.05$), results were compared with Welch's tests. Where

appropriate, independent samples Student t-tests were used to directly compare performance of WT and TG animals. Unless otherwise specified, all results assume equal variances. Data that violated the assumptions of parametric statistics were analysed with analogous non-parametric tests, that is with Mann-Whitney U-tests and Krusal Wallis tests. For all the analyses the α-level was set at $p<0.05$.

Bayesian statistical analyses

Bayesian statistical analyses were conducted using the open-source software JASP 0.9.0.1. Bayesian analysis do not require the data to meet any particular assumption, as the analysis purely calculates the probability that H0 and H1 attribute to the observed data. For all analyses, the strength of the evidence in favour of H0 (B_{01}) was assessed, where factors > 1 indicated more evidence for B_{01} than B_{10} ($B_{01} = 1/B_{10}$). The data were analysed with Bayesian independent samples Student t-tests, whereby the robustness of Bayes factors was evaluated by testing prior distributions of different widths. As the width of the prior distribution did not notably affect the size of Bayes factors, the default prior distribution (Cauchy scale =0.707) was used in all tests.

2.3. Biochemical assays

Brain tissue was collected to examine the effects of the three mutations on brain biochemistry and to possibly uncover biochemical mechanisms underlying behavioural phenotypes. Western blots were used to quantify the expression of different glutamate receptors in synaptosomal preparations.

2.3.1. Brain samples

Brain tissue was collected at rest. The animals were sacrificed by cervical dislocation and the brains were immediately removed. The left hemisphere was dissected to remove hippocampus and frontal cortex. The frontal cortex dissection was defined as the most frontal third of the cortex (~4mm). The samples were immediately snap frozen on liquid nitrogen and stored at -80°C until further processing.

For the Dp1Tyb, brain samples were collected from a single cohort at 20 months of age. For the Dp3Yey and the Dp2Yey, brain samples were collected from two different cohorts, one at 14 months and the other at 21-22 months of age.

2.3.2. Synaptosome extraction

A Synaptic Protein Extraction Reagent (Syn-PER) (ThermoFisher Scientific) was used to extract proteins and fractionate brain samples into purified synaptosomal and cytosolic fractions. Syn-PER reagent was added to each sample at 10µL/1mg of tissue together with a protease inhibitor cocktail (Set III, 1:100, Merck Millipore) and a phosphatase inhibitor cocktail (Set III, 1:50, Merck Millipore). The tissue was then homogenised manually with a tissue grinder, for approximately 40 seconds, to obtain a homogeneous solution without solid residues. The samples were then centrifuged for 10 minutes at 1200 × *g* in a refrigerated microcentrifuge at 4°C. The supernatant was carefully removed and the insoluble pellet was discarded. The supernatant was further centrifuged for 30 minutes at 4°C at 1300 × *g*. This resulted in a supernatant containing the cytosolic fraction and an insoluble pellet containing the synaptosome fraction of neuronal cells. The supernatant was collected, while the insoluble pellet was re-suspended into Syn-PER at 1.5µL/1mg of original tissue weight. Both fractions were stored at -20°C until further processing.

2.3.2.1. Bicinchoninic Acid Assay

A Bicinchoninic Acid Assay (BCA) kit (ThermoFisher Scientific) was used to quantify the protein concentration of synaptosome samples. Standards were prepared with 1:2 serial dilutions of Bovine Serum Albumin (BSA) (Pierce, ThermoFisher Scientific), resulting in protein concentrations from 2 to 0.008mg/mL and a dH2O blank control. A 96-well plate

was used to load in duplicate the BSA standards, blank control, sample blank (SynPER plus protease and phosphatase inhibitor cocktails) and samples. For standards and blank control, 25µL were loaded while 1µL was loaded for sample blank and samples. To each well, 200µL of BCA working reagent (50 parts of Reagent A and 1 part of Reagent B) were added. The plate was mixed on a plate shaker for 30 seconds and incubated at 37°C for 30 minutes. The light absorbance was read with a spectrophotometer at 540nm. Microsoft Excel 2013 was used to generate a standard curve based on the absorbance of the BSA standards and to then calculate the protein concentration of the samples.

2.3.3. Western blotting

Western blots were used to quantify the expression of proteins in synaptosome samples of the hippocampus or frontal cortex. The samples were diluted at 1:3 with 3x sample buffer (6.3mM TrisBase, 0.8% [w/v] SDS (BioRad), 20% [v/v] Glycerol, 10% [v/v] β-mercaptoethanol, 2% [v/v] bromophenol blue, dH2O to 50ml) and reduced for 40 minutes at 90°C prior to the first use. For subsequent uses, samples were thawed for 5 minutes at 70°C. The samples were loaded onto a 7.5% polyacrylamide gel (dH2O, 2.5% [v/v] acrylamide (BioRad), 1.25% [v/v] Tris HCl, 0.1% [v/v] SDS, 0.05% [v/v] APS, 0.005% [v/v] TEMED (Sigma Aldrich)) and sodium dodecyl sulfate-polyacrylamide gel electrophoresis (SDS-PAGE) was used to separate proteins based on their molecular weight. A protein concentration of 20µg was loaded for the samples and 10µl were loaded for the molecular weight marker (Precision Plus Protein All Blue Standards, BioRad). The electrophoresis was first run for 30 minutes at 40mV and then at 140mV for approximately 90 minutes, in running buffer (25mM Tris base, 190mM glycine, 0.05% [v/v] SDS, pH 8.3). The gel was blotted onto a 0.45µm nitrocellulose electrode membrane (GE Healthcare Life Sciences) soaked in semi-dry blotting buffer (42.9mM Tris base, 38.9mM glycine, 0.038% SDS, in MeOH) for 1 hour at 39mA. After the blotting, the membrane was washed for 30 seconds in Tris-buffered saline with Tween (TBS-T) (2mM Tris base, 15 mM NaCl, 0.1% Tween-20 (Fisher), pH 7.5), blocked for 1 hour at room temperature in 5% blotto (5% [w/v] non-fat milk powder (Tesco) in TBS-T) and then washed again for 30 seconds in TBS-T. The membrane was cut into different strips, allowing simultaneous incubation into different primary antibodies. The membranes were incubated into primary antibodies in 1% blotto either overnight at 4°C or for 2 hours at room temperature, on a roller. Optimal dilutions for each antibody were determined beforehand and are reported in table 2.4. After primary antibody incubation, membranes were washed in TBS-T three times for 10 minutes each and incubated into horseradish peroxidase (HRP)-conjugated secondary antibodies (rabbit 1:15000, Vector Laboratories; or mouse 1:15000, (Vector Laboratories) in 1% blotto for 2 hours (90 minutes for β-actin) at room temperature, on a roller. The membranes were then

washed again three times for 10 minutes each in TBS-T. Finally, the membranes were incubated for 5 minutes in a luminol-based enhanced chemiluminescence HRP substrate (SuperSignal West dura Extended duration substrate (ThermoFisher Scientific) or Pierce ECL western blotting substrate (ThermoFisher Scientific)) and then exposed in succession to an automated chemiluminescence machine (G:BOX Chemi XX6, Syngene) to detect immunoreactions. For further probing, the membranes were washed in TBS-T for 30 seconds and incubated for 5 minutes into a stripping buffer (Restore Western blot stripping buffer; ThermoFisher Scientific) prior to repeating the antibody incubation procedure described above.

Table 2.4: List of primary antibodies. Target, species, dilution and origin of the antibodies are reported. All antibodies were polyclonal except for monoclonal β-actin.

Antibody	Target	Species	Dilution	Origin
GluA1	AMPA glutamate receptor 1	rabbit	1:2500	abcam
pGluA1(S845)	GluA1 receptor phosphorylated at ser845	rabbit	1:2500	abcam
GluK5	Kainate glutamate receptor 5	rabbit	1:500	Novus Biologicals
GluN1	NMDA glutamate receptor 1	mouse	1:500	BD Biosciences
GluN2A	NMDA glutamate receptor 2A	rabbit	1:1000	Merck Millipore
GluN2B	NMDA glutamate receptor 2B	rabbit	1:500	Merck Millipore
pGluN2B(Y1472)	GluN2B receptor phosphorylated at tyr1472	rabbit	1:750	Merck Millipore
PSD95	Postsynaptic density protein 95	rabbit	1:1000	abcam
β-actin (HRP conjugated)	β-actin	mouse	1:15000	Sigma-Aldrich

2.3.3.1. Validation of synaptosome extraction

An illustrative western blot assessing synaptic markers (GluN1 and PSD95) in synaptosome and cytosolic fractions of the hippocampus and frontal cortex was carried out to validate the synaptosome extraction protocol, demonstrating the purity of the fractions. Brain samples were obtained from three naïve WT animals (female, 16 months old) and protein concentration was measured for both synaptosome and cytosolic fractions with the BCA. The western blot was carried out using primary antibody dilutions optimised for synaptosome sample. Figure 2.7 shows the western blot results. Across brain regions and subjects, the expression of GluN1 and PSD95 was visibly higher in synaptosome relative to cytosolic sample. The expression of the housekeeping cytoskeletal protein β-actin was equivalent in both types of sample. These qualitative results confirmed that the synaptosome extraction protocol reliably produced a synaptically enriched sample.

Figure 2.7: Illustrative western blot to validate the synaptosome extraction protocol. Synaptic markers (GluN1 and PSD95) were visibly higher in synaptosome than cytosolic fractions, while β-actin levels were equivalent. syn= synaptosome; cyt = cytosol; n = 3 WT.

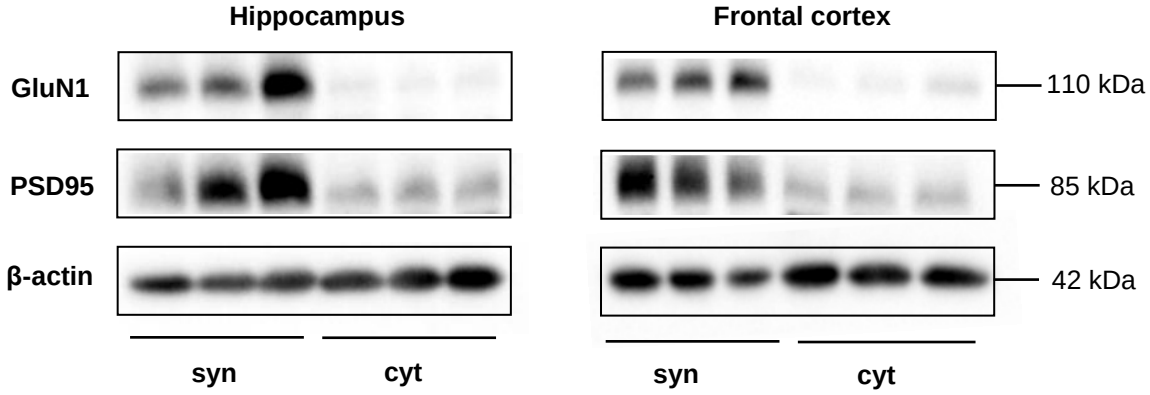

2.3.4. Data analyses

Western blots were analysed with the open-source software NIH ImageJ (1.8.0) to quantify protein expression based on the optical density of each sample band. Background noise was removed and optical density scores were normalised to internal controls and to the expression of other relevant proteins (e.g. β-actin or PSD95) using Microsoft Excel 2013, as described in the relevant chapter. Statistical analyses were conducted using IBM SPSS Statistics 23 as described in section 2.2.3.

Chapter 3: Behavioural phenotypes

Overview

This chapter begins with an introduction on memory systems and their neural substrates, focusing on recognition memory. Recognition memory relies on a network of structures within the medial temporal lobe, including the hippocampus. Individuals with DS and mouse models of DS report aberrant hippocampal morphology and impairments in recognition memory. To determine the contribution of the Mmu16, Mmu17 and Mmu10 trisomy to recognition memory function, Dp1Tyb, Dp3Yey and Dp2Yey animals were tested on a battery of memory tasks assessing different attributes and retention-spans of recognition memory. Behavioural experiments are reported in this chapter. The three mouse lines revealed distinct patterns of recognition memory performance, implicating distinct Hsa21 syntenic portions in the regulation of distinct features of recognition memory.

3.1. Introduction

The capacity to record, retain and recall everyday experiences constitutes a central part of human life and is key to survival in animal species. For example, recognising familiar faces or driving the way to work are behaviours essential to the daily life and rely on the recollection of past experiences. For a mouse, discriminating between safe and noxious food or navigating the way to a hideout are behaviours essential to its subsistence. Memory is however a hypothetical construct and as such, it needs to be modelled into theoretical frameworks in order to be studied. Studies of brain-injured patients and brain-lesioned animals revealed essential for the contemporary understanding of memory processes. Such studies rely on the concept of dissociation, whereby injury to a given brain region is observed to impair performance in a memory task while sparing performance in a different memory task. This type of findings provide evidence for the existence of distinct, independent functional subsystems within memory that are subserved by activity of distinct brain regions (Eichenbaum, Yonelinas, & Ranganath, 2007; Squire & Zola-Morgan, 1991).

3.1.1. Memory systems

One of the earliest models of memory was developed by Atkinson and Shiffrin (1968). Their Multi-store model consisted of three different storage systems: sensory memory, short-term memory (STM) and long-term memory (LTM). According to the model, new information is presented in the form of a sensory input (e.g. a visual or acoustic stimulus) detected by the sensory systems, entering sensory memory. Information that is attentively attended is then transferred to STM for brief, temporary storage. Active maintenance rehearsal processes enable transfer of the information to LTM for permanent storage, while unrehearsed information decays and is eventually forgotten. Upon recall, information is retrieved from LTM and momentarily returned to STM for immediate availability.

The existence of separate storage systems operating on different timescales as postulated by the Multi-store model has been corroborated by patient studies reporting dissociations between STM and LTM memory performance (Drachman & Arbit, 1966; Shallice & Warrington, 1970). One of the most notorious case studies in memory research is patient H.M. (Scoville & Milner, 1957). In an attempt to treat epilepsy, patient H.M. underwent the bilateral resection of the medial temporal lobe, a system of anatomically and functionally related structures comprising the hippocampus. Unexpectedly, the operation resulted in severe anterograde amnesia. The patient could recall episodes that occurred prior to the surgical intervention but was unable to form new lasting memories, showing a complete memory loss for events subsequent the surgery. Interestingly, despite the impairment in the long-term retention of new information, H.M. performed normally when

asked to memorise and immediately recall a series of digits, indicating intact STM under conditions of severely impaired LTM. The same dissociation was observed in other amnesic patients who suffered bilateral hippocampal lesions (Cave & Squire, 1992; Drachman & Arbit, 1966) and in animal models of medial temporal lobe lesions (Clark, West, Zola, & Squire, 2001; Overman, Ormsby, & Mishkin, 1990). These findings point to a critical role of the medial temporal lobe, in LTM but not STM.

At this juncture, it is important to note that the Multi-store model of memory encompasses a very narrow definition of STM, postulating STM to retain memories for only extremely brief time intervals, namely under 30 seconds (Atkinson & Shiffrin, 1968). Although patient studies suggest that STM functions independently of the medial temporal lobe, there is evidence indicating that the medial temporal lobe is involved in STM when retention intervals exceed a handful of seconds. For example, rats with hippocampal lesions showed normal memory performance after a 4 seconds delay but were impaired after one minute (Clark et al., 2001). Similarly, monkeys with medial temporal lobe lesions reported intact memory up until 10 seconds and were impaired afterwards (Overman et al., 1990). Indeed, patient H.M. would generally forget newly learned information in under a minute and his short-term retention ability strongly depended upon continuous verbal rehearsal of the learned material (Milner, Squire, & Kandel, 1998). Finally, neuroimaging studies on healthy subjects demonstrate the involvement of the medial temporal lobe in STM tasks (Ranganath & D'Esposito, 2001).

Given that the current research aimed to study the role of the medial temporal lobe in memory, such largely HPC-independent, immediate memories lie outside its scope. With regards to the Atkinson and Shiffrin model, it can be reasoned that the current research aimed to examine LTM after shorter and longer retention intervals. Therefore, a theoretical framework conceiving memory as a single, unitary storage system would be more appropriate. Cowan (1988) developed a unitary-store model of memory, proposing that all memories are stored in LTM. In this model, STM is defined as an activated portion of LTM. Within STM, a subset of activated items lies in the focus of attention, that is, in the immediate awareness of an individual. The strength of a given memory representation stored in LTM can vary, making the memory more or less likely to become activated, enter the focus of attention and be retrieved. For example, memories of recently, frequently or attentively experienced stimuli are postulated to be more strongly consolidated in LTM. The presentation of memory cues (e.g. relevant context) is predicted to facilitate memory retrieval by activating associated LTM representations.

An important factor that both Atkinson and Shiffrin's and Cowan's memory model fail to address, is the nature of the memoranda. Both models postulate memory subsystems operating on different timescales but do not distinguish between different types of

information, implying that all permanent memories are stored in the same system regardless of their nature. However, patients with memory dissociations provide clear evidence for the existence of separate storage systems for different types of information. For example, despite the overwhelming incapacity to retain new facts and episodes, patient H.M. could successfully acquire and retain new motor skills indefinitely (Corkin, 1968). Similarly, patients with Parkinson's disease were found unable to learn a procedural task but able to recall episodic details of the study, while amnesic patients with bilateral damage to the HPC reported the opposite pattern (Knowlton, Mangels, & Squire, 1996).

Based on these and similar findings, LTM was postulated to consist of distinct storage systems for different types of information, a view currently widely accepted (Squire & Zola-Morgan, 1991; Tulving, 1984). The main distinction lies between implicit (non-declarative) and explicit (declarative) memory. Implicit memory entails knowledge on how to carry out procedures, where the output is often an automatic motor response expressed through performance (e.g. playing an instrument or driving a car). This type of memory is independent of the medial temporal lobe and relies mainly on the striatum. Instead, explicit memory entails knowledge on facts and events, where the output is easily verbalised and expressed through recollection. Explicit memory relies on the medial temporal lobe system and can be further divided into semantic memory (knowledge on facts, e.g. recalling the date of the graduation ceremony) and episodic memory (knowledge on past episodes, e.g. recalling the events that took place during the graduation ceremony). Focus of the current research lies on recognition memory, a sub-type of episodic memory.

3.1.2. The medial temporal lobe system

Episodic memory is the recollection of personally experienced events, whereby a given life episode is mentally re-lived. In the case of recalling the graduation ceremony, the episodic memory would be a combined representation of the content of the event ("*what*"), along with its contextual details, namely location ("*where*") and time ("*when*") of the event (Tulving, 2002).

Anatomical studies of the human, primate and rodent brain identified the anatomical components of the medial temporal lobe system subserving episodic / episodic-like memory (Burwell, Witter, & Amaral, 1995; Suzuki & Amaral, 1994). There is general agreement that the medial temporal lobe system comprises the HPC and the adjacent entorhinal, perirhinal and parahippocampal (postrhinal in rodents) cortices. These structures are densely interconnected and together they form a functional network underpinning the acquisition of new declarative memories.

On the basis of the observed connectivity within the medial temporal lobe system, memory formation is widely viewed as a hierarchical process originating from sensory

systems and converging in the HPC (Eichenbaum et al., 2007; Squire & Zola-Morgan, 1991). New information acquired through the sensory systems is processed by unimodal and polymodal neocortical association areas via two different pathways projecting to distinct medial temporal lobe structures. The ventral "*what stream*" extends along the temporal lobe and processes information regarding the features of a given item. Temporal neocortical areas send item-information to the PRH cortex, which then projects to the lateral entorhinal cortex. Representations of items (e.g. objects, people, events) are thus formed in the PRH and lateral entorhinal cortex. In contrast, the dorsal "*where stream*" extends along the parietal lobe and processes information regarding the context of a given item. Parietal neocortical areas send context-information to the parahippocampal cortex, which then projects to the medial entorhinal cortex. Representations of contexts (e.g. spatial locations, temporal information) are thus formed in the parahippocampal and medial entorhinal cortices. Information from the *"what"* and the *"where"* streams is then converged in the HPC, receiving inputs from the lateral and medial entorhinal cortex. As a consequence of this anatomical organisation, the HPC is postulated to be essential for the binding of item- and context-information into a cohesive episodic memory. Feedback connections within this system support memory retrieval, with the HPC projecting to the entorhinal cortex, respectively feeding back to the PRH and parahippocampal cortices, ultimately returning signals to neocortical areas of the corresponding stream. Reciprocal connections between the HPC and the medial prefrontal cortex also support memory consolidation and retrieval. Figure 3.1 provides a schematic representation of the information flow within the medial temporal lobe system. Evidence supporting the existence of separate pathways within the medial temporal lobe system is presented in the following section, focusing on recognition memory.

Figure 3.1: Information flow underlying formation and retrieval of episodic memory. The ventral "*what*" stream engages temporal neocortical areas to process object information (e.g. different object types) while the dorsal *"where"* stream engages parietal neocortical areas to process contextual information (e.g. spatial location in an open field maze). The streams travel through distinct medial temporal lobe regions to ultimately reach the HPC, where object and context information are integrated (e.g. location of a given object in the maze). Feedback connections within the system and with the medial prefrontal cortex support memory consolidation and retrieval.

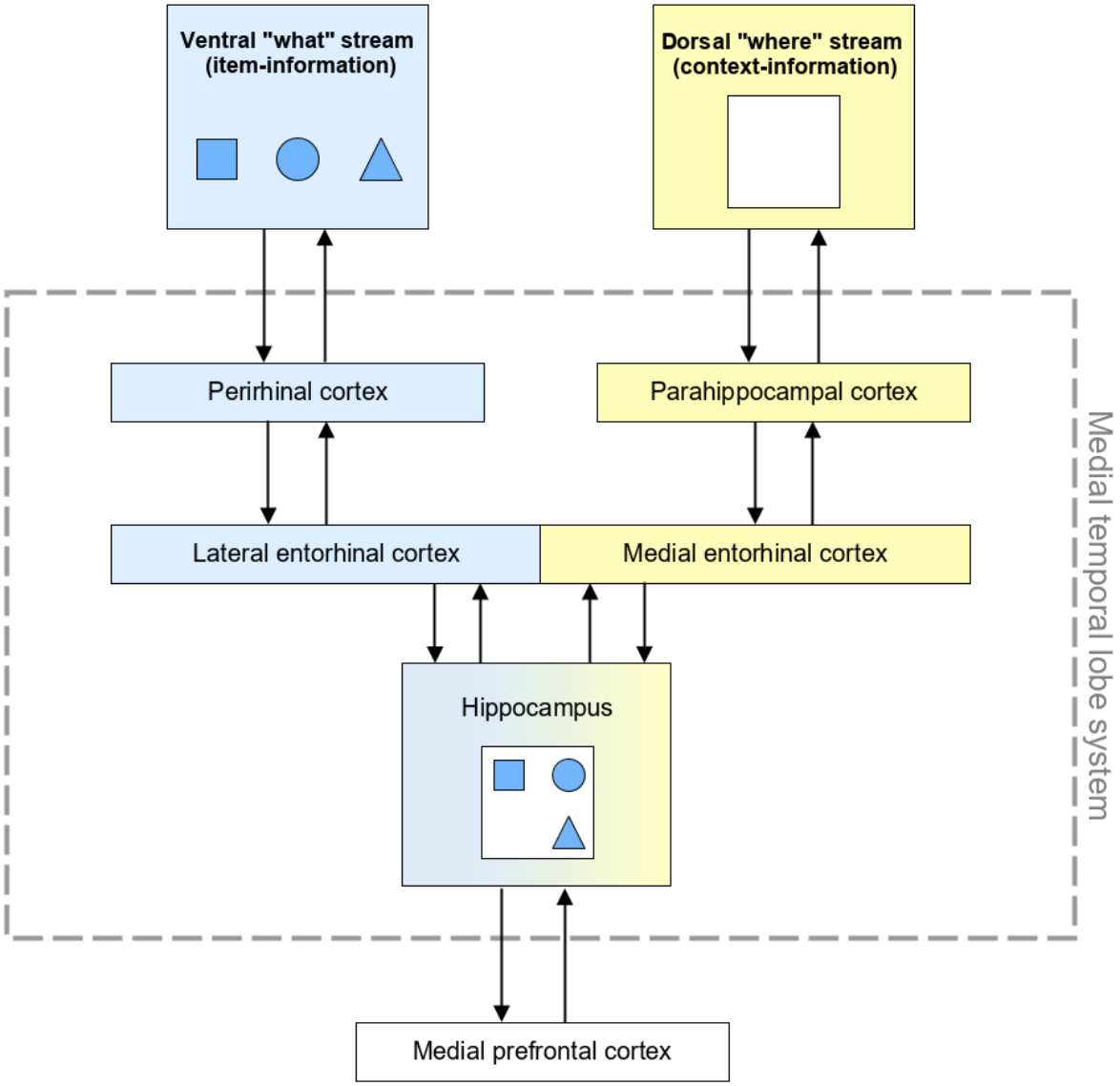

3.1.2.1. Recognition memory

Recognition memory concerns the ability to remember whether a stimulus has been previously encountered or not. The processes involved in recognition memory have been addressed by two major classes of models (Eichenbaum et al., 2007). Dual-process models view recognition memory as consisting of two qualitatively different components, familiarity and recollection. Familiarity is the knowledge that an item was encountered before, while contextual details of the episode are not remembered. Recognition memory based on familiarity processes is commonly assessed by testing the discrimination between novel and familiar individual stimuli, such as recognising the prior occurrence of a given object. Recollection is instead the full, detailed retrieval of the episode in which an item was encountered (i.e. "*what-where-when*") and relies on activity within the medial temporal lobe system (Eichenbaum et al., 2007). Recognition memory based on recollection processes is commonly assessed by testing the discrimination between novel and familiar associations, such as recognising the prior occurrence of an object in a given spatial location or at a given time point. Alternatively, single-process models view recognition memory as a unitary process, whereby familiarity and recollection only differ quantitatively in the strength of the retrieved episodic memory (Eichenbaum et al., 2007).

Tests of recognition memory in amnesic subjects provide evidence for a dissociation between familiarity and recollection processes, supporting a dual-process view (Aggleton et al., 2005). The contribution of patient studies is however limited, as the brain damage frequently concerns more than a single component of the medial temporal lobe system. In this respect, animal studies provide a better tool to investigate recognition memory processes and their neural underpinnings. In animals, recognition memory is commonly tested with behavioural paradigms relying on either the trained (delayed non-match-to-sample tasks) or natural (spontaneous exploration tasks) tendency to prefer novelty (Eichenbaum et al., 2007; Ennaceur & Delacour, 1988; Joubert & Vauclair, 1986). In these tasks, animals are first presented with a set of stimuli during an acquisition phase and after a retention interval, they are presented with previously encountered and novel stimuli. By this means, preference for novelty is contingent upon the retrieval of the prior encounter with the stimuli, permitting inferences on recognition memory processes from the behaviour displayed by the animal.

In rats, lesions of the PRH cortex were found to impair the recognition of a novel object among familiar objects, while lesions of the HPC did not impair object discrimination (Barker & Warburton, 2011b; Mumby, Gaskin, Glenn, Schramek, & Lehmann, 2002). Similarly, monkeys with lesions of the PRH cortex failed to choose novel objects paired with a food reward over familiar objects, while monkeys with lesions of the HPC, parahippocampal cortex or entorhinal cortex performed normally (Nemanic, Alvarado, & Bachevalier, 2004).

By contrast, recognition memory was found impaired by hippocampal lesions in tasks involving the recollection of places or contexts associated to individual stimuli (Bachevalier & Nemanic, 2008; Barker & Warburton, 2011b; Mumby et al., 2002). For example, Mumby et al. (2002) showed that while rats with hippocampal lesions displayed normal preference for exploring a novel object, they were unable to detect novelty when a familiar object was placed in a novel spatial position or presented in a novel test room. Interestingly, recognition memory relying on the binding of item- and context- information was also affected by lesions of other components of the medial temporal system. Monkeys and rats with lesions of either the HPC, PRH cortex, parahippocampal cortex or medial prefrontal cortex failed to display preference for familiar stimuli that exchanged position over stationary familiar stimuli, suggesting that integrated activity within the medial temporal lobe is necessary for the retrieval of associations (Barker & Warburton, 2011b; Bechavalier & Nemanic, 2008).

Overall, animal lesion studies suggest that the PRH cortex and the HPC play distinct roles in recognition memory processes. Further evidence comes from electrophysiological and cell activity studies. Recordings from the monkey and rat brain showed that repeated presentation of a stimulus significantly decreased neuronal responses in the PRH cortex, while activity did not or only mildly decreased in the HPC (Xiang & Brown, 1998; Zhu, Brown, & Aggleton, 1995). Neurons in the PRH cortex and temporal cortex also showed higher responses to features of visual stimuli, such as colour and shape, compared to hippocampal and parahippocampal neurons (Riches, Wilson, & Brown, 1991). Instead, neurons in the HPC were found to selectively respond to visual stimuli occurring in particular spatial positions (Rolls et al., 1989). Similarly, the presentation of images of familiar items in novel spatial arrangements resulted in increased hippocampal and postrhinal neural activity, leaving PRH and temporal cortex activity levels unaltered, as measured by the expression of the immediate-early-gene c-fos (Wan, Aggleton, & Brown, 1999).

Taken together, these findings identify the PRH cortex as fundamental for the recognition of individual items and the HPC for the recognition of spatial or contextual aspects associated to individual items. This widely accepted view, matches the hierarchical information flow underlying episodic memories outlined in section 3.1.2 and reflects a dual-process model of recognition memory. Neurons in the PRH cortex encode primarily item-information ("*what stream*"), whereby neuronal activity levels signal the familiarity of a stimulus and serve familiarity judgments based on single item-recognition processes. Hippocampal neurons encode context-information ("*where stream*"), bind it to item-information and serve recollection judgments based on associative-recognition processes.

In DS, medial temporal lobe structures exhibit abnormal morphology and individuals with DS report in fact impairments in the recognition of previously presented items and their spatial position (Clark et al., 2017; Vicari et al., 2000). To investigate the role of Hsa21

orthologous regions in recognition memory dysfunction, recognition memory was assessed in the Dp1Tyb, Dp3Yey and Dp2Yey mouse lines. A widely employed experimental paradigm to investigate single item- and associative-recognition processes in rodents are object-recognition memory tasks.

Object-recognition memory tasks

Object-recognition paradigms for use with rodents are based on spontaneous exploration tasks. These rely on the natural tendency of rodents to explore novel stimuli (Ennaceur & Delacour, 1988). The advantage of these tasks is that they do not require prior training or reinforcements, and the same basic paradigm can be used to test different processes and retention-spans of recognition memory.

All object-recognition memory tasks consists of a sample phase in which the animal encodes an array of objects, and of a test phase, in which the presence of familiar objects is postulated to activate the representation of the sample episode and enable the animal to detect the presence of novel objects. Firstly, the animal is placed in an open field maze and allowed to freely explore an object array (*sample phase*). After a time delay, the animal is re-exposed to an object array consisting of previously encountered and novel objects (*test phase*). Object exploration times are used to create an index of novelty preference, whereby preference for novelty indicates intact recognition memory processes. In the test phase, different aspects of the object array can be altered to result in novelty, such as object type, object location or encounter recency. Distinct sample-test phase incongruences are used to assess single item- or associative-recognition processes, as described below.

In the current research, four different types of object-recognition memory tasks were used: Novel Object Recognition (NOR), Object-in-Place (OiP), Object Location (Loc), Temporal Order (TOr). Although the exact protocols might slightly differ between laboratories, these four tasks are widely employed in mouse memory research (Ennaceur, 2010; Warburton & Brown, 2015). In the NOR, novelty detection relies solely on single item-recognition (*"what"*), whereby the animal is tested with two familiar objects and one new object (fig. 2.4a). In the OiP, novelty detection relies on the recognition of associations between single items and their spatial location (*"what-where"*), whereby the animal is tested with one stationary object and two familiar objects that exchanged location (fig. 2.4b). In the Loc, novelty detection relies on single spatial-recognition irrespective of object type (*"where"*), whereby the animal is tested with two stationary objects and one familiar object in a new location (fig. 2.4c). In the TOr, novelty detection relies on the recognition of associations between single items and their encounter time (*"what-when"*), whereby the animal is tested with a recently encountered and a remotely encountered object (fig. 2.4d).

In reference to the neural underpinnings of recognition memory presented previously, reasonable assumptions can be made on the medial temporal lobe components that

underlie each of the four object-recognition memory tasks. The PRH cortex is expected to play a critical role in the single item-recognition processes that enable object novelty judgments in the NOR, while the item-in-context associative-recognition processes tested in the OiP and TOr would rely more on network activity within the medial temporal lobe. Finally, the single context-recognition processes that enable spatial novelty judgments in the Loc would mainly rely on the postrhinal cortex and the HPC.

Indeed, these assumptions are corroborated by studies that explicitly aimed to investigate the neural basis of object-recognition memory tasks. Research by Barker and Warburton (2011b) used rats to test the effects of bilateral lesions of either the PRH cortex, the HPC or the medial prefrontal cortex (mPFC) on performance in the four object-recognition memory tasks presented above. Unsurprisingly, PRH lesions impaired the detection of object novelty in the NOR task, while HPC or mPFC lesions did not affect performance. Instead, HPC but not PRH or mPFC lesions impaired the detection of novel spatial locations in the Loc task. Performance in the OiP and TOr tasks was affected by lesion of either of the three regions. In all tasks, impairments were observed both when memory was tested after short (5-min) and long (24-h) retention intervals. To confirm the necessity of integrated network activity in the OiP and TOr tasks, the authors also tested groups of rats with unilateral HPC lesions together with PRH or mPFC lesions in either the ipsilateral or contralateral hemisphere. According to the anatomy of the medial temporal lobe system, contralateral but not ipsilateral lesions disconnect network connectivity. Predictably, animals with crossed lesions were impaired in both tasks, while ipsilaterally lesioned animals performed normally.

The crucial role of the PRH, but not of the HPC or mPFC, in novel object recognition tasks, has been amply demonstrated by several studies, as well as the importance of the HPC in object location tasks and of the three regions PRH, HPC and mPFC in object-in-place and temporal order tasks (Barker, Bird, Alexander, & Warburton, 2007; Cross, Brown, Aggleton, Warburton, 2013; Good, Barnes, McGregor, & Honey, 2007; Mitchell & Laiacona, 1998; Mumby et al., 2002; Mumby, Piterkin, Lecluse, & Lehmann, 2007). Together, studies employing object-recognition memory tasks converged to a clear dissociation pattern. A summary of the characteristics of each object-recognition memory task is reported in table 3.1.

Nonetheless, a few studies reported the involvement of other brain regions as well. For example, performance in the NOR and Loc tasks was impaired by lesions of the nucleus accumbens (Nelson, Thur, Marsden, & Cassaday, 2010). Lesions of the retrosplenial cortex impaired OiP but not NOR performance (Vann & Aggleton, 2002) and lesions of the mediodorsal thalamic nucleus impaired both OiP and TOr performance (Cross et al., 2013). Therefore, although HPC, PRH and mPFC emerged as the key regions underlying

performance in object-recognition memory tasks, activity in other brain structures is also potentially relevant.

In order to make appropriate inferences on memory processes from exploration times observed in object-recognition memory tasks, some key aspects of the tasks need to be considered. For one, as discussed by Ennaceur (2010), the choice of the object array must be given extensive thought. Although object exploration engages different sensory modalities, such as vision, olfaction and haptic perception, object discrimination relies mainly on the visual system. Vision in mice is however poor, with 97% of the mouse retina consisting of rods and having only two cone types, resulting in dichromatic, low, daylight vision (Jacobs, Williams, & Fenwick, 2004; Jeon, Strettoi, & Masland, 1998). Object discrimination thus should not be primarily based on colour as any object preference potentially observed in the test phase is unlikely to reflect recognition memory processes. Instead, objects that clearly differ in size or shape, or that present distinct high-contrast patterns, are more appropriate. The selected object array must at the same time prevent a priori object preferences. For example, objects that are particularly stimulating in terms of visual patterns, odour or surface protrusions, may profit from higher exploration times irrespective of the memory representations established during the task (Ennaceur, 2010).

A final observation tackles a more conceptual aspect of object-recognition memory tasks. These tasks are designed to assess recognition memory, a specific type of episodic memory in which the cued recall of past experiences is used for novelty judgments. Under the perspective of Cowan's memory model (1988), as the mouse is re-placed in the maze for the test phase, familiar cues, such as the environment and some of the objects, activate the associated LTM representations, namely the episodic memory of the sample phase. Activated representations become readily available and allow novelty detection as the animal explores the objects. In this regard, as argued by Ennaceur (2010), it must be noted that the value of the four object-recognition memory tasks presented here in the study of episodic-like memory is limited, as these tasks only assess certain aspects of a given episode and not the triangular "*what-where-when*" schema. Additionally, the recognition memory processes postulated to take place in these tasks are tightly linked to the visual system. Generalisation of the findings to other sensory modalities, or to recognition or episodic memory in general, is thus potentially problematic. Nonetheless, if conducted properly, object-recognition memory tasks provide a valuable tool to study the neural basis of visual recognition memory processes.

At this juncture, it must be noted that while the presented model of recognition memory provides the advantage of differentiating between attributes of recognition memory, the *what-where-when* approach does not propose a psychological mechanism enabling familiarity judgments to be made. An alternative framework to study recognition memory

processes is the Sometimes-Opponent-Process model (SOP) (Wagner, 1981). The SOP model allows to address recognition memory processes in terms of habituation to familiar stimuli, leading to reduced responding and thus preference for novelty. Performance in object-recognition memory tasks will be discussed in the context of the SOP model in the general discussion (chapter 5).

Table 3.1: Characteristics of object-recognition memory tasks. Novelty was operationalised differently in each task to test different single- or associative recognition memory processes, known to rely on different medial temporal lobe structures. Primarily based on Barker and Warburton (2011b).

Task	Novelty	Recognition memory process	Neural basis
NOR	Novel object	Single item *("what")*	PRH
OiP	Familiar object in different location	Item-in-context association *("what-where")*	PRH HPC mPFC
Loc	Novel location	Single context *("where")*	HPC
TOr	Familiar object presented long ago	Item-in-context association *("what-when")*	PRH HPC mPFC

3.1.3. Study rationale

Down Syndrome is a neurodevelopmental disorder caused by an extra copy of Hsa21. Memory function in DS is severely impaired (Godfrey & Lee, 2018; section 1.2.2.2). Although DS individuals show relatively preserved memory in immediate recall tests, memory is impaired after retention intervals exceeding a few minutes. Subjects with DS report deficits in the recognition of previously presented objects and their spatial location, along with learning deficits in visuospatial navigation tasks (Clark et al., 2017; Courbois et al., 2013; Lavenex et al., 2015; Purser et al., 2015; Vicari et al., 2000; Vicari et al., 2005). Patient studies and lesion studies in rodents demonstrate that the medial temporal lobe and the HPC in particular, are crucial for the formation of new episodic memories (Cave & Squire, 1992; Clark et al., 2001; Drachman & Arbit, 1966; Scoville & Milner, 1957). In DS, the HPC is characterised by reduced volume and aberrant cytoarchitecture (Guidi et al., 2008; Pinter et al., 2001a; Pinter et al., 2001b). These changes are already visible in DS foetuses and persist through adulthood.

DS is also characterised by age-related cognitive decline and increased incidence of early-onset AD (Lott & Head, 2000; Wisniewski, et al., 1985). AD is a neurodegenerative disorder characterised by episodic memory impairments and hippocampal degeneration, due to Aβ accumulation. Virtually all DS brains present signs of amyloid pathology, even at early age. Increased Aβ accumulation in DS has been associated to trisomy of key genes located on Hsa21, such as *APP* and *S100B* (Lott & Head, 2000).

Although a number of genes on Hsa21 has been implicated in cognition, such as *DYRK1A*, *APP*, *RCAN1*, *S100B* and *CBS*, the role that Hsa21 genes play in the regulation of memory function is poorly understood. The long arm of Hsa21 shares conserved synteny with the mouse genome, mapping to conserved regions on Mmu16, Mmu17, Mmu10 (Lana-Elola et al., 2011). Based on this synteny, mouse models of segmental DS trisomic for distinct portions of the conserved regions have been generated via genetic engineering techniques, as reviewed in section 1.3. Indeed, mouse models of DS recreate a number of physical and cognitive DS-like features (Belichenko et al., 2009a; Holtzmann et al., 1996; Fernandez & Garner, 2007; Kleschevnikov et al., 2012; Li et al., 2007; Olson et al., 2007; Pereira et al., 2009; Richtsmeier et al., 2000; Richtsmeier et al., 2002; Souchet et al., 2019).

The Dp1Tyb, Dp3Yey and Dp2Yey models were recently generated and they carry a complete and exact trisomy of the Mmu16, Mmu17, Mmu10 conserved regions, respectively (Yu et al., 2010b). By contrast, other mouse models such as the Ts65dn, Ts1Cje or Dp1Yah, carry trisomy of genes that are not syntenic to Hsa21 and/or lack trisomy of Hsa21 syntenic genes, in addition to the intended trisomy (Duchon et al., 2011b; Pereira et al., 2009). As such, the Dp1Tyb, Dp3Yey and Dp2Yey models represent the most valid tool to determine the separate contribution of each conserved region to DS-like phenotypes.

As previously discussed (section 3.1.2.1), several lesion studies have demonstrated that novelty/familiarity and associative recognition processes rely on different medial temporal lobe structures, engaging the HPC to a different extent. As such, the pattern of memory performance observed in object-recognition memory tasks permit inferences about putatively aberrant medial temporal lobe circuits. These tasks are widely employed in the study of DS mouse models, with previous evidence revealing trisomy-dependent impairments, suggesting that distinct genetic portions regulate distinct processes and timeframes of recognition memory.

Performance on object-recognition tasks is however contingent upon the locomotor behaviour of the animal and its willingness to approach novelty. Altered locomotor activity and anxiety levels can impact contact times with the objects and mask novelty detection, ultimately confounding inferences on memory processes. In DS, motor function is aberrant, with individuals presenting hypotonia, gait abnormalities, and difficulties in balance and postural control (Weijerman & de Winter, 2010). Additionally, children and adolescents with DS also frequently report anxiety disorders, impulsivity and decreased attention. The prevalence of attention-deficit/hyperactivity disorders in DS has been estimated to almost 45% (Ekstein, Glick, Weill, Kay, & Berger, 2011). Indeed, delayed motor development and impairments in motor coordination and balance have been observed in several DS models, including the Dp1Tyb (Costa et al., 1999; Goodliffe et al., 2016).

A meta-analysis by Viggiano (2008) identified the entorhinal-hippocampal-septal-prefrontal cortex-olfactory bulb axis as the system regulating activity levels and lesions of the HPC are known to result in hyperactivity (Bannerman et al., 2002). Furthermore, in addition to underlying memory function and activity levels, the HPC has also been implicated in emotional processing. On the EPM, rats with complete lesions of the HPC spent significantly more time in open arms compared to sham-operated rats, suggesting reduced anxiety (Bannerman et al., 2002). Similarly, Tg2576 mice, a mouse model of hippocampal amyloid pathology similar to AD, showed increased locomotor activity on the open-field test and reduced anxiety on the EPM (Lalonde, Lewis, Strazielle, Kim, & Fukuchi., 2003). Activity and anxiety phenotypes can thus be indicative of aberrant hippocampal function.

In the present study, the impact of the Mmu16, Mmu17 and Mmu10 segmental trisomies on recognition memory processes and age-related cognitive decline was assessed. Cohorts of adult (12-13 months) and aged (18-20 months) Dp1Tyb, Dp3Yey and Dp2Yey animals underwent a battery of object-recognition memory tasks testing shorter (10-min) and longer (3-h or 24-h) retention intervals. To investigate locomotor activity and anxiety phenotypes in the trisomies and to disambiguate these variables from performance

in memory tasks, the three mouse lines also underwent the EPM test. The three models were predicted to display distinct patterns of memory performance, as detailed below.

Several Hsa21 genes that have been implicated in learning and memory map to the Mmu 16 segment, such as *App, Dyr1kA* and *Rcan1* (Lana-Elola et al., 2011). Mouse models of Mmu16 trisomy – Ts65Dn, Ts1Cje, Ts1Rhr mice – exhibit abnormal hippocampal morphology and impaired hippocampal LTP, along with deficits in HPC-dependent memory tasks, such as the MWM, CFC, T-maze test, Loc and OiP tasks (Belichenko et al., 2007; Belichenko et al., 2009a; Fernandez & Garner, 2007; Kleschevnikov et al., 2012; Sago et al., 2000). Similar phenotypes have been reported in Dp1Tyb mice (Goodliffe et al., 2016; Souchet et al., 2019; Yu et al., 2010b). Therefore, the Dp1Tyb mouse line was hypothesised to display impaired performance on the three HPC-dependent object-recognition memory tasks, namely the OiP, TOr and Loc tasks. Additionally, models of Mmu16 trisomy, including the Dp1Tyb, show impaired object novelty recognition, especially following long retention intervals (Belcihenko et al., 2009a; Kleschevnikov et al., 2012; Souchet et al., 2019). For example, Ts65dn mice were unable to detect object novelty after a 24-h delay but were unimpaired after a 10-min delay (Kleschevnikov et al., 2012). Therefore, the Dp1Tyb mouse line was also hypothesised to display impairments on the 24-h NOR test. Finally, because of the *App* trisomy, any spared NOR memory was predicted to deteriorate with age, as observed in mouse models of AD pathology (Hall et al., 2016; Webster, Bachstetter, Nelson, Schmitt, & Van Eldik, 2014).

The *Cbs* gene has also been implicated in cognitive dysfunction and maps to the Mmu17 segment (Almuqbil et al., 2019; Marechal et al., 2019). Previous evidence on the Dp3Yey model reports enhanced hippocampal LTP and intact performance on the MWM and CFC task (Yu et al., 2010b). In a mouse model of incomplete Mmu17 trisomy, the Dp1Yah, novel object recognition was found impaired after a 1-h delay (Pereira et al., 2009). Therefore, the Dp3Yey mouse line was hypothesised to display memory deficits on the NOR task, possibly both on the 10-min and the 24-h test. If that were the case, further testing with the OiP and TOr tasks would be impracticable, as these tasks depend on intact object memory (Barker & Warburton, 2011b). Performance on the Loc task would however be testable and expected to report no impairments, in line with previous evidence on the Dp3Yey model showing intact performance in HPC-dependent tasks (Yu et al., 2010b). Ageing was not predicted to impact memory function.

The *S100b gene* has been implicated in AD-pathology and maps to the Mmu10 segment (Block et al., 2015). Previous evidence on the Dp2Yey model reports normal hippocampal LTP and intact performance in the MWM and CFC task at 2-4 months of age (Yu et al., 2010b). Therefore, younger Dp2Yey animals were hypothesised to display intact memory in HPC-dependent object-recognition memory tasks (OiP, TOr, Loc). Given trisomy

of *S100b*, Dp2Yey mice were hypothesised to display age-dependent cognitive decline, resulting in impaired memory performance on the NOR task at older age, as observed in mouse models of AD-pathology (Hall et al., 2016; Webster, et al., 2014).

To date, no study has ever systematically examined recognition memory in the Dp1Tyb, Dp3Yey and Dp2Yey models. The current study aimed to provide a better understanding of memory dysfunction in DS by identifying gene portions associated to specific memory deficits, indicative of aberrant activity in specific medial temporal lobe structures.

3.2. Methods

The general methods are described in chapter 2. Further details on the two behavioural tests are provided below.

3.2.1. Object-recognition memory tasks

Object-recognition memory tasks were run as described in section 2.2.1. To obtain an initial evaluation of the impact of each trisomy on recognition memory, adult animals (12-13 months) were first tested on the NOR and OiP tasks, each with a 10-min and a 24-h retention interval. Animals underwent the two tasks in counterbalanced order. In case of memory impairments, the mouse line was subsequently tested on the Loc and/or TOr task. Following the testing of adult animals, cohorts of older animals (18-20 months) were tested in the same way. Because memory impairments were observed in adult Dp1Tyb mice, a cohort of younger (4 months) mice was additionally tested on the OiP task. In total, 4 experiments (Exp. 1a, 1b, 1c, 1d) were run on the Dp1Tyb, 2 on the Dp3Yey (Exp. 2a, 2b), and 2 on the Dp2Yey (Exp. 3a, 3b).

Animal subjects

For the Dp1Tyb, a cohort of 12-month-old animals (11 WT and 12 Dp1Tyb) was used in Exp. 1a and 1b. The same cohort was used in Exp. 1c at 20 months of age (9 WT and 7 Dp1Tyb). A different cohort of 4-month-old animals (11 WT and 12 Dp1Tyb) was used in Exp. 1d. For the Dp3Yey, a cohort of 13-month-old animals (12 WT and 12 Dp3Yey) was used in Exp. 2a and a different cohort of 18-month-old animals (9 WT and 12 Dp3Yey) was used in Exp. 2b. For the Dp2Yey, a cohort of 13-month-old animals (12 WT and 12 Dp2Yey) was used in Exp. 3a and a different cohort of 20-month-old animals (9 WT and 12 Dp2Yey) was used in Exp. 3b.

Materials

As described in section 2.2.1.1.

Procedure

As described in section 2.2.1.2.

Data analysis

Statistical analyses were conducted as described in section 2.2.3. The analyses were run separately for each mouse line and each object-recognition memory task. Total contact time with the objects was averaged over the total number of objects, resulting in mean contact times with one object for sample phases and mean contact times with one novel

and one familiar object for test phases. In tasks testing two delays, contact times during the sample phases were collapsed and averaged over the delays.

For sample phases, contact times with the objects were analysed using repeated measures two-way ANOVAs, with genotype as between-subjects factor and sample phase as within-subjects factor. For test phases, contact times with familiar and novel objects were analysed using repeated measures three-way ANOVAs, with genotype as between-subjects factor and object and delay as within-subjects factors. In tasks that tested only one delay, the same analysis was run without the within-subject factor of delay.

Mean discrimination ratios (calculated as described in 2.2.1.2) were analysed with repeated measures two-way ANOVAs, with genotype as between-subjects factor and delay as within-subjects factor. In tasks that tested only one delay, independent samples Student's t-tests were used. Mean discrimination ratios were also compared against chance (0.5) with one-sample t-tests.

To corroborate results obtained with classical statistical analyses and confirm that TG animals performed normally, mean discrimination ratios were further analysed with Bayesian statistics as described in 2.2.3.

3.2.2. Elevated plus maze test

Cohorts of adult Dp1Tyb, Dp3Yey and Dp2Yey animals were tested as described in section 2.2.2.

Animal subjects

For the Dp1Tyb experiments, a cohort of 12-month-old animals (8 WT and 11 Dp1Tyb) was used, the same of Exp. 1d. For the Dp3Yey experiments, a cohort of 8-month-old animals (12 WT and 12 Dp3Yey) was used, later tested on Exp. 2a. For the Dp2Yey experiments, a cohort of 8-month-old animals (12 WT and 12 Dp2Yey) was used, later tested on Exp. 3a.

Materials

As described in section 2.2.2.1.

Procedure

As described in section 2.2.2.2. A break of approximately 5 weeks separated EPM and object-recognition tests.

Data analysis

Statistical analyses were conducted as described in section 2.2.3 and run separately for each mouse line. The percentage of time spent in open arms during the entire trial duration was calculated as follows: (seconds in open arms / (seconds in open arms + seconds in closed arms)) * 100%). The percentage of time spent in open arms was compared between the groups with independent samples Student's t-tests. The following measures –velocity, distance moved, number of arm entries – were analysed with repeated measures two-way ANOVAs with genotype as between-subjects factor and arm type as within-subjects factor. Latency to first entry into open arms and total number of head dips were compared between WT and TG mice with independent samples Student's t-tests. The overall distance moved on the EPM in the first trial minute was compared to the last minute with paired samples t-tests within each mouse line.

3.3. Dp1Tyb results

To characterise the behavioural phenotypes associated to trisomy of the Mmu16 conserved region, the same cohorts of Dp1Tyb animals underwent four experiments involving object-recognition memory tasks (exp 1a, 1b, 1c, 1d) and the EPM test (Exp. 1e).

3.3.1. Exp. 1a: Delay-dependent impairment in object-in-place memory

Adult Dp1Tyb and their WT littermates were first tested on the NOR and the OiP task, each with a 10-min and a 24-h delay. Respectively, the two tasks assessed the ability to recognise a novel object among familiar objects (*what*) and to recognise objects that exchanged position among stationary objects (*what-where*). Subsequently, to determine whether impairments observed in the OiP task were a result of a general impairment in the retention of spatial locations or concerned specifically the retention of object-in-place associations, the animals were tested on the Loc task. This task assessed the ability to detect when an object moved to a previously vacant (and thus novel) location relative to other identical but stationary objects (*where*). Results are reported separately for each task. Mean contact times with the objects during sample and test phases are shown in table 3.2.

Novel Object recognition task

During the two sample phases, Dp1Tyb and WT displayed similar contact times with the objects (two-way ANOVA – genotype: $F_{(1,21)}$=0.944, p=0.342; genotype x sample phase: $F_{(1,21)}$=0.056, p=0.815). The two sample phases were identical and habituation from the first to the second sample phase took place in both groups, as indicated by significantly reduced contact times (two-way ANOVA – sample phase: $F_{(1,21)}$=21.172, p<0.001).

In the test phase, intact memory for object identity was inferred from longer contact times with novel than familiar objects. Overall, contact times with novel objects were significantly higher than with familiar objects (three-way ANOVA object: $F_{(1,21)}$=62.915, p<0.001). However, contact times with novel objects by Dp1Tyb mice were significantly lower compared to wildtypes (three-way ANOVA – genotype: $F_{(1,21)}$=6.573, p=0.018; genotype x object: $F_{(1,21)}$=9.539, p=0.006; simple main effects of object – WT: $F_{(1,21)}$=58.195, p<0.001; Dp1Tyb: $F_{(1,21)}$=12.262, p=0.002; simple main effects of genotype – novel, Welch's corrected: $F_{(1,15)}$=9.093, p=0.008, familiar: $F_{(1,21)}$=0.820, p=0.375). This reduction was not linked to a specific delay (three-way ANOVA – genotype x delay: $F_{(1,21)}$=0.223, p=0.641; genotype x object x delay: $F_{(1,21)}$=1.980, p=0.174). In both groups, contact times with novel objects were significantly lower at the 24-h than the 10-min delay (three-way ANOVA – delay: $F_{(1,21)}$=7.361, p=0.013; delay x object: $F_{(1,21)}$=10.811, p=0.004; simple main effects of delay – novel object: $F_{(1,21)}$=10.437, p=0.004; familiar object: $F_{(1,21)}$=0.529, p=0.475).

To investigate preference for novelty independently of total overall contact times during the test phase, mean discrimination ratios were analysed (fig. 3.2a). In agreement with the previous analysis, both groups displayed significantly above chance preference for novel objects, at both delays (one sample t-test – $WT_{10\text{-min}}$: $t_{(10)}=5.253$, $p<0.001$; $WT_{24\text{-h}}$: $t_{(10)}=5.039$, $p=0.001$; $Dp1Tyb_{10\text{-min}}$: $t_{(11)}=4.697$, $p=0.001$; $Dp1Tyb_{24\text{-h}}$: $t_{(11)}=4.002$, $p=0.002$). Furthermore, mean discrimination ratios did not significantly differ between the groups, although they were numerically lower in the Dp1Tyb group, at both delays (two-way ANOVA – genotype: $F_{(1,21)}=0.947$, $p=0.342$; genotype x delay: $F_{(1,21)}=0.438$, $p=0.515$). In line with the contact time analysis, novelty preference was generally lower at the 24-h than the 10-min delay (two-way ANOVA – delay: $F_{(1,21)}=4.088$, $p=0.056$).

To further investigate whether novelty preference in the Dp1Tyb was no different from the WT group, mean discrimination ratios were also compared with Bayesian statistics. The estimated Bayes factors (B_{01}) reported that the data were 1.776 times and 2.471 times more likely to occur under H0 than H1 for the 10-min and the 24-h delay respectively, providing supporting evidence in favour of group similarity.

Together, these findings indicate that Dp1Tyb animals were able to discriminate between familiar and novel objects, both after the 10-min and the 24-h retention interval. Dp1Tyb animals explored novel objects to a lesser extent than their WT littermates, but there was still a marked preference for Dp1Tyb mice to explore novel objects across delay intervals.

Object-in-place task

One Dp1Tyb animals was excluded from this analysis due to insufficient contact time with the objects during the sample phases (< 3 sec). In the sample phases, there was no difference in contact times displayed by Dp1Tyb and WT animals (two-way ANOVA – genotype: $F_{(1,20)}=0.149$, $p=0.703$). Contact times dropped significantly across the two identical sample phases in both groups, and this decrease was significantly larger in the WT than the Dp1Tyb group (two-way ANOVA – sample phase: $F_{(1,20)}=47.134$, $p<0.001$; genotype x sample phase: $F_{(1,20)}=5.305$, $p=0.032$; simple main effects of sample phase – WT: $F_{(1,20)}=42.033$, $p<0.001$; Dp1Tyb: $F_{(1,20)}=10.407$, $p=0.004$; simple main effects of genotype – S1: $F_{(1,20)}=1.799$, $p=0.195$; S2: $F_{(1,20)}=0.478$, $p=0.497$).

In the test phase, intact memory for object-in-place associations was inferred from longer contact times with objects that exchanged position (i.e. novel place) than stationary objects (i.e. familiar place). Overall, contact times were significantly higher for novel place than familiar place objects and did not differ between the groups (three-way ANOVA – genotype: $F_{(1,20)}=0.130$, $p=0.722$; object: $F_{(1,20)}=7.673$, $p=0.012$; object x genotype: $F_{(1,20)}=4.269$, $p=0.052$). However, mean contact times (table 3.2) with novel place objects were generally lower in the Dp1Tyb group. This observation is supported by the fact that

the interaction between object type and genotype approached significance. Additionally, the ANOVA revealed that contact times were significantly lower at the 10-min than the 24-h delay, but the decrease was not specifically linked to either object type or genotype (three-way ANOVA – delay: $F_{(1,20)}$=5.252, p=0.033; delay x object: $F_{(1,20)}$=2.006, p=0.172; delay x genotype: $F_{(1,20)}$=0.013, p=0.910; genotype x delay x object: $F_{(1,20)}$=2.898, p=0.104).

As suggested by mean contact times, the mean discrimination ratio (fig. 3.2b) of Dp1Tyb mice was not significantly above chance at the 10-min delay, in contrast to the WT group who performed significantly above chance (one sample t-test – $WT_{10\text{-}min}$: $t_{(10)}$=2.810, p=0.018; $Dp1Tyb_{10\text{-}min}$: $t_{(10)}$=0.872, p=0.404). In contrast, however, the Dp1Tyb mice but not WT mice, showed a significantly above chance novelty preference on the 24-h test (one sample t-tests – $WT_{24\text{-}h}$: $t_{(10)}$=1.800, p=0.102; $Dp1Tyb_{24\text{-}h}$: $t_{(10)}$=2.899, p=0.016). Differences between the groups failed however to reach statistical significance, at either delay (two-way ANOVA – genotype: $F_{(1,20)}$=3.414, p=0.079; genotype x delay $F_{(1,20)}$=3.252, p=0.086). Overall, the tested delay did not significantly affect novelty preference (two-way ANOVA – delay: $F_{(1,20)}$=1.324, p=0.263).

To further investigate whether Dp1Tyb animals performed normally, mean discrimination ratios were compared between groups with Bayesian statistics. For the 10-min delay, the estimated Bayes factor (B_{01}) reported that the data were only 0.457 times more likely to occur under H0 than H1. Instead, for the 24-h delay the data were 2.556 times in favour of H0. To corroborate the Bayesian results, performance was directly compared between the groups with classical Student's t-tests. Novelty preference was significantly lower in the Dp1Tyb group compared to the WT group at the 10-min delay, but there was no difference at the 24-h delay (Student's t-test – 10-min: $t_{(20)}$=2.281, p=0.034; 24-h: $t_{(20)}$=0.215, p=0.832).

Together, these findings indicate that Dp1Tyb animals were less sensitive to novel object-in-place associations than their WT littermates. The evidence reports that Dp1Tyb animals were not consistently able to discriminate between novel and familiar object-in-place associations, with memory deficits emerging after the 10-min but not the 24-h retention interval.

Object location task

To examine whether the impairment on the OiP task concerned short-term memory for the spatial organisation of the objects or specifically concerned object-in-place associations, the mice were tested on the Loc task with a 10-min delay. In the sample phases, there was no significant difference between the contact times of WT and Dp1Tyb animals (two-way ANOVA – genotype: $F_{(1,20)}$=3.542, p=0.074). Unexpectedly, contact times did not drop across the two identical sample phases, possibly due to a floor effect (i.e. three

copies of the same object; two-way ANOVA – sample phase: $F_{(1,20)}$=0.654, p=0.428, sample phase x genotype: $F_{(1,20)}$=0.264, p=0.613).

In the test phase, intact memory for spatial locations was inferred from higher contact times with objects moved to a novel, previously vacant locations (i.e. novel location objects) than with stationary objects (i.e. familiar location objects). Both groups showed significantly higher contact times with novel than familiar location objects, to a similar extent (two-way ANOVA – object: $F_{(1,20)}$=24.809, p<0.001; genotype: $F_{(1,20)}$=0.036, p=0.851; object x genotype: $F_{(1,20)}$=0.569, p=0.460).

Mean discrimination ratios (fig. 3.2c) were significantly above chance in both the WT and the Dp1Tyb group (one sample t-test – $WT_{10\text{-}min}$: $t_{(10)}$=5.114, p<0.001; $Dp1Tyb_{10\text{-}min}$: $t_{(10)}$=5.320, p<0.001). Novelty preference was compared between the groups with classical and Bayesian Student's t-tests. Respectively, the tests reported no statistically significant difference between the groups ($t_{(20)}$=1.094, p=0.287) and an estimated Bayes factor (B_{01}) indicating that the data were 1.699 times more likely to occur under H0 than H1.

Together, these findings indicate that following a 10-min delay, Dp1Tyb animals were able to discriminate between familiar objects occupying a novel, previously vacant spatial location and identical, stationary objects to WT levels. Memory for spatial information was thus not overall defective in the Dp1Tyb following a 10-min delay.

Table 3.2: Mean contact times of 12-month-old Dp1Tyb mice in object-recognition memory tasks. Sample phases comprised a total of three objects. Test phases comprised one novel and two familiar objects / locations in the NOR and Loc task, and two novel and one familiar place object in the OiP task. Values are mean contact times with one object, ± 1 SD. For NOR and Loc n= 11 WT, 12 Dp1Tyb. For OiP n=11 WT, 11 Dp1Tyb.

			Mean contact times (sec)	
			WT	**Dp1Tyb**
NOR	Sample phase	S1	7.09 (±1.95)	6.45 (±2.38)
		S2	5.36 (±1.74)	4.53 (±2.01)
	Test - 10-min	Familiar	4.56 (±2.32)	4.19 (±3.02)
		Novel	12.68 (±5.95)	7.68 (±4.28)
	Test - 24-h	Familiar	4.48 (±1.50)	3.48 (±1.72)
		Novel	8.22 (±3.23)	5.21 (±1.48)
OiP	Sample phase	S1	7.08 (±1.41)	6.15 (±1.80)
		S2	4.33 (±1.65)	4.78 (±1.45)
	Test - 10-min	Familiar	3.31 (±2.04)	4.56 (±2.60)
		Novel	5.20 (±3.21)	3.52 (±1.35)
	Test - 24-h	Familiar	4.47 (±2.11)	4.20 (±2.23)
		Novel	6.11 (±2.63)	5.75 (±2.45)
Loc	Sample phase	S1	5.63 (±2.01)	3.71 (±2.24)
		S2	5.00 (±3.03)	3.57 (±2.04)
	Test - 10-min	Familiar	3.68 (±1.61)	3.11 (±1.57)
		Novel	6.00 (±2.01)	6.26 (±3.53)

Figure 3.2: Mean discrimination ratios of 12-month-old Dp1Tyb mice on the NOR (a), OiP (b) and Loc (c) task. Bars originate from a 0.5 discrimination ratio, representing chance. Upward bars indicate preference for novelty, downward bars indicate preference for familiarity. Values are means ± 1 SEM. For NOR and Loc n= 11 WT, 12 Dp1Tyb. For OiP n=11 WT, 11 Dp1Tyb.

a) NOR

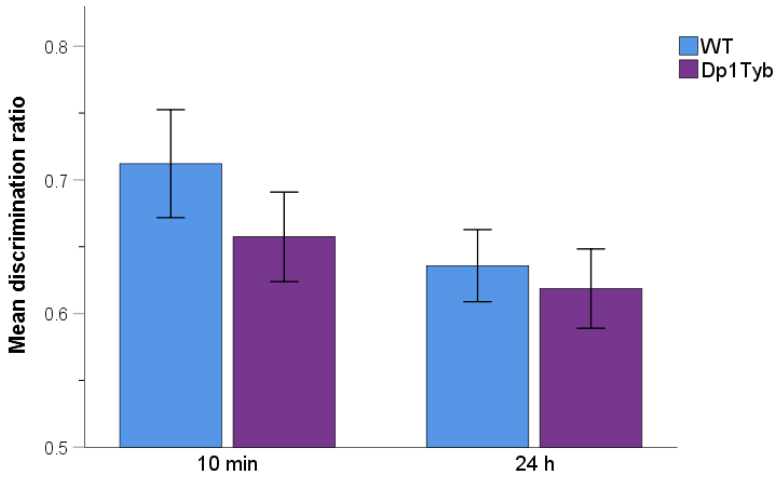

b) OiP

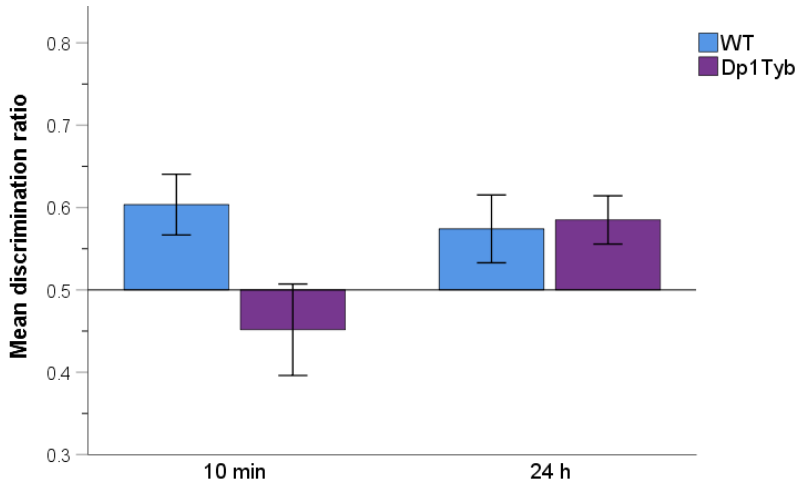

c) Loc

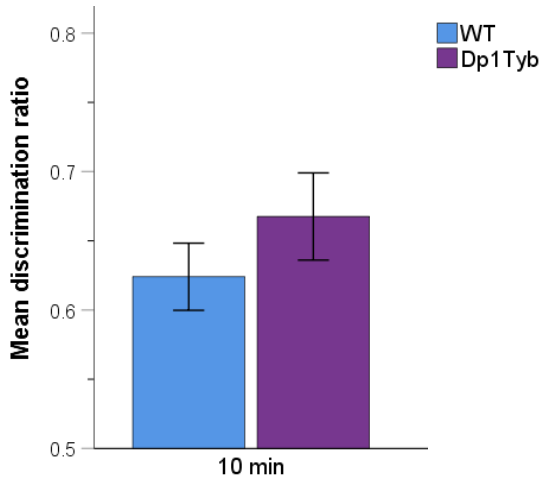

3.3.2. Exp. 1b: Delay-dependent impairment in temporal order memory

To further characterise the pattern of memory deficits in Dp1Tyb mice, the same mice used in Exp. 1a were tested on the TOr task, with a 10-min and a 3-h delay. This allowed assessment of the critical 10-min retention interval on a different feature of associative recognition memory. The TOr task assessed the ability to discriminate between more recently and less recently encountered objects (*what-when*). Unlike other object-recognition memory tasks in which animals were exposed to two identical sample phases, the TOr task employed two different sample phases, effectively halving the time to sample a set of objects. Because a shorter sampling time could influence novelty detection in the test phase, the animals underwent a preliminary experiment to examine novelty detection in the NOR task after a single sample phase, with a 10-min delay (fig. 3.3). Dp1Tyb animals successfully discriminated between novel and familiar objects, implicating that performance on the TOr task would not be a priori impaired by the use of a single sample phase for each object pair. Mean contact times with the objects during sample and test phases of the TOr and 1-sample NOR task are shown in table 3.3.

Figure 3.3: Design of the 1-sample NOR task. Two identical objects were used in the sample phase (S1) and a novel object was presented in the Test phase (T) after a 10-min delay.

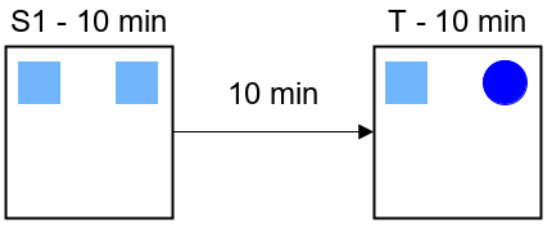

1-sample Novel object recognition task

One WT animal was excluded from this analysis as contact time with the objects during the sample phase met the exclusion criteria (< 3 sec). One Dp1Tyb animal was identified as an outlier as assessed with boxplots and z-scores (smaller / greater ± 3), and excluded from the analysis. Contact times displayed in the single sample phase did not significantly differ between the WT and the Dp1Tyb group (Student's t-test – $t_{(18)}$=0.208, p=0.838). In the test phase, both WT and Dp1Tyb mice displayed significantly higher contact times with the novel than the familiar object, to a similar extent (two-way ANOVA – genotype: $F_{(1,18)}$=1.329, p=0.264; object: $F_{(1,18)}$=12.532, p=0.002; genotype x object: $F_{(1,18)}$=0.038, p=0.847). In line with these results, mean discrimination ratios (fig. 3.4a) were significantly above chance in both the WT and the Dp1Tyb group (one sample t-test – WT:

$t_{(9)}$=2.536, p=0.032; Dp1Tyb: $t_{(9)}$=4.768, p=0.001). Novelty preference was compared between the groups with classical and Bayesian Student's t-tests. Respectively, the tests reported no statistically significant difference between the groups ($t_{(18)}$=1.550, p=0.139) and an estimated Bayes factor (B_{01}) indicating that the data were 1.110 times more likely to occur under H0 than H1. In sum, Dp1Tyb animals were able to detect object novelty after a single sample phase and a 10-min retention interval.

Temporal order task

One Dp1Tyb and one WT animal were excluded from the analysis as contact times with the objects displayed during the sample phases met the exclusion criteria (< 3 sec). During sample phases, Dp1Tyb animals spent significantly less time sampling the objects than wildtypes (two-way ANOVA – genotype: $F_{(1,18)}$=9.866, p=0.006). Contact times remained stable across the two different phases in both groups, indicating that the two pairs of objects were explored to a similar extent (two-way ANOVA – sample phase: $F_{(1,18)}$=0.476, p=0.499; sample phase x genotype: $F_{(1,18)}$=0.118, p=0.735).

In the test phase, intact recognition memory for temporal order information was inferred from higher contact times with less recently presented objects (i.e. old objects) than with more recently encountered objects (i.e. recent objects). Overall, the groups displayed significantly higher contact times with old than recent objects (three-way ANOVA – object: $F_{(1,18)}$=35.440, p<0.001). However, overall contact times were significantly lower in the Dp1Tyb group compared to the WT group (three-way ANOVA – genotype: $F_{(1,18)}$=12.001, p=0.003). The interaction between genotype and object was significant, confirming that WT mice displayed higher contact times than Dp1Tyb mice for both object types and showing that this difference was significantly larger for old than recent objects (three-way ANOVA – genotype x object: $F_{(1,18)}$=5.979, p=0.025; simple main effects of object – WT: $F_{(1,18)}$=35.266, p<0.001; Dp1Tyb: $F_{(1,18)}$=6.153, p=0.023; simple main effects of genotype – old: $F_{(1,18)}$=14.548, p=0.001; recent: $F_{(1,18)}$=6.194, p=0.023). In other words, generally low contact times in the Dp1Tyb group were more evident towards old objects. According to mean contact times (table 3.3), the old object preference in the Dp1Tyb was particularly low on the 10-min test. There was however no significant difference between the tested delays, in either group and towards either object type (three-way ANOVA – delay: $F_{(1,18)}$=2.612, p=0.123; delay x genotype: $F_{(1,18)}$=0.577, p=0.457; delay x object: $F_{(1,18)}$=0.035, p=0.854; delay x genotype x object: $F_{(1,18)}$=1.725, p=0.206).

To account for the difference in overall contact time, mean discrimination ratios were analysed (fig. 3.4b). In the WT group, mean discrimination ratios were significantly above chance on both the 10-min and the 3-h test (one sample t-test – $WT_{10\text{-}min}$: $t_{(9)}$=4.040, p=0.003; $WT_{3\text{-}h}$: $t_{(9)}$=2.920, p=0.017). In the Dp1Tyb group instead, only the 3-h mean discrimination ratio was significantly above chance (one sample t-test – $Dp1Tyb_{10\text{-}min}$:

$t_{(9)}$=0.126, p=0.903; Dp1Tyb$_{3\text{-}h}$: $t_{(9)}$=2.947, p=0.016). Despite these findings, group differences failed to reach statistical significance (two-way ANOVA – genotype: $F_{(1,18)}$=3.502, p=0.078; genotype x delay: $F_{(1,18)}$=3.592, p=0.074). Overall, the tested delay did not significantly affect novelty preference (two-way ANOVA – delay: $F_{(1,18)}$=0.230, p=0.637).

Although ANOVAs are theoretically robust against violations of the underlying assumptions (Blanca, Alarcón, Arnau, Bono, & Bendayan, 2017), the distribution of the discrimination ratios violated the assumption of normality in the Dp1Tyb group at the 10-min delay. Therefore, mean discrimination ratios were further analysed with classical and Bayesian Mann-Whitney U-tests. At the 10-min delay, Dp1Tyb animals performed significantly lower than WT animals (U=20, p=0.023) and the estimated Bayes factor (B_{01}) reported that these data were only 0.253 times more likely to occur under H0 than H1. At the 3-h delay, there was no significant difference between the groups (U=58, p=0.579) and the estimated Bayes factor (B_{01}) reported that these data were 2.147 times in favour of H0.

Together, these findings report that Dp1Tyb animals were not able to discriminate between old and recent objects after the 10-min interval, while temporal order discrimination was intact following the 3-h retention interval. Additionally, Dp1Tyb mice generally displayed reduced contact times.

Table 3.3: Mean contact times of 12-month-old Dp1Tyb mice in the TOr and 1-sample NOR task. Sample phases comprised a total of two objects, different for each phase. Test phases comprised one novel / old and one familiar / recent object. Values are mean contact times with one object, ± 1 SD. n= 10 WT, 10 Dp1Tyb.

			Mean contact times (sec)	
			WT	**Dp1Tyb**
TOr	Sample	S1	7.89 (±1.87)	5.12 (±2.16)
		S2	7.45 (±2.04)	4.98 (±2.25)
	Test - 10-min	Recent	5.37 (±1.49)	4.70 (±1.50)
		Old	8.40 (±2.67)	5.18 (±2.41)
	Test - 3-h	Recent	7.72 (±3.04)	4.78 (±2.40)
		Old	9.85 (±3.63)	6.46 (±3.42)
1-sample NOR	Sample	S1	5.04 (±1.32)	4.84 (±2.77)
	Test – 10-min	Familiar	5.08 (±1.62)	3.58 (±2.02)
		Novel	7.26 (±3.76)	6.01 (±4.00)

Figure 3.4: Mean discrimination ratios of 12-month-old Dp1Tyb mice on the 1-sample NOR (a) and TOr (b) task. Bars originate from a 0.5 discrimination ratio, representing chance. Upward bars indicate preference for novel resp. old objects, downward bars indicate preference for familiar resp. recent objects. Values are means ± 1 SEM. n= 10 WT, 10 Dp1Tyb.

a) 1-sample NOR

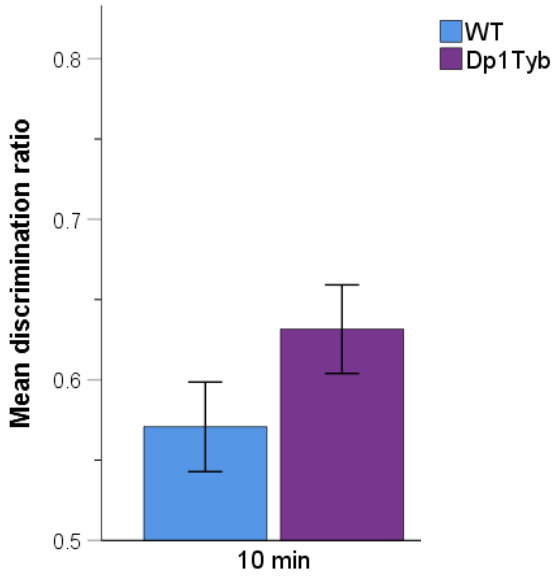

b) TOr

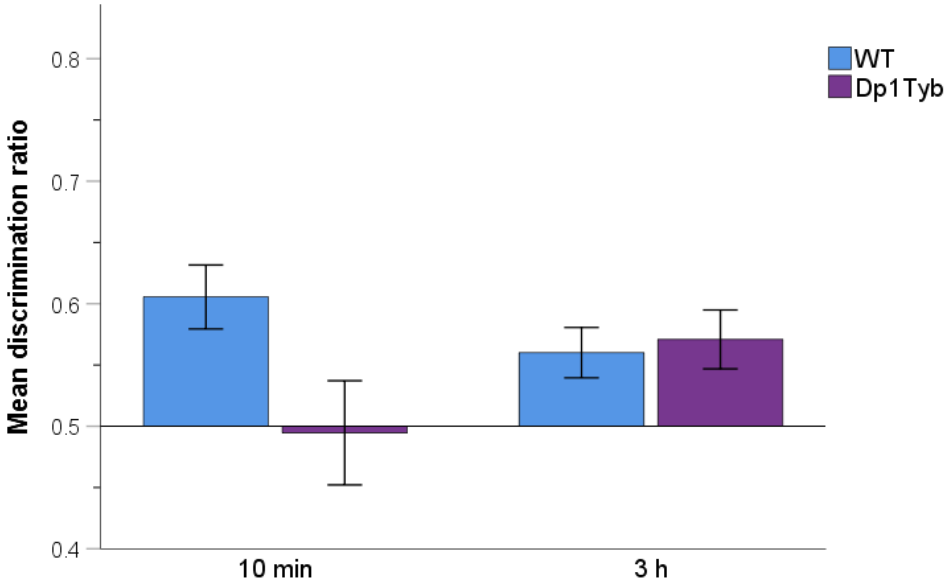

3.3.3. Exp. 1c: Ageing did not impair memory for objects

Mouse models of Aβ-pathology report impairments in novel object recognition, especially following long-term delays (Hall et al., 2016; Webster et al., 2014). To determine whether the Mmu16 trisomy – which includes the *App* gene – in conjunction with ageing had detrimental effects on memory performance, the animals used in Exp. 1a and 1b were re-tested on the NOR task at 20 months of age, with a 10-min and a 24-h delay. Mean contact times with the objects during sample and test phases of the NOR task are shown in table 3.4.

Novel object recognition task

During the sample phases, Dp1Tyb and WT animals displayed similar object sampling behaviour (two-way ANOVA – genotype: $F_{(1,14)}$=1.532, p=0.236). Unexpectedly, habituation did not take place in either group, as indicated by stable contact times across the two identical sample phases (two-way ANOVA – sample phase: $F_{(1,14)}$=2.533, p=0.134; sample phase x genotype: $F_{(1,14)}$=0.263, p=0.616).

In the test phase, contact times were significantly higher with novel than familiar objects and, in contrast to NOR findings in Exp. 1a, there was no difference between the groups (three-way ANOVA – object: $F_{(1,14)}$=76.041, p<0.001; genotype: $F_{(1,14)}$=0.669, p=0.427; genotype x object: $F_{(1,14)}$=0.095, p=0.762). As observed in Exp.1a, contact times were generally lower at the 24-h than the 10-min delay (three-way ANOVA – delay: $F_{(1,14)}$=10.091, p=0.007). This decrease was once again due to significantly reduced contacts with novel objects on the 24-h test, in both groups (three-way ANOVA – delay x object: $F_{(1,14)}$=5.636, p=0.032; simple main effects of delay – familiar: $F_{(1,14)}$=2.346, p=0.148; novel: $F_{(1,14)}$=12.368, p=0.003; two-way ANOVA – delay x genotype: $F_{(1,14)}$=0.470, p=0.504; delay x genotype x object: $F_{(1,14)}$=2.373, p=0.146).

In line with the above findings, mean discrimination ratios (fig. 3.5) were significantly above chance in both the WT and the Dp1Tyb group, for the 10-min and the 24-h delay (one sample t-test – $WT_{10\text{-}min}$: $t_{(8)}$=16.807, p<0.001; $WT_{24\text{-}h}$: $t_{(8)}$=4.970, p=0.001; $Dp1Tyb_{10\text{-}min}$: $t_{(6)}$=5.418, p=0.002; $Dp1Tyb_{24\text{-}h}$: $t_{(6)}$=9.014, p<0.001). Surprisingly, novelty preference was numerically higher in the Dp1Tyb group but the difference failed to reach statistical significance (two-way ANOVA – genotype: $F_{(1,14)}$=3.663, p=0.076). Although the contact time analysis reported lower contacts with novel objects at the 24-h delay, mean discrimination ratios did not significantly differ between the delays, in either group (two-way ANOVA – delay: $F_{(1,14)}$=0.818, p=0.381; genotype x delay: $F_{(1,14)}$=0.411, p=0.532).

To further investigate whether Dp1Tyb animals performed normally, mean discrimination ratios were compared between groups with Bayesian statistics. Estimated Bayes factors (B_{01}) reported that the data were 1.762 times more likely to occur under H0

than H1 for the 10-min delay but were only 0.861 times in favour of H0 for the 24-h delay. To corroborate the Bayesian results, performance on the 24-h test was directly compared between the groups with a classical Student's t-test, reporting no significant difference ($t_{(14)}$=1.775, p=0.098).

Together, these findings indicate that even at 20 months of age, Dp1Tyb animals were able to discriminate between familiar and novel objects, after the 10-min and the 24-h retention interval.

Table 3.4: Mean contact times of 20-month-old Dp1Tyb mice in the NOR task. Sample phases comprised a total of three objects. Test phases comprised one novel and two familiar objects. Values are mean contact times with one object, ± 1 SD. n= 9 WT, 7 Dp1Tyb.

			Mean contact times (sec)	
			WT	**Dp1Tyb**
NOR	Sample	S1	14.20 (±4.47)	10.66 (±6.83)
		S2	11.84 (±4.22)	9.46 (±5.58)
	Test - 10-min	Familiar	10.78 (±3.91)	9.26 (±9.66)
		Novel	30.60 (±10.80)	24.36 (±12.64)
	Test - 24-h	Familiar	8.61 (±4.56)	5.84 (±4.65)
		Novel	19.08 (±8.35)	18.95 (±9.53)

Figure 3.5: Mean discrimination ratios of 20-month-old Dp1Tyb mice on the NOR task. Bars originate from a 0.5 discrimination ratio, representing chance. Upward bars indicate preference for novelty, downward bars indicate preference for familiarity. Values are means ± 1 SEM. n= 9 WT, 7 Dp1Tyb.

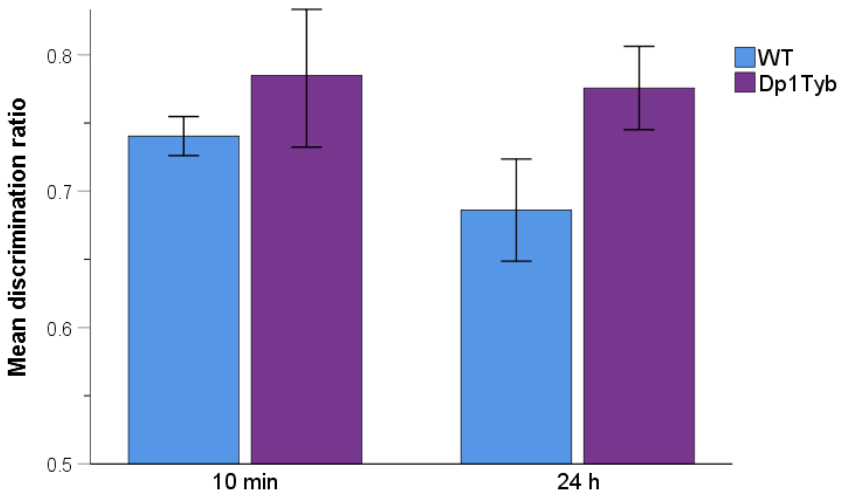

3.3.4. Exp. 1d: Delay-dependent memory impairments at young age

To determine whether the 10-min impairment in associative-recognition memory observed in Exp.1a and 1b emerged in adulthood or was present already at younger age, a cohort of 4-month-old Dp1Tyb was tested on the OiP task, with a 10-min and a 3-h delay. The 3-h delay was chosen as pilot tests revealed the 24-h retention interval was too challenging for animals of this age to successfully discriminate between novel and familiar object-in-place associations. Mean contact times with the objects during sample and test phases of the OiP task are shown in table 3.5.

Object-in-place task

Two WT and one Dp1Tyb animal were excluded from the analysis due to insufficient contact times with the objects during the sample phases (< 3 sec). During the first sample phase, Dp1Tyb mice spent significantly more time sampling the objects than wildtypes, while there was no group difference in the second sample phase (two-way ANOVA – genotype: $F_{(1,18)}$=1.873, p=0.188; sample phase: $F_{(1,18)}$=8.187, p=0.010; genotype x sample phase: $F_{(1,18)}$=4.996, p=0.038; simple main effects of genotype – S1: $F_{(1,18)}$=5.467, p=0.031; S2: $F_{(1,18)}$<0.001, p=0.998). Contact times decreased significantly across the two sample phases in the Dp1Tyb group, while contact times in the WT group did not decrease further in the second sample phase (simple main effects of sample phase – Dp1Tyb: $F_{(1,18)}$=14.430, p=0.001; WT: $F_{(1,18)}$=0.178, p=0.678).

In the test phase, overall contact times were significantly higher with objects that exchanged location (i.e. novel place objects) than with stationary objects (i.e. familiar place objects), and did not differ between the groups, at either delay (three-way ANOVA – object: $F_{(1,18)}$=4.868, p=0.041; genotype: $F_{(1,18)}$=2.630, p=0.122; genotype x delay: $F_{(1,18)}$=0.301, p=0.590; genotype x object: $F_{(1,18)}$=0.161, p=0.693; delay: $F_{(1,18)}$=1.320, p=0.266; delay x object: $F_{(1,18)}$=0.619, p=0.442). Nonetheless, similarly to OiP findings in Exp. 1a, mean contact times (table 3.5) indicate that while Dp1Tyb animals preferred novel place objects at the 3-h delay, this was clearly not the case at the 10-min delay. This interaction just failed however to meet statistical significance (three-way ANOVA – genotype x delay x object: $F_{(1,18)}$=12.653, p=0.066).

In line with mean contact times, mean discrimination ratios (fig. 3.6) for the 10-min delay were significantly above chance in the WT but not the Dp1Tyb group (one sample t-test – $WT_{10\text{-}min}$: $t_{(8)}$=3.454, p=0.009; $Dp1Tyb_{10\text{-}min}$: $t_{(10)}$=0.750, p=0.471). Instead, mean discrimination ratios for the 3-h delay were significantly above chance in the Dp1Tyb but not the WT group (one sample t-test – $WT_{3\text{-}h}$: $t_{(8)}$=1.842, p=0.103; $Dp1Tyb_{3\text{-}h}$: $t_{(10)}$=2.222, p=0.050). In agreement with these results, differences between the mean discrimination ratios of the groups approached statistical significance, suggesting a weaker novel place

preference in the Dp1Tyb on the 10-min test (two-way ANOVA – genotype: $F_{(1,18)}$=3.825, p=0.066; genotype x delay: $F_{(1,18)}$=4.335, p=0.052). Overall, novelty preference did not differ between the two tested delays (two-way ANOVA – delay: $F_{(1,18)}$=0.728, p=0.405).

To further investigate whether Dp1Tyb mice performed normally, mean discrimination ratios were compared between the groups with Bayesian statistics. For the 10-min delay, the estimated Bayes factor (B_{01}) reported that the data were only 0.091 times more likely to occur under H0 than H1. Instead, for the 3-h delay the data were 2.505 times in favour of H0. To corroborate the Bayesian results, classical Student's t-tests were carried out. Novelty preference was significantly lower in the Dp1Tyb group compared to the WT group at the 10-min delay, but there was no difference at the 3-h delay (10-min: $t_{(18)}$=3.343, p=0.004; 3-h: $t_{(18)}$=0.057, p=0.955).

These findings are similar to the results of Exp.1a, indicating that at 4 months of age, Dp1Tyb animals were less sensitive to changes in object-in-place associations. Once again, memory impairments were restricted to the 10-min retention interval.

Table 3.5: Mean contact times of 4-month-old Dp1Tyb mice in the OiP task. Sample phases comprised a total of three objects. Test phases comprised two novel place and one familiar place object. Values are mean contact times with one object, ± 1 SD. n= 9 WT, 11 Dp1Tyb.

			Mean contact times (sec)	
			WT	**Dp1Tyb**
OiP	Sample	S1	5.10 (±2.26)	7.40 (±2.14)
		S2	4.78 (±2.34)	4.78 (±2.09)
	Test - 10-min	Familiar	2.51 (±1.57)	5.09 (±1.91)
		Novel	4.33 (±2.30)	4.89 (±2.25)
	Test - 3-h	Familiar	4.37 (±4.72)	4.45 (±2.37)
		Novel	5.23 (±2.70)	6.50 (±3.43)

Figure 3.6: Mean discrimination ratios of 4-month-old Dp1Tyb mice on the OiP task. Bars originate from a 0.5 discrimination ratio, representing chance. Upward bars indicate preference for novelty, downward bars indicate preference for familiarity. Values are means ± 1 SEM. **p<0.01. n= 9 WT, 11 Dp1Tyb.

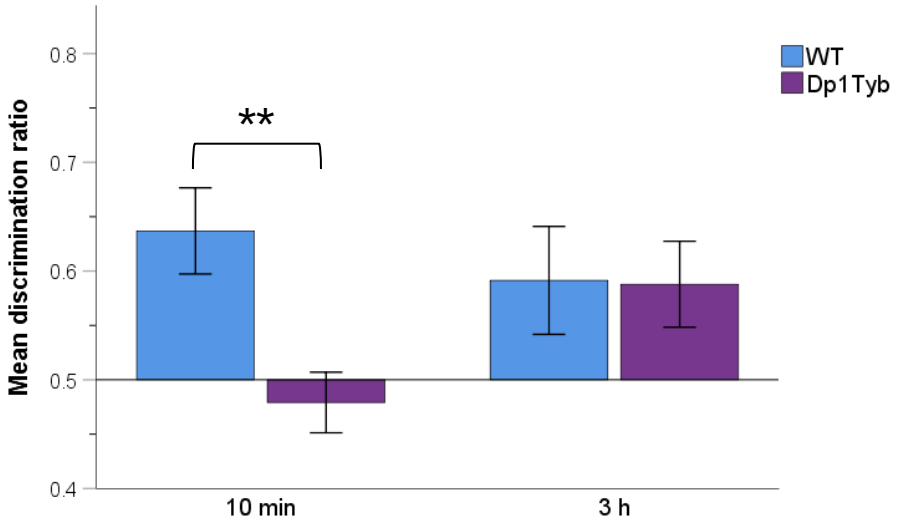

3.3.5. Exp. 1e: Increased anxiety and activity levels on the EPM

The EPM test was used to assess anxiety and general locomotor activity levels in adult (12-month-old) Dp1Tyb animals. The exploratory behaviour of the animal during a 5-min trial on the EPM was tracked with a computerised system (EthoVision XT 13) and compared between closed and open arms.

All WT mice visited the open arms of the maze, while one Dp1Tyb animal did not enter them and remained within closed arms throughout the entire trial duration. On average, Dp1Tyb mice spent over twice as much time exploring closed arms than open arms, while wildtypes showed no clear preference between the two arm types (table 3.6). Respectively, the WT and the Dp1Tyb group spent ~47% and ~32% of the trial time within the open arms of the maze (fig. 3.7a), a difference that was however not statistically significant (Student's t-test – $t_{(17)}$=1.346, p=0.196. On average, Dp1Tyb entered open arms for the first time after ~22 seconds on the EPM, taking significantly longer compared to the ~9 second latency displayed by wildtypes (fig. 3.7b) (Student's t-test, equal variances not assumed – $t_{(11)}$=2.395, p=0.035). One Dp1Tyb animal was excluded from this comparison since it was identified as an outlier (latency = 105 sec) as assessed with boxplots and z-scores (smaller / greater ± 3) .Dp1Tyb displayed 21 head dips in contrast to 31 in the WT group, but this difference was not statistically significant (table 3.6) (Student's t-test – $t_{(17)}$=1.433, p=0.170).

The locomotor activity of Dp1Tyb and WT animals on the EPM per minute is shown in fig. 3.7c. Overall, there was no difference in the locomotor behaviour of the two groups and activity decreased significantly over time in both the WT and the Dp1Tyb group, indicating habituation to the maze (two-way ANOVA Greenhouse-Geisser corrected – genotype: $F_{(1,17)}$=1.780, p=0.200; time: $F_{(3,46)}$=8.227, p<0.001; genotype x time: $F_{(3,46)}$=1.664, p=0.192). In fact, in both groups the distance moved during the last trial minute was significantly lower compared to the first minute (paired t-test – WT: $t_{(7)}$=3.369, p=0.012; Dp1Tyb: $t_{(10)}$=3.326, p=0.008).

A comparison between the two arm types (fig. 3.7d) revealed that throughout the entire trial, Dp1Tyb mice moved a significantly larger distance than WT in closed arms and that while Dp1Tyb moved significantly more in closed than open arms, WT didn't show a preference for either arm type (two-way ANOVA – genotype: $F_{(1,17)}$=1.833, p=0.194; arm type: $F_{(1,17)}$=18.992, p<0.001; arm type x genotype: $F_{(1,17)}$=7.553, p=0.014; simple main effects of arm type – WT: $F_{(1,17)}$=1.119, p=0.305; Dp1Tyb: $F_{(1,17)}$=29.984, p<0.001; simple main effects of genotype – closed arms, Welch's corrected: $F_{(1,15)}$=6.268, p=0.024; open arms: $F_{(1,17)}$=1.782, p=0.199).

The total number of arm entries did not significantly differ between the two groups, but Dp1Tyb mice entered closed arms a significantly higher number of times compared to wildtypes, showing instead a significant preference for entering open over closed arms (fig.

3.7e) (two-way ANOVA – genotype: $F_{(1,17)}$=0.034, p=0.857; arm type: $F_{(1,17)}$=7.715, p=0.013; arm type x genotype: $F_{(1,17)}$=7.303, p=0.015; simple main effects of arm type – WT: $F_{(1,17)}$=12.968, p=0.002; Dp1Tyb: $F_{(1,17)}$=0.003, p=0.954; simple main effects of genotype – closed arms, Welch's corrected: $F_{(1,16)}$=5.065, p=0.039; open arms: $F_{(1,17)}$=1.474, p=0.241). Overall, there was no difference in the mean velocity of WT and Dp1Tyb mice, and both groups moved significantly more slowly in open than in closed arms (table 3.6) (two-way ANOVA – genotype: $F_{(1,16)}$=1.420, p=0.251; arm type: $F_{(1,16)}$=20.121, p<0.001; arm type x genotype: $F_{(1,16)}$=1.596, p=0.225).

Together, these results indicate that Dp1Tyb mice were less prone than WT littermates to explore open arms, suggesting increased anxiety levels. Dp1Tyb also reported signs of increased locomotor activity, but exclusively within closed arms. Representative locomotor tracks and mean heat maps are shown in fig. 3.8.

Figure 3.7: Explorative behaviour of Dp1Tyb mice on the EPM (a-e). Values are means ± 1 SEM, *p<0.05, **p<0.01, ***p<0.001. n = 8 WT, 11 Dp1Tyb.

a) Proportion of time in open arms

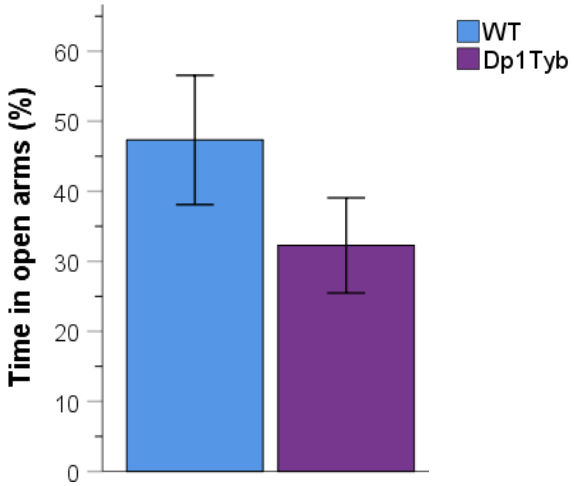

b) Latency to first open arm entry

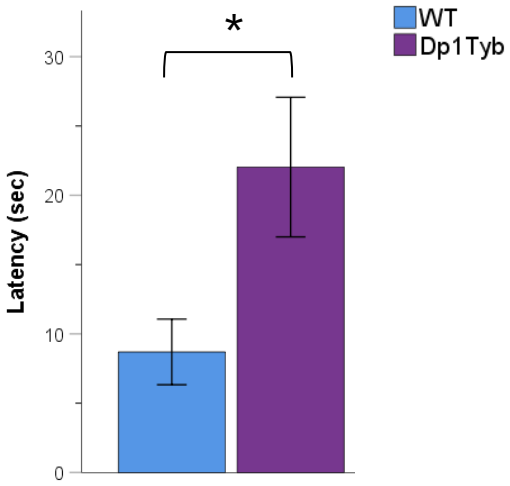

c) Overall distance moved per minute

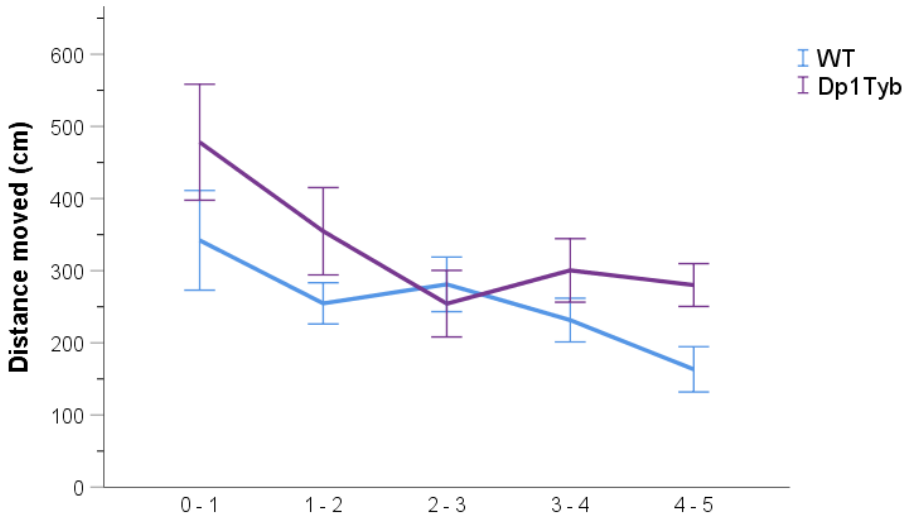

d) Distance moved per arm type

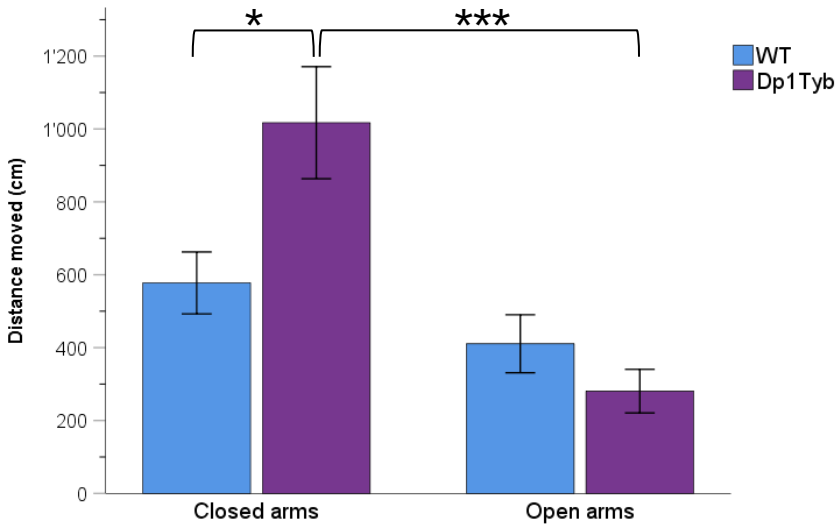

e) Number of entries

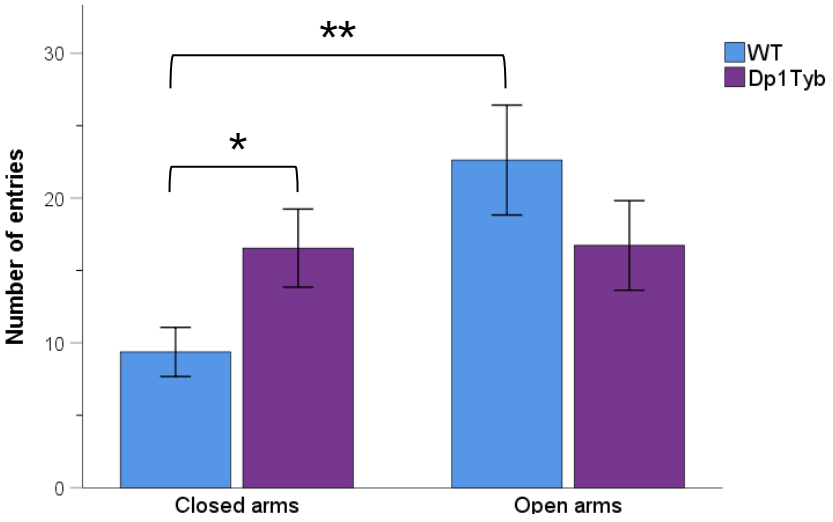

Table 3.6: Explorative behaviour of Dp1Tyb mice on the EPM. Values are means ± 1 SD. No significant differences between the groups. n = 8 WT, 11 Dp1Tyb.

	WT		Dp1Tyb	
	Closed arms	Open arms	Closed arms	Open arms
Time (sec)	124.19 (±63.01)	111.24 (±62.49)	163.07 (±64.13)	75.95 (±55.93)
Head dips (freq)		31 (±16.39)		21.36 (±12.97)
Velocity (cm/sec)	5.83 (±3.05)	3.61 (±1.03)	7.15 (±3.77)	3.83 (±1.31)

Figure 3.8: Representative locomotor tracks and mean heat maps of Dp1Tyb mice on the EPM. a) WT group; b) Dp1Tyb group. On the tracking, closed arms are represented in orange, open arms in pink and the centre in light blue. For heat maps, warmer and colder colours indicate longer and shorter exploration times respectively. n = 8 WT, 11 Dp2Yey.

a) WT

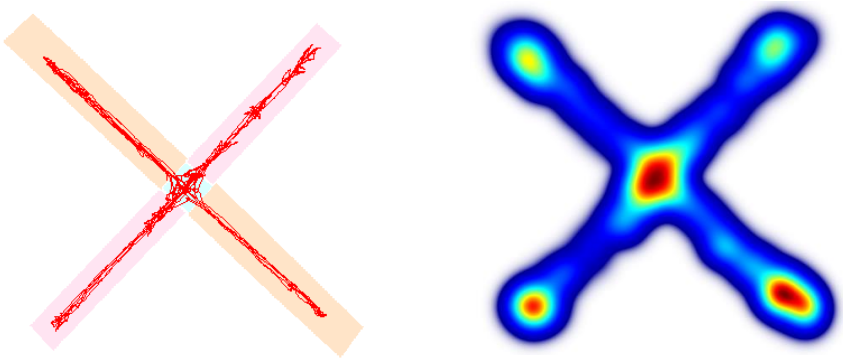

b) Dp1Tyb

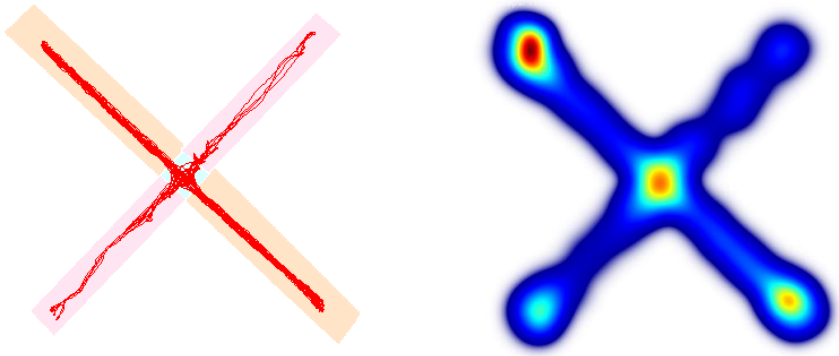

3.4. Dp3Yey results

To characterise the behavioural phenotypes associated to trisomy of the Mmu17 conserved region, Dp3Yey animals underwent two experiments employing object-recognition memory tasks (Exp. 2a and 2b) and the EPM test (Exp. 2c).

3.4.1. Exp. 2a: Intact recognition memory

Dp3Yey and their WT littermates were first tested on the NOR (*what*) and the OiP (*what-where*) task at 13 months of age, each with a 10-min and a 24-h delay. The results are reported separately for each task. Mean contact times with the objects during sample and test phases are shown in table 3.7.

Novel Object recognition task

During the sample phases, WT and Dp3Yey animals displayed similar contact times with the objects (two-way ANOVA – genotype: $F_{(1,22)}<0.001$, $p=0.998$). Habituation took place in both groups, as indicated by significantly reduced contact times across the two sample phases (two-way ANOVA – sample phase: $F_{(1,22)}=56.125$, $p<0.001$; genotype x sample phase: $F_{(1,22)}=0.038$, $p=0.848$).

In the test phase, intact recognition memory for objects was inferred from higher contact times with novel objects. Overall, both groups displayed significantly higher contact times with novel than familiar objects, on both the 10-min and the 24-h test (three-way ANOVA – object: $F_{(1,22)}=34.626$, $p<0.001$; genotype: $F_{(1,22)}=1.739$, $p=0.201$; genotype x object: $F_{(1,22)}=0.273$, $p=0.606$). Contact times did not differ between the tested delays, in either group and for either object type (three-way ANOVA – delay: $F_{(1,22)}=0.803$, $p=0.380$; delay x genotype: $F_{(1,22)}=0.044$, $p=0.835$; delay x object: $F_{(1,22)}=0.197$, $p=0.661$; delay x genotype x object: $F_{(1,22)}=0.047$, $p=0.830$).

Mean discrimination ratios (fig. 3.9a) were analysed to investigate preference for novelty independently of total contact time during the test phase. In line with the above findings, mean discrimination ratios were significantly above chance in both the WT and the Dp3Yey group, for the 10-min and the 24-h delay (one sample t-test – $WT_{10\text{-}min}$: $t_{(11)}=2.876$, $p=0.015$; $WT_{24\text{-}h}$: $t_{(11)}=2.351$, $p=0.038$; $Dp3Yey_{10\text{-}min}$: $t_{(11)}=3.325$, $p=0.007$; $Dp3Yey_{24\text{-}h}$: $t_{(11)}=4.970$, $p<0.001$). Novelty preference did not differ between the groups at either delay and delay did not significantly affect novelty preference (two-way ANOVA – genotype: $F_{(1,22)}=0.155$, $p=0.698$; delay: $F_{(1,22)}=0.447$, $p=0.511$; genotype x delay: $F_{(1,22)}=0.008$, $p=0.928$). To confirm that Dp3Yey animals performed normally, mean discrimination ratios were further compared with Bayesian statistics. The estimated Bayes factors (B_{01}) reported that the data were 2.634 times and 2.522 times more likely to occur under H0 than H1 for the 10-min and the 24-h delay respectively.

Dp3Yey animals were therefore able to discriminate between familiar and novel objects similar to WT levels, both after the 10-min and the 24-h retention interval.

Object-in-place task

During the sample phases, there was again no difference between Dp3Yey and WT animals, and contact times dropped significantly across the two identical sample phases (two-way ANOVA – genotype: $F_{(1,22)}$=0.014, p=0.906; sample phase: $F_{(1,22)}$=47.275, p<0.001; genotype x sample phase: $F_{(1,22)}$=0.269, p=0.609).

In the test phase, intact memory for object-in-place associations was inferred from higher contact times with objects that exchanged position (i.e. novel place objects) than with stationary objects (i.e. familiar place objects). Overall, both groups displayed significantly higher contact times with novel place than familiar place objects, on both the 10-min and the 24-h test (three-way ANOVA – object: $F_{(1,22)}$=35.030, p<0.001; genotype: $F_{(1,22)}$<0.001, p=0.985; genotype x object: $F_{(1,22)}$=0.125, p=0.727; delay x genotype: $F_{(1,22)}$=0.002, p=0.967). The tested delay did not significantly affect contact times (three-way ANOVA – delay: $F_{(1,22)}$=2.906, p=0.102; delay x object: $F_{(1,22)}$=0.680, p=0.418; delay x genotype x object: $F_{(1,22)}$=0.181, p=0.674).

In line with the above findings, mean discrimination ratios (fig. 3.9b) were significantly above chance in both the WT and the Dp3Yey group, for the 10-min and the 24-h delay (one sample t-test – $WT_{10\text{-}min}$: $t_{(11)}$=3.345, p=0.007; $WT_{24\text{-}h}$: $t_{(11)}$=3.398, p=0.006; $Dp3Yey_{10\text{-}min}$: $t_{(11)}$=3.452, p=0.005; $Dp3Yey_{24\text{-}h}$: $t_{(11)}$=3.113, p=0.010). Novel place preference did not differ between the groups at either delay and delay did not significantly affect novelty preference (two-way ANOVA – genotype: $F_{(1,22)}$=0.190, p=0.667; delay: $F_{(1,22)}$=2.192, p=0.153; genotype x delay: $F_{(1,22)}$=0.818, p=0.376). To confirm that Dp3Yey animals performed normally, mean discrimination ratios were further compared with Bayesian statistics. Estimated Bayes factors (B_{01}) reported that the data were 2.623 times and 1.644 times more likely to occur under H0 than H1 for the 10-min and the 24-h delay respectively.

Together, these findings indicate that Dp3Yey animals were consistently able to discriminate between novel and familiar object-in-place associations similar to WT levels, both after the 10-min and the 24-h retention interval.

Table 3.7: Mean contact times of 13-month-old Dp3Yey mice in object-recognition memory tasks. Sample phases comprised a total of three objects. Test phases comprised one novel and two familiar objects in the NOR, and two novel and one familiar place object in the OiP task. Values are mean contact times with one object, ± 1 SD. n= 12 WT, 12 Dp3Yey.

			Mean contact times (sec)	
			WT	**Dp3Yey**
NOR	Sample phase	S1	13.70 (±4.33)	13.82 (±4.82)
		S2	9.11 (±2.83)	8.99 (±2.16)
	Test - 10-min	Familiar	8.56 (±2.87)	7.37 (±3.78)
		Novel	13.48 (±5.96)	11.28 (±4.93)
	Test - 24-h	Familiar	9.85 (±3.17)	8.06 (±3.27)
		Novel	13.95 (±6.49)	11.69 (±4.77)
OiP	Sample phase	S1	13.22 (±5.17)	12.70 (±4.73)
		S2	8.37 (±2.69)	8.53 (±3.20)
	Test - 10-min	Familiar	7.18 (±3.11)	7.23 (±4.41)
		Novel	11.32 (±5.12)	11.39 (±4.56)
	Test - 24-h	Familiar	8.73 (±4.51)	9.18 (±3.47)
		Novel	12.44 (±3.30)	11.99 (±4.88)

Figure 3.9: Mean discrimination ratios of 13-month-old Dp3Yey mice on the NOR (a) and OiP (b) task. Bars originate from a 0.5 discrimination ratio, representing chance. Upward bars indicate preference for novelty, downward bars indicate preference for familiarity. Values are means ± 1 SEM. n= 12 WT, 12 Dp3Yey.

a) NOR

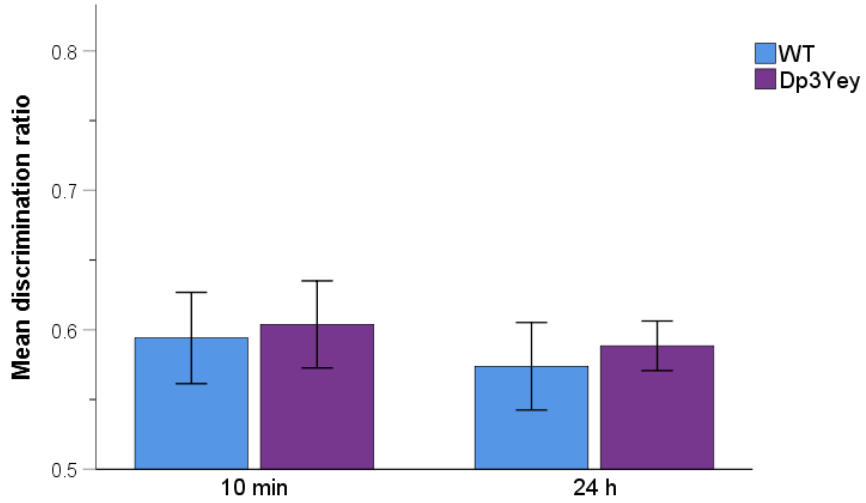

b) OiP

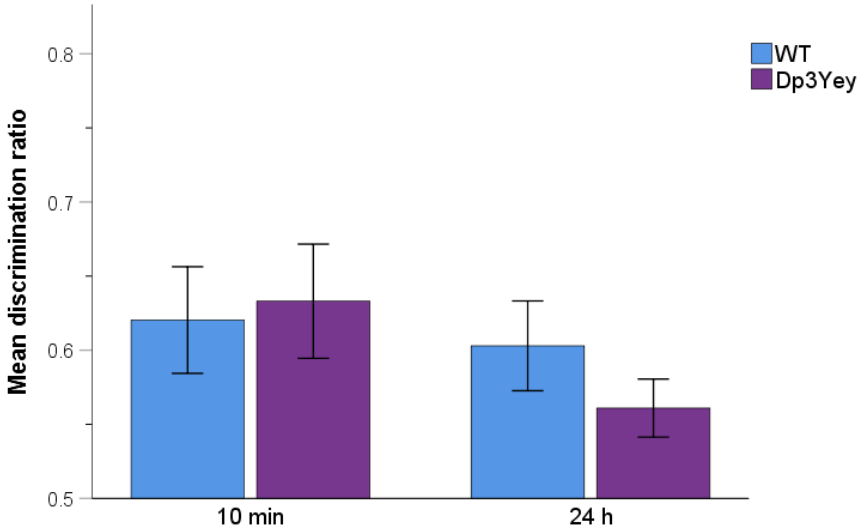

3.4.2. Exp. 2b: Ageing did not impair recognition memory

To determine whether the Mmu17 trisomy in conjunction with ageing processes had detrimental effects on memory performance, a cohort of Dp3Yey animals was tested on the NOR and the OiP task at 18 months of age, with a 10-min and a 3-h delay. The 3-h delay was chosen as previous data revealed that the 24-h retention interval failed to consistently produce preference for novelty in wildtypes. Results are reported separately for each task. Mean contact times with the objects during sample and test phases are reported in table 3.8.

Novel Object recognition task

During the sample phases, Dp3Yey and WT mice showed similar object sampling behaviour (two-way ANOVA – genotype: $F_{(1,19)}$=0.603, p=0.447). Although contact times dropped from the first to the second sample phase in both groups (table 3.8), this effect just failed to reach statistical significance (two-way ANOVA – sample phase: $F_{(1,19)}$=3.810, p=0.066; sample phase x genotype: $F_{(1,19)}$=0.086, p=0.772).

In the test phase, both groups displayed significantly higher contact times with novel than familiar objects, on both the 10-min and the 3-h test (three-way ANOVA – object: $F_{(1,19)}$=22.544, p<0.001; genotype: $F_{(1,19)}$=0.186, p=0.671; genotype x object: $F_{(1,19)}$=0.006, p=0.940; delay x genotype: $F_{(1,19)}$=0.421, p=0.524). The tested delay did not significantly affect contact times, in either group and for either object type (three-way ANOVA – delay: $F_{(1,19)}$=0.339, p=0.567; delay x object: $F_{(1,19)}$=0.025, p=0.875; delay x genotype x object: $F_{(1,19)}$=1.550, p=0.228).

Similarly to what was observed in Exp.1a with younger mice, mean discrimination ratios (fig. 3.10a) were significantly above chance in both the WT and the Dp3Yey group, for the 10-min and the 3-h delay (one sample t-test – $WT_{10\text{-}min}$: $t_{(8)}$=3.695, p=0.006; $WT_{3\text{-}h}$: $t_{(8)}$=4.720, p=0.002; $Dp3Yey_{10\text{-}min}$: $t_{(11)}$=2.930, p=0.014; $Dp3Yey_{3\text{-}h}$: $t_{(11)}$=4.444, p=0.001). Novelty preference did not differ between the groups at either delay and delay did not significantly affect novelty preference (two-way ANOVA – genotype: $F_{(1,19)}$=0.082, p=0.778; delay: $F_{(1,19)}$=0.164, p=0.690; genotype x delay: $F_{(1,19)}$=0.413, p=0.528). To confirm that Dp3Yey animals performed normally, mean discrimination ratios were further compared with Bayesian statistics. Estimated Bayes factors (B_{01}) reported that the data were 2.287 times and 2.477 times more likely to occur under H0 than H1 for the 10-min and the 3-h delay respectively.

Together, these findings indicate that ageing did not influence the ability of Dp3Yey animals to discriminate between familiar and novel objects similar to WT levels, both after the 10-min and the 3-h retention interval.

Object-in-place task

One Dp3Yey animal was excluded from this analysis due to insufficient contact times (< 3 sec) and one WT animal was excluded as it fell ill during the experimental period. In the sample phases, there was again no difference between the groups and contact times dropped significantly across the two sample phases (two-way ANOVA – genotype: $F_{(1,17)}$=1.301, p=0.270; sample phase: $F_{(1,17)}$=5.201, p=0.036; genotype x sample phase: $F_{(1,17)}$=0.025, p=0.876).

In the test phase, both WT and Dp3Yey mice displayed significantly higher contact times with novel place than familiar place objects, although overall contact times were significantly higher in the Dp3Yey than WT group (three-way ANOVA – object: $F_{(1,17)}$=29.118, p<0.001; genotype: $F_{(1,17)}$=4.805, p=0.043; genotype x object: $F_{(1,17)}$=0.132, p=0.721). Once again, the tested delay did not significantly affect contact times in either group, for either object type (three-way ANOVA – delay: $F_{(1,17)}$=0.010, p=0.922;, p=0.454; delay x genotype: $F_{(1,17)}$=0.588; delay x object: $F_{(1,17)}$=0.578, p=0.458; delay x genotype x object: $F_{(1,17)}$=0.064, p=0.804).

Similarly to what was observed in Exp. 2a with younger mice, mean discrimination ratios (fig. 3.10b) were significantly above chance at both delays in the WT group and were at the edge of significance and significantly above chance in the Dp3Yey group for the 10-min and the 3-h delay respectively (one sample t-test – $WT_{10\text{-}min}$: $t_{(7)}$=3.426, p=0.011; $WT_{3\text{-}h}$: 2.612, p=0.035; $Dp3Yey_{10\text{-}min}$: $t_{(10)}$=2.194, p=0.053; $Dp3Yey_{3\text{-}h}$: $t_{(10)}$=2.705, p=0.022). Novelty preference did not differ between the groups at either delay and delay did not significantly affect novelty preference (two-way ANOVA – genotype: $F_{(1,17)}$=0.190, p=0.669; delay: $F_{(1,17)}$=0.012, p=0.916; genotype x delay: $F_{(1,17)}$<0.001, p=0.993). To confirm that Dp3Yey animals performed normally, mean discrimination ratios were further compared with Bayesian statistics. Estimated Bayes factors (B_{01}) reported that the data were 2.412 times and 2.395 times more likely to occur under H0 than H1 for the 10-min and the 3-h delay respectively.

Together, these findings indicate that ageing did not affect the ability of Dp3Yey to discriminate between novel and familiar object-in-place associations similar to WT levels, both after the 10-min and the 3-h retention interval.

Table 3.8: Mean contact times of 18-month-old Dp3Yey mice in object-recognition memory tasks. Sample phases comprised a total of three objects. Test phases comprised one novel and two familiar objects in the NOR, and two novel and one familiar place object in the OiP task. Values are mean contact times with one object, ± 1 SD. For NOR n= 9 WT, 12 Dp3Yey. For OiP n= 9 WT, 11 Dp3Yey.

			Mean contact times (sec)	
			WT	**Dp3Yey**
NOR	Sample phase	S1	9.08 (±2.83)	10.17 (±3.18)
		S2	7.91 (±2.71)	8.58 (±3.20)
	Test - 10-min	Familiar	5.91 (±2.96)	6.58 (±6.22)
		Novel	11.16 (±4.26)	10.08 (±4.86)
	Test - 3-h	Familiar	5.62 (±2.73)	5.83 (±2.60)
		Novel	8.75 (±3.04)	10.98 (±6.29)
OiP	Sample phase	S1	8.56 (±3.33)	9.78 (±2.66)
		S2	7.11 (±2.80)	8.52 (±2.50)
	Test - 10-min	Familiar	4.95 (±2.44)	6.22 (±3.07)
		Novel	8.36 (±5.76)	9.61 (±5.46)
	Test - 3-h	Familiar	4.99 (±3.04)	7.58 (±3.04)
		Novel	6.83 (±2.84)	10.19 (±2.87)

Figure 3.10: Mean discrimination ratios of 18-month-old Dp3Yey mice on the NOR (a) and OiP (b) task. Bars originate from a 0.5 discrimination ratio, representing chance. Upward bars indicate preference for novelty, downward bars indicate preference for familiarity. Values are means ± 1 SEM. For NOR n= 9 WT, 12 Dp3Yey. For OiP n= 9 WT, 11 Dp3Yey.

a) NOR

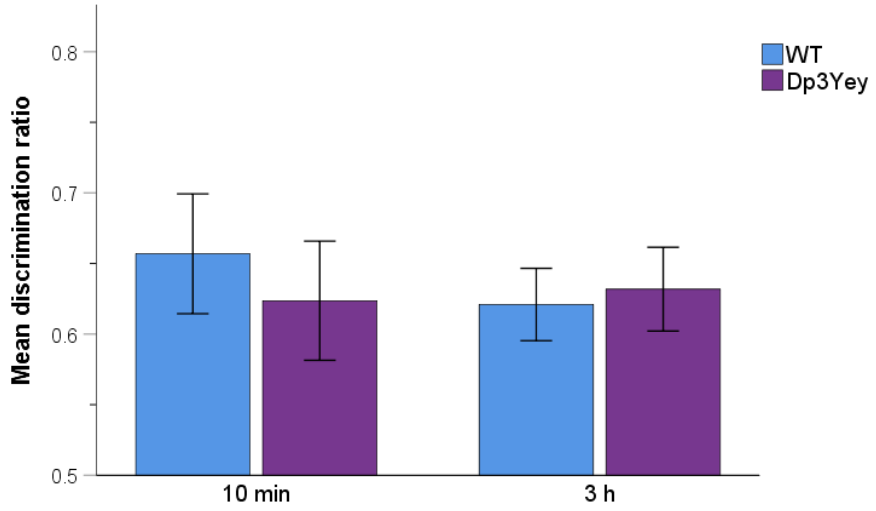

b) OiP

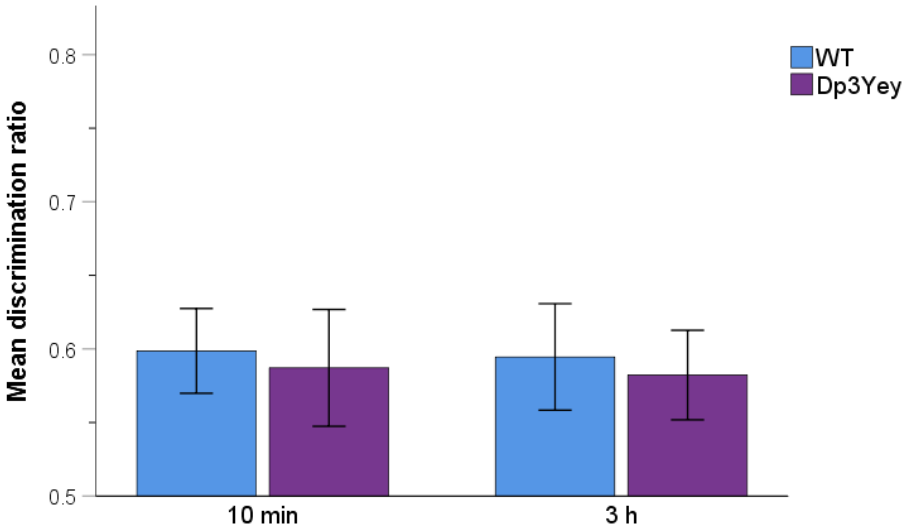

3.4.3. Exp. 2c: Increased activity levels on the EPM

Adult Dp3Yey (8 months old) underwent a 5-min trial on the EPM to assess anxiety and general activity levels. All WT and all Dp3Yey mice visited the open arms of the maze andboth groups spent more time within closed than open arms (table 3.9). There was no significant difference between the groups in the proportion of time spent in open arms, with WT and Dp3Yey animals spending respectively ~28% and ~24% of the trial time in open instead of closed arms (fig. 3.11a) (Student's t-test: $t_{(22)}$=1.009, p=0.324)..

The latency to enter open arms for the first time (table 3.9) was similar in both groups, taking on average ~ 10 seconds (Student's t-test – $t_{(20)}$=0.690, p=0.498). One WT and one Dp3Yey were excluded from this analysis because they were identified as outliers (latency WT = 111 sec; latency Dp3Yey = 127 sec), as assessed with boxplots and z-scores (smaller / greater ±3). There was also no significant difference in the number of head dips displayed by the groups (table 3.9), 24 and 22 in the WT and Dp3Yey group respectively (Student's t-test – $t_{(22)}$=0.708, p=0.487).

The locomotor activity of Dp3Yey and WT animals per minute on the EPM is shown in fig. 3.11b. Overall, Dp3Yey mice moved a significantly greater distance compared to wildtypes but activity decreased significantly over time in both groups, indicating habituation to the maze (two-way ANOVA – genotype: $F_{(1,22)}$=6.795, p=0.016; time: $F_{(4,88)}$=30.696, p<0.001; time x genotype: $F_{(4, 88)}$=0.885, p=0.477). In fact, the distance moved during the last trial minute was significantly lower compared to the first minute in both groups (paired t-test – WT: $t_{(11)}$=7.808, p<0.001; Dp3Yey: $t_{(11)}$=4.137, p=0.002).

A comparison between the two arm types (table 3.9) revealed that Dp3Yey displayed significantly higher locomotor activity compared to wildtypes in either arm type and that both groups moved a significantly larger distance in closed than open arms (two-way ANOVA – genotype: $F_{(1,22)}$=9.596, p=0.005; arm type: $F_{(1,22)}$=512.974, p<0.001; arm type x genotype: $F_{(1,22)}$=3.728, p=0.067). The total number of arm entries did not differ between WT and Dp3Yey mice, and both groups entered closed arms a significantly higher number of times compared to open arms (two-way ANOVA – genotype: $F_{(1,22)}$=2.147, p=0.157; arm type: $F_{(1,22)}$=57.441, p<0.001; arm type x genotype: $F_{(1,22)}$=1.078, p=0.310). There was also no difference between the groups in mean velocity and both groups moved significantly more slowly in open arms (two-way ANOVA – genotype: $F_{(1,22)}$=1.069, p=0.312; arm type: $F_{(1,22)}$=219.570, p<0.001; arm type x genotype: $F_{(1,22)}$=0.325, p=0.574).

Together, these results report that the exploratory behaviour of Dp3Yey mice towards open arms was similar to wildtypes, indicating no anxiety phenotype. Dp3Yey mice showed however a general increase in locomotor activity. Representative locomotor tracks and mean heat maps for the Dp3Yey and the WT group are shown in fig. 3.12.

Figure 3.11: Explorative behaviour of Dp3Yey mice on the EPM (a-b). Values are means ± 1 SEM. Significant main effect of group in b) with *p<0.05. n = 12 WT, 12 Dp3Yey.

a) Proportion of time in open arms

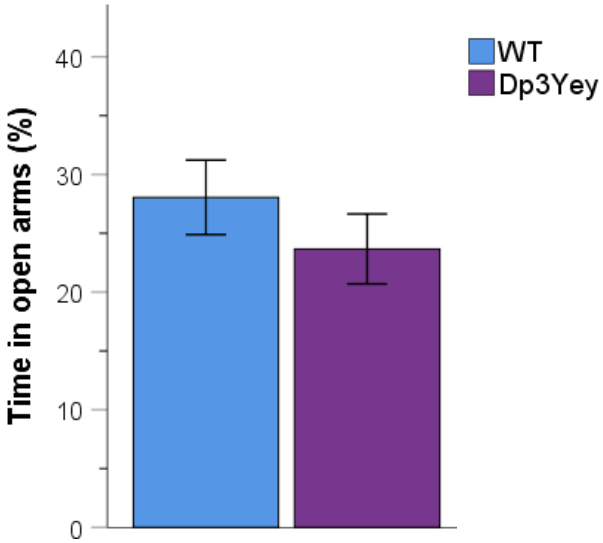

b) Overall distance moved per minute

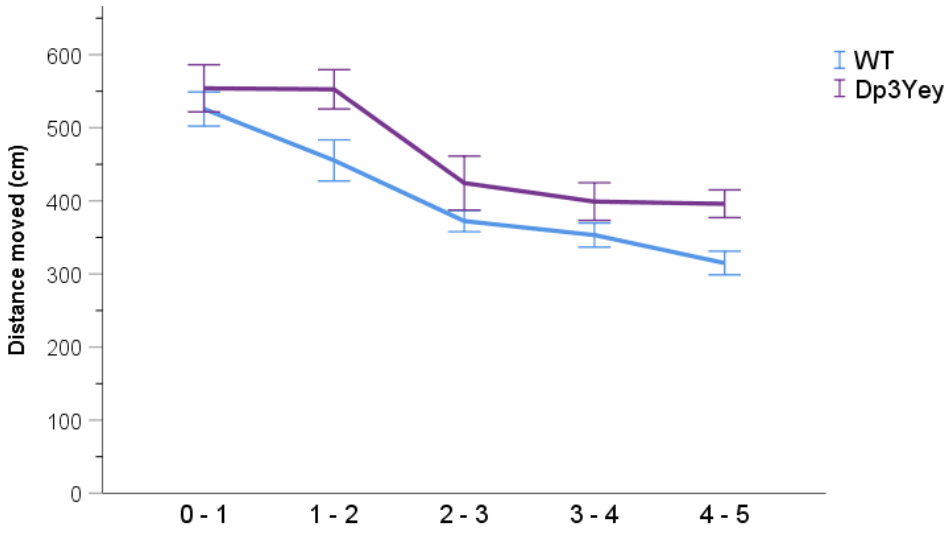

Table 3.9: Explorative behaviour of Dp3Yey mice on the EPM. Values are means ± 1 SD. No significant differences between the groups. n = 12 WT, 12 Dp3Yey.

	WT		Dp3Yey	
	Closed arms	Open arms	Closed arms	Open arms
Time (sec)	133.57 (±21.12)	52.56 (±21.43)	154.22 (±23.24)	48.14 (±22.05)
Latency first entry (sec)		8.30 (±9.56)		11.40 (±11.46)
Head dips (freq)		24.3 (±6.67)		22 (±9.27)
Distance moved (cm)	1280.97 (±170.78)	227.92 (±105.58)	1514.95 (±196.78)	265.63 (±170.65)
Arm entries (freq)	22.92 (±2.90)	12.42 (±5.30)	26.92 (±4.66)	13.08 (±8.03)
Velocity (cm/sec)	9.70 (±1.36)	4.28 (±1.01)	10.03 (±1.87)	5.00 (±1.66)

Figure 3.12: Representative locomotor tracks and mean heat maps of Dp3Yey mice on the EPM. a) WT group; b) Dp3Yey group. On the tracking, closed arms are represented in orange, open arms in pink and the centre in light blue. For heat maps, warmer and colder colours indicate longer and shorter exploration times respectively. n = 12 WT, 12 Dp3Yey.

a) WT

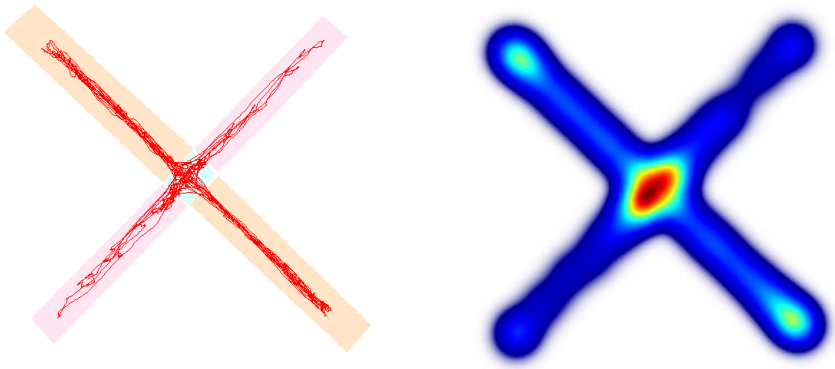

b) Dp3Yey

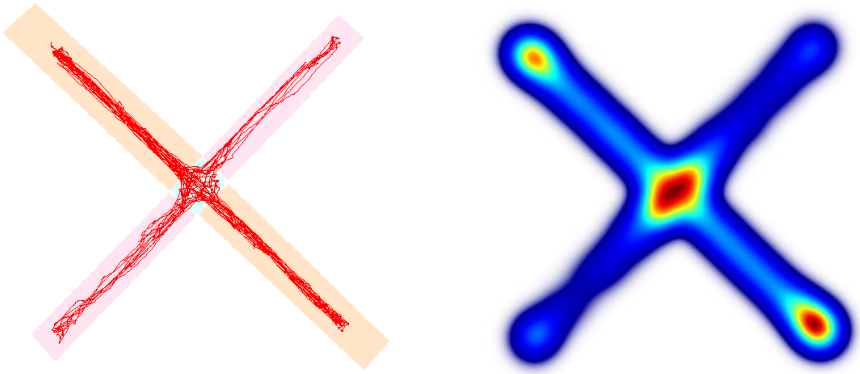

3.5. Dp2Yey results

To characterise the behavioural phenotypes associated to trisomy of the Mmu10 conserved region, Dp2Yey animals underwent two experiments employing object-recognition memory tasks (Exp. 3a and 3b) and the EPM test (Exp. 3c).

3.5.1. Exp. 3a: Intact recognition memory

Dp2Yey and their WT littermates were first tested on the NOR (*what*) and the OiP (*what-where*) task at 8 months of age, each with a 10-min and a 24-h delay. Because Dp2Yey mice performed at chance levels on the 24-h tests, the cohort was subsequently tested on the Loc task (*where*), to determine whether Dp2Yey mice were able to detect novelty at all after a 24-h retention interval. The results are reported separately for each task. Mean contact times with the objects during sample and test phases are shown in table 3.10.

Novel Object recognition task

During the sample phases, Dp2Yey mice spent significantly less time sampling the objects than WT mice in the first, but not the second sample phase (two-way ANOVA – genotype: $F_{(1,22)}$=2.739, p=0.112; genotype x sample phase: $F_{(1,22)}$=11.336, p=0.003; simple main effects of genotype, Welch's corrected – S1: $F_{(1,18)}$=5.489, p=0.031; S2: $F_{(1,18)}$=0.240, p=0.631). Habituation to the objects took place in both groups, as indicated by significantly reduced contact times from the first to the second sample phase (two-way ANOVA – sample phase: $F_{(1,22)}$=48.592, p<0.001; simple main effects of sample phase – WT: $F_{(1,22)}$=53.433, p<0.001; Dp2Yey: $F_{(1,22)}$=6.494, p=0.018).

In the test phase, intact recognition memory for object identity was inferred from higher contact times with novel objects. Although mean contact times with novel objects were numerically lower in the Dp2Yey (table 3.10), there was no significant difference between groups and both groups showed significantly higher contact times with novel than familiar objects (three-way ANOVA – object: $F_{(1,22)}$=21.827, p<0.001; genotype: $F_{(1,22)}$=0.943, p=0.342; genotype x object: $F_{(1,22)}$=0.619, p=0.440). Total contact times were significantly higher on the 24-h than the 10-min test, an increase that was not specifically associated to either group or object type (three-way ANOVA –delay: $F_{(1,22)}$=5.305, p=0.031; delay x object: $F_{(1,22)}$=2.161, p=0.156; delay x genotype: $F_{(1,22)}$=0.178, p=0.677; delay x object x genotype: $F_{(1,22)}$=1.088, p=0.308).

Mean discrimination ratios (fig. 3.13a) were analysed to investigate preference for novelty independently of total contact time during the test phase. In the WT group, mean discrimination ratios were significantly above chance at both tested delays (one sample t-tests – $WT_{10\text{-min}}$: $t_{(11)}$=5.269, p<0.001; $WT_{24\text{-h}}$: $t_{(11)}$=2.867, p=0.015). In contrast, preference

for novelty in the Dp2Yey group was significantly above chance at the 10-min but not the 24-h delay (one sample t-tests – $Dp2Yey_{10\text{-}min}$: $t_{(11)}=3.904$, $p=0.002$; $Dp2Yey_{24\text{-}h}$: $t_{(11)}=0.929$, $p=0.373$). Overall, mean discrimination ratios were significantly lower at the 24-h than the 10-min delay, but group differences were not statistically significant (two-way ANOVA – delay: $F_{(1,22)}=6.838$, $p=0.016$; genotype: $F_{(1,22)}=1.480$, $p=0.237$; genotype x delay: $F_{(1,22)}=0.306$, $p=0.586$).

To further investigate whether Dp2Yey animals performed normally, mean discrimination ratios were compared with Bayesian statistics. Estimated Bayes factors (B_{01}) reported that the data were 1.497 times and 2.572 times more likely to occur under H0 than H1 for the 10-min and the 24-h delay respectively.

Together, these findings indicate that Dp2Yey animals were able to discriminate between novel and familiar objects to WT levels, both after the 10-min and a 24-h retention interval. Preference for novel objects in Dp2Yey mice was however at chance levels on the 24-h test and suggests a subtle deficit in performance.

Object-in-place task

During the sample phases, Dp2Yey and WT mice spent a similar amount of time sampling the objects and contact times dropped significantly across the two phases (two-way ANOVA – genotype: $F_{(1,22)}=1.140$, $p=0.297$; sample phase: $F_{(1,22)}=32.329$, $p<0.001$; genotype x sample phase: $F_{(1,22)}=2.922$, $p=0.101$).

In the test phase, intact recognition memory for object-in-place associations was inferred from higher contact times with objects that exchanged position (i.e. novel place objects) than with stationary objects (i.e. familiar place objects). Although mean contact times (table 3.10) with novel place objects were generally lower in the Dp2Yey, there was no significant difference between groups and both groups showed significantly higher contacts with novel place than familiar place objects (three-way ANOVA – object: $F_{(1,22)}=12.739$, $p<0.002$; genotype: $F_{(1,22)}=1.199$, $p=0.285$; genotype x object: $F_{(1,22)}=0.452$, $p=0.509$). Total contact times were significantly higher on the 24-h than the 10-min test, an increase that was not specifically associated to either group or object type (three-way ANOVA – delay: $F_{(1,22)}=10.130$, $p=0.004$; delay x object: $F_{(1,22)}=0.649$, $p=0.429$; delay x genotype: $F_{(1,22)}=0.002$, $p=0.964$; delay x object x genotype: $F_{(1,22)}=0.003$, $p=0.955$).

As observed in the NOR task, mean discrimination ratios (fig. 3.13b) of the WT group were significantly above chance at both tested delays, while preference for novelty in the Dp2Yey group was significantly above chance at the 10-min but not the 24-h delay (one sample t-test – $WT_{10\text{-}min}$: $t_{(11)}=2.769$, $p=0.018$; $WT_{24\text{-}h}$: $t_{(11)}=2.277$, $p=0.044$; $Dp2Yey_{10\text{-}min}$: $t_{(11)}=2.255$, $p=0.045$; $Dp2Yey_{24\text{-}h}$: $t_{(11)}=1.088$, $p=0.300$). However, novelty preference did not differ between the groups, at either tested delay (two-way ANOVA – genotype: $F_{(1,22)}=0.257$,

p=0.617; genotype x delay: $F_{(1,22)}$=0.059, p=0.811). Delay did not significantly affect mean discrimination ratios (two-way ANOVA –delay: $F_{(1,22)}$=1.710, p=0.205).

Mean discrimination ratios were further compared between the groups with Bayesian statistics. Estimated Bayes factors (B_{01}) reported that the data were 2.656 times and 2.353 times more likely to occur under H0 than H1 for the 10-min and the 24-h delay respectively.

Together, these findings indicate that Dp2Yey animals were able to discriminate between novel and familiar object-in-place associations to WT levels, both after the 10-min and the 24-h retention interval. However, in Dp2Yey mice preference for novel object-in-place associations was at chance levels on the 24-h test and suggests a subtle deficit in performance.

Object location task

To determine whether Dp2Yey animals were at all unable to detect novelty above chance levels following a 24-h retention interval, this delay was further tested with the Loc task. During sample phases, there was no difference between WT and Dp2Yey mice and contact times dropped significantly across the two sample phases (two-way ANOVA – genotype: $F_{(1,22)}$=0.994, p=0.330; sample phase: $F_{(1,22)}$=12.641, p=0.002; genotype x sample phase: $F_{(1,22)}$=2.590, p=0.122).

In the test phase, intact memory for spatial locations was inferred from higher contact times with objects moved to a novel, previously vacant locations (i.e. novel location objects) than with stationary objects (i.e. familiar location objects). Overall, contact times were significantly higher with novel than familiar location objects and there was no difference between WT and Dp2Yey animals (two-way ANOVA – object: $F_{(1,22)}$=34.366, p<0.001; genotype: $F_{(1,22)}$=0.043, p=0.837; object x genotype: $F_{(1,22)}$=1.335, p=0.269).

In contrast to NOR and OiP findings, both WT and Dp2Yey animals showed a significantly above chance mean discrimination ratio after 24-h (fig. 3.13c) (one sample t-test – $WT_{24\text{-}h}$: $t_{(11)}$=7.526, p<0.001; $Dp2Yey_{24\text{-}h}$: $t_{(11)}$=5.592, p<0.001). Novelty preference was compared between the groups with classical and Bayesian independent samples Student's t-tests. Respectively, the tests reported no statistically significant difference between the groups ($t_{(22)}$=1.215, p=0.237) and an estimated Bayes factor (B_{01}) reporting that the data were 1.575 times more likely to occur under H0 than H1.

Together, these findings indicate that following a 24-h delay, Dp2Yey animals were able to discriminate between familiar objects occupying a novel, previously vacant, spatial location and identical, stationary objects. Dp2Yey mice were thus able to display above chance novelty preference following a 24-h retention interval.

Table 3.10: Mean contact times of 13-month-old Dp2Yey mice in object-recognition memory tasks. Sample phases comprised a total of three objects. Test phases comprised one novel and two familiar objects / locations in the NOR and Loc task, and two novel and one familiar place object in the OiP task. Values are mean contact times with one object, ± 1 SD. n= 12 WT, 12 Dp2Yey.

			Mean contact times (sec)	
			WT	**Dp2Yey**
NOR	Sample phase	S1	13.66 (±5.35)	9.40 (±3.32)
		S2	8.08 (±3.88)	7.45 (±2.14)
	Test - 10-min	Familiar	6.36 (±2.56)	5.73 (±3.26)
		Novel	12.98 (±9.59)	9.23 (±5.16)
	Test - 24-h	Familiar	10.88 (±4.92)	9.41 (±4.74)
		Novel	13.02 (±5.02)	12.15 (±8.73)
OiP	Sample phase	S1	13.15 (±4.46)	10.56 (±3.81)
		S2	8.87 (±3.69)	8.26 (±3.74)
	Test - 10-min	Familiar	8.76 (±6.63)	7.21 (±4.51)
		Novel	12.60 (±7.16)	10.11 (±5.83)
	Test - 24-h	Familiar	11.77 (±5.77)	10.24 (±6.15)
		Novel	14.45 (±3.59)	11.80 (±4.43)
Loc	Sample phase	S1	6.01 (±2.84)	4.55 (±2.05)
		S2	3.35 (±1.52)	3.55 (±1.24)
	Test - 24-h	Familiar	5.89 (±3.01)	4.83 (±2.40)
		Novel	8.98 (±4.49)	9.44 (±5.08)

Figure 3.13: Mean discrimination ratios of 13-month-old Dp2Yey mice on the NOR (a), OiP (b) and LOC (c) task. Bars originate from a 0.5 discrimination ratio, representing chance. Upward bars indicate preference for novelty, downward bars indicate preference for familiarity. Values are means ± 1 SEM. n= 12 WT, 12 Dp2Yey.

a) NOR

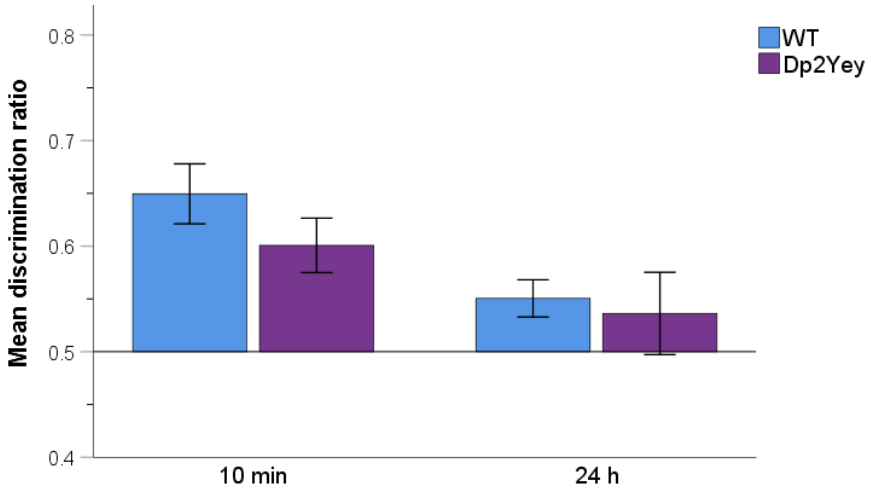

b) OiP

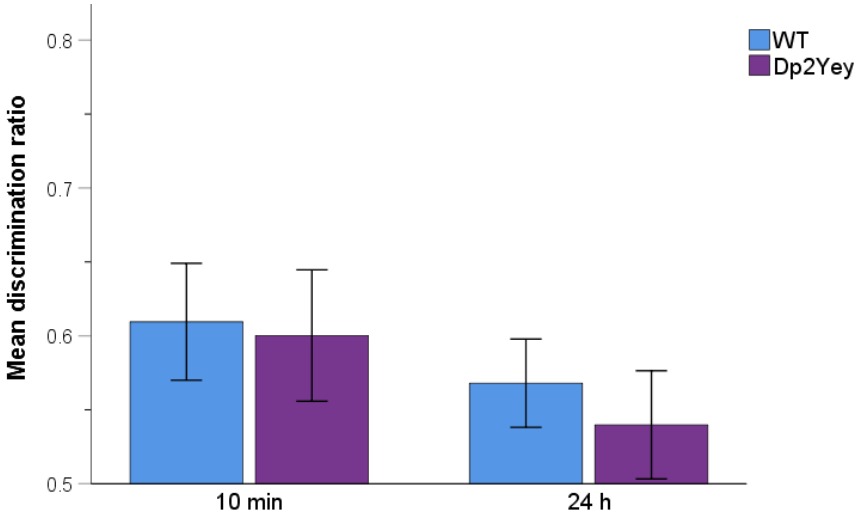

c) Loc

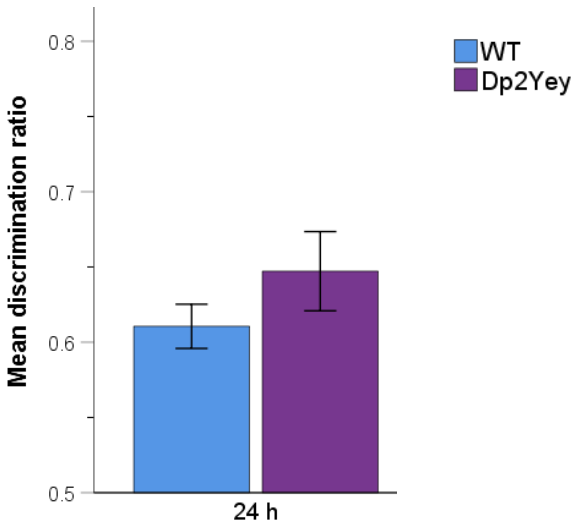

3.5.2. Exp. 3b: Ageing impaired memory for objects

To determine whether the Mmu10 trisomy in conjunction with ageing had detrimental effects on memory performance, a cohort of Dp2Yey animals was tested at 20 months of age. Since younger Dp2Yey animals showed signs of potentially impaired long-term NOR memory and since intact memory for object identity was a requirement for testing on the OiP task, NOR memory was first assessed, with a 10-min and a 3-h delay. The 3-h delay was chosen as previous data revealed that the customary 24-h retention interval failed to consistently produce preference for novelty in wildtype mice. Subsequently, to determine whether NOR impairments observed in aged animals were a result of a general age-related impairment in novelty detection or concerned specifically the retention of object information, the animals were tested on the Loc-task, with a 10-min delay. Since identical objects are used in the Loc task, performance does not depend on intact memory for objects. One WT mouse was excluded from all the analyses as it displayed a strong preference for familiar objects in all tests (mean discrimination ratios < 0.25), indicating a profound impairment in novelty detection. Results are reported separately for each task. Mean contact times with the objects during sample and test phases are reported in table 3.11.

Novel object recognition task

During the sample phases, WT and Dp2Yey mice spent a similar amount of time sampling the objects and contact times dropped significantly from the first to the second sample phase in both groups (two-way ANOVA – genotype: $F_{(1,18)}$=1.233, p=0.282; sample phase: $F_{(1,18)}$=8.126, p=0.011; sample phase x genotype: $F_{(1,18)}$=0.871, p=0.363).

In the test phase, contact times were significantly higher with novel than familiar objects and did not differ between the groups (three-way ANOVA – genotype: $F_{(1,18)}$=0.147, p=0.706; object: $F_{(1,18)}$=19.242, p<0.001). However, mean contact times (table 3.11) suggest that preference for novel objects was lower in the Dp2Yey than the WT group, at both the 10-min and the 3-h delay. The interaction between genotype and object type failed nevertheless to reach statistical significance (three-way ANOVA – genotype x object: $F_{(1,18)}$=4.092, p=0.058). The tested delay did not significantly affect contact times, in either group and for either object type (three-way ANOVA – delay: $F_{(1,18)}$=1.020, p=0.326; delay x genotype: $F_{(1,18)}$=1.427, p=0.248; delay x object: $F_{(1,18)}$=0.292, p=0.595; delay x genotype x object: $F_{(1,18)}$=1.357, p=0.259).

Normalisation of novelty preference over total contact time in the test phase allowed group differences to emerge. In the WT group, mean discrimination ratios (fig. 3.14a) were significantly above chance at both delays, while in the Dp2Yey group, mean discrimination ratios were no different from chance (one sample t-test – $WT_{10\text{-}min}$: $t_{(7)}$=3.888, p=0.006; $WT_{3\text{-}h}$: $t_{(7)}$=3.530, p=0.010; $Dp2Yey_{10\text{-}min}$: $t_{(11)}$=0.358, p=0.727; $Dp2Yey_{3\text{-}h}$: $t_{(11)}$=0.138, p=0.893).

In fact, mean discrimination ratios displayed by Dp2Yey mice were significantly lower compared to wildtypes, independently of the tested delay (two-way ANOVA – genotype: $F_{(1,18)}$=9.647, p=0.006; delay: $F_{(1,18)}$=0.233, p=0.635; delay x genotype: $F_{(1,18)}$=0.001, p=0.980).

To confirm impaired novelty detection in the Dp2Yey group, mean discrimination ratios were further compared with Bayesian statistics. The estimated Bayes factors (B_{01}) reported that the data were only 0.827 times and 0.327 times more likely to occur under H0 than H1 for the 10-min and the 3-h delay respectively.

These findings indicate that at 20 months of age, Dp2Yey animals were unable to discriminate between novel and familiar objects, both after a 10-min and a 3-h retention interval.

Object location task

To determine whether impairments in novelty detection of aged Dp2Yey mice were restricted to object identity, the animals were further tested on the Loc task. One Dp2Yey animal was excluded from the analysis due to insufficient contact time with the objects during the test phase (< 3 sec).

During the sample phases, WT and Dp2Yey mice spent a similar amount of time sampling the objects (two-way ANOVA – genotype: $F_{(1,17)}$=0.002, p=0.968). In both groups, contact times remained however stable across the two sample phases, possibly due to a floor effect (i.e. three copies of the same object) (two-way ANOVA – sample phase: $F_{(1,17)}$=1.214, p=0.286, sample phase x genotype: $F_{(1,17)}$=0.051, p=0.823).

In the test phase, there was no difference between the groups and contact times were significantly higher with novel than familiar location objects (two-way ANOVA – object: $F_{(1,17)}$=21.996, p<0.001; genotype: $F_{(1,17)}$=0.207, p=0.655; object x genotype: $F_{(1,17)}$=0.014, p=0.907).

In line with the above analysis, mean discrimination ratios of both WT and Dp2Yey animals were significantly above chance (fig. 3.14b) (one sample t-test – $WT_{10\text{-}min}$: $t_{(7)}$=7.440, p<0.001; $Dp2Yey_{10\text{-}min}$: $t_{(10)}$=3.501, p=0.006). Novelty preference was compared between the groups with classical and Bayesian independent samples Student's t-tests. Respectively, the tests reported no significant difference between the groups (equal variances not assumed: $t_{(14)}$=0.151, p=0.882) and an estimated Bayes factor (B_{01}) indicating that the data were 2.437 times more likely to occur under H0 than H1.

These findings indicate that despite the impairments observed in the NOR task, 20-month-old Dp2Yey animals were able to detect spatial novelty, successfully discriminating between objects occupying a novel, previously vacant spatial location and identical, stationary objects. Novelty elicited exploration per se was therefore not pervasively impaired in aged Dp2Yey mice.

Table 3.11: Mean contact times of 20-month-old Dp2Yey mice in the NOR and Loc task. Sample phases comprised a total of three objects. Test phases comprised one novel and two familiar objects / locations. Values are mean contact times with one object, ± 1 SD. For NOR n= 8 WT, 12 Dp2Yey. For Loc n= 8WT, 11 Dp2Yey.

			Mean contact times (sec)	
			WT	**Dp2Yey**
NOR	Sample phase	S1	4.21 (±1.87)	3.78 (±1.39)
		S2	3.71 (±1.63)	2.80 (±0.98)
	Test – 10-min	Familiar	1.66 (±0.77)	2.17 (±1.02)
		Novel	3.00 (±0.83)	3.23 (±3.18)
	Test – 3-h	Familiar	2.53 (±1.36)	2.58 (±1.52)
		Novel	4.24 (±2.06)	2.65 (±1.44)
Loc	Sample phase	S1	3.54 (±1.51)	3.60 (±2.08)
		S2	3.18 (±1.16)	3.05 (±2.83)
	Test – 10-min	Familiar	1.79 (±1.07)	2.05 (±1.50)
		Novel	3.21 (±1.33)	3.54 (±1.98)

Figure 3.14: Mean discrimination ratios of 20-month-old Dp2Yey mice on the NOR (a) and LOC (b) task. Bars originate from a 0.5 discrimination ratio, representing chance. Upward bars indicate preference for novelty, downward bars indicate preference for familiarity. Values are means ± 1 SEM. Significant main effect of genotype on the NOR task ($p<0.01$). N= 8 WT, 12 Dp2Yey.

a) NOR

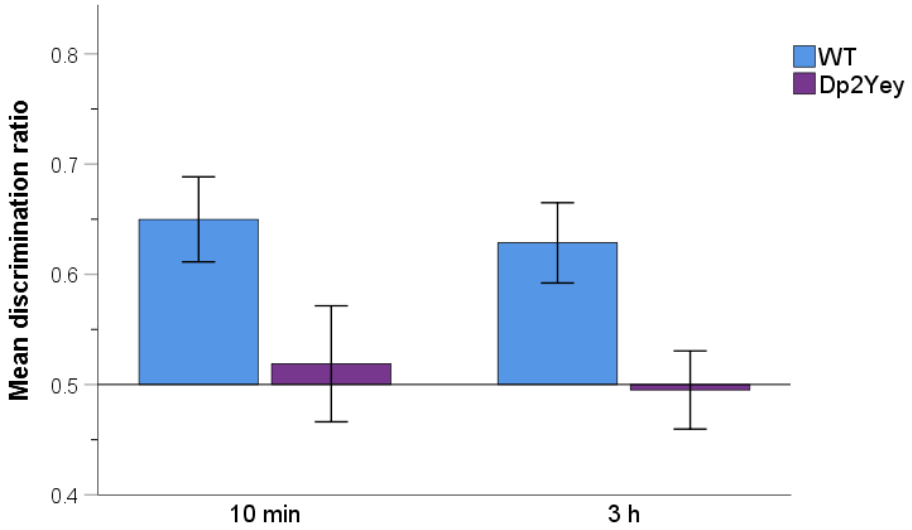

b) Loc

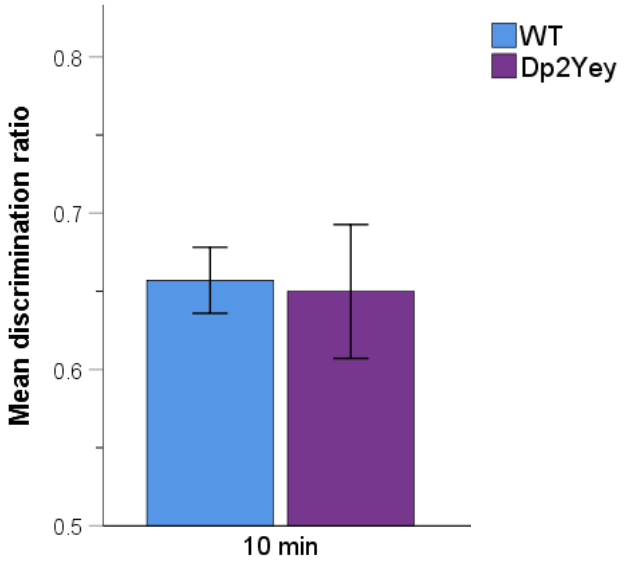

3.5.3. Exp. 3c: Normal anxiety and activity levels on the EPM

Adult (8 months old) Dp2Yey underwent a 5-min trial on the EPM to assess anxiety and general activity levels. All WT mice entered the open arms of the maze, although one Dp2Yey mouse did not visit the open arms throughout the entire duration of the trial. Both WT and Dp2Yey animals spent more time within closed than open arms (table 3.12) and there was no significant group difference in the proportion of time spent in open relative to closed arms, with WT and Dp2Yey spending respectively ~22% and ~23% of the trial time within open arms (fig. 3.15a) (Student's t-test – $t_{(22)}$=0.306, p=0.762). On average, it took Dp2Yey ~ 13 seconds and wildtypes ~24 seconds to enter open arms for the first time (table 3.12), but this difference was not statistically significant (Student's t-test – $t_{(19)}$=1.255, p=0.225). One WT and one Dp2Yey were excluded from this analysis because they were identified as outliers (latency WT = 178 sec; latency Dp2Yey = 104 sec), as assessed with boxplots and z-scores (smaller / greater ± 3). On average, both WT and Dp2Yey mice displayed a total of ~15 head dips (Student's t-test – $t_{(22)}$=0.143, p=0.887).

The locomotor activity of Dp2Yey and WT animals per minute on the EPM is shown in fig. 3.15b. Overall, Dp2Yey and WT mice moved a similar distance on the EPM and activity decreased significantly over time in both groups, indicating habituation to the environment (two-way ANOVA – genotype: $F_{(1,22)}$=0.149, p=0.703; time: $F_{(4,88)}$=15.847, p<0.001; time x genotype: $F_{(4, 88)}$=2.003, p=0.101). In fact, in both groups the distance moved during the last trial minute was significantly lower compared to the first minute (paired t-test – WT: $t_{(11)}$=4.448, p=0.001; Dp2Yey: $t_{(11)}$=2.465, p=0.031).

A comparison between the two arm types (table 3.12) confirmed that locomotor activity of Dp2Yey mice was similar to wildtypes in both arm types and revealed that both groups moved a significantly larger distance in closed than open arms (two-way ANOVA – genotype: $F_{(1,22)}$=0.233, p=0.634; arm type: $F_{(1,22)}$=622.019, p<0.001; arm type x genotype: $F_{(1,22)}$=0.132, p=0.720). There was also no significant group difference in the number of arm entries and both groups entered closed arms a significantly higher number of times compared to open arms (two-way ANOVA – genotype: $F_{(1,22)}$=0.263, p=0.613; arm type: $F_{(1,22)}$=92.499, p<0.001; arm type x genotype: $F_{(1,22)}$=0.129, p=0.723). Mean velocity on the EPM also did not significantly differ between the groups and both groups moved significantly more slowly in open arms (two-way ANOVA – genotype: $F_{(1,21)}$<0.001, p=0.995; arm type: $F_{(1,21)}$=76.003, p<0.001; arm type x genotype: $F_{(1,21)}$=1.244, p=0.277).

Together, these results indicate that the exploratory behaviour of Dp2Yey mice was similar to wildtypes, suggesting no anxiety or activity phenotypes. Representative locomotor tracks and mean heat maps on the EPM for the Dp2Yey and the WT group are shown in fig. 3.16.

Figure 3.15: Explorative behaviour of Dp2Yey mice on the EPM (a-b). Values are means ± 1 SEM. n = 12 WT, 12 Dp2Yey.

a) Proportion of time in open arms

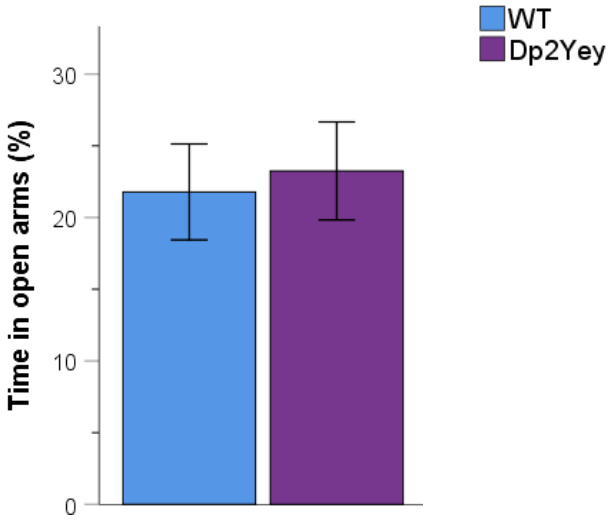

b) Overall distance moved per minute

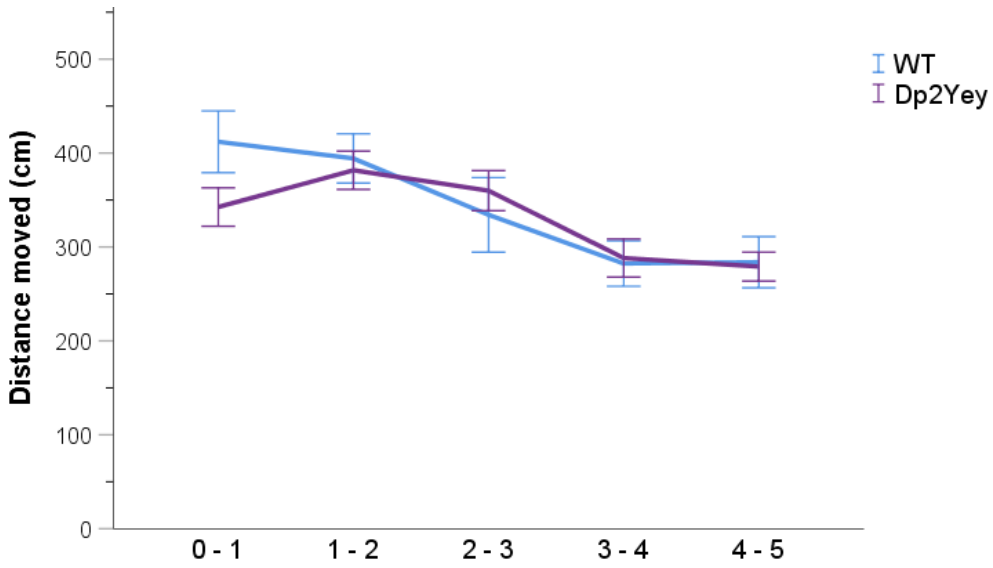

Table 3.12: Explorative behaviour of Dp2Yey mice on the EPM. Values are mean ± 1 SD. No significant differences between the groups. n = 12 WT, 12 Dp2Yey.

	WT		Dp2Yey	
	Closed arms	Open arms	Closed arms	Open arms
Time (sec)	149.25 (±29.27)	41.36 (±22.80)	134.22 (±21.67)	41.22 (±20.26)
Latency first entry (sec)		23.96 (±22.54)		13.19 (±15.83)
Head dips (freq)		15.25 (±6.69)		15.58 (±4.50)
Distance moved (cm)	1076.66 (±240.77)	190.63 (±115.18)	1063.38 (±163.96)	151.17 (±69.18)
Arm entries (freq)	19.58 (±5.63)	9.17 (±5.37)	18.42 (±2.84)	8.75 (±3.84)
Velocity (cm/sec)	7.59 (±2.34)	4.26 (±1.57)	8.09 (±1.89)	3.78 (±0.81)

Figure 3.16: Representative locomotor tracks and mean heat maps of Dp2Yey mice on the EPM. a) WT group, (b) Dp2Yey group. On the tracking, closed arms are represented in orange, open arms in pink and the centre in light blue. For heat maps, warmer and colder colours indicate longer and shorter exploration times respectively. n= 12 WT, 12 Dp2Yey.

a) WT

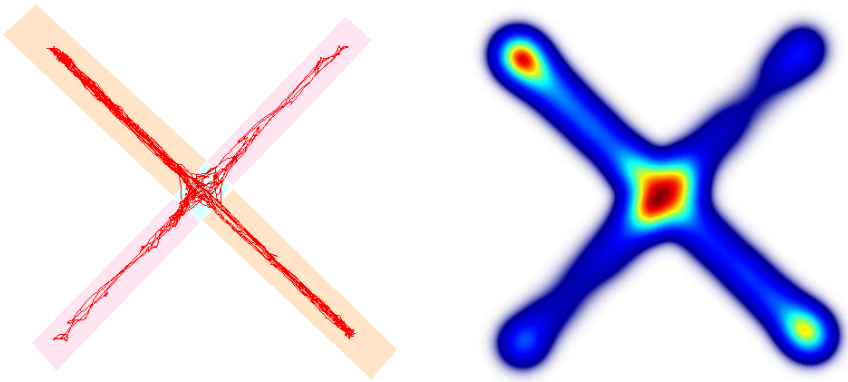

b) Dp2Yey

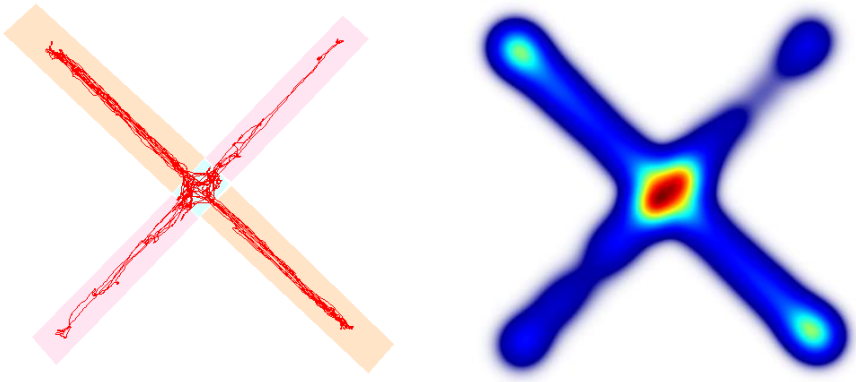

3.6. Discussion

Individuals with DS have severe difficulties in the long-term retention of episodic memories. The role that Hsa21 genes play in the regulation of memory function is however unclear. Here, to determine the separate contribution of the Mmu16, Mmu17 and Mmu10 conserved regions to memory impairments, the Dp1Tyb, Dp3Yey and Dp2Yey mouse models of segmental DS were studied on a battery of object-recognition memory tasks and anxiety tests. For each mouse line, adult (12 months) and aged (18-20 months) animals were tested on a series of object-recognition memory tasks, assessing different features and retention-spans of recognition memory. As anticipated, the mouse lines revealed distinct memory profiles, implicating over-dosage of distinct Has21 syntenic regions in the production of distinct phenotypes. Table 3.13 provides a summary of the phenotypes observed in each mouse line.

Mmu16 and the Dp1Tyb model

Dp1Tyb animals displayed an age-independent, dissociation in recognition memory. Performance on the NOR task was unimpaired (Exp. 1a), indicating that Dp1Tyb successfully recognised novel objects after short (10-min) and long (24-h) retention intervals. However, Dp1Tyb mice were unable to detect spatial novelty associated to specific objects in the OiP task (Exp. 1a) and to judge object temporal recency in the TOr task (Exp. 1b). These impairments emerged exclusively after a 10-min retention interval, while performance was consistently above chance following longer intervals (24-h or 3-h). Importantly, the OiP impairment was not due to a deficit in the processing or retention of information about the spatial organisation of objects, as Dp1Tyb mice performed normally and above chance on the Loc task (Exp. 1a). Hence, the Mmu16 trisomy did not affect memory for single items (*what*) and for spatial organisation (*where*), but specifically impaired short-term memory for item-in-place and item-order associations (*what-where* and *what-when*). Impairments in associative-recognition memory were already observed at 4 months of age (Exp. 1d) and memory for single objects was intact even at 20 months of age (Exp. 1c).

The observation of intact long-term NOR memory is in contrast to previous findings on the Dp1Tyb model. Two studies reported that following a 24-h retention interval, Dp1Tyb mice failed to display a preference for exploring a novel over a familiar object (Nguyen et al., 2018; Souchet et al., 2019). However, the methods of these two studies differed substantially from the present protocol. Most importantly, the animals were given only a single 10-min sample phase, in contrast to the two employed here. It is possible that doubling the acquisition time in the present study prevented the emergence of a memory deficit. Indeed, although Dp1Tyb successfully discriminated between familiar and novel

objects, contact times with novel objects were significantly reduced compared to controls, implying a weaker memory trace. Here, Dp1Tyb mice were also tested on a one-sample version of the NOR task and showed normal object memory, but the task was carried out only with a 10-min delay (fig. 3.4a).

Intact long-term NOR memory in the Dp1Tyb is also in contrast to other models of Mmu16 trisomy. Recognition of novel objects was impaired in Ts65Dn and Ts1Rhr mice after 24-h, but normal in the Ts1Cje (Belichenko et al., 2009a; Fernandez & Garner, 2007; Kleschevnikov et al., 2012). This suggests that trisomy of the DSCR is sufficient to produce the deficit (Ts1Rhr), but that the deficit disappears under DSCR trisomy in conjunction with trisomy of a small portion of Mmu16 homologs (Ts1Cje), re-appears under trisomy of a longer Mmu16 portion (Ts65Dn) and would seem to disappear again under complete trisomy of Mmu16 homologs (Dp1Tyb). This pattern underlines the necessity to understand how simultaneous over-dosage of distinct Mmu16 homologs affects gene transcription and ultimately memory function. When NOR memory was assessed in a transchromosomic DS model, the Tc1, trisomic animals were impaired on short-term memory but showed unimpaired long-term object memory, suggesting that simultaneous over-dosage of Hsa21 genes mapping to all three conserved regions does not interfere with long-term object memory (Hall et al., 2016).

Although no previous published study has ever tested memory in Dp1Tyb mice following shorter delays, current results are in line with Ts65Dn mice displaying intact 10-min NOR memory (Kleschevnikov et al., 2012). By contrast, evidence in the Tc1 line found that despite normal 24-h performance, Tc1 mice were unable to recognise a novel object following a 10-min delay (Hall et al., 2016). This suggests that Hsa21 genes mapping to Mmu10 or Mmu17 but not Mmu16, might be involved in the regulation of short-term object memory.

Dp1Tyb animals were expected to display impairments in HPC-dependent memory tests, yet, despite evidence of disrupted OiP memory, they performed normally on the Loc task (Exp. 1a). This suggests that Dp1Tyb mice possess a subtle spatial memory impairment. By contrast, Ts65Dn mice were repeatedly found unable to detect spatial novelty in different versions of object-recognition memory tasks (Kleschevnikov et al., 2012; Smith, Kesner, & Korenberg, 2014). The Ts65Dn is however a controversial model as these animals lack trisomy of some Hsa21-syntenic genes and are trisomic for 60 genes on Mmu17 that are not syntenic to Hsa21 (Duchon et al., 2011b). In fact, behavioural and physical phenotypes are generally more severe in the Ts65Dn strain compared to other DS mouse models (Belichenko et al., 2009a). The HPC of Ts65Dn mice is affected by important structural anomalies, such as reduced neuronal and synapse numbers (Chakrabarti et al., 2007; Chakrabarti et al., 2010). By contrast, although research on Dp1Tyb brain structure

is still in its infancy, this mouse line does not seem to be characterised by obvious alterations in hippocampal cytoarchitecture (Goodliffe et al., 2016).

Nevertheless, Dp1Tyb mice exhibited a delay-dependent deficit on the OiP and TOr tasks (Exp. 1a and 1b), known to depend on a network of structures that includes the HPC. Importantly, although Dp1Tyb mice failed to display a preference for the less recently presented object in the TOr task, they also did not show a preference for the more recently presented object. The lack of a preference towards either object implicates that neither object was perceived as novel. Thus, Dp1Tyb mice reported a specific difficulty in judging the temporal context associated to each object, while recognising both objects as previously encountered.

Memory for object-in-place and object temporal order associations requires the integration of object and place / temporal context-information, a role that has been repeatedly attributed to the HPC. Indeed, performance of rats with lesions of either the PRH, the HPC or the mPFC is impaired on the OiP and TOr tasks, demonstrating the necessity of integrated activity within the medial temporal lobe (Barker & Warburton, 2011b). Instead, NOR and Loc performance was exclusively affected by lesions of the PRH and the HPC respectively. Based on the Dp1Tyb memory profile, it can be postulated that independent activity of subregions within the medial temporal lobe appears normal but network activity is aberrant, whereby HPC-mediated input integration and/or recall of integrated events is defective. In line with this interpretation, Dp1Tyb animals have been repeatedly found impaired in tasks requiring the integration of visuospatial / contextual information, such as the MWM and the contextual fear conditioning task, known to be sensitive to hippocampal dysfunction (Aziz et al., 2018; Goodliffe et al., 2016; Jiang et al., 2015; Yu et al., 2010b; Zhang et al., 2014).

The memory deficits following brain lesions observed by Barker and Waburton (2011b) were however not restricted to a specific time window but affected both short (5-min) and long (24-h) retention intervals. The pattern of impaired short-term but preserved long-term associative-recognition memory in the Dp1Tyb is peculiar, but not unprecedented. Tc1 mice displayed the same delay-dependent memory performance on the NOR task and on the MWM (Hall et al., 2016; Morice et al., 2008). Moreover, this behavioural pattern was reflected in synaptic plasticity, whereby in vivo hippocampal LTP was significantly reduced in Tc1 mice after tetanic stimulation, but LTP maintenance levels were normal 24-h later (Morice et al., 2008). In the Dp1Tyb, in vitro hippocampal LTP was significantly reduced up to 1 hour after induction, but longer intervals have never been assessed (Yu et al., 2010b; Zhang et al., 2014). Based on the behavioural evidence it can be speculated that, analogously to the Tc1 model, long-term maintenance of LTP may be normal in the Dp1Tyb.

Memory performance was expected to deteriorate with age in Dp1Tyb mice, as a result of *App* trisomy promoting AD-like pathology. In the Ts65Dn model, brain APP levels were found significantly increased at 10 months of age, while no difference was observed at younger ages (Choi et al., 2009). Ts65Dn mice have also been found to display elevated Aβ-levels in the HPC and treatment with a γ-secretase inhibitor restored both normal Aβ-levels and performance on the MWM (Netzer et al., 2010). In the Dp1Tyb model, previous research reported that APP overexpression in the HPC was evident already at 4 months of age, but Aβ-deposits were not investigated (Yu et al., 2010b).

Mouse models of AD commonly display diffuse Aβ-plaques after the age of 8 months and impairments are observed in HPC-dependent and NOR tasks (as reviewed in Webster et al., 2014). On the NOR task, Tg2576 mice displayed intact recognition memory after a 10-min delay but were impaired after 24-h, suggesting a critical role of APP in the regulation of long-term object memory (Hall et al., 2016). This interpretation is agreement with Tc1 mice –not functionally trisomic for *App* – who display intact 24-h NOR memory (Hall et al., 2016). Here however, 20-month-old Dp1Tyb mice showed intact 24-h NOR memory (Exp. 1c). Furthermore, memory deficits observed on the OiP task were already present in 4-month-old mice (Exp. 1d). These results demonstrate that *App* trisomy in conjunction with duplication of all Mmu16 homologs did not affect long-term memory for objects and that ageing did not represent a crucial factor in the performance of Dp1Tyb mice.

These seemingly inconsistent findings highlight once again the importance of gene-to-gene interactions, whereby deleterious effects of a given gene depend on the dosage of other Hsa21 homologs. In this perspective, it is worth pointing out that while Tc1 mice do not exhibit amyloid pathology, Tc1 mice crossed with a mouse line overexpressing APP were found to display significantly increased hippocampal Aβ-levels and Aβ-plaque number in comparison to mice solely overexpressing APP (Wiseman et al., 2018). This suggests that in DS, genes on Hsa21 other than *APP* contribute to AD pathology, exacerbating Aβ-aggregation.

Dosage-sensitive genes linked to the memory deficits observed in the Dp1Tyb are potentially located within the DSCR. By crossing Dp1Tyb mice with mutant mice monosomic for the DSCR, Zhang et al. (2014) generated offspring carrying normal copy number of DSCR genes and trisomy of all other Mmu16 homologs. In contrast to the Dp1Tyb, the crossed mouse line reported normal performance on the MWM and normal hippocampal LTP, attributing DSCR genes a causative role in aberrant hippocampal function (Zhang et al., 2014). A candidate gene located within the DSCR is *DYRK1A*. This gene codes for a kinase involved in numerous cellular pathways in the developing and adult brain. Alterations in *DYRK1A* dosage have been repeatedly associated to cognitive dysfunction. Studies of DS individuals report a gene dosage-dependent expression of DYRK1A, with western blots

indicating a ~1.5 fold increase in different brain regions (Dowjat et al., 2007). A similar increase in DYRK1A expression has also been found in the Ts65Dn, the Tc1 and the Dp1Tyb model (Ahmed et al., 2013; Dowjat et al., 2007; Souchet et al. 2014).

The molecular mechanisms altered by *DYRK1A* over-dosage impairing cognition are not fully understood and are discussed in more detail in chapter 4. Certainly, DYRK1A plays a fundamental role during embryonic development as demonstrated by the mid-gestation mortality of *Dyrk1A* deficient transgenic mice (Fotaki et al., 2002). Reducing *Dyrk1A* to one functional copy (-/+) increased death rates as well, with surviving pups presenting reduced body size and brain volume (Fotaki et al., 2002). Although overdosage of *Dyrk1A* does not affect litter viability or gross brain morphology, increased DYRK1A levels have been associated to neuronal and behavioural abnormalities, including memory impairments on the MWM, the T-maze spontaneous alternation test and the NOR task (Altafaj et al., 2001; De la Torre et al., 2014; Souchet et al., 2014).

To better understand the contribution of DYRK1A to the memory deficits observed in DS, a few studies have crossed trisomic and *Dyrk1A* (+/-) mice to generate offspring with normal *Dyrk1A* copy number on an otherwise trisomic background. In the Ts65Dn model, normalisation of *Dyrk1A* copy number rescued memory performance on the MWM and restored normal hippocampal LTP (García-Cerro et al., 2014). In the Dp1Tyb model, normalisation of *Dyrk1A* partially rescued in vitro hippocampal LTP and significantly improved spontaneous alternation rates on the T-maze test and freezing levels on the contextual fear conditioning task, although performance did not reach normal levels (Jiang et al., 2015). By contrast, normalisation of *Dyrk1A* together with half DSCR (~13 genes) did not rescue either memory deficits or LTP, reiterating the importance of gene-to-gene interactions in DS (Jiang et al, 2015).

In addition to memory deficits, the Mmu16 trisomy resulted in an increase in anxiety and activity levels on the EPM (Exp. 1e). Compared to wildtypes, Dp1Tyb mice were less inclined to explore the open arms of the maze and they moved a larger distance in closed arms, suggesting that within a sheltered environment Dp1Tyb mice are hyperactive. Measures of anxiety and locomotor activity are important as these variables can interfere with explorative behaviour and thus memory performance in object-recognition memory tasks. Such confounds would however equally affect performance in all tasks, at all tested delays. It is therefore extremely unlikely that anxiety and activity phenotypes participated in the very specific pattern of memory dissociation displayed by Dp1Tyb animals.

Additionally, contact behaviour during the sample phases did not differ between Dp1Tyb and WT mice. The only exception was in the TOr task (Exp. 1b), with Dp1Tyb mice spending less time with the objects in both sample and test phases. Reduced contacts are however unlikely to have confounded the performance, since TOr memory was not fully

compromised in the Dp1Tyb but only at the 10-min delay. The reason why Dp1Tyb displayed lower contact times than wildtypes in the TOr task is unclear. The TOr was the last task of a series of experiments and it is possible that Dp1Tyb mice were more sensitive to repeated testing than wildtypes, resulting in reduced task engagement.

Activity levels have been assessed before in Dp1Tyb mice but produced inconsistent evidence. On the open-field test, Dp1Tyb mice were found to display normal, reduced or increased locomotor activity (Aziz et al., 2018; Goodliffe et al., 2016; Souchet et al., 2019). Here, findings on the Dp1Tyb activity profile were expanded, revealing a hyperactivity phenotype in unexposed maze areas (i.e. closed arms). It is possible that discrepant findings in the literature resulted from differences in acclimation to the testing environment, especially in light of an anxiety phenotype. Increased anxiety levels are consistent with previous evidence reporting increased thigmotaxis in Dp1Tyb mice (Goodliffe et al., 2016).

Altered activity and anxiety levels have been observed in other Mmu16 trisomy models and associated to aberrant hippocampal function. Partially in line with Dp1Tyb findings, Ts65Dn mice displayed increased locomotor activity on the open-field maze but reduced anxiety on the EPM (Sago et al., 2000; Yin et al., 2017). Instead, Ts1Cje were found hypoactive on the open-field test but showed increased thigmotaxis, suggesting elevated anxiety (Sago et al., 2000). Interestingly, DYRK1A activity has also been implicated in altered anxiety and activity levels. Transgenic mice overexpressing *Dyrk1A* displayed reduced anxiety levels on the EPM and increased activity on the open-field maze (Altafaj et al., 2001). In the Ts65Dn, normalisation of *Dyrk1A* copy number reduced hyperactivity (García-Cerro et al., 2014).

Overall, the behavioural profile of the Dp1Tyb strain recreated some, but not all, of the phenotypes observed in other Mmu16 trisomy models. Occurrence and nature of memory deficits seem to depend on genetic differences between the Mmu16 models. However, rather than being specific Mmu16 genes or Mmu16 portions whose over-dosage is directly responsible for the manifestation of given memory deficits, it seems that phenotypes depend primarily on dosage-dependent interactions between Mmu16 homologs.

Mmu17 and the Dp3Yey model

Dp3Yey animals displayed intact recognition memory. Performance was normal on the NOR and the OiP task (Exp. 2a), indicating that Dp3Yey mice successfully recognised novel objects and novel object-in-place associations, both after short (10-min) and long (24-h) retention intervals. Intact OiP memory automatically implied normal memory for single spatial locations. Hence, the Mmu17 trisomy did not affect either single- or associative-recognition memory processes. As predicted, memory was not affected by ageing (Exp. 2b).

Based on the memory profile displayed by Dp3Yey mice, it can be concluded that there is no evidence that the Mmu17 trisomy alters activity of medial temporal lobe structures, even at advanced age. Genes syntenic to Hsa21 located on Mmu17 thus do not seem to contribute to either cognitive decline or hippocampal dysfunction characteristic of DS. This interpretation is in line with previous evidence on the Dp3Yey model reporting intact memory on the MWM and the contextual fear conditioning task (Yu et al., 2010b).

Further support for the lack of involvement of Mmu17 homologs in the regulation of hippocampal activity comes from mouse lines with partial Mmu17 mutations. Both animals trisomic (Dp1Yah) or monosomic (Ms2Yah) for a portion of Mmu17 homologs did not display memory deficits in HPC-dependent tasks (Pereira et al., 2009; Sahún et al., 2014). In fact, visuospatial learning on the MWM and associative memory on the contextual fear conditioning task were significantly increased in the Dp1Yah and Ms2Yah respectively.

Nevertheless, intact NOR memory in the Dp3Yey diverges from previous findings on the Dp1Yah model. Following a 1-h delay, Dp1Yah mice were found unable to discriminate between a novel and a familiar object, suggesting that over-dosage of a portion of Mmu17 syntenic genes interferes with normal activity of the PRH cortex (Marechal et al., 2019; Pereira et al., 2009). The task was however carried out with a single sample phase. Whether memory for objects following exposure to a single sample phase and after a 1-h retention interval would be impaired in Dp3Yey mice, is currently unknown. This seems however highly unlikely, since present results found no evidence for a reduction in novelty preference.

Based on the above findings, it can be concluded that genes trisomic in the Dp3Yey but not the Dp1Yah model determine the emergence of impairments in object memory. As per the importance of gene-to-gene interactions noted for Mmu16 trisomy models, it seems plausible that over-dosage of the few genes exclusive to the Dp3Yey model (~5 genes) might compensate for the deleterious effects produced by over-dosage of the remaining Mmu17 homologs. A possible candidate gene implicated in NOR impairments is the *Cbs* gene, trisomic in both the Dp3Yey and the Dp1Yah model. The *Cbs* gene codes for an enzyme involved in the synthesis of cysteine, an amino acid relevant for metabolism

function (Marechal et al., 2019). Mutations in the *CBS* gene have been associated to homocystinuria, a metabolic disorder affecting a wide range of body systems, including the central nervous system. Individuals with homocystinuria have intellectual disability (Almuqbil et al., 2019).

In DS individuals, CBS expression in the brain is over twice as much the levels of control subjects (Ichinohe et al, 2005). CBS levels in Dp3Yey mice are unknown but Dp1Yah mice reported an increase in different brain regions, including the HPC (Pereira et al., 2009). Interestingly, normalisation of *Cbs* dosage in Dp1Yah animals restored normal memory for objects (Marechal et al., 2019). Moreover, transgenic mice deficient for *Cbs* showed normal NOR memory, while transgenic mice overexpressing *Cbs* were impaired and the deficit could be rescued by treatment with CBS-inhibitors, attributing CBS overexpression a causative role in object memory impairments (Marechal et al., 2019). It is possible that in the Dp3Yey model, simultaneous over-dosage of all Mmu17 homologs downregulates CBS expression, preventing memory deficits in the NOR task. This hypothesis could potentially be confirmed by measuring CBS levels in Dp3Yey brains.

Interactions between genes do not only occur between genes located on the same conserved region, but also between genes on different chromosomes, reiterating the genetic complexity of DS. For example, while Dp1Yah mice and transgenic mice overexpressing DYRK1A displayed impaired NOR memory, crossing the two mouse lines resulted in offspring with intact NOR memory, implicating that interactions between Mmu17 homologs and *Dyrk1A* prevent the deficit (Marechal et al., 2019). Indeed, DYRK1A levels have been associated to CBS expression (Marechal et al., 2019). However, simultaneous Dp1Yah trisomy and DYRK1A overexpression produced a new deficit on the MWM, confirming the importance of *Dyrk1A* dosage in HPC-dependent tasks (Marechal et al., 2019).

Although trisomy of Mmu17 homologs did not result in memory deficits, phenotypes were observed on the EPM (Exp. 2c). While Dp3Yey mice explored open arms to a similar extent as wildtypes, indicating no anxiety phenotype, the overall distance walked on the EPM was significantly larger in the Dp3Yey group. Importantly, despite the increase in locomotor activity, Dp3Yey habituated normally to the maze, suggesting that hyperactivity was not the result of a cognitive defect in accustoming to the environment. Increased activity levels in the Dp3Yey are unlikely to have interfered with performance on object-recognition memory tasks, as novelty preference of Dp3Yey mice was no different from controls, in any task. On the contrary, contact behaviour towards the objects was remarkably similar to wildtypes, both in sample and test phases.

Normal anxiety levels are in agreement with previous EPM evidence on the Dp1Yah model, adding to the interpretation that Mmu17 homologs are not involved in the regulation

of anxiety (Pereira et al., 2009). Interestingly, while Dp1Yah and mice overexpressing CBS reported normal locomotor levels on the open-field test, normalising *Cbs* copy number in the Dp1Yah produced hyperactivity (Marechal et al., 2019). As noted for object memory, it seems plausible that genes trisomic in the Dp3Yey but not the Dp1Yah model downregulate the expression of CBS, in this case generating a hyperactivity phenotype.

Based on the current findings it can be postulated that syntenic genes located on Mmu17 play an important role in the regulation of activity levels, potentially contributing to attention deficit / hyperactivity disorders observed in the DS population. Although hyperactivity has been previously associated to hippocampal dysfunction, this interpretation would be in contrast with present and previous evidence reporting no impairments in HPC-dependent memory tasks in Dp3Yey mice.

Overall, the memory profile of Dp3Yey mice was consistent with previous findings reporting normal performance in HPC-dependent tasks. The findings were however in strong contrast to a model of incomplete Mmu17 trisomy. Once again, gene-to-gene interactions seem crucial in determining the emergence of behavioural phenotypes.

Mmu10 and the Dp2Yey model

Dp2Yey animals displayed an age-dependent, deficit in recognition memory. At 12 months of age, performance on the NOR and the OiP task was no different from controls, both after short (10-min) and long (24-h) retention intervals (Exp. 3a). In both tasks however, performance of the Dp2Yey on the 24-h test was at chance levels. Low novelty discrimination concerned specifically the retention of objects and object-in-place associations, since memory for single spatial locations assessed with the Loc task was above chance after 24-h (Exp. 3a).

At 20 months of age, Dp2Yey mice displayed a pervasive impairment in object memory. In the NOR task, aged Dp2Yey mice were no longer able to discriminate between familiar and novel objects, both after short (10-min) and long (3-h) retention intervals (Exp. 3b). Consequently, associative-recognition memory processes relying on object memory assessed in the OiP and TOr task could not be evaluated and further testing was only practicable with the Loc task (Exp. 3b). Aged Dp2Yey mice were still able to discriminate between novel and familiar spatial locations, excluding the possibility that NOR deficits were caused by non-specific perceptual or attentional impairments. Hence, although the Mmu10 trisomy alone did not significantly affect single- or associative-recognition memory, the Mmu10 trisomy in conjunction with ageing resulted in impaired memory for single items (*what*), sparing memory for single locations (*where*).

Electrophysiological and cellular studies repeatedly demonstrated that the processing of item information relies on activity of the PRH cortex and lesions of the PRH cortex were repeatedly demonstrated to impair memory for objects. On the NOR task, pharmacological

inactivation of the PRH cortex prior to the sample phase, during the retention interval or prior to the test phase, resulted in impaired performance (Winters & Bussey, 2005). These results strongly indicate that activity of the PRH cortex is necessary during encoding, consolidation and retrieval of object memory. Here, 20-month-old but not 12-mont-old Dp2Yey animals were unable to recognise novel objects among familiar objects on the NOR task (Exp. 3b). Therefore, it can be reasonably concluded that the Mmu10 trisomy progressively impaired function of the PRH cortex.

Although memory for objects was impaired in 20-month-old Dp2Yey, memory for single spatial locations assessed with the Loc task was preserved (Exp.3b). Spatial / contextual information is primarily processed by the postrhinal cortex and the HPC. It could thus be assumed that the Mmu10 trisomy did not impair activity of the HPC. However, present findings do not permit one to definitively draw this conclusion, as HPC-dependent associative-recognition memory processes could not be tested in the presence of defective object memory. Although associative-recognition memory processes would be impaired in 20-month-old Dp2Yey mice due to defective processing of object-information, it cannot be excluded that the HPC-dependent integration of object- and context information might also be defective.

In 12-month-old Dp2Yey animals, memory for object-in-place associations was unimpaired, suggesting no hippocampal dysfunction at this age (Exp. 3a). However, Dp2Yey mice performed only at chance levels on the 24-h test. Since performance was also low on the 24-h test of the NOR task (Exp. 3a), it cannot be determined whether low performance in the OiP task was due to a defect in HPC-dependent input integration or a consequence of already degrading object memory. This ambiguity could potentially be clarified by investigating associative-recognition memory processes in Dp2Yey mice at an earlier age.

Although previous evidence on the Dp2Yey model is scarce, findings indeed seem to suggest that the Mmu10 trisomy does not interfere with hippocampal function. Dp2Yey animals aged 2-4 months reported normal visuospatial learning on the MWM and normal associative learning on the contextual fear conditioning task (Yu et al., 2010b). Nevertheless, since performance on these tasks requires the HPC-mediated integration of item- and contextual-information, it can be predicted that Dp2Yey mice would display memory deficits if tested at a later age.

Whether Mmu10 syntenic genes contribute to the hippocampal dysfunction characteristic of DS was also addressed with crossed transgenic mouse lines. Duchon et al. (2011a) generated mice monosomic for the entirety of the Mmu10 syntenic region, the Ms4Yah. These animals were crossed with Tc1 mice, producing offspring with normal copy number of the Mmu10 region on the trisomic background of the Tc1 line. The animals were

tested on the short-term version of the MWM, assessing performance following repeated training trials separated by brief time intervals. Visuospatial learning was intact in Ms4Yah mice but impaired in both Tc1 mice and Tc1 mice with normal Mmu10 dosage, suggesting once again that Mmu10 genes do not play a key role in the regulation of hippocampal function.

Although the Mmu10 trisomy does not seem to contribute to aberrant hippocampal function, the deficit in the NOR task indicates that it is involved in the object memory impairments observed in DS. In the Tc1 line, trisomic mice displayed a deficit on the NOR task together with spared memory for novel spatial locations on the Loc task, exactly as observed here in aged Dp2Yey (Hall et al., 2016). Since Dp2Yey but not Dp1Tyb or Dp3Yey mice reported a NOR deficit, it is plausible that over-dosage of Hsa21 genes mapping to Mmu10 causes aberrant memory for objects in DS. The assessment of Tc1 mice with normal Mmu10 copy number on the NOR task could potentially confirm this hypothesis, with crossed animals expected to perform normally.

Tc1 mice displayed however the NOR deficit already at 4-7 months of age, while here, 12-month-old Dp2Yey mice still performed no different from controls. Additionally, Tc1 mice were impaired exclusively after a 10-min delay, while here, 20-month-old Dp2Yey mice were also impaired after longer retention intervals. At younger age, signs of a weaker memory trace were present in the Dp2Yey, but only in long-term memory. It can be speculated that in the Tc1 model, trisomy of Mmu10 homologs in conjunction to the remaining Hsa21 homologs, exacerbates memory deficits, revealing them at an earlier age. At the same time, the complete Hsa21 trisomy in the Tc1 model might result in compensatory mechanisms rescuing long-term memory performance.

A candidate Hsa21 gene for the age-dependent cognitive decline observed in the Dp2Yey model is the *S100B* gene, which maps to Mmu10. This gene is primarily expressed by astrocytes, encoding for the S100 calcium-binding protein B (Cristóvão & Gomes, 2019). S100B can act as neurotrophic factor, contributing to cell proliferation, differentiation and growth and has also been involved in synaptic plasticity, as discussed in chapter 4. S100B can also play a role in neuroinflammation, acting as a pro-inflammatory cytokine. As such, S100B has been repeatedly implicated in the pathogenesis of AD.

In AD, the formation of Aβ-aggregates and consequent neuronal cell death elicit an immune response, resulting in glial cells activation and cytokine expression, including S100B (Cristóvão & Gomes, 2019). Immunohistochemical analyses report that cortical and hippocampal levels of S100B are elevated in AD-patients and mouse models of AD (Griffin et al., 1989; Yeh et al, 2015). Moreover, Tg2576 mice crossed with transgenic mice overexpressing human S100B show a significant increase in Aβ-deposits in HPC and entorhinal cortex, in comparison to Tg2576 mice (Mori et al., 2010). Respectively, genetic

ablation of *S100b* in a mouse model of AD resulted in a significant decrease in cortical Aβ-density (Roltsch, Holcomb, Young, Marks, & Zimmer, 2010).

Such findings provide evidence for the involvement of S100B in the amyloidgenic cleavage of APP. Although the exact cellular mechanisms are unclear, S100B has been found to upregulate the expression of APP and vice versa, in a self-propagating cycle exacerbating AD pathology (as reviewed in Wilcock & Griffin, 2013). In this perspective, the higher incidence of AD in the DS population is unsurprising, since trisomy 21 combines over-dosage of both the *S100B* and the *APP* gene. Indeed, S100B expression is already elevated in DS foetuses and progressively increases with age (Griffin et al., 1989; Royston et al., 1999). Moreover, cortical S100B levels were found to positively correlate with Aβ-deposition levels in DS individuals (Royston et al., 1999).

Considering the previous evidence, it can be postulated that in the Dp2Yey model – trisomic for *S100b* but not *App* – overexpression of S100B progressively leads to increased Aβ accumulation, promoting neurodegeneration and cognitive decline. In fact, transgenic mice overexpressing S100B were found to display dendritic spine loss at 1 year of age, along with aberrant cytoskeletal morphology and impaired memory on the MWM (Whitaker-Azmitia et al., 1997). Importantly, the detrimental effect of S100B overexpression depended on age, whereby 5-week-old transgenic mice actually displayed an increase in dendritic spine density.

In line with the reciprocally upregulating relationship between S100B and APP, levels of S100B were found increased in Ts1Cje mice, trisomic for *App* but not *S100b* (Créau et al., 2016). This increase was once again age-dependent, observed at 12- and 17- but not 4-months of age. In the Dp2Yey, hippocampal levels of both S100B and APP were found elevated at 8 months of age (Block et al., 2015). Based on current and previous evidence, it can be hypothesised that brains of aged Dp2Yey animals are characterised by neurodegenerative processes and Aβ-aggregation, causing memory impairments.

On the EPM (Exp. 3c), the propensity of Dp2Yey mice to explore the open arms of the maze was similar to wildtypes, as well as locomotor activity levels. This suggests that Hsa21 syntenic genes located on Mmu10 are not involved in the regulation of anxiety or activity levels. In line with this interpretation, Ms4Yah mice reported normal locomotor activity and normal thigmotaxis levels on the open-field test (Duchon et al., 2011a).

It must however be noted, that only 12-month-old Dp2Yey animals were tested on the EPM. It cannot be excluded that the Mmu10 trisomy might generate anxiety or activity phenotypes at a later age, as was the case for memory function. Consequently, it remains unclear whether these measures might have interfered with performance in object-recognition memory tasks at 20-months of age. Nevertheless, the available evidence demonstrates that there was no difference in the explorative behaviour of Dp2Yey and WT

animals during the sample phases. Additionally, performance of aged Dp2Yey mice was not overall impaired, but only in the NOR task. It is unlikely that possible anxiety or activity phenotypes produced such a selective deficit.

Overall, the memory profile of Dp2Yey mice provided no evidence of abnormal hippocampal function, in line with previous findings on this model. This interpretation is however limited by aberrant memory for objects. The Mmu10 trisomy was nevertheless associated to age-dependent abnormal function of the PRH cortex. No anxiety or activity phenotypes were associated to the Mmu10 trisomy.

Conclusion

These results identify the Mmu16 conserved region as the primary source of aberrant HPC-dependent recognition memory processes. Instead, the Mmu10 conserved region was identified as the source of aberrant memory for objects and age-related cognitive decline. The Mmu17 and the Mmu16 trisomy were related to increased activity and anxiety levels.

Together, phenotypes observed in the Dp1Tyb, Dp3Yey and Dp2Yey recapitulated phenotypes observed in the triple trisomic (TTS) model. Analogously to the Dp1Tyb line, TTS mice were found to display deficits in HPC-dependent tasks, namely the MWM and the contextual fear conditioning task (Yu et al., 2010a). TTS mice also displayed a deficit in the NOR task after a 24-h delay, as observed in aged Dp2Yey (Belichenko et al., 2015). Finally, TTS mice showed increased locomotor activity on the open-field test, analogously to what observed in the Dp3Yey and to some extent in the Dp1Tyb on the EPM (Belichenko et al., 2015).

Comparison of current findings with other models of the Mmu16, Mmu17 and Mmu10 trisomy revealed that gene-to-gene interactions are fundamental in determining the manifestation of phenotypes, rather than specific genes or gene segments. For example, while dosage normalisation of the DSCR in the Dp1Tyb rescued performance on the MWM, normalisation of the DSCR plus trisomy of the Mmu17 conserved region reinstated the MWM deficit (Zhang et al., 2014). By contrast, dosage normalisation of the DSCR in the Dp1Tyb plus trisomy of the Mmu10 conserved region did not prevent DSCR normalisation to rescue the MWM deficit. This implicates that genes on Mmu17 but not on Mmu10, interact with Mmu16 genes outside the DSCR, reinstating the memory deficit. Further studies assessing performance of crossed mouse lines on the NOR task would allow to uncover whether Mmu10 genes interact with Mmu16 or Mmu17 in the regulation of object memory.

The cellular mechanisms through which syntenic genes on Mmu16, Mmu17 and Mmu10 regulate each other's expression in DS, affecting brain development, synaptic plasticity and memory function, still need clarification. In this respect, the utility of mouse models of segmental DS is limited.

Table 3.13: Overview of behavioural findings. Performance in object-recognition memory tasks and on the EPM test for the cohorts of Dp1Tyb, Dp3Yey and Dp2Yey animals. Red: impaired memory performance / EPM phenotype; green: intact memory performance / no EPM phenotype; yellow: chance memory performance.

		Task							
		NOR		OiP		Loc	TOr		EPM
Mouse line	**Age**	10-min	3-h/24-h	10-min	3-h/24-h	10-min/24-h	10-min	3-h	
Dp1Tyb	12-mo	✓	✓	✗	✓	✓	✗	✓	Anxiety, hyperactivity in closed arms
	20-mo	✓	✓						
	4-mo			✗	✓				
Dp3Yey	12-mo	✓	✓	✓	✓				Hyperactivity
	18-mo	✓	✓	✓	✓				
Dp2Yey	12-mo	✓	≈	✓	≈	✓			No phenotype
	20-mo	✗	✗			✓			

Chapter 4: Expression of glutamate receptors

Overview

This chapter begins with an introduction on synaptic plasticity mechanisms and glutamate receptors. Expression and activity of glutamate receptors is fundamental for the changes in synaptic transmission postulated to underpin memory function. Indeed, altered activity of glutamate receptors has been associated to memory impairments and altered glutamate receptor levels are observed in the hippocampus of DS mouse models. Therefore, to determine the impact of the Mmu16, Mmu17 and Mmu10 trisomy on glutamate receptor expression and to reveal molecular mechanisms possibly associated to impairments in object-recognition memory tasks observed in chapter 3, glutamate receptor expression was examined in the hippocampus of Dp1Tyb, Dp3Yey and Dp2Yey mice. Western blot experiments are reported in this chapter. The three mouse lines revealed distinct patterns of glutamate receptor expression, possibly related to over-dosage of key genes located on the respective trisomic segment.

4.1. Introduction

In object-recognition memory tasks, successful recall of the sample episode implies that the episode was first encoded and then consolidated into a stable memory representation. Biochemical processes such as gene expression and protein synthesis in the neural networks that encode the memory, take place seconds to years thereafter and are proposed to represent the cellular basis of LTM (Dudai, Karni, & Brown, 2015). In this chapter, the focus lies on glutamate receptors involved in the molecular mechanisms underlying the cellular consolidation of episodic-like memories formed during object-recognition memory tasks.

4.1.1. Synaptic plasticity

Neurons communicate via the transmission of electrochemical signals exchanged at synapses. Signals are transmitted from the axon terminal of the presynaptic neuron to dendritic spines on the postsynaptic neuron through the release of neurotransmitters. Receptors on the postsynaptic neuron are activated by the neurotransmitter and open to allow the influx of positively charged ions. Sufficient depolarisation of the postsynaptic neuron triggers transmission of the signal via the same mechanism to connecting neurons (Purves et al., 2012).

At cellular level, memories are postulated to be stored in the strength of the synapses connecting the neural circuit encoding the memory (Citri & Malenka, 2008; Dudai et al., 2015; Hebb, 1949). During memory consolidation, molecular mechanisms modify the strength of the connections, inducing long-term changes in the efficacy of synaptic transmission. These changes can either facilitate, and thus strengthen communication between neurons, or hinder, and thus weaken communication. Long-lasting, experience dependent changes in synaptic transmission are referred to as synaptic plasticity.

There are two main models of synaptic plasticity, long-term potentiation (LTP) and long-term depression (LTD). The most common and most extensively studied mechanism of LTP and LTD involves the rapid redistribution of postsynaptic receptors. In this type of synaptic plasticity, receptors are either added to the synapse to enhance synaptic transmission (LTP) or removed from the synapse to decrease synaptic transmission (LTD).

Long-term potentiation was first demonstrated in the HPC, by electrophysiological studies (Bliss & Gardner-Medwin, 1973a; Bliss & Lomo, 1973b). These studies reported that repetitive high-frequency stimulation of excitatory synapses resulted in increased postsynaptic potentials, lasting for hours and days. Frequent synaptic activation thus enhanced transmission efficacy.

Numerous studies investigated the molecular mechanisms underlying synaptic potentiation, concentrating on the HPC. These studies tested the effects of pharmacological inactivation of different postsynaptic receptors or signalling molecules on electrophysiological LTP (Lee, Barbarosie, Kameyama, Bear, & Huganir, 2000; Malenka et al., 1989; Malenka, 1991; Shi, Hayashi, Esteban, & Malinow, 2001). The resulting evidence converged towards a relatively uniform picture of the LTP-intracellular cascades, as summarised by Citri and Malenka (2008).

Upon neuronal activation, the excitatory neurotransmitter glutamate is released at the synapse from the presynaptic neuron. Glutamate binds to ionotropic α-amino-3-hydroxy-5-methyl-4-isoxazolepropionic acid receptors (AMPARs) and N-methyl-D-aspartate receptors (NMDARs) located on the surface membrane of the postsynaptic neuron, causing AMPAR channels to open and allowing sodium ions (Na^+) to enter the postsynaptic neuron, gradually depolarising it. NMDAR channels are, however, blocked by magnesium and remain largely impermeable. Once the postsynaptic neuron is sufficiently depolarised, the magnesium block is expelled from NMDAR pores allowing further Na^+ influx and importantly, the influx of calcium ions (Ca^{2+}). A large increase in Ca^{2+} concentration activates the calcium / calmodulin-dependent protein kinase II (CaMKII), which potentiates the synapse in two ways. For one, CaMKII phosphorylates AMPAR subunits causing an increase in the conductance of AMPAR channels. For another, CaMKII triggers the exocytosis of new AMPARs from intracellular vesicles and their insertion into the postsynaptic membrane. These NMDAR-dependent events increase speed and likelihood of future postsynaptic depolarisation upon glutamate release, potentiating the communication between the neurons. Molecular mechanisms of the LTP-cascade are schematically represented in fig. 4.1.

The synaptic changes described above have been observed to occur in the first hours after electrophysiological stimulation to induce LTP. The subsequent molecular mechanisms allowing LTP to be maintained for hours and days are not fully understood, but evidence indicates that they depend upon Ca^{2+}-mediated synthesis of new proteins. For example, hippocampal injections of the protein synthesis inhibitor anisomycin in freely moving rats blocked the expression of LTP 3-4 hours after synaptic stimulation, while initial LTP was normal (Krug, Lössner, & Ott, 1984). The available evidence suggests the existence of two distinct phases of LTP: an initial induction phase that does not depend on protein synthesis, and a later phase that necessitates the synthesis of new proteins for the long-lasting stabilisation of LTP. The late-phase of LTP has also been associated to morphological changes in the postsynaptic neuron, such as enlargement and growth of dendritic spines (Matsuzaki, Honkura, Ellis-Davies, & Kasai, 2004).

The idea that synaptic plasticity and, LTP in particular, embody the biological mechanism of memory storage, is supported by several studies. For example, injection of NMDAR antagonists in the mouse HPC blocked the expression of LTP and produced deficits in spatial memory (Morris et al., 1986). Mice that were trained to learn a new stimulus-context association in an avoidance task, showed increased AMPAR phosphorylation levels and increased excitatory postsynaptic potentials (Whitlock, Heynen, Shuler, & Bear, 2006). Further support for the idea that memories are stored in the distribution of varying degrees of synaptic strength within a neural circuit, comes from electrophysiological experiments observing NMDAR-dependent LTD, proving the existence of a mechanism able to modify synaptic strength in the opposite direction to LTP. Dudek and Bear (1992) found that repetitive low-frequency stimulation of excitatory synapses in rat hippocampal slices resulted in decreased postsynaptic potentials. Importantly, the application of NMDAR-antagonists blocked the expression of LTD and high-frequency stimulation of previously depressed synapses could reverse LTD and elicit LTP. This evidence suggests that the direction of synaptic plasticity depends on the intensity of synaptic activation, mediating magnitude and dynamics of postsynaptic Ca^{2+} entry through NMDARs.

The LTD-intracellular signalling cascade (fig. 4.1) has been investigated by several studies (Beattie et al., 2000; Morishita et al., 2001; Mulkey & Malenka, 1992; Mulkey, Endo, Shenolikar, & Malenka, 1994). As summarised by Citry and Malenka (2008), LTD is initiated by a modest release of glutamate, causing weak activation of AMPARs and slow postsynaptic depolarisation. Consequently, NMDAR pores are only partially relieved by the magnesium block, allowing a modest influx of Ca^{2+}. At low levels, Ca^{2+} activates the calcium / calmodulin-dependent phosphatase calcineurin and the protein phosphatase 1 (PP1), which in turn dephosphorylate AMPARs, decreasing their conductivity and triggering AMPAR endocytosis. As for LTP, the maintenance of LTD requires protein synthesis and has been associated to morphological changes, such as NMDAR- and calcineurin-dependent shrinkage of dendritic spines (Manahan-Vaughan, Kulla, & Frey, 2000; Zhou, Homma, & Poo, 2004). Importantly, LTD has been demonstrated as essential as LTP for the storage of new memories, whereby calcineurin-knockout mice reported impaired electrophysiological LTD and memory impairments (Zeng et al., 2001).

Although research has largely focused on NMDAR-dependent postsynaptic LTP and LTD at hippocampal excitatory synapses, other forms of synaptic plasticity have also been observed (Citri & Malenka, 2008). For example, synaptic plasticity can take place in presynaptic neurons, regulating neurotransmitter release. Activity-dependent changes have also been observed at inhibitory synapses and can involve metabotropic glutamate receptors or other types of synaptic receptors. Synaptic plasticity is a dynamic process

aimed to regulate surface expression and channel function of synaptic receptors, primarily ionotropic glutamate receptors. There are three classes of ionotropic glutamate receptors: AMPARs, NMDARs, and kainate receptors (KARs). Receptors actively involved in synaptic transmission are clustered together with other signalling molecules in the postsynaptic density (PSD) of dendritic spines, an area adjacent to presynaptic terminals. The characteristics of each class of ionotropic glutamate receptors are briefly outlined below, following the most recent receptor nomenclature (Collingridge, Olsen, Peters, & Spedding, 2009).

AMPA receptors

AMPARs mediate fast, excitatory synaptic transmission and are expressed throughout the entire brain. AMPARs are composed as dimer-of-dimers of the four subunits GluA1, GluA2, GluA3, GluA4, each encoded by a different gene. AMPARs can be assembled into heterotetrameric or homotetrameric complexes. In the adult rat HPC, the majority of AMPARs are GluA1/2 and GluA2/3 heterotetramers, while GluA4 is mainly expressed during early development (Wenthold, Petralia, Blahos, & Niedzielski, 1996).

Each of the four subunits composing the AMPAR has a binding site for glutamate. Channel conductivity increases as more binding sites are occupied by glutamate or upon phosphorylation of the receptor (Derkach, Barria, & Soderling, 1999; Rosenmund, Stern-Bach, & Stevens, 1998). While all AMPARs allow the influx of Na^+, GluA2-lacking AMPARs also allow the entry of Ca^{2+} (Hollmann, Hartley, & Heinemann, 1991). Evidence suggests that the insertion of Ca^{2+}-permeable AMPARs constitutes the early-phase of LTP and that these are subsequently replaced by Ca^{2+}-impermeable AMPARs to stabilise LTP (Plant et al., 2006).

AMPARs are assembled in the endoplasmic reticulum and trafficked to perisynaptic sites along the dendritic shaft by transmembrane AMPA receptor regulatory proteins (TARPs) (Henley & Wilkinson, 2016). LTP induction triggers the exocytosis of AMPARs, which reach the PSD via lateral diffusion at the membrane surface. AMPARs are then anchored to the PSD by interacting with Ca^{2+}-sensitive TARPs (e.g. stargazin) and synaptic scaffold proteins (e.g. PSD95, SAP97). During LTD induction, AMPARs are internalised at endocytic zones adjacent the PSD, whereby internalised AMPARs are either recycled back to the plasma membrane or sorted for protein degradation by Ca^{2+}-sensitive pathways. In addition to the activity-dependent exocytosis and endocytosis of AMPARs, AMPARs also undergo constitutive recycling at the synapse, resulting in highly-dynamic AMPAR trafficking both during plasticity and basal conditions (Henley & Wilkinson, 2016). Dysregulations in the expression, activity or trafficking of AMPARs at the synapse have been linked to memory impairments, in particular in relation to the GluA1 subunit (Lee et al., 2003; Sanderson & Bannerman, 2012; Wakabayashi, et al., 1999).

NMDA receptors

NMDARs are heterotetrameric receptors composed of two obligatory GluN1 subunits (encoded by one gene with eight splice variants) and two regulatory subunits (GluN2 or GluN3) (Sanz-Clemente, Nicoll, & Roche, 2013). There are four genes encoding the GluN2 regulatory subunit (GluN2 A-D) and two genes encoding GluN3 (A-B). NMDARs are assembled in the endoplasmic reticulum as di-heterotetrameric or tri-heterotetrameric complexes. For the NMDAR pore to open, simultaneous binding of glutamate and glycine (or D-serine) is necessary. NMDARs are considered “molecular coincidence detectors”, as channel gating requires neurotransmitter release from the presynaptic neuron and depolarisation of the postsynaptic neuron to expel the magnesium block. Open NMDAR channels allow the influx of Na^+ and Ca^{2+} ions.

NMDAR expression and channel properties depend on their regulatory subunits, which are developmentally regulated (Sanz-Clemente et al., 2013). GluN3-containing NMDARs exhibit low Ca^{2+} permeability and GluN2C-containing NMDARs are predominantly expressed in the cerebellum. GluN2D- and GluN2B-containing NMDARs are highly expressed during early brain development and found only at lower levels in the adult brain. By contrast, the expression of Glu2NA-containing NMDARS is weak postnatally but increased in adulthood. Regulatory subunits can also determine the subcellular localisation of NMDARs, with GluN2A-containing NMDARs preferentially found at synaptic and GluN2B-containing NMDARs at extrasynaptic sites (Sanz-Clemente et al., 20131). At the synapse, NMDARs are anchored to the PSD by binding to scaffold proteins (e.g. PSD95, SAP102) in a subunit-dependent manner. While AMPARs are rapidly trafficked to and from the synapse, evidence suggests a less dynamic trafficking of NMDARs. Higher mobility and recycling rates have been described for GluN2B- in comparison to GluN2A-containing NMDARs.

Similarly to AMPARs, alterations in activity or surface expression of NMDARs have been associated to memory dysfunction and neurodegenerative conditions, such as AD (Sanz-Clemente et al., 2013). Neurodegenerative cascades seem to be specifically related to the GluN2B subunit (Snyder et al., 2005).

Kainate receptors

In contrast to AMPARs and NMDARs, the role of KARs in synaptic plasticity is less clear. Due to pharmacological limitations (i.e. lack of specific KAR antibodies), this receptor class was not systematically investigated until recently. KARs are tetrameric complexes composed as dimer-of-dimers of the five subunits GluK1, GluK2, GluK3, GluK4, GluK5, each encoded by a distinct gene (Evans, Gurung, Henley, Nakamura, & Wilkinson, 2019). The GluK1-3 subunits can assemble into homotetramers, while the GluK4 and GluK5 subunits must co-assemble with a GluK1, 2 or 3 subunit in order to form functional receptors. Unlike AMPARs and NMDARs, KAR signalling can be induced not only in

response to glutamate binding, but also by G-proteins (Evans et al., 2019). KARs activated by glutamate are permeable to Na^+ and to a degree to Ca^{2+}, while G-protein-activated KARs trigger a series of intracellular events, operating similarly to metabotropic receptors.

KARs are widely distributed throughout the brain and are found both pre- and postsynaptically. In the HPC, GluK4- and GluK-5 subunits are located mainly on pre- and postsynaptic membranes, respectively (Darstein, Petralia, Swanson, Wenthold, & Heinemann, 2003). KARs have been implicated in both hippocampal LTP and LTD, with presynaptic KARs modulating the release of glutamate and inhibitory neurotransmitter, and postsynaptic KARs modulating excitatory responses (Evans et al., 2019). In comparison to AMPARs, KARs generate slower and smaller currents of excitatory postsynaptic potentials and the majority of KAR-mediated forms of synaptic plasticity are independent of NMDAR-activity (Castillo, Malenka, & Nicoll, 1997; Evans et al., 2019).

Several proteins have been involved in KAR anchoring to the PSD (e.g. PSD95), KAR endocytosis (e.g. SNAP25, actinfilin) and KAR channel properties (e.g. NETO1, NETO2) but the exact mechanisms are not clear (Evans et al., 2019). KARs have been associated to several neurological diseases, such epilepsy and mental retardation (Evans et al., 2019). In fact, the gene coding for the GluK1 subunit (Glutamate Receptor Ionotropic Kainate 1, *GRIK1*) is located on Hsa21. Additionally, the GluK5 subunit has been specifically implicated in synaptic plasticity mechanisms underlying recognition memory and is reduced in Tc1 mice (Barker et al., 2006; Hall, 2016).

Figure 4.1: Graphical representation of the intracellular cascade during NMDAR-dependent LTD and LTP. Left: Weak glutamate release results in weak Ca^{2+} influx, activating protein phosphatases (e.g. calcineurin, PP1) that induce the removal of AMPARs from the PSD (light grey area), de-potentiating the synapse (LTD). Right: Strong glutamate release results in the activation of NMDAR channels and a strong Ca^{2+} influx, activating protein kinases (e.g. CaMKII) that induce the insertion of new AMPARs into PSD, potentiating the synapse (LTP). Adapted from Lüscher and Malenka (2012).

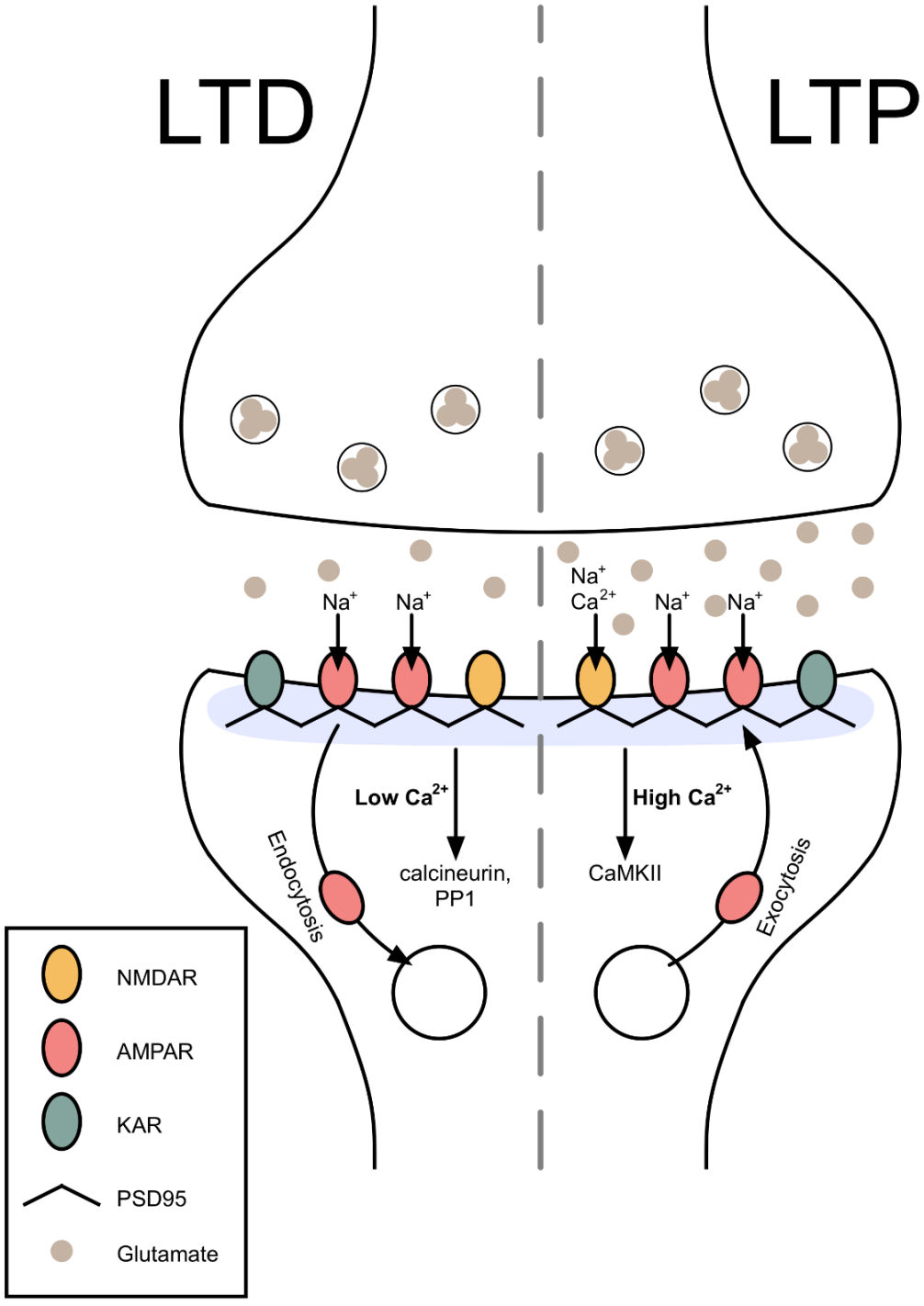

4.1.2. Study rationale

DS is caused by trisomy of Hsa21, a neurodevelopmental disorder characterised by learning and memory impairments (section 1.2). The HPC is the core structure supporting memory function. In individuals with DS, the HPC is characterised by morphological anomalies, such as reduced cell number and dendritic branching (e.g. Becker et al., 1986). At cellular level, memories are proposed to be stored in varying degrees of synaptic transmission efficacy within a neural network encoding the memory (Citri & Malenka, 2008; Dudai et al., 2015; Hebb, 1949). Synaptic transmission efficacy is modulated through plasticity mechanisms that either potentiate (LTP) or depotentiate (LTD) communication between connecting neurons.

The most extensively studied form of plasticity takes place at excitatory synapses, where activity of ionotropic glutamate receptors can induce long-lasting changes in postsynaptic terminals of dendritic spines (section 4.1.1.). This type of synaptic plasticity is dependent on NMDAR-activation and consists primarily on the rapid, activity-dependent redistribution of AMPAR surface expression.

AMPARs are synthesised in the endoplasmic reticulum and subsequently trafficked to dendritic spines (Henley & Wilkinson, 2016). AMPAR trafficking is highly dynamic, with AMPARs undergoing both constitutive and activity-dependent cycling in and out the PSD. Upon synaptic activation, Ca^{2+}- sensitive intracellular signalling cascades involving protein phosphatases and kinases, upregulate (LTP) or downregulate (LTD) AMPAR surface expression, depending on the dynamics of Ca^{2+} entry.

In addition to AMPARs and NMDARs, a third class of ionotropic glutamate receptors – KARs – has also been recently demonstrated to contribute to synaptic plasticity at excitatory synapses in the HPC. At postsynaptic terminals, KAR-mediated plasticity is independent of NMDAR-activation and can operate to regulate AMPAR or KAR surface expression (Carta et al., 2013; Petrovic et al., 2017). Recent evidence indicates that similarly to AMPARs, KARs undergo activity-dependent cycling at the PSD (Gurung et al., 2018).

Fine-tuned regulation of glutamate receptor function is crucial for normal synaptic potentiation and memory function. Antagonism of glutamate receptor activity has been repeatedly demonstrated to impair learning and memory, including performance in object-recognition memory tasks (e.g. Barker et al., 2006; Barker & Warburton, 2015). Unsurprisingly, mouse models of DS exhibit altered expression of glutamate receptors, primarily reduced AMPAR levels in the HPC (Belichenko et al., 2009b; Morice et al., 2008; Souchet et al., 2014). Accordingly, electrophysiological studies report defective hippocampal LTP in a wide range of DS mouse models, including Tc1, Ts1Cje, Ts1Rhr, Ts65Dn, Dp1Tyb and Dp3Yey mice (Belichenko et al., 2007; Belichenko et al., 2009a;

Kleschevnikov et al., 2004; Morice et al., 2008; Yu et al., 2010b). Although a number of Hsa21 genes has been implicated in receptor trafficking, such as *DYRK1A*, *RCAN1* and *SYNJ1*, the link between gene overdosage and altered synaptic composition is unclear.

At dendritic spines, glutamate receptors are anchored to the PSD by binding with scaffold proteins of the membrane-associated guanylate kinase (MAGUK) family (Won, Levy, Nicoll, & Roche, 2017). PSD95 is the major MAGUK scaffold protein, playing a central role in the trafficking and localisation of different molecules in the PSD. PSD95 can bind directly with GluN2A-C, GluK1, GluK2 and GluK5 subunits and indirectly with GluA1 subunits via the TARP stargazin, anchoring NMDARs, KARs and AMPARs to the PSD. In addition to immobilising receptors to the PSD, PSD95 also clusters receptors with intracellular signalling proteins that regulate cycling of synaptic receptors. Consequently, PSD95 plays a key role in determining surface levels of glutamate receptors. Indeed, PSD95 expression has been associated to synaptic potentiation through the delivery of AMPARs and PSD95-knockout mice report reduced AMPAR-mediated and KAR-mediated excitatory postsynaptic potentials, LTP and LTD alterations, and memory deficits (Béïque et al., 2006; Ehrlich & Malinow, 2004; Migaud et al., 1998; Suzuki & Kamiya, 2016).

Because PSD95 is a core structural protein present in all glutamatergic dendritic spines, expression levels of PSD95 may reflect the abundance of postsynaptic terminals (e.g. Chakrabarti et al., 2007; Shao, Mirra, Sait, Sacktor, & Sigurdsson, 2011). Electron microscopy demonstrated in fact, that PSD95-constructed molecular scaffolds are essential not only for synaptic localisation of glutamate receptors, but also for sustaining the three-dimensional molecular structure of the PSD (Chen et al., 2011).

In DS, a number of genes located on Hsa21 have been associated to neuronal cell death and AD pathology, such as *APP*, *S100B* and *TRPM2*. Accordingly, individuals with DS commonly develop early-onset AD, a disorder characterised by hippocampal neurodegeneration and memory impairments. Unsurprisingly, PSD95 levels are downregulated in the HPC of AD patients and mouse models of AD (Counts, Alldred, Che, Ginsberg, & Mufson, 2014; Simón et al., 2009).

Here, the separate impact of the Mmu16, Mmu17 and Mmu10 segmental trisomies on the expression of glutamate receptors in the HPC was examined in cohorts of Dp1Tyb, Dp3Yey and Dp2Yey animals at adult (14 months) and advanced (20-22 months) age. Regrettably, only aged animals were examined for the Dp1Tyb line, as younger animals were not available for tissue collection. Findings from chapter 3 suggest however that ageing does not represent a crucial factor in the Dp1Tyb model, since memory deficits were observed already at 4 months of age (Exp. 1d).

In the three mouse models, expression levels of subunits from each glutamate receptor class were assessed with western blotting. These included GluA1, GluN2A,

GluN2B, GluN1 and GluK5. These subunits are abundantly expressed in the HPC, play a role in synaptic plasticity and have been implicated in object-recognition memory tasks (e.g. Barker et al., 2006). Expression levels of PSD95 were also assessed and used as a marker to evaluate integrity and abundance of postsynaptic terminals.

Trafficking to or away from the PSD is largely determined by dynamic regulation of the receptor's phosphorylation state. To investigate potential mechanisms related to AMPAR or NMDAR expression, phosphorylation levels of GluA1 on serine 845 (S845) and of GluN2B on tyrosine 1472 (Y1472) were also assessed. Dephosphorylation of S845 has been previously implicated in internalisation of GluA1-containing AMPARs and LTD (Lee, Kameyama, Huganir, & Bear, 1998). Similarly, phosphorylation at Y1472 targets GluN2B-containing NMDARs for endocytosis, a mechanism observed in relation to AD pathology (Snyder et al., 2005).

Because the proteins of interest studied here are primarily located at postsynaptic terminals, brain sample was fractionated into cytosol and synaptosome fractions. Synaptosomes were isolated from nerve terminals during nerve tissue homogenisation and contained complete presynaptic and postsynaptic terminals. The extraction protocol was validated beforehand (see section 2.3.3.1). Examination of synaptosomes allowed to selectively study the expression of glutamate receptors potentially involved in synaptic function. In addition to HPC synaptosomes, frontal cortex synaptosome extractions were also analysed. This allowed to determine whether alterations in glutamate receptor expression observed in the HPC affected specifically the HPC or were a more general feature of trisomic brains. The frontal cortex was selected for its involvement in the network supporting object memory processes (Barker & Warburton, 2011b).

Previous evidence on the D1Tyb model reported impaired LTP and decreased AMPAR and NMDAR levels in the HPC (Souchet et al., 2014; Yu et al., 2010b). Indeed, Hsa21 genes implicated in receptor trafficking and phosphorylation (*DYRK1A, RCAN1*, *SYNJ1*) map to Mmu16 and are trisomic in the Dp1Tyb. A further relevant gene trisomic in the Dp1Tyb is *GRIK1*, coding for the GluK1 subunit. In chapter 3, Dp1Tyb animals displayed deficits in HPC-dependent short-term memory (Exp. 1a, 1b, 1d), a retention interval that depends on fast synaptic transmission of GluA1-containing AMPARs (Sanderson & Bannerman, 2012). Therefore, hippocampal sample from Dp1Tyb animals was expected to display reduced GluN1 and GluA1 levels, along with decreased GluA1 phosphorylation at S845. Additionally, since GluK5 subunits must assemble with GluK1, 2, or 3 subunits to form functional KARs, altered expression of GluK5 was also expected.

Previous evidence on the Dp3Yey model reported enhanced hippocampal LTP (Yu et al., 2010b). However, none of the Mmu17 genes have been related to glutamate receptor function or neurodegeneration. Additionally, Dp3Yey animals performed normally in all

memory tasks, both at adult and advanced age (Exp. 2a, 2b). Therefore, normal expression levels of glutamate receptors were expected from Dp3Yey hippocampal sample.

Previous evidence on the Dp2Yey model reported intact hippocampal LTP at 2-4 months of age, consistent with normal memory performance observed here at adult age (Exp. 3a) (Yu et al., 2010b). At older age however, Dp2Yey animals displayed memory impairments (Exp. 3b). Indeed, Hsa21 genes potentially involved in neuronal cell death (*S100B*, *TRPM2*) are located on Mmu10 and are trisomic in the Dp2Yey. Therefore, PSD95 expression was expected to be downregulated in sample from aged but not adult Dp2Yey animals, indicating postsynaptic degeneration. Additionally, the memory deficit displayed by aged Dp2Yey animals was in the NOR task, which has been demonstrated to depend on function of GluN2A-, GluN2B-, and GluK5-containing receptors (Barker et al., 2006). Therefore, levels of these subunits were expected to be downregulated in aged, but not adult, Dp2Yey mice. Since the NOR task does not primarily rely on the HPC, changes in protein expression were not expected to affect exclusively the HPC but potentially include the frontal cortex as well.

To date, no study has ever systematically examined glutamate receptor expression in the Dp1Tyb, Dp3Yey and Dp2Yey models. The current study aimed to provide a better understanding of synaptic plasticity impairments and neurodegeneration in DS, by identifying gene portions associated to specific synaptic phenotypes. Such synaptic phenotypes could, theoretically, underlie aberrant memory function in DS.

4.2. Methods

Brain samples were collected at rest from animals previously used in behavioural experiments, as described in 2.3.1. The tissue was fractionated as described in 2.3.2 and protein expression was assessed with western blotting as described in 2.3.3. Further details on the experiments carried out with each of the three mouse lines are provided below.

Dp1Tyb

Three western blot experiments were performed to analyse HPC synaptosomes (Exp. 4a), frontal cortex synaptosomes (Exp. 4b) and HPC cytosol (Exp. 4c). In Exp. 4c, a rabbit polyclonal DYRK1A antibody was used (Abnova, 1:500) and the concentration of the GluA1 antibody was increased to 1:350. Each experiment was performed on a cohort of 20-month-old animals (6 WT and 5 Dp1Tyb), on a 10% polyacrylamide gel.

Dp3Yey

A western blot experiment (Exp. 5a) was performed to analyse HPC synaptosomes from a cohort of 14-month-old animals (12 WT and 12 Dp3Yey) and a cohort of 21-month-old animals (9 WT and 12 Dp3Yey). The groups were distributed as equally as possible across four 7.5% polyacrylamide gels and one 14-month-old WT animal was randomly selected as internal control.

Dp2Yey

A western blot experiment (Exp. 6a) was performed to analyse HPC synaptosomes from a cohort of 14-month-old animals (10 WT and 11 Dp2Yey) and a cohort of 22-month-old animals (6 WT and 10 Dp2Yey). The groups were distributed as equally as possible across three 7.5% polyacrylamide gels and one 14-month-old WT animal was randomly selected as internal control. A further experiment (Exp. 6b) was performed on frontal cortex synaptosomes from 22-month-old animals (6 WT and 11 Dp2Yey). The groups were distributed as equally as possible across two 7.5% polyacrylamide gels and one WT animal was randomly selected as internal control.

Data analysis

Protein expression was quantified as described in 2.3.4 and statistically analysed as described in 2.2.3. In experiments comprising more than one gel, protein expression was firstly normalised to internal control levels, to account for intra-gel variability. To account for differences in total amount of protein, the expression of proteins of interest was normalised to β-actin levels. Ultimately, to determine increases or decreases in protein expression relative to wildtype levels, protein density levels were normalised to the mean of WT groups.

In experiments comprising wildtype and trisomic animals of different age, differences in protein expression were analysed separately for each protein of interest using two-way ANOVAs with genotype and age as between-subjects factors. In experiments assessing a single age range, differences between wildtype and trisomic animals were compared with independent samples Student's t-tests for each protein of interest. Additionally, to determine gross anatomical differences and evaluate dissection consistency, sample weight was compared between WT and trisomic mice of each model with independent samples Student's t-tests.

4.3. Dp1Tyb results

In chapter 3, Dp1Tyb mice displayed age-independent memory impairments in tasks known to rely on the HPC (Exp. 1a, 1b, 1d), suggesting that the Mmu16 trisomy altered synaptic plasticity mechanisms underlying the assessed memory processes. To test this hypothesis, a total of three western blot experiments was carried out on HPC and frontal cortex sample collected from a cohort of 20-month-old Dp1Tyb animals. The average weight of hippocampal dissections was 15.64mg (±3.57) in the WT and 15.34mg (±1.92) in the Dp1Tyb group, while frontal cortex dissections weighed 29.55mg (±9.54) and 32.64mg (±11.11) respectively. Sample weight did not significantly differ between Dp1Tyb and WT animals (Student's t-test – HPC: $t_{(9)}$=0.173, p=0.866; frontal cortex: $t_{(9)}$=0.497, p=0.631).

4.3.1. Exp. 4a: Downregulation of PSD95 and upregulation of GluA1 in HPC synaptosomes

In the first experiment, the expression of ionotropic glutamate receptors was assessed in purified HPC synaptosome extractions. A subunit from each receptor class was assessed: GluN1 for total NMDARs, GluA1 for AMPARs and GluK5 for KARs. Levels of the postsynaptic scaffold protein PSD95 were also measured. To assess a mechanism potentially involved in AMPAR expression, phosphorylation levels of GluA1 on S845 were also measured. Western blots are shown in fig. 4.2 and quantified results are presented in fig. 4.3.

Hippocampal synaptosomes from Dp1Tyb animals displayed a significant reduction in the expression of PSD95 (Student's t-test – $t_{(9)}$=2.985, p=0.015). Relative to the WT group, levels of PSD95 were reduced by ~35%. Instead, expression of the GluA1 subunit was significantly upregulated in the Dp1Tyb (Student's t-test – $t_{(9)}$=2.371, p=0.042). Relative to the WT group, Dp1Tyb synaptosomes displayed a ~1.5-fold increase in GluA1. Levels of GluN1 and GluK5 subunits did not differ between Dp1Tyb and WT mice (Student's t-test – GluN1: equal variances not assumed $t_{(5)}$=0.394, p=0.709; GluK5: $t_{(9)}$=1.049, p=0.322).

The GluA1 overexpression was not accompanied by increased GluA1 phosphorylation. Total phosphorylation levels of GluA1 on S845 relative to β-actin did not differ between Dp1Tyb and WT animals (Student's t-test – $t_{(9)}$=0.582, p=0.575). To account for differences in total expression of GluA1, a ratio of phosphorylated over total GluA1 was calculated. Relative to the GluA1 upregulation, phosphorylation levels on S845 were significantly decreased in the Dp1Tyb (Student's t-test – $t_{(9)}$=3.075, p=0.013). Compared to the WT group, GluA1 subunits in the Dp1Tyb displayed a ~30% reduction in S845 phosphorylation.

In sum, the Mmu16 trisomy resulted in a reduction of the postsynaptic scaffold protein PSD95 and a selective increase of the GluA1 subunit, while GluN1 and GluK5 levels were normal. Relative to the GluA1 upregulation, phosphorylation at S845 was decreased.

Figure 4.2: Western blots of HPC synaptosomes from Dp1Tyb mice. Blots show downregulation of PSD95, upregulation of GluA1 and downregulation of pGluA1(S845) relative to total GluA1. kDa = kilodalton, molecular weight. n= 6 WT, 5 Dp1Tyb.

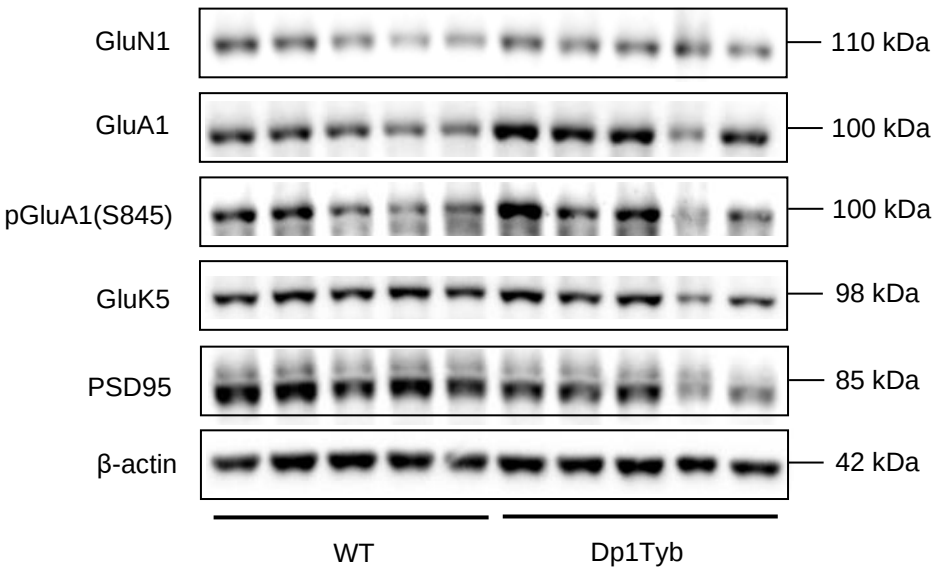

Figure 4.3: Protein density of Dp1Tyb western blots of HPC synaptosomes relative to the WT group. a) Protein expression normalised to β-actin levels. b) Phosphorylated GluA1 at S845 normalised to β-actin or total GluA1 levels. Values are means ± 1 SEM, *p<0.05. n = 6 WT, 5 Dp1Tyb.

a)

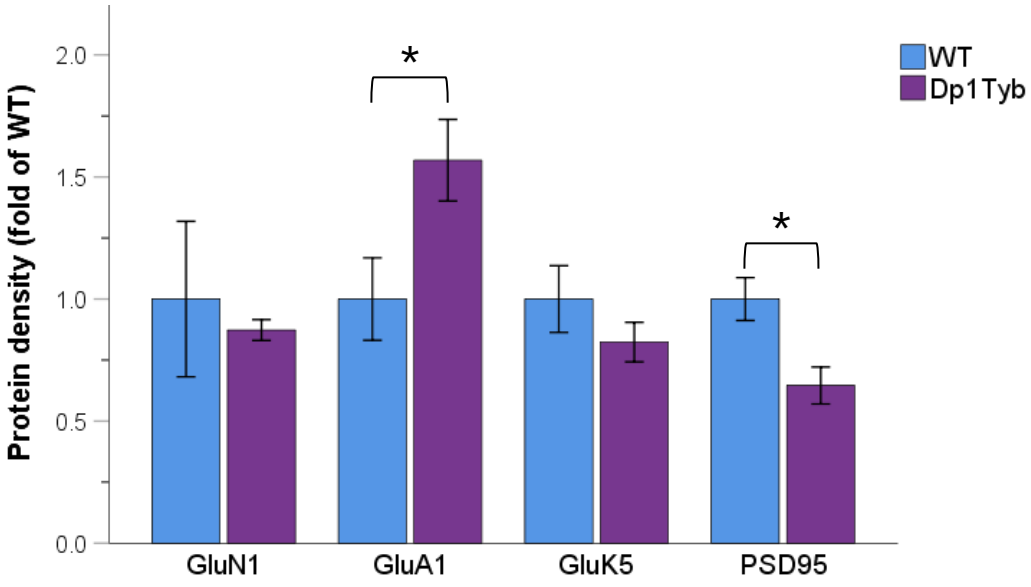

b)

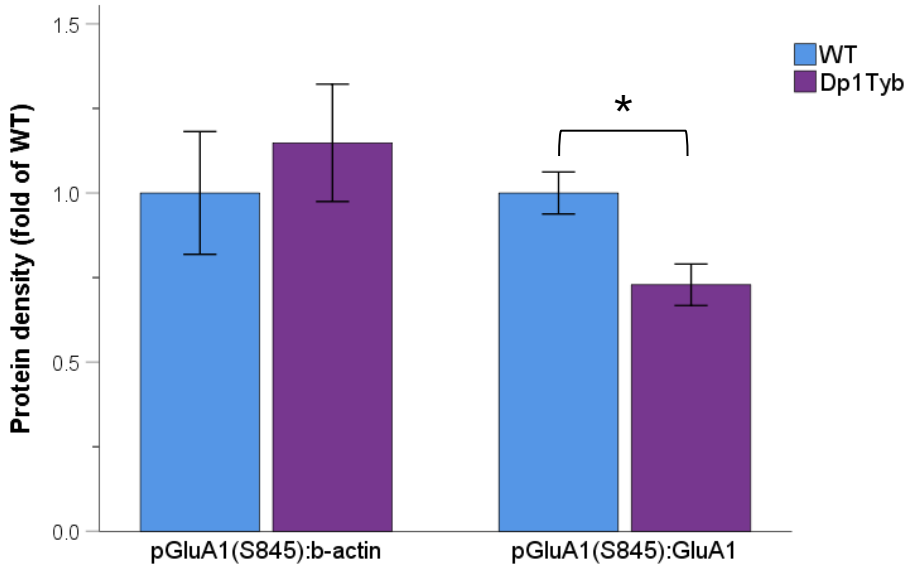

4.3.2. Exp. 4b: Normal PSD95 and GluA1 expression in frontal cortex synaptosomes

To determine whether alterations in PSD95 and GluA1 expression observed in Exp. 3a concerned specifically the HPC or were a more general characteristic of Dp1Tyb brains, PSD95 and GluA1 levels were examined in purified frontal cortex synaptosome extractions. Unlike the HPC, PSD95 and GluA1 levels in the frontal cortex did not significantly differ between Dp1Tyb and WT animals (Student's t-test – PSD95: $t_{(9)}$=0.571, p=0.582; GluA1: $t_{(9)}$=0.726, p=0.486). Western blots are shown in fig. 4.4 and quantified results are presented in fig. 4.5.

Figure 4.4: Western blots of frontal cortex synaptosomes from Dp1Tyb mice. Blots show no difference in protein expression. n= 6 WT, 5 Dp1Tyb.

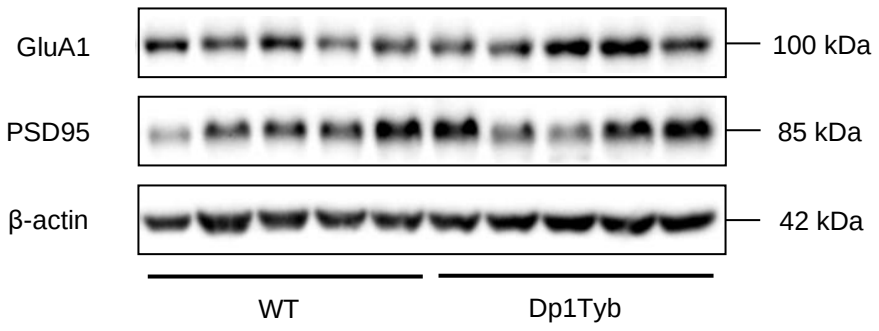

Figure 4.5: Protein density of Dp1Tyb western blots of frontal cortex synaptosomes relative to the WT group. Values are means ± 1 SEM. n = 6 WT, 5 Dp1Tyb.

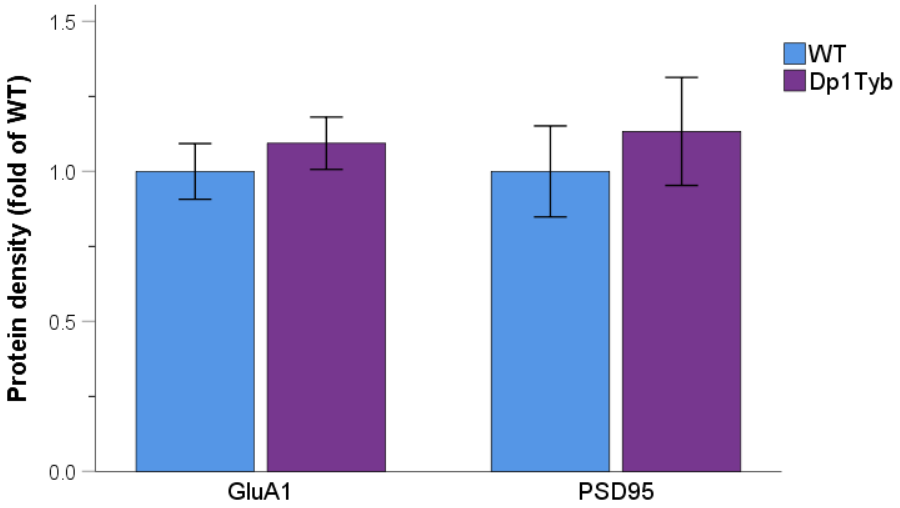

4.3.3. Exp. 4c: Normal GluA1 but upregulated Dyrk1A cytosolic expression in HPC

To determine whether the GluA1 overexpression observed in HPC synaptosomes was accompanied by an increase in the intracellular pool of GluA1 subunits, levels of GluA1 were assessed in HPC cytosol fractions. Additionally, to investigate a cellular mechanism potentially linked to increased surface expression of GluA1, levels of DYRK1A were assessed. Previous literature identified the cytosol as the primary subcellular location of DYRK1A expression (Martí et al., 2003), which was confirmed beforehand with a qualitative western blot comparing DYRK1A levels in synaptosome and cytosol fractions (fig. 4.6).

In the cytosol, expression of GluA1 did not differ between WT and Dp1Tyb sample (Student's t-test – $t_{(9)}$=0.391, p=0.705). Instead, expression of DYRK1A was significantly increased in the Dp1Tyb group (Student's t-test – $t_{(9)}$=3.440, p=0.007). Relative to the WT group, the HPC of Dp1Tyb animals displayed a ~1.7-fold increase in DYRK1A expression. Western blots are shown in fig. 4.7 and quantified results are presented in fig. 4.8.

Figure 4.6: Illustrative western blot to determine the subcellular location of DYRK1A. Levels of DYRK1A were visibly higher in cytosol relative to synaptosome fractions. syn = synaptosome; cyt = cytosol; hom = homogenate; n = 2 WT.

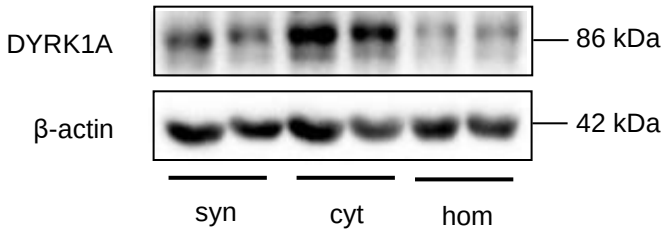

Figure 4.7: Western blots of HPC cytosol fractions from Dp1Tyb mice. Blots show upregulation of DYRK1A. n= 6 WT, 5 Dp1Tyb.

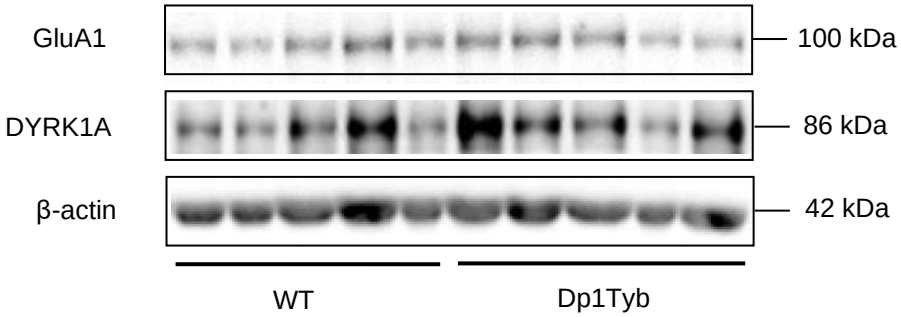

Figure 4.8: Protein density of Dp1Tyb western blots of HPC cytosol fractions relative to the WT group. Values are means ± 1 SEM, **p<0.01. n = 6 WT, 5 Dp1Tyb.

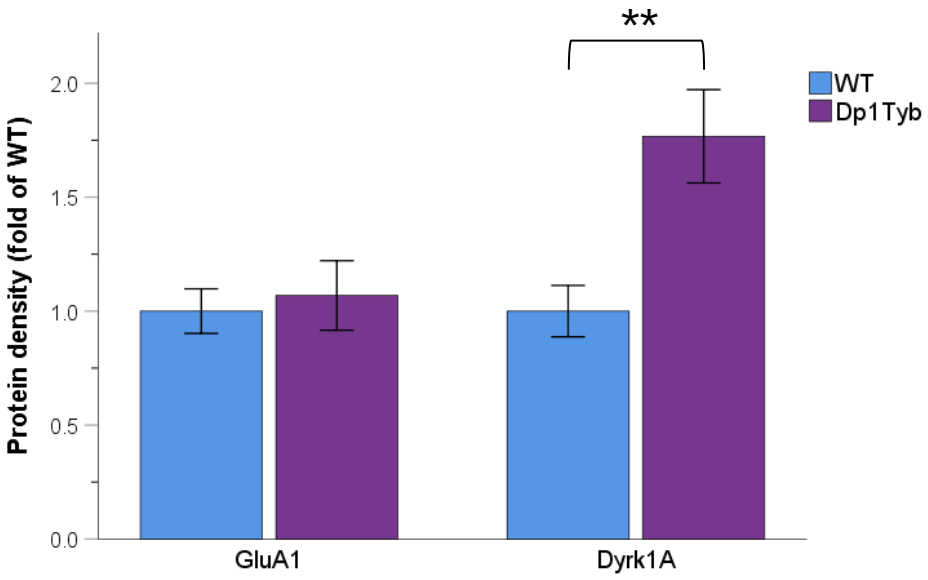

4.4. Dp3Yey results

In chapter 3, Dp3Yey animals reported intact memory performance at all tested ages (Exp. 2a, 2b), suggesting that the Mmu17 trisomy did not interfere with synaptic plasticity mechanisms underlying the assessed memory processes. To investigate this hypothesis, a western blot experiment was carried out on HPC synaptosomes from a cohort of 14-month-old and a cohort of 21-month-old Dp3Yey animals. Hippocampal sample collected at 14 months of age weighed on average 20.11mg (±4.42) in the WT and 18.86mg (±3.68) in the Dp3Yey group, while the respective sample weights were 19.32mg (±2.37) and 17.76mg (±2.72) at 21 months of age. Sample weight did not significantly differ between the groups (Student's t-test – 14 months: $t_{(22)}$=0.753, p=0.459; 21 months: $t_{(19)}$=1.375, p=0.185).

4.4.1. Exp. 5a: Unaltered glutamate receptor levels in HPC synaptosomes

In this experiment, the impact of the Mmu17 trisomy and of ageing on the expression of ionotropic glutamate receptors in the HPC was investigated. A subunit from each receptor class was assessed: GluN1 for total NMDARs, GluA1 for AMPARs and GluK5 for KARs. Levels of the postsynaptic scaffold protein PSD95 were also assessed. Representative western blots are shown in fig. 4.9 and quantified results are presented in fig. 4.10.

Neither the Mmu17 trisomy nor ageing had a significant effect on the expression of glutamate receptor subunits, with sample from WT and Dp3Yey mice displaying comparable levels of GluN1 (two-way ANOVA – genotype: $F_{(1,40)}$=0.181, p=0.673; age: $F_{(1,40)}$=0.720, p=0.401; genotype x age: $F_{(1,40)}$=0.126, p=0.724), GluA1 (two-way ANOVA – genotype: $F_{(1,40)}$=0.011, p=0.916; age: $F_{(1,40)}$=0.007, p=0.932; genotype x age: $F_{(1,40)}$=0.031, p=0.862) and GluK5 (two-way ANOVA – genotype: $F_{(1,40)}$=0.294, p=0.591; age: $F_{(1,40)}$=0.184, p=0.670; genotype x age: $F_{(1,40)}$=1.017, p=0.319). However, ageing significantly increased the expression of PSD95, with sample from 21-month-old mice displaying higher levels of PSD95 compared to sample from 14-month-old mice, irrespective of genotype (two-way ANOVA – genotype: $F_{(1,40)}$=0.080, p=0.779; age: $F_{(1,40)}$=8.312, p=0.006; genotype x age: $F_{(1,40)}$=1.677, p=0.203). Relative to younger animals, the HPC of older animals displayed a ~1.5-fold increase in PSD95.

In sum, the Mmu17 trisomy did not alter the expression of glutamate receptors or of PSD95 in HPC synaptosomes. For this reason, sample from Dp3Yey cohorts was not further examined.

Figure 4.9: Western blots of HPC synaptosomes from 14- and 21-month-old Dp3Yey mice. Blots show upregulation of PSD95 in the older group. At 14-months n= 11 WT, 12 Dp3Yey. At 21-months n= 9 WT, 12 Dp3Yey.

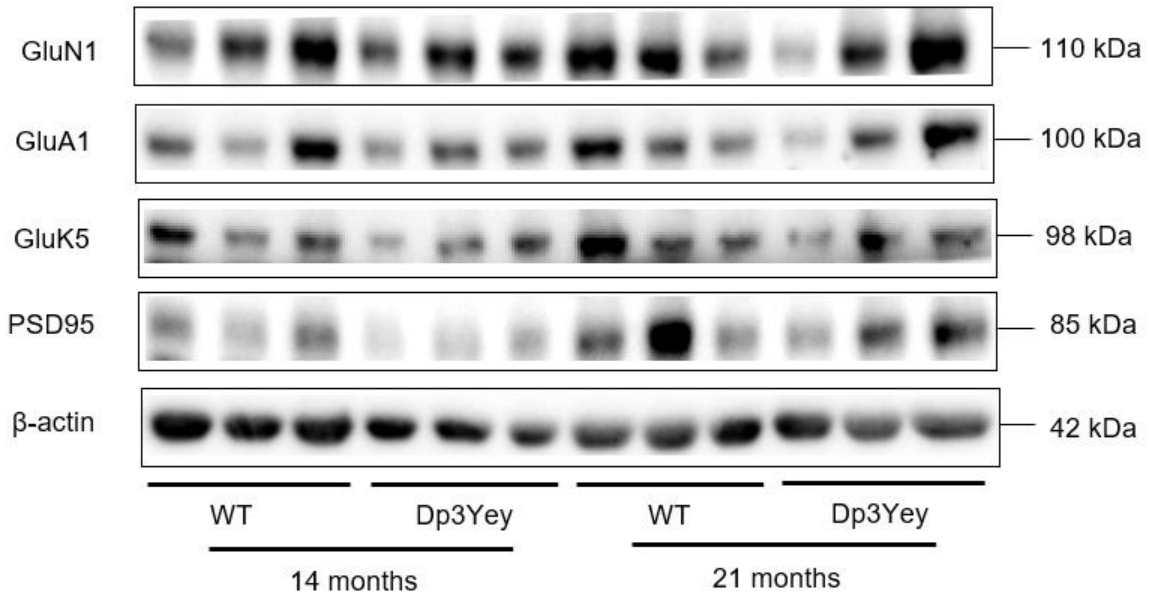

Figure 4.10: Protein density of western blots of HPC synaptosomes from 14- and 21-month old Dp3Yey mice relative to the 14-month-old WT group. Values are means ± 1 SEM, **p<0.01. At 14-months n= 11 WT, 12 Dp3Yey. At 21-months n= 9 WT, 12 Dp3Yey.

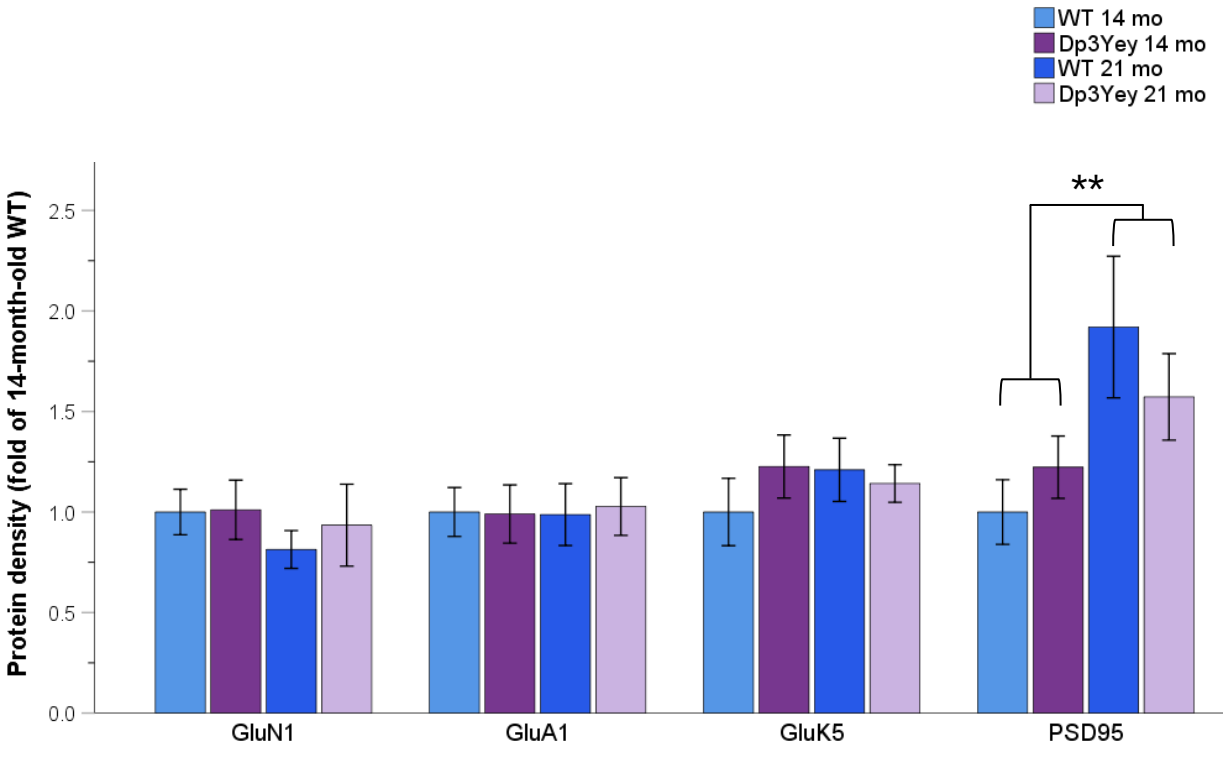

4.5. Dp2Yey results

In chapter 3, Dp2Yey animals reported age-dependent memory impairments (Exp. 1b), suggesting that the Mmu10 trisomy in conjunction with ageing interfered with synaptic plasticity mechanisms underlying the assessed memory processes. To investigate this hypothesis, a western blot experiment was carried out on HPC synaptosomes from a cohort of 14-month-old and a cohort of 22-month-old Dp2Yey animals. To determine specificity of changes observed in the HPC, a further experiment was subsequently carried out on frontal cortex synaptosomes from the older cohort.

Hippocampal sample collected at 14 months of age weighed on average 20.22mg (±1.51) in the WT and 19.55mg (±3.49) in the Dp2Yey group, while the respective sample weights were 19.58mg (±3.43) and 21.14mg (±3.06) at 18 months of age. Frontal cortex sample weighed on average 37.13mg (±10.63) in the WT and 41.87mg (±12.56) in the Dp2Yey group. Sample weight did not significantly differ between the groups (Student's t-test – HPC: 14 months: $t_{(19)}=0.587$, p=0.564; 22 months: $t_{(14)}=0.944$, p=0.361; Frontal cortex: $t_{(15)}=0.781$, p=0.447).

4.5.1. Exp. 6a: Downregulation of PSD95 and GluK5 in HPC synaptosomes

In this experiment, the impact of the Mmu10 trisomy and of ageing on the expression of ionotropic glutamate receptors in the HPC was investigated. A subunit from each receptor type was assessed: GluN1 for total NMDARs, GluA1 for AMPARs and GluK5 for KARs. PSD95 expression was also assessed. Since the NMDAR subunits GluN2A and GluN2B have been previously implicated in the task sensitive to aged Dp2Yey mice (Barker et al., 2006), levels of GluN2A and GluN2B were also measured in this experiment. Additionally, to investigate potential mechanisms related to GluN2B expression, phosphorylation levels of GluN2B at Y1472 were also assessed. Representative western blots are shown in fig. 4.11 and quantified results are presented in fig. 4.12.

Neither the Mmu10 trisomy nor ageing had a significant effect on the expression of GluA1 or NMDAR subunits, with sample from WT and Dp2Yey displaying comparable levels of GluA1 (two-way ANOVA – genotype: $F_{(1,32)}=0.453$, p=0.506; age: $F_{(1,32)}=0.030$, p=0.864; genotype x age: $F_{(1,32)}=2.150$, p=0.152) and GluN1 (two-way ANOVA – genotype: $F_{(1,32)}=2.743$, p=0.107; age: $F_{(1,32)}=2.495$, p=0.124; genotype x age: $F_{(1,32)}=2.460$, p=0.127). Since the distribution of GluN2A and GluN2B scores violated the assumption of normality, group differences were tested with Kruskal-Wallis tests with group as between-subjects factor. There was no significant difference between the four groups in either GluN2A ($\chi^2_{(3)}=0.940$, p=0.816) or GluN2B levels ($\chi^2_{(3)}=2.095$, p=0.553). Levels of GluN2B phosphorylated at Y1472 were also not normally distributed and analysed with Kruskal-

Wallis tests, reporting no difference between the four groups relative to β-actin ($\chi^2_{(3)}$=1.544, p=0.672) or to total GluN2B levels ($\chi^2_{(3)}$=2.434, p=0.487).

By contrast, expression levels of the GluK5 subunit significantly differed between the groups. A significant interaction between the Mmu10 trisomy and ageing was found on the expression of GluK5, with sample from 22-month-old Dp2Yey animals exhibiting lower GluK5 levels compared to age-matched wildtypes, while no group difference was observed at 14 months of age (two-way ANOVA – genotype: $F_{(1,32)}$=5.960, p=0.020; age: $F_{(1,32)}$=0.206, p=0.653; genotype x age: $F_{(1,32)}$=5.556, p=0.025; simple main effects of age – WT: $F_{(1,32)}$=3.334, p=0.077; Dp2Yey: $F_{(1,32)}$=2.222, p=0.146; simple main effects of genotype – 14 months: $F_{(1,32)}$=0.004; p=0.949; 22 months: $F_{(1,32)}$=10.117, p=0.003). HPC synaptosomes of aged Dp2Yey animals displayed a ~50% reduction in GluK5 relative to age-matched wildtypes.

Similarly, expression of PSD95 also depended on the interaction between Mmu10 trisomy and age. While PSD95 expression did not differ between WT and Dp2Yey animals at 14 months of age, 22-month-old Dp2Yey animals displayed significantly reduced PSD95 levels compared to both age-matched wildtypes and to younger Dp2Yey mice (two-way ANOVA – genotype: $F_{(1,32)}$=0.929, p=0.342; age: $F_{(1,32)}$=2.277, p=0.141; genotype x age: $F_{(1,32)}$=4.638, p=0.039; simple main effects of age – WT: $F_{(1,32)}$=0.175, p=0.678; Dp2Yey: $F_{(1,32)}$=8.233, p=0.007; simple main effects of genotype – 14 months: $F_{(1,32)}$=0.821, p=0.372; 22 months: $F_{(1,32)}$=4.270, p=0.047). HPC synaptosomes of aged Dp2Yey animals displayed a ~45% decrease in PSD95 relative to age-matched wildtypes.

In sum, ageing resulted in selective downregulation of the GluK5 subunit and of the scaffold protein PSD95 in animals carrying the Mmu10 trisomy. Levels of GluA1, NMDAR subunits and phosphorylation of GluN2B at Y1472 were unaltered.

Figure 4.11: Western blots of HPC synaptosomes from 14- and 22-month-old Dp2Yey mice. Blots show downregulation of PSD95 and of GluK5 in older Dp2Yey mice. At 14-months n= 9 WT, 11 Dp2Yey. At 22-months n= 6 WT, 10 Dp2Yey.

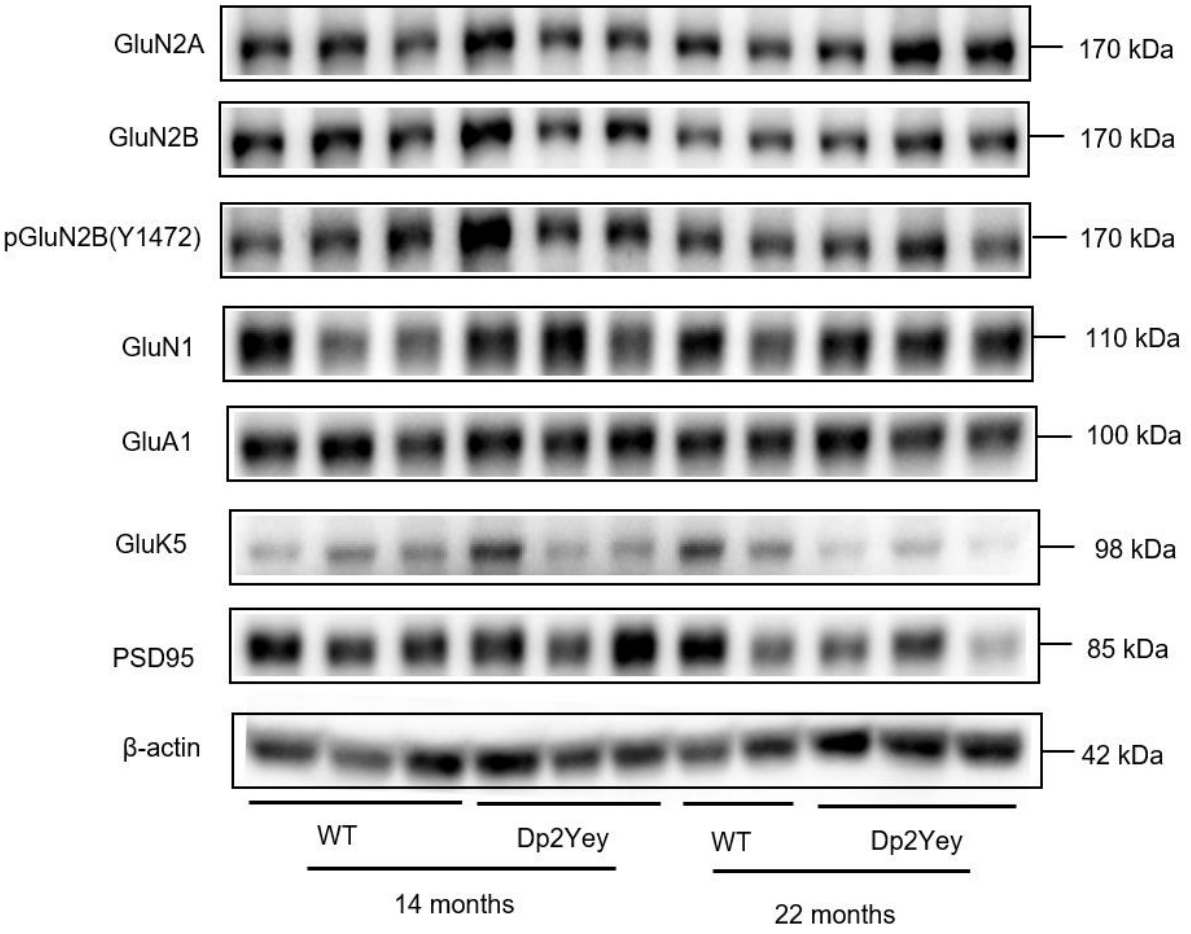

Figure 4.12: Protein density of western blots of HPC synaptosomes from 14- and 22-month old Dp2Yey mice relative to the 14-month-old WT group. a) Protein expression normalised to β-actin levels. b) Phosphorylated GluN2B at Y1472 normalised to β-actin or total GluN2B levels. Values are means ± 1 SEM, *p<0.05, **p<0.01. At 14-months n= 9 WT, 11 Dp2Yey. At 22-months n= 6 WT, 10 Dp2Yey.

a)

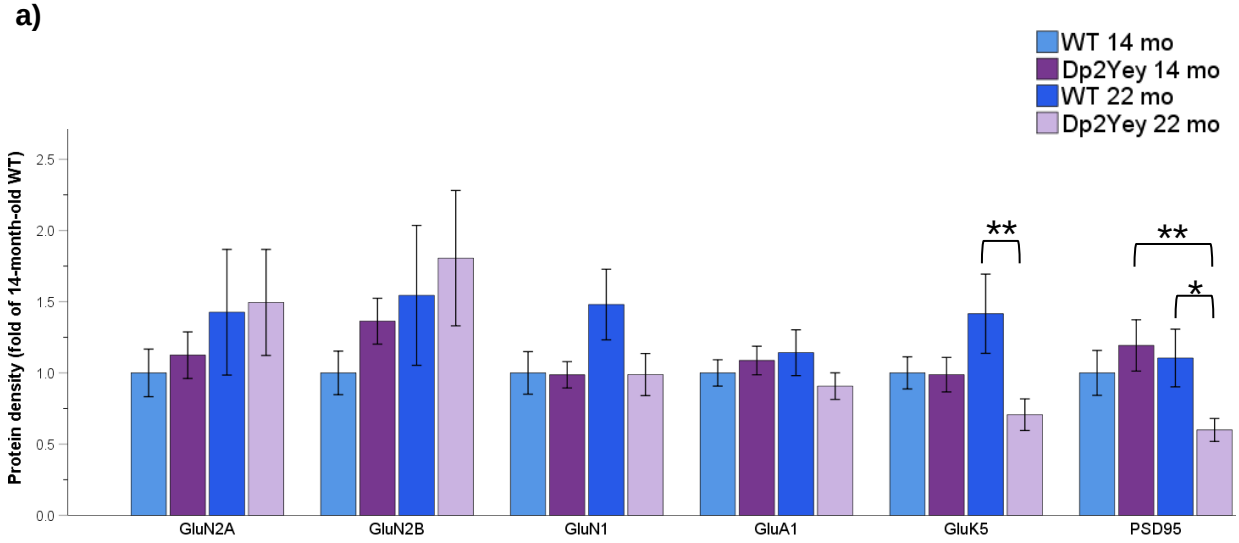

b)

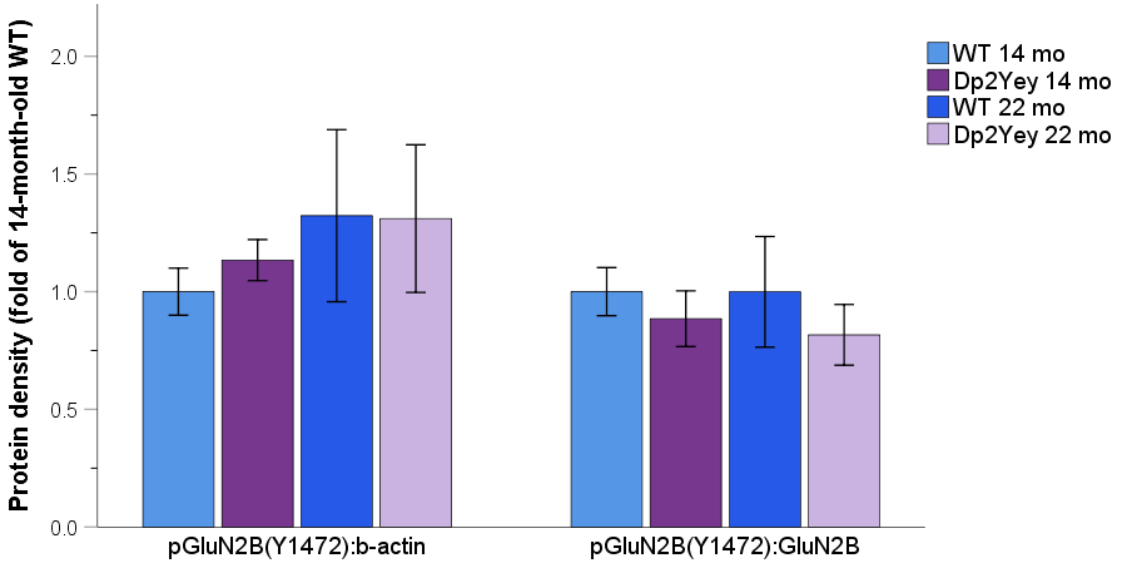

4.5.2. Exp. 6b: Normal PSD95 and GluK5 expression in frontal cortex synaptosomes

To determine whether alterations in protein expression observed in Exp. 3a concerned specifically the HPC or were a more general characteristic of aged Dp2Yey brains, the same proteins were assessed in purified frontal cortex synaptosome extractions collected from the cohort of 22-month-old animals. Representative western blots are shown in fig. 4.13 and quantified results are presented in fig. 4.14.

Analogously to the HPC, there was no significant difference between aged WT and Dp2Yey animals in the levels of GluA1 (Student's t-test – $t_{(14)}$=1.130, p=0.277), GluN1 (Student's t-test – $t_{(14)}$=0.456, p=0.655), GluN2A (Student's t-test – $t_{(14)}$=0.181, p=0.859) or GluN2B (Student's t-test – $t_{(14)}$=0.738, p=0.473) in the frontal cortex. Levels of phosphorylated GluN2B on Y1472 also did not differ between the groups, either when normalised to the β-actin (Student's t-test – $t_{(14)}$=0.668, p=0.515) or to GluN2B expression (Student's t-test – equal variances not assumed $t_{(13)}$=1.765, p=0.101). In contrast to HPC findings, levels of GluK5 (Student's t-test – $t_{(14)}$=0.092, p=0.928) and of PSD95 (Student's t-test – $t_{(14)}$=1.184, p=0.256) did not significantly differ between Dp2Yey and WT animals in the frontal cortex.

Figure 4.13: Western blots of frontal cortex synaptosomes from 22-month old Dp2Yey mice. Blots show no difference in protein expression. n= 5 WT, 11 Dp2Yey.

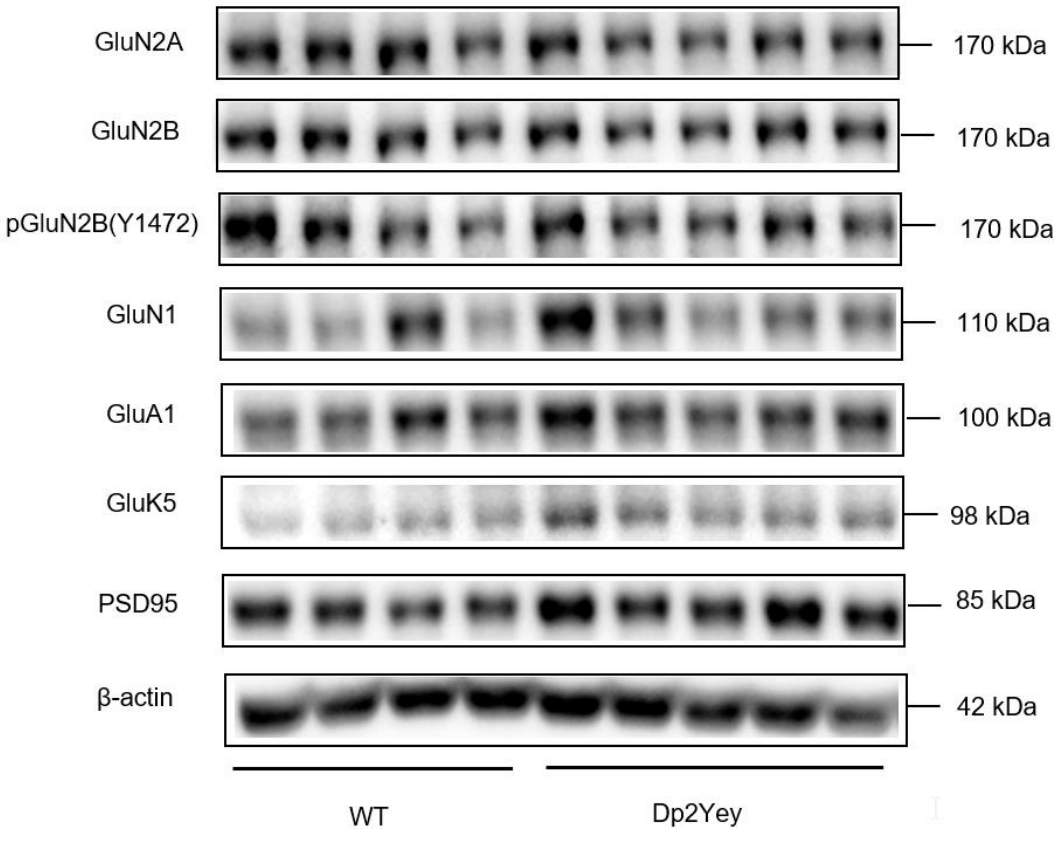

Figure 4.14: Protein density of western blots of frontal cortex synaptosomes from 22-month old Dp2Yey mice relative to the WT group. a) Protein expression normalised to β-actin. b) Phosphorylated GluN2B at Y1472 normalised to β-actin or total GluN2B levels. Values are means ± 1 SEM. n= 5 WT, 11 Dp2Yey.

a)

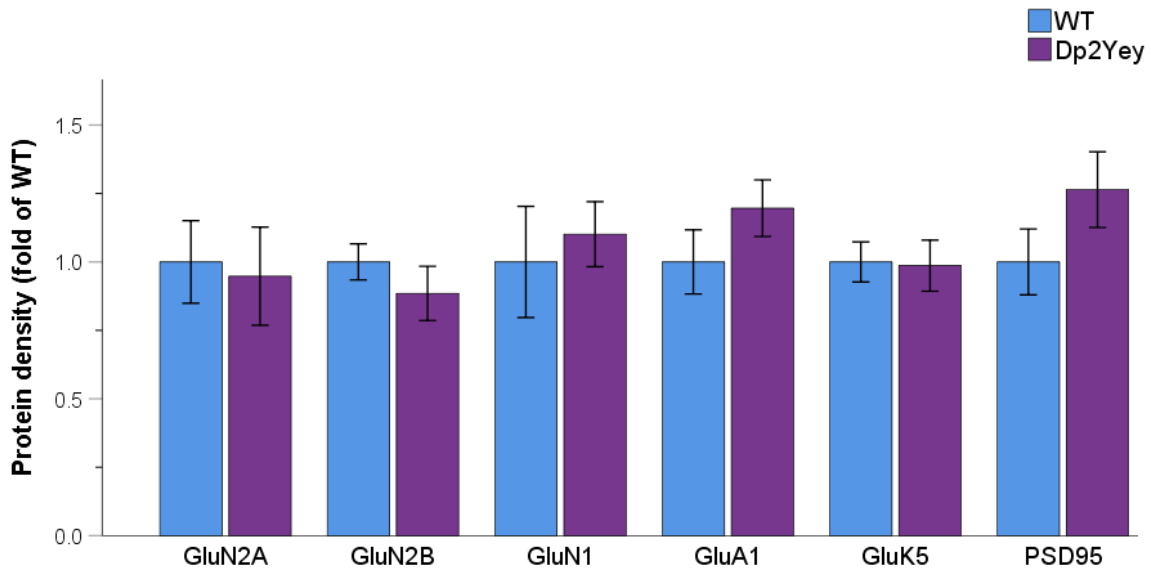

b)

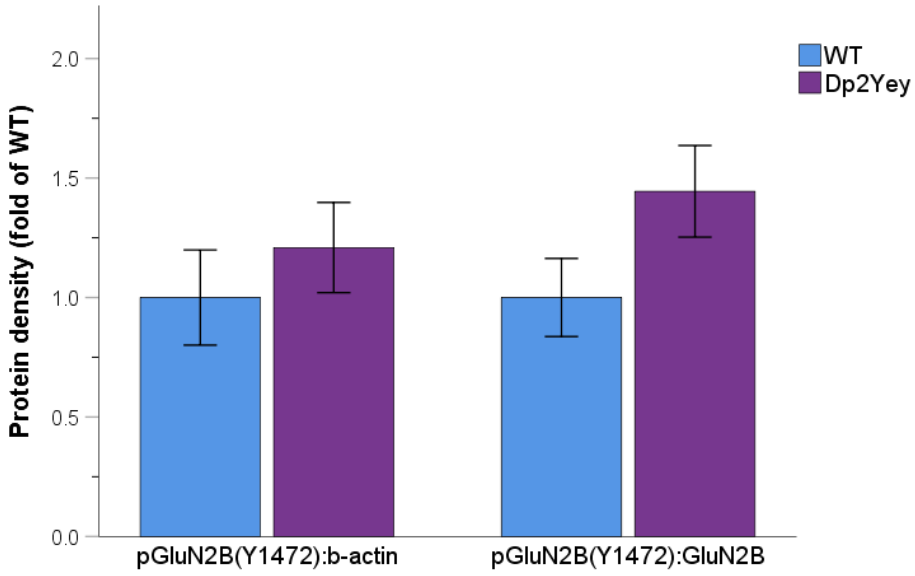

4.6. Discussion

At cellular level, formation and consolidation of new memories is postulated to rely upon synaptic plasticity changes mediated by glutamate receptors. Activity-dependent molecular signalling pathways regulate conductivity and expression of glutamate receptors, ultimately modifying synaptic transmission efficacy. In mouse models of DS, memory deficits have been repeatedly observed in conjunction with aberrant synaptic plasticity in the HPC.

Here, the separate impact of over-dosage of Mmu16, Mmu17 and Mmu10 homologs on expression levels of glutamate receptors (AMPARs, NMDARs, KARs) and the major postsynaptic scaffold protein PSD95, was examined in adult (14 months) and aged (20-22 months) Dp1Tyb, Dp3Yey and Dp2Yey animals in synaptosome extractions with western blotting. As anticipated, protein expression was differentially affected by the three trisomies. Importantly, no difference was observed between trisomic and WT animals in the weight of HPC and frontal cortex sample collected, suggesting that the Mmu16, Mmu17 and Mmu10 trisomy did not alter gross brain volume.

Mmu16 and the Dp1Tyb model

Western blot analysis of HPC synaptosome extractions from Dp1Tyb animals revealed an upregulation of the GluA1 subunit and a downregulation of the scaffold protein PSD95 (Exp. 4a). Expression levels of GluN1 and GluK5 subunits were not different from wildtypes. Moreover, total phosphorylation levels of GluA1 at S845 were unaltered but normalisation to total GluA1 levels revealed a significant reduction in phosphorylation. These protein perturbations localised specifically to the HPC, as levels of GluA1 and PSD95 were normal in frontal cortex synaptosomes (Exp. 4b). Additionally, the hippocampal GluA1 upregulation specifically concerned synaptosomes, as intracellular levels of the GluA1 subunit were unaltered in the cytosol fraction (Exp. 4c). The cytosol displayed instead an increase in DYRK1A expression.

PSD95 is a central coordinator of dendritic spine architecture and association with PSD95 is critical for determining surface levels of glutamate receptors (Béïque et al., 2006; Chen et al., 2011, Ehrlich & Malinow, 2004). In HPC synaptosomes of Dp1Tyb animals, levels of PSD95 were downregulated by ~35% compared to the WT group (Exp. 4a). Given its major role as scaffold protein, PSD95 downregulation implicates a disruption in the molecular structure and composition of postsynaptic densities in the Dp1Tyb. Consequently, the experience-dependent potentiation and depotentiation of synaptic transmission was likely to be compromised in the Dp1Tyb. At the same time, downregulation of PSD95 also suggests a reduction in the number or size of postsynaptic terminals. Since only 20-month old animals were investigated, it remains unclear whether

low PSD95 levels were a result of defective neurodevelopmental processes or progressive neurodegeneration. Both explanations seem possible, as both decreased synaptogenesis and age-related deterioration are common features of DS (Becker et al., 1986; Chakrabarti et al., 2007; Takashima et al., 1994). However, previous research on the Dp1Tyb reported no evidence of neuromorphological anomalies in prenatal or new-born animals, suggesting that current results are unlikely a congenital trait (Aziz et al., 2018; Goodliffe et al., 2016). In fact, hippocampal PSD95 expression was found to be increased in Dp1Tyb animals at 3-4 months of age (Souchet et al., 2014). In Ts65Dn mice, PSD95 levels were reduced in embryos but increased at 4-5 months of age, arguing for a dynamic regulation of PSD95 expression (Chakrabarti et al., 2007; Souchet et al., 2014). It seems thus more likely that PSD95 downregulation in the Dp1Tyb resulted from age-dependent neurodegeneration. This interpretation is compatible with the possibility of the *App* trisomy progressively inducing Aβ-aggregation and ultimately synaptic loss. Indeed, evidence demonstrates that Aβ-oligomers preferentially target postsynaptic regions and PSD95 levels are decreased in AD patients and mouse models of AD pathology (Counts et al., 2014; Lacor et al., 2004; Simón et al., 2009). However, further analyses are necessary to determine whether brains of the 20-month-old Dp1Tyb show evidence of Aβ-accumulation.

An alternative, or concomitant cause for the observed PSD95 downregulation, is glutamate-induced excitotoxicity. Hippocampal synaptosome extractions from Dp1Tyb mice were in fact characterised by a ~1.5-fold upregulation of the GluA1 subunit (Exp. 4a). Overactivation of AMPARs can lead to neurotoxic levels of postsynaptic Ca^{2+} influx, whereby excessive Ca^{2+} activates protease enzymes leading to apoptosis (Dong, Wang, & Qin, 2009). Glutamate excitotoxicity has been implicated in different neurodegenerative disorders, including AD. Given GluA1 overexpression, it seems possible that excitotoxic processes might have damaged hippocampal neurons, resulting in synaptic degeneration and reduced PSD95. Additionally, GluA1 subunits are permeable to Ca^{2+}, potentially contributing directly to excitotoxicity. In a recent study, overexpression of GluA1 was directly implicated in excitotoxic degeneration of cultured motor neurons (Selvaraj et al., 2018).

It must be acknowledged that the upregulation of the GluA1 subunit was not anticipated. Nevertheless, it is equally noteworthy that this effect was not apparent in frontal cortex tissue, suggesting that the upregulation was not a measurement or procedure artefact. Although research on glutamate receptor expression in DS mouse models is scarce, most studies reported a decrease in AMPAR expression (Belichenko et al., 2009b, Morice et al., 2008; Souchet et al., 2014). Even in the Dp1Tyb model, previous research employing western blotting found decreased hippocampal GluA1 levels at 3-4 months of age (Souchet et al., 2014). The discrepancy between current and previous findings on the Dp1Tyb can be explained by several factors. For one, Souchet et al. (2014) did not examine

purified synaptosome extractions, but whole cell lysates. As demonstrated in Exp. 4c, the GluA1 upregulation concerned specifically the synaptosome fraction, since GluA1 levels were normal in the cytosol fraction. It is therefore possible that a potential GluA1 overexpression at synapses was confounded by other cell compartments. For another, it appears that animals examined by Souchet et al. (2014) did not undergo any behavioural training. As reviewed throughout this chapter, AMPAR synaptic insertion represents the chief plasticity mechanism underlying learning and memory. It is therefore possible that the behavioural protocols experienced by Dp1Tyb animals here, played a role in the GluA1 overexpression. Finally, the GluA1 upregulation might be gradually acquired with age, possibly to compensate a downregulation present at earlier age, as observed by Souchet et al. (2014).

Indeed, AMPAR trafficking has been implicated in homeostatic mechanisms aimed to regulate the neuron's own excitability and preserve an overall balance in synaptic strength, specifically through synaptic delivery or removal of GluA1 (Ju et al., 2004; Kim & Ziff, 2014). In homeostatic plasticity, AMPAR surface expression is regulated on the basis of neuronal activity, whereby chronic activity results in AMPAR downregulation and chronic inactivity in AMPAR upregulation. It is possible that the GluA1 overexpression in the Dp1Tyb might be the result of abnormal compensatory mechanisms aimed to upregulate excitability due to an initial GluA1 downregulation. This possibility would fit with the GABAergic over-inhibition hypothesis, whereby Mmu16 mouse models have been observed to generally display increased GABAergic and decreased glutamatergic synaptic transmission (Contestabile et al., 2012). In this regard, examination of synaptosomes from younger Dp1Tyb mice and of markers of inhibitory transmission, would provide valuable information.

Homeostatic synaptic upscaling and downscaling of AMPARs is tightly linked to wake/sleep cycles (Tononi & Cirelli, 2014; Vyazovskiy et al., 2008). Wakefulness has been shown to favour synaptic potentiation while sleep favours synaptic depotentiation, preventing synaptic saturation. In the rat HPC, surface levels of GluA1-containing AMPARs have been shown to increase following wake periods and decrease following sleep (Vyazovskiy et al., 2008). Here, tissue collection took place during the light period, but WT and TG animals of a given mouse line were sacrificed in random order from morning to afternoon. It is therefore possible that sleep intervals occurring throughout the day may have had an influence on GluA1 expression levels via homeostatic plasticity, affecting current results. In this respect, it would be important to investigate whether sleep patterns are altered in the Mmu16 trisomy.

Nevertheless, although unusual, AMPAR upregulation is not completely unprecedented in DS research. Findings on Ts65Dn mice report primarily decreased AMPAR levels, but unaltered or even increased hippocampal GluA1 expression has also

been noted (Siarey et al., 2006; Souchet et al., 2014). Investigations on human DS brains are rare. Immunohistochemical analyses found that cortical GluA1 expression progressively increased with age in DS but not in neurotypical subjects (Arai, Mizuguchi, & Takashima, 1996). Prenatally, cortical levels of the GluA2 and GluA3 subunits were significantly increased in male DS foetuses, but no difference was observed in GluA1 levels (Falsafi, Dierssen, Ghafari, Pollak, & Lubec, 2016).

At present, the cause of GluA1 upregulation in the Dp1Tyb HPC can only be speculated. None of the genes encoding AMPAR subunits are located on Hsa21, implicating that the increase does not reflect gene over dosage, or at least not directly. Given that GluA1 levels were not elevated in the cytosol fraction, the intracellular pool of GluA1 subunits appears to be normal. This suggests a specific impairment in the cycling of AMPARs at the synapse. AMPARs surface levels are tightly regulated by constitutive and activity-dependent trafficking, controlling the insertion of newly synthesised receptors, lateral diffusion of extrasynaptic receptors and endosomal cycling (Henley & Wilkinson, 2016). In endosomal cycling, AMPARs are removed from the surface by endocytosis and trafficked to early endosomes, where they are sorted for either recycling back to the plasma membrane via recycling endosomes or for trafficking to later endosomes for degradation. These trafficking pathways are regulated by distinct molecular pathways involving Ca^{2+}-dependent posttranslational modifications, such as phosphorylation. Fine-tuned phosphorylation of AMPARs is key to the rapid, activity-dependent regulation of AMPARs surface distribution, targeting AMPARs for synaptic insertion or removal. *Dyrk1A* is trisomic in the Dp1Tyb and activity of this protein kinase has been implicated in the regulation of numerous cellular pathways, including regulation of endocytic pathways (Murakami, Bolton, & Hwang, 2009). DYRK1A has also been shown to interact directly with NMDARs, whereby DYRK1A phosphorylation prevented NMDAR internalisation (Grau et al., 2014). Indeed, transgenic mice overexpressing DYRK1A display altered expression levels of different NMDAR subunits and deficits in different memory tasks (Souchet et al., 2014).

In addition to *DYRK1A*, two other genes located on Hsa21 have been involved in the phosphorylation events underlying endosomal cycling, *RCAN1* and *SYNJ1*. Coincidently, both genes map to Mmu16 (Lana-Elola et al., 2011). *RCAN1* codes for the regulator of calcineurin 1, a protein widely expressed in the HPC and upregulated 2-fold in DS foetal and adult brains (Ermak, Morgan, & Davies, 2001; Fuentes et al., 2000). RCAN1 inhibits the activity of the phosphatase calcineurin. Calcineurin has been implicated in different cellular processes, including cell differentiation, gene transcription and synaptic plasticity. As outlined in section 4.1.1, calcineurin plays an important role during LTD, dephosphorylating AMPARs and targeting them for internalisation (Citri & Malenka, 2008). Additionally, similarly to DS mouse models, transgenic mice overexpressing RCAN1 display

reduced hippocampal volume, impaired memory performance on the NOR task, T-maze and MWM, along with anomalies in LTP induction (Martin et al., 2012). RCAN1 overexpression has also been associated to Ca^{2+}-dependent neuronal death (Sun, Wu, Herculano, & Song, 2014).

SYNJ1 codes for the phosphoinositide phosphatase synaptojanin 1, an enzyme located in synaptic terminals that regulates the phosphoinositide metabolism (Di Paolo & De Camilli, 2006). The primary target of synaptojanin 1 is the phosphatidylinositol-4,5-bisphosphate [PI(4,5)P2], a signalling lipid that plays a critical role in vesicle endocytosis. Accordingly, expression of synaptojanin 1 has been demonstrated to regulate both presynaptic neurotransmitter and postsynaptic receptor vesicle endocytosis (Cremona et al., 1999; Gong & De Camilli, 2008). In neuronal cell cultures, knockout of synaptojanin 1 resulted in increased postsynaptic AMPAR levels and decreased AMPAR internalisation (Gong & De Camilli, 2008). Overexpression of synaptojanin 1 has instead been associated to enlargement of early endosomes, a morphological feature observed in DS related to defects in endocytic sorting (Cossec et al., 2012).

Assuming that overdosage of *DYRK1A*, *RCAN1* and *SYNJ1* might directly result in increased gene product is however too simplistic. Expression and activity of these genes is modulated by a complex interplay with other Hsa21 genes, reiterating once again the genetic complexity of DS. For example, RCAN1 activity is induced by DYRK1A phosphorylation and higher RCAN1 levels can be induced by APP (Ermak et al., 2001; Jung et al., 2011.) In turn, the RCAN1-mediated activity of calcineurin stimulates the activity of synaptojanin 1 (Lee, Wenk, Kim, Nairn, & De Camilli, 2004). It can be speculated that in the Dp1Tyb, overexpression of DYRK1A and APP might result in higher RCAN1 activity, with concomitant lower calcineurin activity. Lower calcineurin activity would directly reduce AMPAR internalisation and synaptojanin 1 activity, which would further lower AMPAR internalisation. Unfortunately, numerous western blotting attempts to quantify RCAN1 failed but DYRK1A levels were found significantly increased in the Dp1Tyb HPC (Exp. 4c). This perturbation suggests imbalances in the phosphorylation events downstream of DYRK1A. In line with this possibility, levels of GluA1 phosphorylation at S845 relative to total GluA1 were significantly decreased in the Dp1Tyb (Exp. 4a). It is possible that unbalanced GluA1 phosphorylation states prevented normal cycling of AMPARs, ultimately resulting in GluA1 upregulation.

The S845 phosphorylation site of the GluA1 subunit has been repeatedly implicated in synaptic plasticity and AMPAR trafficking. Using a combination of western blotting and *in vitro* electrophysiology, Lee et al. (2000) found that hippocampal LTD induction caused a decrease in S845 phosphorylation, while LTP induction caused an increase in phosphorylation at a different GluA1 serine site, S831. Furthermore, dephosphorylation and

phosphorylation of S845 have been respectively associated to synaptic removal and insertion of GluA1 subunits (Esteban et al., 2003; Kim & Ziff, 2014; Lee et al., 1998).

In a subsequent study, Lee, Takamiya, He, Song and Huganir (2010) generated phosphomutant mouse lines unable to phosphorylate either S845 or S831. Hippocampal western blots showed that at young age (3 weeks old), S845 and S831 mutants displayed normal levels of total GluA1 and normal phosphorylation levels of the respective non-mutated serine site. At older age however (≥ 3 months old), S831 mutants displayed an increase in total GluA1 and a relative decrease in S845 phosphorylation. No difference was instead observed in older S845 mutants. The findings on older S831 mutants correspond exactly to the pattern observed here in the Dp1Tyb, namely GluA1 upregulation and reduced S845 phosphorylation. This suggests the existence of an age-dependent mechanism mediated by unbalanced phosphorylation events that results in synaptic accumulation of GluA1 subunits. Additionally, LTD was impaired in S845 but not S831 mutants, confirming the crucial role of the S845 site in synaptic depotentiation (Lee et al., 2010). Given the ample evidence implicating S845 in GluA1-internalisation, the reduction in S845 phosphorylation observed in the Dp1Tyb may suggest that surplus GluA1 subunits are potentially targeted for endocytosis. Interestingly, dephosphorylation of S845 is operated by calcineurin, pointing to a key role of RCAN1 in altered AMPAR trafficking, potentially modulated by elevated DYRK1A levels. Of note, Tc1 mice trisomic for *Dyrk1A* but not *Rcan1*, displayed instead a downregulation of hippocampal GluA1 (Morice et al., 2008).

While analysis of synaptosome extractions permitted to quantify receptors located at synaptic terminals, it must be noted that this does not exclusively comprehend receptors anchored to the PSD, actively participating in synaptic transmission, but also reserve pools of receptors adjacent to the PSD. In view of this, it is not possible to know whether surplus GluA1 subunits in the Dp1Tyb were part of functional AMPARs or reserve AMPARs pending endocytic sorting. Generally, an increase in synaptic AMPARs is postulated to potentiate the synapse, enhancing sensitivity to glutamate release and neuronal excitability. However, in the context of prolonged, non-dynamic trafficking, AMPAR upregulation is problematic as it may impair the activity-dependent modulation of synaptic strength through AMPAR redistribution. Additionally, synaptic overexpression of AMPARs could occlude LTP as the synapse cannot be further potentiated (Whitlock et al., 2006). Indeed, electrophysiological studies on Dp1Tyb mice consistently reported impairments in hippocampal LTP induction (Yu et al., 2010b; Zhang et al., 2014).

The lack of alterations in NMDAR expression observed in the Dp1Tyb (Exp. 4a) is in line with previous evidence reporting normal levels of different NMDAR subunits in the Ts65Dn model, but is once again in contrast to the Souchet et al. (2014) study observing

NMDAR downregulation. Literature on KARs is scarcer. In Tc1 mice, trisomic for *Grik1*, levels of GluK1 and GluK5 were normal in the HPC, but GluK5 was downregulated in the PRH cortex (Hall, 2016). In the Dp1Tyb HPC, GluK5 levels were normal, in line with Tc1 findings.

Overall, western blot analysis of Dp1Tyb brains revealed a number of synaptic abnormalities, potentially due to trisomy of key genes involved in synaptic degeneration and receptor trafficking (*App*, *Dyrk1A*, *Rcan1*, *Synj1*). Although the Ts65Dn model is trisomic for the same key genes, literature on AMPAR expression is largely – but not entirely – in contrast to the Dp1Tyb. Inconsistent findings could either be due to the Mmu17 trisomic portion of Ts65Dn mice, the investigation of whole cell lysates instead of synaptosomes, or differences in the age of the examined animals. Indeed, age seems to play an important role in the synaptic phenotypes of the Dp1Tyb. These phenotypes concerned specifically the HPC, suggesting that they might underlie the impairments observed in HPC-dependent memory tasks (Exp. 1a, 1b, 1d) and that Mmu16 homologs are involved HPC dysfunction.

Mmu17 and the Dp3Yey model

Western blot analysis of HPC synaptosome extractions from Dp3Yey animals revealed no trisomy-dependent alterations in protein expression. Levels of GluA1, GluN1, GluK5 and of the scaffold protein PSD95, did not differ between WT and Dp3Yey mice, either at adult (14 months) or advanced (21 months) age (Exp. 5a). The only change observed was a trisomy-independent PSD95 upregulation, whereby older WT and Dp3Yey animals displayed higher PSD95 levels compared to younger animals (Exp. 5a).

This was the first study explicitly investigating glutamate receptors in a mouse model of Mmu17 trisomy. The lack of trisomy-dependent differences was anticipated, given that Dp3Yey animals displayed intact memory function in a series of memory tasks (Exp. 2a, 2b) and that the Mmu17 trisomy does not include genes that code for proteins directly involved in synaptic function.

However, previous evidence on the Dp3Yey model reported significantly increased hippocampal LTP, with Dp3Yey animals exhibiting enhanced and longer lasting potentiation (Yu et al., 2010b). Enhanced hippocampal LTP was also observed in an incomplete Mmu17 trisomy mode, the Dp1Yah (Pereira et al., 2009). These findings implicate that trisomic genes shared by the two models (~12 genes) enhance synaptic potentiation. Current results indicate however that this enhancement is not mediated by altered expression of the GluA1 subunit, total NMDARs or the GluK5 subunit. It is possible that glutamate receptor subunits not assessed here might be differentially expressed in the Dp3Yey, contributing to enhanced LTP. Alternatively, altered phosphorylation events might raise the conductivity of glutamate receptors to atypically large levels during LTP.

Interestingly, transgenic mice overexpressing CBS also reported enhanced hippocampal LTP, attributing once again the *Cbs* gene a crucial role in the Mmu17 trisomy (Régnier et al., 2012). Mutations in CBS are associated to homocystinuria, a metabolic disorder comprising intellectual disability (Almuqbil et al., 2019). It is however unclear how CBS overexpression might influence synaptic activity. One possibility discussed by Régnier et al. (2012) is that CBS might alter hydrogen sulphide concentrations and facilitate NMDAR activity.

Importantly, in contrast to the Dp1Tyb and Dp2Yey, Dp3Yey animals did not display signs of synaptic degeneration, as PSD95 levels did not differ between WT and trisomic animals, at either age (Exp. 5a). As a matter of fact, PSD95 levels were significantly increased in older animals, irrespective of genotype. This finding was unexpected, but robust across the western blots.

Younger and older animals underwent identical treatment during sample collection and sample preparation. They also underwent a similar number of behavioural protocols. One explanation for the age-dependent PSD95 upregulation might be that in the absence of neurodegenerative processes, PSD95 levels normally increase with age. Studies investigating ageing and PSD95 expression in healthy subjects are however rare (as reviewed in Savioz, Leuba, & Vallet, 2014). Nevertheless, a study did in fact report a significant, positive correlation between frontal cortex PSD95 levels and age in ≥ 90 years old individuals (Head et al., 2009). Increased PSD95 levels have also been observed in the cortex of naturally aged rats (Nyffeler, Zhang, Feldon, & Knuesel, 2007).

An alternative explanation for the age-dependent PSD95 increase might lie in the birthplace of older and younger animals. Although both age groups were generated and maintained on a C57BL/6J background and sent to Cardiff University at ~3 months of age, the laboratory breeding the animals moved location, resulting in younger and older animals born in two different facilities. As confirmed by the breeding laboratory, weaning, animal care and housing conditions (including cage enrichment) did not differ between the two facilities. It cannot be excluded however, that non-specific environmental differences experienced during the first 3 months of life might have caused PSD95 upregulation in the older group. Indeed, rats or mice exposed to different housing conditions, such as environmental enrichment, show increased PSD95 levels in different brain areas, including the HPC (Savioz et al., 2014).

Overall, no evidence of altered glutamate receptor expression or neurodegeneration was observed in the Dp3Yey, in line with fully intact memory performance (Exp. 2a, 2b). These findings suggest once again that Mmu17 genes are not involved in either HPC dysfunction or age-dependent neurodegeneration in DS.

Mmu10 and the Dp2Yey model

Western blot analysis of HPC synaptosomes from Dp2Yey animals revealed age-dependent alterations in protein expression in animals carrying the Mmu10 trisomy (Exp. 6a). Synaptic expression of GluA1, GluN1, GluN2A, GluN2B subunits and of GluN2B phosphorylated at Y1472, did not differ between WT and Dp2Yey animals, either at adult (14 months) or advanced (22 months) age. By contrast, although the expression of GluK5 was normal at adult age, GluK5 levels were downregulated in aged Dp2Yey. The same age-dependent phenotype was observed for the scaffold protein PSD95, with aged but not adult Dp2Yey reporting reduced PSD95 expression. Additionally, downregulation of GluK5 and PSD95 was localised specifically to the HPC, since normal protein levels were observed in frontal cortex synaptosomes, as for GluA1, GluN1, GluN2A, GluN2B and pGluN2B Y1472 (Exp. 6b).

PSD95 plays a fundamental role in dendritic spine organisation. In aged (22 months) Dp2Yey, PSD95 was downregulated by almost 50% in the HPC (Exp. 6a). As noted for the Dp1Tyb, PSD95 downregulation suggests a disruption in the normal molecular composition of postsynaptic densities and a reduced number or size of dendritic spines. Importantly, at younger age (14 months) levels of PSD95 did not differ from controls. This strongly suggests the existence of age-dependent neurodegenerative processes induced by the Mmu10 trisomy. Indeed, in older Dp2Yey mice PSD95 was significantly downregulated not only compared to age-matched wildtypes, but also compared to younger Dp2Yey.

As proposed in chapter 3, a candidate gene for progressive neurodegeneration is *S100B*. This astrocytic protein plays an important role in neuroinflammation, aggravates AD pathology and has been repeatedly implicated in apoptotic processes (Cristóvão & Gomes, 2019). Elevated levels of S100B are observed in a wide range of neurodegenerative disorders, including AD. Importantly, S100B gradually increases with age and animal studies have demonstrated harmful effects of S100B overexpression that are progressive with age (Créau et al., 2016; Royston et al., 1999; Whitaker-Azmitia et al., 1997).

Another Hsa21 gene mapping to Mmu10 potentially implicated in cell death is *TRPM2*. This gene codes for the transient receptor potential melastatin 2, a cation channel permeable to Ca^{2+} located in the plasma membrane of neurons and immune cells. TRPM2 activity is induced by oxidative stress and can aggravate neuroinflammation by promoting the production of pro-inflammatory cytokines (Sita, Hrelia, Graziosi, Ravegnini, & Morroni, 2018). Oxidative stress results from an imbalance between the production of prooxidants (i.e. free radicals) and antioxidants, due to dysregulated mitochondrial function. Indeed, mitochondrial dysfunction has been implicated in the pathophysiology of DS and neurodegenerative disorders, such as AD (as reviewed in Valenti et al., 2018). In cell culture, expression of TRPM2 has been associated to Ca^{2+}-dependent cell death following

oxidative stress, while genetic deletion of *Trpm2* or inhibition of TRPM2 activity has been found to protect cell viability (Miller, 2006; Verma et al., 2012). TRPM2 activity has also been noted to exacerbate Aβ-mediated neurotoxicity and deletion of *Trpm2* in a mouse model of AD reverted a number of inflammatory markers to normal levels and rescued synaptic degeneration (Ostapchenko et al., 2015).

Increased susceptibility to oxidative stress, neuroinflammation and disrupted Ca^{2+} homeostasis are normally observed with increasing age (Kregel & Zhang, 2006). Given overdosage of both *S100b* and *Trpm2*, it can be hypothesised that ageing processes are accelerated in the Dp2Yey, by aggravating age-dependent inflammatory processes that ultimately result in cell death. From this perspective, it remains surprising that signs of neurodegeneration (i.e. PSD95 downregulation) were observed only in the HPC and not in the frontal cortex as well (Exp. 6b).

S100B and TRPM2 levels in the Dp2Yey mice examined in the present set of experiments are unknown. However, previous evidence on the Dp2Yey model by Block et al. (2015) reports that S100B expression was increased in the HPC of males and females Dp2Yey, at 7-9 months of age (Block et al., 2015). Of note, the same study also observed an upregulation of APP and RCAN1 in the HPC of male, but not female, Dp2Yey. This implicates that the Mmu10 trisomy promotes accumulation of non-Mmu10 gene products implicated in neurodegeneration and surprisingly, in a sex-dependent manner.

This was the first study explicitly investigating expression of glutamate receptors in a mouse model of Mmu10 trisomy. The Block et al. (2015) study assessed expression of a wide range of proteins in the Dp2Yey, using reverse phase protein arrays. Coincidently, some of these proteins included NMDARs. In line with current findings, Block et al. (2015) reported no difference in the expression of GluN1 or GluN2B in the HPC, in both sexes. The study found however a significant GluN2A increase in male (but not female) Dp2Yey, which was not replicated here. This might be due to the employment of a different method or differences in the age of the animals.

In AD, levels of NMDARs are generally reduced (Proctor, Coulson, & Dodd, 2011). Evidence reports that GluN2B-containing NMDARs are specifically targeted by Aβ-oligomers, triggering a phosphatase cascade resulting in dephosphorylation of GluN2B at the Y1472 site, labelling the receptor for endocytosis (Snyder et al., 2005). Here however, expression levels of the GluN2B subunit and the relative Y1472 phosphorylation levels in the Dp2Yey did not differ from controls. This was the case both in adult and aged animals, both in HPC and frontal cortex synaptosomes (Exp. 6a and 6b). These findings suggest that, unlike AD, neurodegenerative processes taking place in aged Dp2Yey animals did not involve NMDAR expression.

Instead, aged Dp2Yey mice displayed a decrease in KAR expression, whereby the GluK5 subunit was downregulated by 50% (Exp. 6a). Given the memory deficit displayed by older Dp2Yey (Exp. 3b), this age-dependent downregulation was anticipated, as will be discussed in chapter 5. Nevertheless, the cause of the GluK5 downregulation can only be speculated. Since PSD95 binds directly to the GluK5 subunit to anchor KARs to the PSD, it is possible that PSD95 downregulation resulted in the trafficking of KARs away from the synapse. However, PSD95 also binds directly to GluN2 and indirectly to GluA1, yet expression levels of these subunits were unaltered. This might be explained by the fact that synaptic anchoring of NMDARs and AMPARs can also occur through binding with other PSD-MAGUK proteins. For example, all NMDAR subunits display high affinity for SAP102, with GluN2B also binding with PSD93 and GluN2A with SAP97. GluA1 subunits can also bind directly with SAP97 (Won et al., 2017). Indeed, SAP97 was found to rescue deficits in AMPAR currents in PSD93/95 double-knockout neurons (Howard, Elias, Elias, Swat, & Nicoll, 2010). By contrast, although there is evidence that GluK5 subunits can also bind with SAP97, this association is incomplete and weaker compared to the association with PSD95 (Mehta, Wu, Garner, & Marshall, 2001). It is therefore possible that in aged Dp2Yey mice, PSD-MAGUK proteins could compensate for the scarcity of PSD95 and maintain normal pools of GluA1-containing AMPARs and NMDARs, but synaptic anchoring of GluK5-containing KARs could not be restored.

A further explanation for the GluK5 downregulation might lie in over dosage of *Adar2*. This gene codes for adenosine deaminase 2, an enzyme primarily located in the nucleus that edits RNA (Nishikura, 2016). In the brain, ADAR2 edits the pre-mRNA of glutamate receptors, altering their functional properties. In most cases, ADAR2 determines the receptor's permeability to Ca^{2+} ions, by editing a glutamine residue into an arginine residue (Q/R editing). Of relevance, ADAR2 edits GluA2, GluK1 and GluK2 subunits, making them Ca^{2+} impermeable. As described throughout this chapter, maintenance of Ca^{2+} homeostasis is fundamental for normal synaptic function and plasticity.

Heteromers of GluK5 and GluK2 are the most abundant type of KAR in the brain and synaptic expression of GluK5 strongly depends on GluK2 availability (Ball, Atlason, Olayemi, & Molnár, 2010). Q/R editing of GluK2 has been shown to reduce the ability of GluK2 to assemble with other subunits, leading to GluK2 retention in the endoplasmic reticulum (Ball et al., 2010). Thus, it can be hypothesised that in the Dp2Yey, over dosage of *Adar2* might result in over editing of GluK2 subunits, consequently leading to a reduced surface number of GluK5/GluK2 KARs.

At the same time, excessive Ca^{2+}- impermeable KARs at the synapse might be preferentially downregulated through homeostatic scaling, to increase the neuron's excitability. This hypothesis seems plausible, as ADAR2 editing of GluK2 has been

demonstrated to depend on synaptic activity. Chronic suppression of synaptic transmission with tetrodotoxin treatment or NMDAR antagonism resulted in upscaling of synaptic expression of unedited – thus Ca^{2+} permeable – GluK2-containing KARs (Gurung et al., 2018). Importantly, although ADAR2 edits GluA2 subunits as well, surface levels of GluA2 were unaltered, suggesting that KAR trafficking is particularly sensitive to Q/R states.

Whether gene overdosage of *Adar2* could in fact result in increased Q/R editing is unclear. Although Higuchi et al. (2000) demonstrated that GluK2 editing progressively decreases with reduced *Adar2* copy number, Gurung et al. (2018) reported that transient ADAR2 overexpression did not exceed baseline levels of edited GluK2. Additionally, if *Adar2* overdosage played a role in the GluK5 downregulation observed in aged Dp2Yey mice, it remains unclear why the same downregulation was not observed in younger Dp2Yey animals. One possibility is that subtle GluK5 reductions might not be detected by western blotting, while at older age, the combined effect of *Adar2* overdosage and PSD95 downregulation might produce a more obvious, detectable GluK5 downregulation.

Unlike AMPARs and NMDARs, the role of KARs in synaptic plasticity has been less extensively studied. Nevertheless, recent evidence reports the involvement of KARs in a wide range of plasticity mechanisms (Evans et al., 2019). Of particular relevance for the current results, Carta et al. (2013) demonstrated a GluK5-dependent form of LTD aimed to regulate KAR synaptic expression in the HPC. Following synaptic stimulation, CaMKII was observed to phosphorylate GluK5 subunits, weakening the association between GluK5 and PSD95. Phosphorylation enhanced mobility of GluK5-containing KARs through lateral diffusion, resulting in downregulation of KAR surface expression and KAR-mediated excitatory postsynaptic potentials. KAR-dependent LTD was not blocked by antagonism of NMDARs, confirming the key role of KARs in this form of synaptic depotentiation.

A more recent study discovered a form of KAR-mediated LTP. Petrovic et al. (2017) noted that high-frequency stimulation of KARs increased AMPAR surface levels and induced structural changes in dendritic spines, analogously to NMDAR-dependent LTP. KAR-mediated LTP was not observed in GluK2-knockout mice, implicating a crucial role of GluK2 and potentially of co-assembled GluK5 subunits in this form of synaptic potentiation.

Given the GluK5 downregulation and the involvement of KARs in synaptic plasticity, it can be reasonably hypothesised that normal synaptic potentiation and depotentiation in aged Dp2Yey mice was unlikely. Additionally, besides their involvement in neuroinflammation, astrocytic release of S100B and neuronal activity of TRPM2 have also been implicated in synaptic transmission and plasticity (Nishiyama, Knopfel, Endo, & Itohara, 2002; Xie et al., 2011). Electrophysiological studies have however examined hippocampal LTP only in 2-4-month-old Dp2Yey animals (Yu et al., 2010b). At this age, Dp2Yey mice displayed normal potentiation, in line with current findings showing normal

glutamate receptor expression and normal memory performance at adult age (Exp. 3a and 6a).

Overall, western blot analysis of Dp2Yey brains revealed age-dependent synaptic neurodegeneration, potentially due to trisomy of genes involved in neuroinflammation (*S100b*, *Trpm2*). Aged Dp2Yey exhibited reduced PSD95 levels and selective downregulation of the GluK5 receptor subunit. These changes are potentially related to the memory deficits displayed by aged animals (Exp. 3b) and were specifically located in the HPC, suggesting that the Mmu10 trisomy is involved in progressive hippocampal dysfunction in DS.

Conclusion

Western blot analysis of purified HPC synaptosome extractions revealed altered expression of glutamate receptors in the Dp1Tyb and Dp2Yey but not the Dp3Yey model. These changes are likely to affect normal synaptic function and were observed specifically in the HPC, a crucial structure in learning and memory function. Table 4.1. reports a summary of the results observed in each mouse line.

Research on glutamate receptor expression in the TTS model is currently unavailable. Nevertheless, electrophysiological studies of TTS hippocampal slices indicate that simultaneous overdosage of Hsa21 syntenic genes results in impaired LTP (Belichenko et al., 2015; Yu et al., 2010a). Research by Zhang et al. (2014) revealed that functional interactions between triplicated genes determine the emergence of aberrant synaptic plasticity in DS. While gene dosage normalisation of the DSCR rescued hippocampal LTP in the Dp1Tyb, addition of the Mmu17 trisomy in a crossed model reinstated the impairment. By contrast, addition of the Mmu10 trisomy did not prevent DSCR normalisation to rescue LTP in the Dp1Tyb. In TTS mice, DSCR normalisation failed to rescue LTP.

Of the candidate genes reviewed in this discussion, only *Dyrk1A* is located on the DSCR (Lana-Elola et al., 2011). Findings by Zhang et al. (2014) suggest that in addition to the DSCR, interactions between Mmu16 genes and Mmu17 genes result in impaired LTP impairment, while Mmu10 genes appear irrelevant for the phenotype. This conclusion is however too simplistic. Although both Dp1Tyb (Mmu16) and Dp3Yey (Mmu17) mice were found to display abnormal LTP, Dp3Yey mice reported significantly enhanced and not decreased LTP (Yu et al., 2010b). This suggests that in crossed models, interactions between the Mmu16 and Mmu17 segments give rise to a different impairment, at least for the Dp3Yey. Additionally, the current research identified ageing as a decisive factor for the emergence of Mmu10-dependent phenotypes. Electrophysiological investigations have however only been conducted on young animals. Based on current findings it is reasonable to expect that studies on older Dp2Yey animals would reveal that the Mmu10 trisomy indeed affects hippocampal plasticity.

Overall, current results implicate the Mmu16 and Mmu10 but not the Mmu17 trisomy in altered glutamatergic function and neurodegeneration in the HPC. The current study does not permit however, to either identify the cause or the consequences of altered glutamate receptor expression, which can only be hypothesised at this time. Further studies are necessary to investigate the cellular pathways leading to the observed synaptic phenotypes. Based on the assumption that glutamate receptor activity is fundamental for plasticity mechanisms underpinning memory function, western blot findings obtained here provide potential explanations for the memory profile displayed by the three mouse lines in chapter 3. This will be considered further in the general discussion.

Table 4.1: Overview of western blot findings. Protein expression in TG groups of the Dp1Tyb, Dp3Yey and Dp2Yey cohorts relative to the respective age-matched WT groups. Significant increase in the TG group (+), significant decrease in the TG group (-), no difference between the groups (=). Syn = synaptosome fraction, cyt = cytosol fraction; Fr cx = frontal cortex.

		Protein expression								
Mouse line	**Sample**	**GluN2A**	**GluN2B**	**pGluN2B**	**GluN1**	**GluA1**	**pGluA1**	**GluK5**	**PSD95**	**Dyrk1A**
Dp1Tyb (20 mo)	HPC syn				=	+	-	=	-	
	HPC cyt					=				+
	Fr cx syn					=			=	
Dp3Yey (14 mo)	HPC syn				=	=		=	=	
Dp3Yey (21 mo)	HPC syn				=	=		=	=	
Dp2Yey (14 mo)	HPC syn	=	=	=	=	=		=	=	
Dp2Yey (22 mo)	HPC syn	=	=	=	=	=		-	-	
	Fr cx syn	=	=	=	=	=		=	=	

Chapter 5: General discussion

Overview

Following a summary of the main findings of the thesis, behavioural and biochemical phenotypes of the Dp1Tyb, Dp3Yey and Dp2Yey models are joined and discussed together, aiming to link glutamate receptor expression to performance in object-recognition memory tasks. Limitations of the thesis and future research directions are also discussed, followed by a summary of the putative contribution of the Mm16, Mmu17 and Mmu10 orthologous regions to phenotypes of human DS.

5.1. Summary of main findings

The primary aim of this thesis was to reveal the contribution of the Mmu16, Mmu17 and Mmu10 trisomy to memory dysfunction in DS. In chapter 3, a series of object-recognition memory tasks was used to assess different attributes and retention-spans of recognition memory in the three mouse models, at adult and advanced age. To determine differences in anxiety or activity levels potentially confounding memory performance, the animals also underwent the EPM test.

Dp1Tyb animals were found to dissociate attributes and retention-spans of recognition memory (Exp. 1a, 1b). Performance in non-associative tasks assessing recognition of single items or single locations was intact, while performance in associative tasks assessing the retention of object-in-place associations and temporal order of object presentation was impaired. Memory impairments were specifically observed after short-term but not long-term delays and were already present at 4 months of age (Exp. 1d). Recognition memory for objects did not deteriorate with ageing (Exp. 1c). Dp1Tyb mice also displayed increased anxiety and locomotor activity on the EPM (Exp. 1e).

Dp3Yey animals displayed intact recognition memory, performing normally in all object-recognition memory tasks at all tested delays, both at adult and advanced age (Exp. 2a, 2b). On the EPM test, Dp3Yey mice showed normal anxiety levels but increased locomotor activity (Exp. 2c).

Dp2Yey animals were found to display an age-dependent dissociation in recognition memory. At adult age, performance was normal in all object-recognition memory tasks (Exp. 3a) while at advanced age, memory for single objects was impaired both after short-term and long-term delays (Exp. 3b). Despite this impairment, memory for single locations was preserved (Exp. 3b). Anxiety and activity levels on the EPM test were also normal (Exp. 3c).

The secondary aim of this research was to identify molecular mechanisms possibly underlying the memory profile of the three mouse models. In chapter 4, expression of glutamate receptor subunits was assessed in the HPC with western blotting. To determine specificity of changes observed in the HPC, receptor levels were also assessed in the frontal cortex.

Hippocampal synaptosomes from Dp1Tyb animals exhibited a downregulation of the major scaffold protein PSD95 and upregulation of the GluA1 subunit (Exp. 4a). Relative to the GluA1 increase, phosphorylation levels of GluA1 at S845 were decreased (Exp. 4a). These changes were not observed in the frontal cortex (Exp. 4b). In the HPC cytosolic fraction, GluA1 expression was normal but DYRK1A was overexpressed (Exp. 4c).

In the Dp3Yey, no alterations in protein expression were observed in the HPC, either at adult or advanced age (Exp. 5a). In the Dp2Yey, protein expression was normal at adult

age while at advanced age, levels of GluK5 and of PSD95 were downregulated (Exp. 6a). These changes were not observed in the frontal cortex (Exp. 6b).

In this chapter, behavioural and biochemical findings are combined with the aim to link glutamate receptor expression to performance in object-recognition memory tasks.

5.2. Recognition memory and glutamate receptors

Object-recognition memory tasks are widely employed in the study of memory function in rodents and the processes enabling novelty judgments in these tasks have been amply demonstrated to depend on activity of glutamate receptors. A series of studies by Barker and Warburton (2006; 2008b; 2011a; 2015) showed that AMPAR antagonism prior to sample or test phases impaired performance in object-recognition memory tasks, whereby task-specific impairments were observed depending on the region into which antagonists were injected, reflecting the pattern presented in table 3.1. Analogous effects were observed for NMDAR and KAR antagonism prior to sample but not test phases. Thus, memory acquisition in object-recognition memory tasks requires AMPAR, NMDAR and KAR activity, and AMPARs for memory retrieval.

Memories are postulated to be stored via changes in synaptic connection strength, primarily mediated by glutamate receptors. Therefore, it seems that AMPARs, NMDARs and KARs are required for the synaptic plasticity mechanisms underlying performance in object-recognition memory tasks. In order to discuss the behavioural and synaptic phenotypes of the Dp1Tyb, Dp3Yey and Dp2Yey, it is important to present a framework within which recognition memory processes and neural activity can be integrated, such as Wagner's Sometimes-Opponent-Process model (SOP) (1981).

The SOP model can be used to describe recognition memory as short-term and long-term habituation to stimuli. Habituation is the process by which, prolonged or repeated exposure to a stimulus results in reduced responding. According to the SOP model, a stimulus is represented by a set of elements. Elements of stimuli can reside into three different states of activation: a primary active state (A1), a secondary active state (A2) and an inactive state (I). During stimulus presentation, the elements representing the stimulus are into A1, being attentively processed and generating strong responses. As familiarisation with the stimulus takes place, its elements decay into A2, generating lower responses. When the stimulus is removed, elements decay from A2 into the inactive state I.

Importantly, elements into A1 can only transfer into A2 and elements into A2 can only transfer into I, implicating that responses to a stimulus are deemed to decrease with time and cannot be restored unless the stimulus is re-presented, a process called self-generated priming. Upon stimulus re-presentation, inactive elements in I are returned to A1 while at the same time, inactive elements associated to the presented stimulus are retrieved from I and activated into A2, a process called retrieval-generated priming. Associations between elements to be stored in I are formed exclusively while elements are actively processed into A1. According to the SOP model, decay from A1 to A2 is proposed to represent short-term habituation and decay from A2 to I to represent long-term habituation to previously encountered stimuli.

To some extent, the SOP model parallels Cowan's memory model (1988) presented in chapter 3. In Cowan's model, familiar cues activate the associated LTM representations in STM and within STM, only a subset of activated elements can reside in the focus of attention. This is analogous to the cue-dependent retrieval of inactive memories from I into A2, whereby only certain elements are actively processed in A1. The key point of the SOP model lies in the identification of a mechanism enabling memories to decay: habituation.

Based on the SOP model, performance in object-recognition memory tasks can be conceptualised as short-term and long-term habituation to previously presented objects. During sample phases, elements representing the objects initially reside into A1, eliciting strong responses. As time progresses, elements decay into A2, indicating short-term habituation to the objects. This is reflected in contact times generally dropping from the first to the second sample phase. In test phases, elements representing objects that were previously presented in sample phases can be postulated to reside into A2, either due to short-term habituation from a recently experienced sample phase (in the case of the 10-min test) or due to long-term habituation following longer retention intervals and retrieval from I (in the case of the 3-h/24-h test). Objects whose elements are into A2 will elicit weaker responses as animals have habituated to them. By contrast, elements of novel objects or of familiar objects in a novel spatial configuration, will reside into A1 and elicit higher responses. Consequently, animals will display higher exploration times for novel than familiar objects. The SOP model thus provides a psychological mechanism explaining how novelty preference is generated in object-recognition memory tasks. In this perspective, the HPC can be considered a mismatch detector, continuously comparing stored with present information and regulating behavioural responses accordingly (Bannerman et al., 2014).

Evidence for Wagner's dual process account of habituation comes from the study of transgenic mice lacking *Gria1*, the gene coding for the GluA1 subunit (Sanderson & Bannerman, 2012). GluA1$^{-/-}$ mice were found able to discriminate between familiar and novel arms of a Y-maze previously explored over repeated trials separated by 24-h intervals, but unable to discriminate between the arms when sample trials were separated by 1-min intervals (Sanderson et al., 2009). Similarly, GluA1$^{-/-}$ mice were impaired on a NOR and a TOr task with a 2-min retention interval, but unimpaired in an object-in-context task that extended over a period of 5 days (Sanderson et al., 2011).

The dissociation displayed by GluA1$^{-/-}$ mice implicates the existence of GluA1-dependent and GluA1-independent memory processes, whereby GluA1 deletion seems to specifically affect the ability to habituate to stimuli over brief time intervals while preserving habituation over longer time periods (Sanderson & Bannerman, 2012). How GluA1 deletion may impair short-term habituation is unclear. Electrophysiological studies of the rat PRH cortex demonstrate that presentation of novel stimuli elicits high neuronal responses while

responses decrease for familiar or recently presented stimuli, providing a possible neural substrate for habituation processes (Zhu et al., 1995). Given that the GluA1 subunit mediates fast, excitatory neurotransmission, it has been suggested that lack of GluA1 may interfere with the rapid decrease in neuronal cell firing possibly underpinning short-term habituation and resulting in impaired short-term memory performance (Sanderson & Bannerman, 2012). In the following sections, findings on the Dp1Tyb, Dp3Yey and Dp2Yey model are discussed in relation to the SOP / AMPA model.

5.2.1. Mmu16 and the Dp1Tyb: impaired short-term associative recognition memory and GluA1 upregulation

Dp1Tyb mice revealed a paradoxical dissociation on the OiP and TOr task: impaired short-term (10-min) but intact long-term (3-h/24-h) recognition memory. This delay-dependent performance clearly resembles the pattern observed in GluA1$^{-/-}$ mice and can be addressed with the SOP model (Sanderson & Bannerman, 2012). Analogously to GluA1$^{-/-}$ mice, it can be hypothesised that short-term but not long-term habituation processes might be defective in the Dp1Tyb, selectively impairing short-term novelty discrimination. One possibility is that primary active processing may decay more slowly in Dp1Tyb than WT animals. If this were the case, elements representing familiar and novel object-in-place associations during the 10-min test phase of the OiP task would both reside into the primary active state A1, eliciting a similar degree of responses. An alternative route also leading to both object types being processed into A1 would be via a more rapid decay from A2 into I, resulting in the re-activation of familiar objects into A1.

On the 10-min TOr task, Dp1Tyb animals were unable to discriminate between less recently and more recently presented objects but spent a similar amount of time exploring both objects. The lack of a preference between the objects suggests that in the test phase, both object types generated similar responses, possibly being processed into A1. At this point, it must be pointed out that although Dp1Tyb mice were impaired on the 10-min OiP and TOr tests, short-term performance was instead intact on the NOR, 1-sample NOR and Loc task. This implicates that if defective short-term habituation processes caused memory impairments in the Dp1Tyb, such processes were affected selectively for habituation to object-in-context associations but not for habituation to independent object- or spatial-information. This seems possible, given that these attributes of recognition memory rely on different structures within the medial temporal lobe (section 3.1.2.1).

A further characteristic observed in GluA1$^{-/-}$ mice was enhanced long-term memory performance (Sanderson & Bannerman, 2012). The authors interpreted the enhancement as a consequence of increased A1 processing, enabling the formation of stronger associations to be stored into I for long-term retrieval. Interestingly, Dp1Tyb animals

performed numerically (but not significantly) better than WT mice on both OiP and TOr long-term memory tests (Exp. 1a, 1b). On the 24-h OiP task, wildtypes performed at chance level while Dp1Tyb mice showed significantly above chance preference for novelty. Moreover, the Bayesian analysis indicated that at 20 months of age, Dp1Tyb mice performed better than wildtypes on the 24-h NOR task (Exp. 2d). Thus, findings on the Dp1Tyb model match performance of GluA1$^{-/-}$ mice and predictions of the SOP model in more than one way.

Nevertheless, although the SOP model provides a valid framework for understanding Dp1Tyb findings, predictions of the model are in contrast with two important points. Firstly, if A1 processing is increased in the Dp1Tyb, this should be reflected in higher contact times with the objects, as in fact observed in GluA1$^{-/-}$ mice (Sanderson et al., 2011). Secondly, contact times should remain stable across identical sample phases, i.e., habituation to the sample should be slower in Dp1Tyb mice. Neither of these predictions are supported by the behaviour of Dp1Tyb mice. Although Dp1Tyb mice displayed signs of hyperactivity on the EPM, contact times in object-recognition memory tasks were similar to WT mice and decreased across sample phases. One explanation is that intact habituation processes concerning object- and spatial-information features might have enabled Dp1Tyb mice to show a reduction in contact across sample phases.

At cellular level, a possible mechanism for the short-term memory impairments of the Dp1Tyb is provided by the hippocampal overexpression of the GluA1 subunit. In view of the SOP model, it can be hypothesised that GluA1 overexpression might result in increased cell firing, delaying short-term habituation processes. Respectively, increased cell firing might enable stronger consolidation and thus enhanced memory in long-term tests. It remains however unclear how a similar cellular mechanism might be responsible for short-term impairments in a model that completely lacks GluA1 (GluA1$^{-/-}$ mice). Of note, impaired short-term but intact long-term recognition memory was also observed in Tc1 mice, along with reduced hippocampal GluA1 levels (Hall et al., 2016; Hall, 2016; Morice et al., 2008).

While it seems clear that alterations in GluA1 expression selectively affect short-term memory, the synaptic mechanisms still need clarification. Altered GluA1 expression is likely to affect excitatory neurotransmission and surface redistribution of AMPARs during LTP / LTD, consequently affecting the rate of cell firing. In line with the memory deficits, alterations in GluA1 may specifically affect the early-phase and not the late-phase of synaptic plasticity.

Irrespective of the exact synaptic mechanisms, pharmacological studies by Barker and Warburton (2008b; 2011a; 2015) indeed confirm the necessity of AMPAR activity in the HPC during object-recognition memory tasks, supporting the interpretation that hippocampal GluA1 upregulation might be responsible for memory deficits in the Dp1Tyb. In rats, bilateral infusions of AMPAR antagonists into the PRH or mPFC cortex, or crossed unilateral AMPAR antagonism into PRH-mPFC, HPC-PRH or HPC-mPFC, all produced a

deficit on the OiP task following short (5-min) and long (1-h) retention intervals (Barker & Warburton 2008b; 2015). Similarly, bilateral AMPAR antagonism into the PRH or mPFC cortex, or crossed unilateral antagonism into the PRH-mPFc cortex, all produced deficits on the 3-h TOr task (Barker & Waburton, 2011a). These findings demonstrate once again that associative-recognition memory relies on integrated activity within the medial temporal lobe, requiring concomitant glutamatergic neurotransmission via AMPARs in the HPC, PRH and mPFC. Although speculative, these data raise the possibility that an imbalance in AMPAR expression in part of the recognition network could lead to disrupted activity and subsequent disruption of information integration necessary for associative recognition memory.

In addition to AMPARs, blockade of NMDARs and GluK5 into the same three key regions also impaired performance on the OiP and TOr tasks (Baker & Warburton, 2008b; 2011a; 2015). Moreover, although glutamate receptors play an important role in memory processes, they are not the only class of receptor involved. For example, antagonism of muscarinic receptors was also found to impair performance on the OiP and TOr tasks, implicating that cholinergic neurotransmission is a requirement for associative-recognition memory (Barker & Warburton 2008a; 2011a). At this point, it cannot be excluded that alterations in cholinergic neurotransmission might have contributed to memory impairments in the Dp1Tyb. Indeed, degeneration of basal forebrain cholinergic neurons is observed in DS individuals (Casanova, Walker, Whitehouse, & Price, 1985).

In summary, impairments in associative-recognition memory displayed by Dp1Tyb mice suggested a dysfunction of the HPC, which was supported by overexpression of the GluA1 subunit in the HPC. The mechanisms leading to Dp1Tyb phenotypes are unclear, but they may involve defective habituation or retrieval processes as described by the SOP model, mediated by altered AMPAR neurotransmission.

5.2.2. Mmu17 and the Dp3Yey: normal recognition memory and normal glutamate receptor expression

Dp3Yey mice were found to perform normally in all object-recognition memory tasks, both after short-term (10-min) and long-term (3-h / 24-h) retention intervals. In terms of SOP, this would suggest that habituation processes proceeded normally in these mice. In line with this, mean contact times with familiar objects progressively decreased from the first to the second sample phase and furthermore in test phase (table 3.7, 3.8).

The assumption of normal habituation processes is however in disagreement with Dp3Yey mice displaying hyperactivity on the EPM test. Hyperactivity can potentially signify a deficit in habituating to a novel environment, whereby exploratory locomotor behaviour remains elevated over time. Analysis of locomotor activity in the EPM per minute reveals however, that although Dp3Yey travelled larger distances compared to wildtypes, activity

significantly decreased from the first to the last trial minute, demonstrating that Dp3Yey gradually habituated to the EPM.

Considering the hyperactivity trait, it is surprising that contact times with the objects did not differ between WT and Dp3Yey mice in object-recognition memory tasks. A possible explanation may lie in the habituation sessions before the start of the testing period. During these sessions, animals were habituated to the open-field maze and to the presence of objects. It is possible that elevated activity levels may have gradually normalised during the habituation sessions, as observed in the EPM.

Normal recognition memory function in Dp3Yey mice was supported by normal expression of glutamate receptor subunits in the HPC. It cannot however be excluded that other types of synaptic receptors or proteins might be altered in the HPC of Dp3Yey mice, generating the hyperactivity phenotype on the EPM.

5.2.3. Mmu10 and the Dp2Yey: age-dependent recognition memory deficits and GluK5 downregulation

In Dp2Yey mice, recognition memory was intact at adult but impaired at advanced ages, both after short (10-min) and long (3-h) retention intervals. In relation to the SOP model, this suggests that both short-term and long-term habituation processes were impaired in aged Dp2Yey mice. It can be hypothesised that novel and familiar objects were both processed in the primary active state A1, eliciting equally strong responses and thus preventing novelty discrimination. Given that aged Dp2Yey mice were impaired both at short-term and long-term level, it seems that elements representing the objects did not cycle through A1-A2-I, failing to generate a progressive decay in behavioural responses.

This interpretation is however in contrast to the fact that contact times were not generally increased in aged Dp2Yey mice and that contacts decreased across the sample phases, indicating indeed habituation to the objects. Habituation processes taking place during the sample phases are however likely to not only reflect object recognition but also non-specific adjustments to the testing situation. Additionally, memory for spatial locations was preserved in aged Dp2Yey mice, showing that they were nonetheless capable of habituating to redundant spatial information. It is thus possible that contact times decreased across the sample phases due to a non-specific acclimation to the testing situation and the object array. In line with this possibility, mean contact times with familiar objects further decreased from the second sample phase to test phase in the WT group, while they remained practically stable in aged Dp2Yey mice, suggesting that, following an initial acclimation, the processing of familiar objects remained elevated (table 3.11).

A possible mechanism for the age-dependent memory impairment is provided by the age-dependent downregulation of the GluK5 subunit in the HPC. As proposed by

Sanderson et al. (2009), neural activity during A1 processing of a stimulus might be necessary to form associations between elements representing the stimulus for subsequent retrieval from I. Given the pervasive memory deficit of aged Dp2Yey mice, it seems plausible that neural activity might have been insufficient to retain object-information, possibly due to decreased kainate-mediated excitatory neurotransmission.

Although the role of KARs in memory function has been less extensively studied in comparison to AMPARs and NMDARs, Barker et al. (2006) demonstrated that KAR activity is a requirement for novel object recognition, involving specifically the GluK5 subunit (Barker et al., 2006).

Lesion studies demonstrate that novel object recognition depends on the PRH cortex (e.g. Barker & Warburton, 2011b). Indeed, bilateral infusions of AMPAR or NMDAR antagonists into the HPC or crossed unilateral AMPAR or NMDAR antagonism into the HPC-PRH or HPC-mPFC, did not impair performance on the NOR task (Barker & Warburton, 2015). By contrast, bilateral antagonism of AMPARs, NMDARs or of the GluK5 subunit into the PRH cortex all produced a deficit in the NOR task (Winter & Bussey, 2005; Barker et al., 2006). More precisely, GluK5 antagonism impaired NOR memory following short (20-min) but not long (24-h) retention intervals, while NMDAR antagonism produced the opposite pattern (Barker et al., 2006). Additionally, for NMDAR antagonism to be effective, simultaneous GluN2A and GluN2B blockade was required, as NOR performance was unaffected when only one NMDAR subtype was blocked.

Pharmacological studies thus confirm that object recognition necessitates glutamatergic activity within the PRH cortex, implicating aberrant PRH cortex activity in aged Dp2Yey mice. Expression levels of glutamate receptors in the PRH cortex were however not investigated but altered protein expression was observed in the HPC. Although a large number of studies demonstrate that object recognition does not depend on the HPC, some studies have indeed reported hippocampal involvement in object recognition, especially following long delays (24-h) (Clark, Zola, & Squire, 2000). Therefore, it seems possible that altered glutamate receptor expression in the HPC might have played a role in the memory deficits of aged Dp2Yey mice. Indeed, in line with the critical role of the GluK5 subunit for NOR memory, levels of GluK5 were found downregulated in the HPC of aged Dp2Yey mice. Levels of total NMDAR, GluN2A and GluN2B were instead normal. Although the GluK5 subunit has been specifically implicated in short retention intervals, the long-term delay assessed in aged Dp2Yey mice was considerably shorter compared to the Barker et al. study (2006) (3-h vs. 24-h). Hence, it is possible that the GluK5 downregulation may be implicated in both short-term and long-term impairments of aged Dp2Yey mice. At the same time, hippocampal GluK5 downregulation could theoretically affect performance in HPC-dependent memory tasks but aged Dp2Yey mice were found to preserve recognition

memory for novel spatial locations. Additionally, although the GluK5 downregulation did not extend to the frontal cortex, it cannot be excluded that GluK5 levels may also be reduced in the PRH cortex of aged Dp2Yey mice.

In summary, age-dependent impairments in recognition memory were supported by age-dependent downregulation of the GluK5 subunit in the HPC, but levels in the PRH cortex are unknown. The mechanisms leading to Dp2Yey phenotypes are unclear, but they may involve defective habituation processes in relation to defective KAR-mediated excitatory transmission.

5.3. Research limitations

The primary limitation of the current research lies in the use of animals to study a human syndrome. Despite their phylogenetic relatedness, mice and humans are very different organisms. Psychological and biochemical processes are likely to differ between human and mice, implicating that current findings may not translate to human DS. Additionally, segmental Hsa21 trisomies corresponding exactly to single orthologous regions do not occur in human DS.

Although the validity of mouse models in DS research may be questioned, DS mouse models indeed recapitulate several physical and cognitive phenotypes of DS, suggesting that they are a suitable tool to study human DS. The use of models of segmental trisomy represents however both a strength and a limitation of the current research. While segmental trisomies allow to investigate the contribution of distinct gene portions to DS phenotypes, findings on segmental trisomies might represent phenotypes of independent syndromes rather than components of trisomy 21. This is especially true in view of the widespread gene-to-gene interactions noted to occur in DS. Indeed, crossing of different mouse models has been shown to give rise to a different set of phenotypes (Jiang et al., 2015; Zhang et al., 2014).

A further limitation of the thesis concerns the use of exclusively male mice. Sex differences have been observed in both human DS and mouse models of DS, implicating that effects of gene over-dosage can depend on sex (de Sola et al., 2015; Falsafi et al., 2016). For example, in the Dp2Yey, 72 out of 102 assessed proteins were differentially expressed in male and female brains, including proteins coded by Hsa21 candidate genes (Block et al., 2015).

Together, these factors limit generalisation of the present findings to human DS. In a critical perspective it could be argued that present experiments merely describe phenotypes generated in male mice with selective Mmu16, Mmu17 and Mmu10 trisomy.

On a more practical level, further limitations concern the employed experimental methods. Here, object-recognition memory tasks were all carried out with a total of 3 objects and two sample phases (except for the TOr task). This design was chosen to match previous research on the Tc1 model (Hall et al., 2016; Morice et al., 2008) and to employ the same number of objects across all tasks, maintaining memory load unvaried. Most studies however, carry out object-recognition memory tasks with a total of 2 objects and a single sample phase (e.g. Marechal et al., 2019; Nguyen et al., 2018; Pereira et al., 2009; Souchet et al., 2019). Therefore, a direct comparison between current and previous findings is challenged by these differences.

Concerning the biochemistry, the most limiting aspect lies in the fact that brain samples were collected at rest. This implicates that expression and phosphorylation levels

of glutamate receptors merely describe a baseline synaptic state and are not directly related to memory function. Current results thus do not provide any information on how exposure to objects and the associated recognition processes may alter hippocampal expression and activity of synaptic glutamate receptors in the three mouse models. Additional control groups and finely timed experiments would be required to investigate this.

Another limitation of the biochemical analysis is that brain samples were analysed with western blotting. Although this technique permitted the simultaneous assessment of a large number of proteins, protein quantification with western blotting provides only an approximative measure, which may fail to detect small changes in protein expression. Western blotting also does not allow to differentiate between subregions of a structure. This is particularly important as different roles have been noted for dorsal and ventral HPC, and different expression patterns of glutamate receptors have been observed at CA1, CA3 and DG synapses (Bannerman et al., 2002; Evans et al., 2019; Henley & Wilkinson, 2016). This implicates that current results cannot be linked to specific hippocampal subfields or subnetworks.

5.4. Future directions

Moving forward from present findings, biochemical changes postulated to occur in Dp1Tyb, Dp3Yey and Dp2Yey brains should be first investigated. It would be important to confirm that neurodegenerative processes were taking place in the HPC of Dp1Tyb and aged Dp2Yey mice. This could be investigated with immunohistochemical analyses aimed to quantify numbers of neuronal cells and of synaptic terminals. At the same time, hippocampal levels of Aβ and S100B should be quantified with western blotting or Enzyme Linked Immunosorbent Assay (ELISA), possibly identifying mechanisms responsible for neurodegeneration.

In the Dp1Tyb, both behavioural and synaptic phenotypes could be related to aberrant RCAN1 activity. Therefore, quantification of RCAN1 and calcineurin levels could provide evidence for the involvement of this gene in accumulation of GluA1 subunits and memory deficits. In aged Dp2Yey, memory deficits were specifically associated to impaired PRH cortex function, but this region could not be investigated with western blotting. Expression of glutamate receptors should thus be investigated in the PRH cortex with immunohistochemistry, possibly revealing GluK5 downregulation as observed in the HPC. In the Dp3Yey, memory and activity phenotypes could be associated to CBS downregulation, which could be confirmed by measuring CBS levels with western blotting.

To test the validity of assumptions made in relation to the SOP model, an immediate-early-gene study could be carried out. For example, c-fos levels in the HPC could be examined in the three mouse lines following single or repeated exposure to an array of objects. In the Dp1Tyb, c-fos levels would be expected to be elevated in comparison to wildtypes, especially following repeated object presentation. In aged Dp2Yey, c-fos levels would be expected to be generally reduced, while normal c-fos expression would be expected for the Dp3Yey. Special care should be dedicated to design of the study, given the delicate temporal dynamics of c-fos expression.

The present work identified behavioural and synaptic phenotypes associated to the three orthologous regions of Hsa21, but the cellular cascades initiated by gene over-dosage impairing memory function remain largely unclear. In a broader perspective, future work on the Dp1Tyb, Dp3Yey and Dp2Yey should thus attempt to better characterise the link between gene over-dosage, synaptic function and memory impairments. This could be investigated by administrating drug treatments aimed to reduce activity of proteins coded by candidate genes of the respective trisomy. For example, OiP memory could be tested in Dp1Tyb mice following treatment with DYRK1A activity inhibitors. Indeed, such a treatment has been reported to rescue memory impairments in Ts65Dn mice (De la Torre et al., 2014). In the Dp2Yey, the efficacy of anti-inflammatory drugs against age-dependent memory decline could be tested. Again, such a treatment rescued memory deficits in Ts65Dn mice

(Lockrow et al., 2009). Additionally, previous pharmacological studies using AMPAR agonists or GABA antagonists aiming to increasing excitatory activity have proved effective in treating memory impairments of Tc1 and Ts65Dn mice (Hall, 2016; Kleschevnikov et al., 2012). In light of altered glutamate receptor expression, pharmacological modulation of glutamate receptor activity could also rescue memory deficits in Dp1Tyb and aged Dp2Yey mice, further clarifying aberrant molecular mechanisms involved in the respective impairments.

5.5. Conclusion

The present work demonstrates for the first time the distinct contribution of the three Hsa21 orthologous regions to recognition memory in DS. The three segmental trisomy models were also associated to specific patterns of glutamate receptor expression in the HPC, revealing possible cellular mechanism underlying the respective memory profile. Together, phenotypes observed in the three mouse models of segmental DS recapitulated cognitive phenotypes observed in human DS. Figure 5.1 reports a summary of the main findings, along with proposed cellular mechanisms.

Overall, the Mmu16 trisomy was associated to hippocampal dysfunction, as hypothesised. Activity of a number of trisomic gene products was proposed to be implicated in memory deficits and altered protein expression in the Dp1Tyb, whereby DYRK1A and RCAN1 emerged as particularly relevant. Despite *App* trisomy, the Mmu16 trisomy was not associated to age-related cognitive decline. The Mmu17 trisomy was associated to normal hippocampal function and normal ageing as hypothesised but did not reveal the expected impairments in object memory. Instead, the Mmu17 trisomy revealed increased activity levels. This might reflect the elevated prevalence of attention-deficit/hyperactivity disorders in the DS population. Finally, as hypothesised, the Mmu10 trisomy was associated to age-dependent cognitive decline. Trisomy of *S100b* and *Trpm2* were proposed to aggravate neuroinflammatory processes, resulting in synaptic degeneration.

Despite a large body of literature dedicated to understanding the pathophysiology of DS, the intricated relationship between gene overdosage and memory dysfunction remains largely unclear. The generation of mouse models of segmental DS carrying breakdown mutations of Mmu16, Mmu17 and Mmu10 could help narrow down specific genes related to specific phenotypes. Indeed, models trisomic for portions of Mmu16 have already been created, the Dp2Tyb, Dp3Tyb and Dp9Tyb (personal communication with the Francis Crick Institute). Although these models risk to represent unique trisomies rather than trisomy 21, the absence of a given phenotype would at least point towards the necessity of specific gene-to-gene interactions for the production of such phenotype.

A better understanding of the genes and molecular processes regulating memory function in DS would not only contribute to a better understanding of DS pathophysiology but also of memory function in general. Such findings could potentially lead to the development of drug treatments aimed to enhance memory function or prevent cognitive decline in DS individuals and individuals affected by other neurological disorders.

Figure 5.1: Overview of phenotypes observed in the three mouse models and their relation to human DS. Western blot findings are reported on the green background, behavioural findings on the yellow background. The discussed molecular processes possibly implicated in the observed phenotypes are reported in grey. ADHD = attention-deficit/hyperactivity disorder

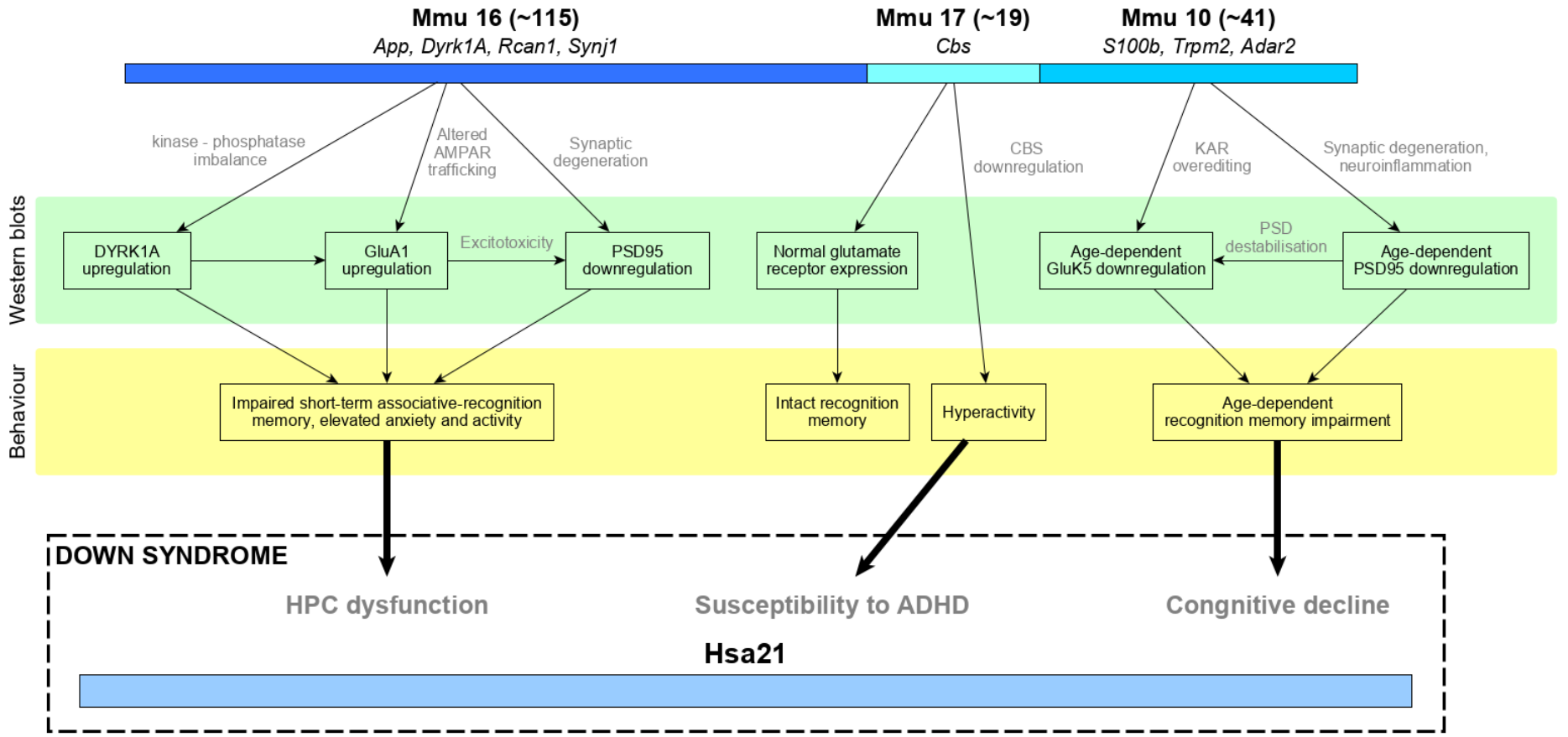

References

Aggleton, J. P., Vann, S. D., Denby, C., Dix, S., Mayes, A. R., Roberts, N., & Yonelinas, A. P. (2005). Sparing of the familiarity component of recognition memory in a patient with hippocampal pathology. *Neuropsychologia, 43* (12), 1810-1823.

Ahmed, M. M., Dhanasekaran, A. R., Tong, S., Wiseman, F. K., Fisher, E. M., Tybulewicz, V. L., & Gardiner, K. J. (2013). Protein profiles in Tc1 mice implicate novel pathway perturbations in the Down syndrome brain. *Human Molecular Genetics, 22* (9), 1709-1724.

Alberts, B., Johnson, A., Lewis, J., Raff, .M., Roberts, K., & Walter, P. (2002). *Molecular Biology of the Cell, 4th edition*. New York, NY: Garland Science.

Alexander, G. E., Saunders, A. M., Szczepanik, J., Strassburger, T. L., Pietrini, P., Dani, A., . . . Schapiro, M. B. (1997). Relation of age and apolipoprotein E to cognitive function in Down syndrome adults. *NeuroReport, 8* (8), 1835-1840.

Allen, E. G., Freeman, S. B., Druschel, C., Hobbs, C. A., O'Leary, L. A., Romitti, P. A., . . . Sherman, S. L. (2009). Maternal age and riso for trisomy 21 assessed by the origin of chromosome nondisjunction: a report from the Atlanta and National Down Syndrome Projects. *Human Genetics, 125* (1), 41-52.

Almuqbil, M. A., Waisbren, S. E., Levy, H. L., & Picker, J. D. (2019). Revising the psychiatric phenotype of Homocystinuria. *Genetics in Medicine, 21* (8), 1827-1831.

Altafaj, X., Dierssen, M., Baamonde, C., Martí, E., Visa, J., Guimerà, J., . . . Estivill, X. (2001). Neurodevelopmental delay, motor abnormalities and cognitive deficits in transgenic mice overexpressing Dyrk1A (minibrain), a murine model of Down's syndrome. *Human Molecular Genetics, 10* (18), 1915-1923.

Antonarakis, S. E., Lyle, R., Chrast, R., & Scott, H. S. (2001). Differential gene expression studies to explore the molecular pathophysiology of Down syndrome. *Brain Research Reviews, 36* (2-3), 265-274.

Arai, Y., Mizuguchi, M., & Takashima, S. (1996). Excessive glutamate receptor 1 immunoreactivity in adult Down syndrome brains. *Pediatric Neurology, 15* (3), 203-206.

Arumugam, A., Raja, K., Venugopalan, M., Chandrasekaran, B., Kovanur Sampath, K., Muthusamy, H., & Shanmugam, N. (2016). Down syndrome – A narrative review with a focus on anatomical features. *Clinical Anatomy, 29* (5), 568-577.

Atkinson, R. C., & Shiffrin, R. M. (1968). Human Memory: A proposed system and its control processes. *Psychology of Learning and Motivation, 2*, 89-195.

Aziz, N. M., Guedj, F., Pennings, J. L. A., Olmos-Serrano, J. L., Siegel, A., Haydar, T. F., & Bianchi, D. W. (2018). Lifespan analysis of brain development, gene expression and behavioral phenotypes in the Ts1Cje, Ts65Dn and Dp(16)1/Yey mouse models of Down syndrome. *Disease Models & Mechanisms, 11* (6), dmm031013.

Bachevalier, J., & Nemanic, S. (2008). Memory for spatial location and object-place associations are differently processed by the hippocampal formation, parahippocampal areas TH/TF and perirhinal cortex. *Hippocampus, 18* (1), 64-80.

Ball, S. M., Atlason, P. T., Shittu-Balogun, O. O., & Molnár, E. (2010). Assembly and intracellular distribution of kainate receptors is determined by RNA editing and subunit composition. *Journal of Neurochemistry, 114* (6), 1805-1818.

Bannerman, D. M., Deacon, R. M., Offen, S., Friswell, J., Grubb, M., & Rawlins, J. N. (2002). Double dissociation of function within the hippocampus: spatial memory and hyponeophagia. *Behavioral Neuroscience, 116* (5), 884-901.

Bannerman, D. M., Sprengel, R., Sanderson, D. J., McHugh, S. B., Rawlins, J. N., Monyer, H., & Seeburg, P. H. (2014). Hippocampal synaptic plasticity, spatial memory and anxiety. *Nature Reviews Neuroscience, 15* (3), 181-192.

Barker, G. R., Bird, F., Alexander, V., & Warburton, E. C. (2007). Recognition memory for objects, place, and temporal order: a disconnection analysis of the role of the medial prefrontal cortex and perirhinal cortex. *The Journal of Neuroscience, 27* (11), 2948-2957.

Barker, G. R., Warburton, E. C., Koder, T., Dolman, N. P., More, J. C., Aggleton, J. P., . . . Brown, M. W. (2006). The different effects on recognition memory of perirhinal kainate and NMDA glutamate receptor antagonism: implications for underlying plasticity mechanisms. *The Journal of Neuroscience, 26* (13), 3561-3566.

Barker, G. R., & Warburton, E. C. (2008a). Critical role of the cholinergic system for object-in-place associative recognition memory. *Learning & Memory, 16* (1), 8-11.

Barker, G. R., & Warburton, E. C. (2008b). NMDA receptor plasticity in the perirhinal and prefrontal cortices is crucial for the acquisition of long-term object-in-place associative memory. *The Journal of Neuroscience, 28* (11), 2837-2844.

Barker, G. R., & Warburton, E. C. (2011a). Evaluating the neural basis of temporal order memory for visual stimuli in the rat. *European Journal of Neuroscience, 33* (4), 705-716.

Barker, G. R., & Warburton, E. C. (2011b). When is the hippocampus involved in recognition memory? *The Journal of Neuroscience, 31* (29), 10721-10731.

Barker, G. R., & Warburton, E. C. (2015). Object-in-place associative recognition memory depends on glutamate receptor neurotransmission within two defined hippocampal-cortical circuits: a critical role for AMPA and NMDA receptors in the hippocampus, perirhinal, and prefrontal cortices. *Cerebral Cortex, 25* (2), 472-481.

Beattie, E. C., Carroll, R. C., Yu, X., Morishita, W., Yasuda, H., von Zastrow, M., & Malenka, R. C. (2000). Regulation of AMPA receptor endocytosis by a signaling mechanism shared with LTD. *Nature Neuroscience, 3* (12), 1291-12300.

Becker, L. E., Armstrong, D. L., & Chan, F. (1986). Dendritic atrophy in children with Down's syndrome. *Annals of Neurology, 20* (4), 520-526.

Béïque, J. C., Lin, D. T., Kang, M. G., Aizawa, H., Takamiya, K., & Huganir, R. L. (2006). Synapse-specific regulation of AMPA receptor function by PSD-95. *Proceedings of the National Academy of Sciences, 103* (51), 19535-19540.

Belichenko, N. P., Belichenko, P. V., Kleschevnikov, A. M., Salehi, A., Reeves, R. H., & Mobley, W. C. (2009a). The "Down syndrome critical region" is sufficient in the mouse model to confer behavioral, neurophysiological, and synaptic phenotypes characteristic of Down syndrome. *The Journal of Neuroscience, 29* (18), 5938-5948.

Belichenko, P. V., Kleschevnikov, A. M., Becker, A., Wagner, G. E., Lysenko L. V., Yu, Y. E., & Mobley, W.C. (2015). Down syndrome cognitive phenotypes modelled in mice trisomic for all HSA21 homologues. *PLOS One, 10* (7), e0134861.

Belichenko, P. V., Kleschevnikov, A. M., Masliah, E., Wu, C., Takimoto-Kimura, R., Salehi, A., & Mobley, W. C. (2009b). Excitatory-inhibitory relationship in the fascia dentata in the Ts65Dn mouse model of Down syndrome. *The Journal of Comparative Neurology, 512* (4), 453-466.

Belichenko, P. V., Kleschevnikov, A. M., Salehi, A., Epstein, C. J., & Mobley, W. C. (2007). Synaptic and cognitive abnormalities in mouse models of Down syndrome: exploring genotype-phenotype relationships. *The Journal of Comparative Neurology, 504* (4), 329-345.

Belichenko, P. V., Masliah, E., Kleschevnikov, A. M., Villar, A. J., Epstein, C. J., Salehi, A., & Mobley, W. C. (2004). Synaptic structural abnormalities in the Ts65Dn mouse model of Down Syndrome. *The Journal of Comparative Neurology, 480* (3), 281-298.

Blanca, M. J., Alarcón, R., Arnau, J., Bono, R., & Bendayan, R. (2017). Non-normal data: Is ANOVA still a valid option? *Psicothema, 29* (4), 552-557.

Bliss, T. V., & Gardner-Medwin, A. R. (1973a). Long-lasting potentiation of synaptic transmission in the dentate area of the unanaestetized rabbit following stimulation of the perforant path. *The Journal of Physiology, 232* (2), 357-374.

Bliss, T. V., & Lomo, T. (1973b). Long-lasting potentiation of synaptic transmission in the dentate area of the anaesthetized rabbit following stimulation of the perforant path. *The Journal of Physiology, 232* (2), 331-356.

Block, A., Ahmed, M. M., Dhanasekaran, A. R., Tong, S., & Gardiner, K. J. (2015). Sex differences in protein expression in the mouse brain and their perturbations in a model of Down syndrome. *Biology of Sex Differences, 6*, 24.

Burwell, R. D., Witter, M. P., & Amaral, D. G. (1995). Perirhinal and postrhinal cortices of the rat: a review of the neuroanatomical literature and comparison with findings from the monkey brain. *Hippocampus, 5* (5), 390-408.

Carlesimo, G. A., Marotta, L., & Vicari, S. (1997). Long-term memory in mental retardation: evidence for a specific impairment in subjects with Down's syndrome. *Neuropsychologia, 35* (1), 71-79.

Carretti, B., Lanfranchi, S., & Mammarella, I. C. (2013). Spatial-simultaneous and spatial-sequential working memory in individuals with Down syndrome: the effect of configuration. *Research in Developmental Disabilities, 34* (1), 669-675.

Carta, M., Opazo, P., Veran, J., Athané, A., Choquet, D., Coussen, F., & Mulle, C. (2013). CaMKII-dependent phosphorylation of GluK5 mediates plasticity of kainate receptors. *The EMBO Journal, 32* (4), 496-510.

Casanova, M. F., Walker, L. C., Whitehouse, P. J., & Price, D. L. (1985). Abnormalities of the nucleus basalis in Down's syndrome. *Annals of Neurology, 18* (3), 310-313.

Castillo, P. E., Malenka, R. C., & Nicoll, R. A. (1997). Kainate receptors mediate a slow postsynaptic current in hippocampal CA3 neurons. *Nature, 388* (6638), 182-186.

Cave, C. B., & Squire, L. R. (1992). Intact verbal and nonverbal short-term memory following damage to the human hippocampus. *Hippocampus, 2* (2), 151-163.

Chakrabarti, L., Best, T. K., Cramer, N. P., Carney, R. S., Isaac, J. T., Galdzicki, Z., & Haydar, T. F. (2010). Olig1 and Olig2 triplication causes developmental brain defects in Down syndrome. *Nature Neuroscience, 13* (8), 927-934.

Chakrabarti, L., Galdzicki, Z., & Haydar, T. F. (2007). Defects in embryonic neurogenesis and initial synapse formation in the forebrain of the Ts65Dn mouse model of Down syndrome. *The Journal of Neuroscience, 27* (43), 11483-11495.

Chen, X., Nelson, C. D., Li, X., Winters, C. A., Azzam, R., Sousa, A. A., . . . Reese, T. S. (2011). PSD-95 is required to sustain the molecular organization of the postsynaptic density. *The Journal of Neuroscience, 31* (17), 6329-6338.

Choi, J. H., Berger, J. D., Mazzella, M. J., Morales-Corraliza, J., Cataldo, A. M., Nixon, R. A., . . . Mathews, P. M. (2009). Age-dependent dysregulation of brain amyloid precursor protein in the Ts65Dn Down syndrome mouse model. *Journal of Neurochemistry, 110* (6), 1818-1827.

Citri, A, & Malenka, R. C. (2008). Synaptic plasticity: multiple forms, functions, and mechanisms. *Neuropsychopharmacology, 33* (1), 18-41.

Clark, C. A. C., Fernandez, F., Sakhon, S., Spanò, G., & Edgin, J. O. (2017). The medial temporal memory system in Down syndrome: Translating animal models of hippocampal compromise. *Hippocampus, 27* (6), 683-691.

Clark, R. E., West, A. N., Zola, S. M., & Squire, L. R. (2001). Rats with lesions of the hippocampus are impaired on the delayed nonmatching-to-sample task. *Hippocampus, 11* (2), 176-186.

Clark, R. E., Zola, S. M., & Squire, L. R. (2000). Impaired recognition memory in rats after damage to the hippocampus. *The Journal of Neuroscience, 20* (33), 8853-8860.

Collingridge, G. L., Olsen, R. W., Peters, J., & Spedding, M. (2009). A nomenclature for ligand-gated ion channels. *Neuropharmacology, 56* (1), 2–5.

Constestabile, A., Magara, S., & Cancedda, L. (2017). The GABAergic Hypothesis for Cognitive Disabilities in Down Syndrome. *Frontiers in cellular Neuroscience, 11*, 54.

Corkin, S. (1968). Acquisition of motor skill after bilateral medial temporal-lobe excision. *Neuropsychologia, 6* (3), 255-265.

Cossec, J. C., Lavaur, J., Berman, D. E., Rivals, I., Hoischen, A., Stora, S., . . . Potier, M. C. (2012). Trisomy for synaptojanin1 in Down syndrome is functionally linked to the enlargement of early endosomes. *Human Molecular Genetics, 21* (14), 3156-3172.

Costa, A. C., Walsh, K., & Davisson, M. T. (1999). Motor dysfunction in a mouse model for Down syndrome. *Physiology & Behavior, 68* (1-2), 211-220.

Counts, S. E., Alldred, M. J., Che, S., Ginsberg, S. D., & Mufson, E. J. (2014). Synaptic gene dysregulation within hippocampal CA1 pyramidal neurons in mild cognitive impairment. *Neuropharmacology, 79*, 172-179.

Courbois, Y., Farran, E. K., Lemahieu, A., Blades, M., Mengue-Topio, H., & Sockeel, P. (2013). Wayfinding behaviour in Down syndrome: a study with virtual environments. *Research in Developmental Disabilities, 34* (5), 1825-1831.

Cowan, N. (1988). Evolving conceptions of memory storage, selective attention, and their mutual constraints within the human information-processing system. *Psychological Bulletin, 104* (2), 163-191.

Créau, N., Cabet, E., Daubigney, F., Souchet, B., Bennaï, S., & Delabar, J. (2016). Specific age-related molecular alterations in the cerebellum of Down syndrome mouse models. *Brain Research, 1646*, 342-353.

Cremona, O., Di Paolo, G., Wenk, M. R., Lüthi, A., Kim, W. T., Takei, K., . . . De Camilli, P. (1999). Essential role of phosphoinositide metabolism in synaptic vesicle recycling. *Cell, 99* (2), 179-188.

Cristóvão, J. S., & Gomes, C. M. (2019). S100 Proteins in Alzheimer's Disease. *Frontiers in Neuroscience, 13*, 463.

Cross, L., Brown, M. W., Aggleton, J. P., & Warburton, E. C. (2012). The medial dorsal thalamic nucleus and the medial prefrontal cortex of the rat function together to support associative recognition and recency but not item recognition. *Learning & Memory, 20* (1), 41-50.

Cruz, A. P., Frei, F., & Graeff, F. G. (1994). Ethopharmacological analysis of rat behavior on the elevated plus-maze. *Pharmacology Biochemistry and Behavior, 49* (1), 171-176.

Darstein, M., Petralia, R. S., Swanson, G. T., Wenthold, R. J., & Heinemann, S. F. (2003). Distribution of kainate receptor subunits at hippocampal mossy fiber synapses. *The Journal of Neuroscience, 23* (22), 8013-8019.

De la Torre, R., De Sola, S., Pons, M., Duchon, A., de Lagran, M. M., Farré, M., . . . Dierssen, M. (2014). Epigallocatechin-3-gallate, a DYRK1A inhibitor, rescues cognitive deficits in Down syndrome mouse models and in humans. *Molecular Nutrition & Food Research, 58* (2), 278-288.

De Sola, S., De la Torre, R., Sánchez-Benavides, G., Benejam, B., Cuenca-Royo, A., Del Hoyo, L., . . . Dierssen, M. (2015). A new cognitive evaluation battery for Down syndrome and its relevance for clinical trials. *Frontiers in Psychology, 6*, 708.

Deacon, R. M., Bannerman, D. M., Kirby, B. P., Croucher, A., & Rawlins, J. N. (2002). Effects of cytotoxic hippocampal lesions in mice on a cognitive test battery. *Behavioural Brain Research, 133* (1), 57-68.

Delabar, J. M., Theophile, D., Rahmani, Z., Chettouh, Z., Blouin, J. L., Prieur, M., . . . Sinet, P. M. (1993). Molecular mapping of twenty-four features of Down syndrome on chromosome 21. *European Journal of Human Genetics, 1* (2), 114-124.

Derkach, V., Barria, A., & Soderling, T. R. (1999). Ca2+/calmodulin-kinase II enhances channel conductance of alpha-amino-3-hydroxy-5-methyl-4-isoxazolepropionate type glutamate receptors. *Proceedings of the National Academy of Sciences, 96* (6), 3269-3274.

Di Paolo, G., & De Camilli, P. (2006). Phosphoinositides in cell regulation and membrane dynamics. *Nature, 443* (7112), 651-657.

Dierssen, M. (2012). Down syndrome: the brain in trisomic mode. *Nature Reviews Neuroscience, 13* (112), 844-858.

Dong, X. X., Wang, Y., & Qin, Z. H. (2009). Molecular mechanisms of excitotoxicity and their relevance to pathogenesis of neurodegenerative diseases. *Acta Pharmacologica Sinica, 30* (4), 379-387.

Dowjat, W. K., Adayey, T., Kuchna, I., Nowicki, K., Palminiello, S., Hwang, Y. W., & Wegiel, J. (2007). Trisomy-driven overexpression of DYRK1A kinase in the brain of subjects with Down syndrome. *Neuroscience Letters, 413* (1), 77-81.

Drachman, D. A., & Arbit, J. (1966). Memory and the hippocampal complex. II. Is memory a multiple process? *Archives of Neurology, 15* (1), 52-61.

Duarte, C. P., Covre, P., Braga, A. C., & de Macedo, E. C. (2011). Visuospatial support for verbal short-term memory in individual with Down syndrome. *Research in Developmental Disabilities, 32* (5), 1918-1923.

Duchon, A., Pothion, S., Brault, V., Sharp, A. J., Tybulewicz, V. L., Fisher, E. M., & Herault, Y. (2011a). The telomeric part of the human chromosome 21 from Cstb to Prmt2 is not necessary for the locomotor and short-term memory deficits observed in the Tc1 mouse model of Down syndrome. *Behavioural Brain Research, 217* (2), 271-281.

Duchon, A., Raveau, M., Chevalier, C., Nalesso, V., Sharp, A. J., & Herault, Y. (2011b). Identification of the translocation breakpoints in the Ts65Dn and Ts1Cje mouse lines: relevance for modelling Down syndrome. *Mammalian Genome, 22* (11-12), 674-684.

Dudai, Y., Karni, A., & Born, J. (2015). The Consolidation and Transformation of Memory. *Neuron, 88* (1), 20-32.

Dudek, S. M., & Bear, M. F. (1992). Homosynaptic long-term depression in area CA1 of hippocampus and effects of N-methyl-D-aspartate receptor blockade. *Proceedings of the National Academy of Sciences, 89* (10), 4363-4367.

Edgin, J. O, Pennington, B. F., & Mervis, C. B. (2010). Neuropsychological components of intellectual disability: the contributions of immediate, working, and associative memory. *Journal of Intellectual Disability Research, 54* (5), 406-417.

Ehrlich, I., & Malinow, R. (2004). Postsynaptic density 95 controls AMPA receptor incorporation during long-term potentiation and experience-driven synaptic plasticity. *The Journal of Neuroscience, 24* (4), 916-927.

Eichenbaum, H., Yonelinas, A. P., & Ranganath, C. (2007). The medial temporal lobe and recognition memory. *Annual Review of Neuroscience, 30*, 123-152.

Ekstein, S., Glick, B., Weill, M., Kay, B., & Berger, I. (2011). Down syndrome and attention-deficit/hyperactivity disorder (ADHD). *Journal of Child Neurology, 26* (10), 1290-1295.

Ennaceur, A. (2010). One-trial object recognition in rats and mice: methodological and theoretical issues. *Behavioural Brain Research, 215* (2), 244-254.

Ennaceur, A., & Delacour, J. (1988). A new one-trial test for neurobiological studies of memory in rats. 1: Behavioral data. *Behavioural Brain Research, 31* (1), 47-59.

Ermak, G., Morgan, T. E., & Davies, K. J. (2001). Chronic overexpression of the calcineurin inhibitory gene DSCR1 (Adapt78) is associated with Alzheimer's disease. *The Journal of Biological Chemistry, 276* (42), 38787-38794.

Esteban, J. A, Shi, S. H., Wilson, C., Nuriya, M., Huganir, R. L., & Malinow, R. (2003). PKA phosphorylation of AMPA receptor subunits controls synaptic trafficking underlying plasticity. *Nature Neuroscience, 6* (2), 136-143.

Evans, A. J., Gurung, S., Henley, J.M., Nakamura, Y., & Wilkinson, K. A. (2019). Exciting Times: New Advances Towards Understanding the Regulation and Roles of Kainate Receptors. *Neurochemical Research, 44* (3), 572-584.

Falsafi, S. K., Dierssen, M., Ghafari, M., Pollak, A., & Lubec, G. (2016). Reduced cortical neurotransmitter receptor complex levels in fetal Down syndrome brain. *Amino Acids, 48* (1), 103-116.

Fernandez, F., & Garner, C. C. (2007). Object recognition memory is conserved in Ts1Cje, a mouse model of Down syndrome. *Neuroscience Letters, 421* (2), 137-141.

Ferrer, I., & Gullotta, F. (1990). Down's syndrome and Alzheimer's disease: dendritic spine counts in the hippocampus. *Acta Neuropathologica, 79* (6), 680-685.

Fotaki, V., Dierssen, M., Alcántara, S., Martínez, S., Martí, E., Casas, C., . . . Arbonés, M. L. (2002). Dyrk1A haploinsufficiency affects viability and causes developmental delay and abnormal brain morphology in mice. *Molecular and Cellular Biology, 22* (18), 6636-6647.

Frenkel, S, & Bourdin, B. (2009). Verbal, visual, and spatio-sequential short-term memory: assessment of the storage capacities of children and teenager with Down's syndrome. *Journal of Intellectual Disability Research, 53* (2), 152-160.

Galante, M., Jani, H., Vanes, L., Daniel, H., Fisher, E. M., Tybulewicz, V. L., . . . Morice, E. (2009). Impairments in motor coordination without major changes in cerebellar plasticity in the Tc1 mouse model of Down syndrome. *Human Molecular Genetics, 18* (8), 1449-1463.

García-Cerro, S., Martínez, P., Vidal, V., Corrales, A., Flórez, J., Vidal, R., . . . Martínez-Cué, C. (2014). Overexpression of Dyrk1A is implicated in several cognitive, electrophysiological and neuromorphological alterations found in a mouse model of Down syndrome. *PLOS One, 9* (9), e106572.

Gardiner, K. (2004). Gene-dosage effects in Down syndrome and trisomic mouse models. *Genome Biology, 5* (10), 244.

Godfrey, M., & Lee, N. R. (2018). Memory profiles in Down syndrome across development: a review of memory abilities through the lifespan. *Journal of Neurodevelopmental Disorders, 10* (1), 5.

Gong, L. W., & De Camilli, P. (2008). Regulation of postsynaptic AMPA responses by synaptojanin 1. *Proceedings of the National Academy of Sciences, 105* (45), 17561-17566.

Good, M. A., Barnes, P., Staal, V., McGregor, A., & Honey, R. C. (2007). Context- but not familiarity-dependent forms of object recognition are impaired following excitotoxic hippocampal lesions in rats. *Behavioral Neuroscience, 121* (1), 218-223.

Goodliffe, J. W., Olmos-Serrano, J. L., Aziz, N. M., Pennings, J. L., Guedj, F., Bianchi, D. W., & Haydar, T. F. (2016). Absence of prenatal forebrain defects in the Dp(16)1Yey/+ mouse model of Down syndrome. *The Journal of Neuroscience, 36* (10), 2926-2944.

Grau, C., Arató, K., Fernández-Fernández, J. M., Valderrama, A., Sindreu, C., Fillat, C., . . . Altafaj, X. (2014). DYRK1A-mediated phosphorylation of GluN2A at Ser(1048) regulates the surface expression and channel activity of GluN1/GluN2A receptors. *Frontiers in Cellular Neuroscience, 8*, 331.

Grieco, J., Pulsifer, M., Seligsohn, K., Skotko, B., & Schwartz, A. (2015). Down syndrome: Cognitive and behavioral functioning across the lifespan. *American Journal of Medical Genetics Part C (Seminars in Medical Genetics), 169* (2), 135-149.

Griffin, W. S., Stanley, L. C., Ling, C., White, L., MacLeod, V., Perrot, L. J., . . . Araoz, C. (1989). Brain interleukin 1 and S-100 immunoreactivity are elevated in Down syndrome and Alzheimer disease. *Proceedings of the National Academy of Sciences, 86* (19), 7611-7615.

Guidi, S., Bonasoni, P., Ceccarelli, C., Santini, D., Gualtieri, F., Ciani, E., & Bartesaghi, R. (2008). Neurogenesis impairment and increased cell death reduce total neuron number in the hippocampal region of fetuses with Down syndrome. *Brain Pathology, 18* (2), 180-197.

Gurung, S., Evans, A. J., Wilkinson, K. A., & Henley, J. M. (2018). ADAR2-mediated Q/R editing of GluK2 regulates kainate receptor upscaling in response to suppression of synaptic activity. *Journal of Cell Science, 131* (24), jcs222273.

Hall, B. (1965). Delayed ontogenesis in human trisomy syndrome. *Hereditas, 52* (3), 334-344.

Hall, J. H. (2016). *Dissociating Aberrant Properties of Recognition Memory in the Tc1 Mouse Model of Trisomy-21*. PhD Thesis, Cardiff University. Retrieved from Online Research @ Cardiff.

Hall, J. H., Wiseman, F. K., Fisher, E. M., Tybulewicz, V. L., Harwood, J. L., & Good, M. A. (2016). Tc1 mouse model of trisomy-21 dissociates properties of short- and long-term recognition memory. *Neurobiology of Learning and Memory, 130*, 118-128.

Hattori, M., Fujiyama, A., Taylor, T. D., Watanabe, H., Yada, T., Park, H. S., . . . Yaspo, M. L. (2000). The DNA sequence of human chromosome 21. *Nature, 405* (6784), 311-319.

Head, E., Corrada, M. M., Kahle-Wrobleski, K., Kim, R. C., Sarsoza, F., Goodus, M., & Kawas, C. H. (2009). Synaptic proteins, neuropathology and cognitive status in the oldest-old. *Neurobiology of Aging, 30* (7), 1125-11234.

Head, E., Powell, D., Gold, B. T., & Schmitt, F. A. (2015). Alzheimer's Disease in Down Syndrome. *European Journal of Neurodegenerative Diseases, 1* (3), 353-364.

Hebb, D. O. (1949). *The organization of behavior; A neuropsychological theory*. New York, NY: Wiley.

Henley, J.M., & Wilkinson, K. A. (2016). Synaptic AMPA receptor composition in development, plasticity and disease. *Nature Reviews Neuroscience, 17* (6), 337-350.

Herault, Y., Delabar, J. M., Fisher, E. M. C., Tybulewicz, V. L. J., Yu, E., & Brault, V. (2017). Rodent models in Down syndrome research: impact and future opportunities. *Disease Models & Mechanisms, 10* (10), 1165-1186.

Hickey, F., Hickey, E., & Summar, K. L. (2012). Medical update for children with Down syndrome for the pediatrician and family practioner. *Advances in Pediatrics, 59* (1), 137-157.

Higuchi, M., Maas, S., Single, F. N., Hartner, J., Rozov, A., Burnashev, N., . . . Seeburg, P. H. (2000). Point mutation in an AMPA receptor gene rescues lethality in mice deficient in the RNA-editing enzyme ADAR2. *Nature, 406* (6791), 78-81.

Hollmann, M., Hartley, M., & Heinemann, S. (1991). Ca2+ permeability of KA-AMPA--gated glutamate receptor channels depends on subunit composition. *Science, 252* (5007), 851-853.

Holtzman, D. M., Santucci, D., Kilbridge, J., Chua-Couzens, J., Fontana, D. J., Daniels, S. E., . . . Mobley, W. C. (1996). Developmental abnormalities and age-related neurodegeneration in a mouse model of Down Syndrome. *Proceedings of the National Academy of Sciences, 93* (23), 13333-13338.

Howard, M. A., Elias, G. M., Elias, L. A., Swat, W., & Nicoll, R. A. (2010). The role of SAP97 in synaptic glutamate receptor dynamics. *Proceedings of the National Academy of Sciences, 107* (8), 3805-3810.

Ichinohe, A., Kanaumi, T., Takashima, S., Enokido, Y., Nagai, Y., & Kimura, H. (2005). Cystathionine beta-synthase is enriched in the brains of Down's patients. *Biochemical and Biophysical Research Communications, 338* (3), 1547-1550.

Iglewicz, B., Hoaglin, D. (1993). *Volume 16: How to Detect and Handle Outliers*. *The ASQC Basic* References in Quality Control: Statistical Techniques.

Jacobs, G. H., Williams, G. A., & Fenwick, J. A. (2004). Influence of cone pigment coexpression on spectral sensitivity and color vision in the mouse. *Vision Research, 44* (14), 1615-1622.

Jarrold, C., Baddeley, A. D., & Phillips, C. E. (2002). Verbal short-term memory in Down syndrome: a problem of memory, audition, or speech? *Journal of Speech, Language, and Hearing Research, 45* (3), 531-544.

Jeon, C. J., Strettoi, E., & Masland, R. H. (1998). The major cell populations of the mouse retina. *The Journal of Neuroscience, 18* (21), 8936-8946.

Jiang, X., Liu, C., Yu, T., Zhang, L., Meng, K., Xing, Z., . . . Yu, Y. E. (2015). Genetic dissection of the Down syndrome critical region. *Human Molecular Genetics, 24* (22), 6540-6551.

Joubert, A., & Vauclair, J. (1986). Reaction to novel objects in a troop of Guinea Baboons: Approach and manipulation. *Behaviour, 96* (1-2), 92-104.

Ju, W., Morishita, W., Tsui, J., Gaietta, G., Deerinck, T. J., Adams, S. R., . . . Malenka, R. C. (2004). Activity-dependent regulation of dendritic synthesis and trafficking of AMPA receptors. *Nature Neuroscience, 7* (3), 244-253.

Jung, M. S., Park, J. H., Ryu, Y. S., Choi, S. H., Yoon, S. H., Kwen, M. Y., . . . Chung, S. H. (2001). Regulation of RCAN1 protein activity by Dyrk1A protein-mediated phosphorylation. *The Journal of Biological Chemistry, 286*(46), 40401-40412.

Kim, S., & Ziff, E. B. (2014). Calcineurin mediates synaptic scaling via synaptic trafficking of Ca2+-permeable AMPA receptors. *PLOS Biology, 12* (7), e1001900.

Kirsammer, G., Jilani, S., Liu, H., Davis, E., Gurbuxani, S., Le Beau, M. M., & Crispino, J. D. (2008). Highly penetrant myeloproliferative disease in the Ts65Dn mouse model of Down syndrome. *Blood, 111* (2), 767-775.

Kleschevnikov, A. M., Belichenko, P. V., Faizi, M., Jacobs, L. F., Htun, K., Shamloo, M., & Mobley, W. C. (2012). Deficits in cognition and synaptic plasticity in a mouse model of Down syndrome ameliorated by GABAB receptor antagonists. *The Journal of Neuroscience, 32* (27), 9217-9227.

Kleschevnikov, A. M., Belichenko, P. V., Villar, A. J., Epstein, C. J., Malenka, R. C., & Mobley, W. C. (2004). Hippocampal long-term potentiation suppressed by increased inhibition in the Ts65Dn mouse, a genetic model of Down syndrome. *The Journal of Neuroscience, 24* (37), 8153-8160.

Knowlton, B. J., Mangels, J. A., & Squire, L. R. (1996). A neostriatal habit learning system in humans. *Science, 273* (5280), 1399-1402.

Kogan, C. S., Boutet, I., Cornish, K., Graham, G. E., Berry-Kravis, E., Drouin, A., & Milgram, N. W. (2009). A comparative neuropsychological test battery differentiates cognitive signatures of Fragile X and Down syndrome. *Journal of Intellectual Disability Research, 53* (2), 125-142.

Korbel, J. O., Tirosh-Wagner, T., Urban, A. E., Chen, X. N., Kasowski, M., Dai, L., . . . Korenberg, J. R. (2009). The genetic architecture of Down syndrome phenotypes revealed by high-resolution analysis of human segmental trisomies. *Proceedings of the National Academy of Sciences, 106* (29), 12031-12036.

Kregel, K. C., & Zhang, H. J. (2007). An integrated view of oxidative stress in aging: basic mechanisms, functional effects, and pathological considerations. *American Journal of Physiology Regulatory, Integrative, Comparative Physiology, 292* (1), R18-36.

Krug, M., Lössner, B., & Ott, T. (1984). Anisomycin blocks the late phase of long-term potentiation in the dentate gyrus of freely moving rats. *Brain Research Bulletin, 13* (1), 39-42.

Kurt, M. A., Kafa, M. I., Dierssen, M., & Davies, D. C. (2004). Deficits of neuronal density in CA1 and synaptic density in the dentate gyrus, CA3 and CA1, in a mouse model of Down syndrome. *Brain Research, 1022* (1-2), 101-109.

Lacor, P. N., Buniel, M. C., Chang, L., Fernandez, S. J., Gong, Y., Viola, K. L., . . . Klein, W. L. (2004). Synaptic targeting by Alzheimer's-related amyloid β oligomers. *The Journal of Neuroscience, 24* (45), 10191-10200.

Lalonde, R., Lewis, T. L., Strazielle, C., Kim, H., & Fukuchi, K. (2003). Transgenic mice expressing the $\beta APP_{695}SWE$ mutation: effects on exploratory activity, anxiety, and motor coordination. *Brain Research, 977* (1), 38-45.

Lana-Elola, E., Watson-Scales, S. D., Fisher, E. M., & Tybulewicz, V. L. (2011). Down syndrome: searching for the genetic culprits. *Disease Models & Mechanisms, 4* (5), 586-595.

Lana-Elola, E., Watson-Scales, S., Slender, A., Gibbins, D., Martineau, A., Douglas, C., . . . Tybulewicz, V. L. J. (2016). Genetic dissection of Down syndrome-associated congenital heart defects using a new mouse mapping panel. *eLIFE, 5*, e11614.

Lavenex, P.B., Bostelmann, M., Brandner, C., Costanzo, F., Fragnière, E., Klencklen, G., . . . Vicari, S. (2015). Allocentric spatial learning and memory deficits in Down syndrome. *Frontiers in Psychology, 6* (62), 1-17.

Laws, G. (2002). Working memory in children and adolescents with Down syndrome: evidence from a colour memory experiment. *Journal of Child Psychology and Psychiatry, 43* (3), 353-364.

Lee, H. K., Barbarosie, M., Kameyama, K., Bear, M. F., & Huganir, R. L. (2000). Regulation of distinct AMPA receptor phosphorylation sites during bidirectional synaptic plasticity. *Nature, 405* (6789), 955-959.

Lee, H. K., Kameyama, K., Huganir, R. L., & Bear, M. F. (1998). NMDA induces long-term synaptic depression and dephosphorylation of the GluR1 subunit of AMPA receptors in hippocampus. *Neuron, 21* (5), 1151-1162.

Lee, H. K., Takamiya, K., Han, J. S., Man, H., Kim, C. H., Rumbaugh, G., . . . Huganir, R. L. (2003). Phosphorylation of the AMPA receptor GluR1 subunit is required for synaptic plasticity and retention of spatial memory. *Cell, 112* (5), 631-643.

Lee, H. K., Takamiya, K., He, K., Song, L., & Huganir, R. L. (2010). Specific roles of AMPA receptor subunit GluR1 (GluA1) phosphorylation sites in regulating synaptic plasticity in the CA1 region of hippocampus. *Journal of Neurophysiology, 103* (1), 479-489.

Lee, S. Y., Wenk, M. R., Kim, Y., Nairn, A. C., & De Camilli, P. (2004). Regulation of synaptojanin 1 by cyclin-dependent kinase 5 at synapses. *Proceedings of the National Academy of Sciences, 101* (2), 546-551.

Lejeune, J., Gautier, M., & Turpin, R. (1959). Study of somatic chromosomes from 9 mongoloid children. *Comptes Rendus hebdomadaires des séances de l'Académie des sciences, 248* (11), 1721-1722.

Li, Z., Yu, T., Morishima, M., Pao, A., LaDuca, J., Conroy, J., . . . Yu, Y. E. (2007). Duplication of the entire 22.9 Mb human chromosome 21 syntenic region on mouse chromosome 16 causes cardiovascular and gastrointestinal abnormalities. *Human Molecular Genetics, 16* (11), 1359-1366.

Loane, M., Morris, J. K., Addor, M. C., Arriola, L., Budd, J., Doray, B., . . . Dolk, H. (2013). Twenty-year trends in the prevalence of Down syndrome and other trisomies in Europe: impact of maternal age and prenatal screening. *European Journal of Human Genetics, 21* (1), 27-33.

Lockrow, J., Prakasam, A., Huang, P., Bimonte-Nelson, H., Sambamurti, K., & Granholm, A. C. (2009). Cholinergic degeneration and memory loss delayed by vitamin E in a Down syndrome mouse model. *Experimental Neurology, 216* (2), 278-289.

Lott, I. T., & Dierssen, M. (2010). Cognitive deficits and associated neurological complications in individuals with Down's syndrome. *The Lancet Neurology, 9* (6), 623-633.

Lott, I. T., & Head, E. (2001). Down syndrome and Alzheimer's disease: a link between development and aging. *Mental Retardation and Developmental Disabilities, 7* (3), 172-178.

Lüscher, C., & Malenka, R. C. (2012). NMDA receptor-dependent long-term potentiation and long-term depression (LTP/LTD). *Cold Spring Harbor Perspectives in Biology, 4* (6), a005710.

Malenka, R. C. (1991). Postsynaptic factors control the duration of synaptic enhancement in area CA1 of the hippocampus. *Neuron, 6* (1), 53-60.

Malenka, R. C., Kauer, J. A., Perkel, D. J., Mauk, M. D., Kelly, P. T., Nicoll, R. A., & Waxham, M. N. (1989). An essential role for postsynaptic calmodulin and protein kinase activity in long-term potentiation. *Nature, 340* (6234), 554-557.

Manahan-Vaughan, D., Kulla, A., & Frey, J. U. (2000). Requirement of translation but not transcription for the maintenance of long-term depression in the CA1 region of freely moving rats. *The Journal of Neuroscience, 20* (22), 8572-8576.

Marechal, D., Brault, V., Leon, A., Martin, D., Lopes Pereira, P., Loaëc, N., . . . Herault, Y. (2019). Cbs overdosage is necessary and sufficient to induce cognitive phenotypes in mouse models of Down syndrome and interacts genetically with Dyrk1a. *Human Molecular Genetics, 28* (9), 1561-1577.

Martí, E., Altafaj, X., Dierssen, M., de la Luna, S., Fotaki, V., Alvarez, M., . . . Estivill, X. (2003). Dyrk1A expression pattern supports specific roles of this kinase in the adult central nervous system. *Brain Research, 964* (2), 250-263.

Martin, K. R., Corlett, A., Dubach, D., Mustafa, T., Coleman, H. A., Parkington, H. C., . . . Pritchard, M. A. (2012). Over-expression of RCAN1 causes Down syndrome-like hippocampal deficits that alter learning and memory. *Human Molecular Genetics, 21* (13), 3025-3041.

Matsuzaki, M., Honkura, N., Ellis-Davies, G. C., & Kasai, H. (2004). Structural basis of long-term potentiation in single dendritic spines. *Nature, 429* (6993), 761-766.

Mehta, S., Wu, H., Garner, C. C., & Marshall, J. (2001). Molecular mechanisms regulating the differential association of kainate receptor subunits with SAP90/PSD-95 and SAP97. *The Journal of Biological Chemistry, 276* (19), 16092-16099.

Migaud, M., Charlesworth, P., Dempster, M., Webster, L. C., Watabe, A. M., Makhinson, M., . . . Grant, S. G. (1998). Enhanced long-term potentiation and impaired learning in mice with mutant postsynaptic density-95 protein. *Nature, 396* (6710), 433-439.

Milner, B., Squire, L. R., & Kandel, E. R. (1998). Cognitive neuroscience and the study of memory. *Neuron, 20* (3), 445-468.

Mitchell, J. B., & Laiacona, J. (1998). The medial frontal cortex and temporal memory: tests using spontaneous exploratory behaviour in the rat. *Behavioural Brain Research, 97* (1-2), 107-113.

Mori, T., Koyama, N., Arendash, G. W., Horikoshi-Sakuraba, Y., Tan, J., & Town, T. (2010). Overexpression of human S100B exacerbates cerebral amyloidosis and gliosis in the Tg2576 mouse model of Alzheimer's disease. *Glia, 58* (3), 300-314.

Morice, E., Andreae, L. C., Cooke, S. F., Vanes, L., Fisher, E. M., Tybulewicz, V. L., & Bliss, T. V. (2008). Preservation of long-term memory and synaptic plasticity despite short-term impairments in the Tc1 mouse model of Down syndrome. *Learning & Memory, 15* (7), 492-500.

Morishita, W., Connor, J. H., Xia, H., Quinlan, E. M., Shenolikar, S., & Malenka, R. C. (2001). Regulation of synaptic strength by protein phosphatase 1. *Neuron, 32* (6), 1133-1148.

Morris, J. K., Alberman, E., Mutton, D., & Jacobs, P. (2012). Cytogenetic and epidemiological findings in Down syndrome: England and Wales 1989-2009. *American Journal of Medical Genetics Part A, 158A* (5), 1151-1157.

Morris, R. G., Anderson, E., Lynch, G. S., & Baudry, M. (1986). Selective impairment of learning and blockade of long-term potentiation by an N-methyl-D-aspartate receptor antagonist, AP5. *Nature, 319* (6056), 774-776.

Morris, R. G., Garrud, P., Rawlins, J. N., & O'Keefe, J. (1982). Place navigation impaired in rats with hippocampal lesions. *Nature, 297* (5868), 681-683.

Mulkey, R. M., Endo, S., Shenolikar, S., & Malenka, R. C. (1994). Involvement of a calcineurin/inhibitor-1 phosphatase cascade in hippocampal long-term depression. *Nature, 369* (6480), 486-488.

Mulkey, R. M., & Malenka, R. C. (1992). Mechanisms underlying induction of homosynaptic long-term depression in area CA1 of the hippocampus. *Neuron, 9* (5), 967-975.

Mumby, D. G., Gaskin, S., Glenn, M. J., Schramek, T. E., & Lehmann, H. (2002). Hippocampal damage and exploratory preferences in rats: memory for objects, places, and contexts. *Learning & Memory, 9* (2), 49-57.

Mumby, D. G., Piterkin, P., Lecluse, V. , & Lehmann, H. (2007). Perirhinal cortex damage and anterograde object-recognition in rats after long retention intervals. *Behavioural Brain Research, 185* (2), 82-87.

Murakami, N., Bolton, D., & Hwang, Y. W. (2009). Dyrk1A binds to multiple endocytic proteins required for formation of clathrin-coated vesicles. *Biochemistry, 48* (39), 9297-92305.

Nelson, L., Johnson, J. K., Freedman, M., Lott, I., Groot, J., Chang, M., . . . Head, E. (2005). Learning and memory as a function of age in Down syndrome: a study using animal-based tasks. *Progress in Neuro-Psychopharmacology & Biological Psychiatry, 29* (3), 443-453.

Nelson, A. J., Thur, K. E., Marsden, C. A., & Cassaday, H. J. (2010). Dissociable roles of dopamine within the core and medial shell of the nucleus accumbens in memory for objects and place. *Behavioral Neuroscience, 124* (6), 789-799.

Nemanic, S., Alvarado, M. C., & Bachevalier, J. (2004). The hippocampal/parahippocampal regions and recognition memory: insights from visual paired comparison versus object-delayed nonmatching in monkeys. *The Journal of Neuroscience, 24* (8), 2013-2026.

Netzer, W. J., Powell, C., Nong, Y., Blundell, J., Wong, L., Duff, K., . . . Greengard, P. (2010). Lowering β-amyloid levels rescues learning and memory in a Down syndrome mouse model. *PLOS One, 5* (6), e10943.

Nguyen, T. L., Duchon, A., Manousopoulou, A., Loaëc, N., Villiers, B., Pani, G., . . . Herault, Y. (2018). Correction of cognitive deficits in mouse models of Down syndrome by a pharmacological inhibitor of DYRK1A. *Disease Models & Mechanisms, 11* (9), dmm035634.

Nishikura, K. (2016). A-to-I editing of coding and non-coding RNAs by ADARs. *Nature Reviews Molecular Cell Biology, 17* (2), 83-96.

Nishiyama, H., Knopfel, T., Endo, S., & Itohara, S. (2002). Glial protein S100B modulates long-term neuronal synaptic plasticity. *Proceedings of the National Academy of Sciences, 99* (6), 4037-4042.

Nyffeler, M., Zhang, W. N., Feldon, J., & Knuesel, I. (2007). Differential expression of PSD proteins in age-related spatial learning impairments. *Neurobiology of Aging, 28* (1), 143-155.

O'Doherty, A., Ruf, S., Mulligan, C., Hildreth, V., Errington, M. L., Cooke, S., . . . Fisher, E. M. (2005). An aneuploid mouse strain carrying human chromosome 21 with Down syndrome phenotypes. *Science, 309* (5743), 2033-2037.

Olson, L. E., Richtsmeier, J. T., Leszl, J., & Reeves R. H. (2004a). A chromosome 21 critical region does not cause specific Down syndrome phenotypes. *Science, 306* (5696), 687-690.

Olson, L. E., Roper, R. J., Baxter, L. L., Carlson, E. J., Epstein, C. J., & Reeves, R. H. (2004b). Down syndrome mouse models Ts65Dn, Ts1Cje, and Ms1Cje/Ts65Dn exhibit variable severity of cerebellar phenotypes. *Developmental Dynamics, 230* (3), 581-589.

Olson, L. E., Roper, R. J., Sengstaken, C. L., Peterson, E. A., Aquino, V., Galdzicki, Z., . . . Reeves, R. H. (2007). Trisomy for the Down syndrome 'critical region' is necessary but not sufficient for brain phenotypes of trisomic mice. *Human Molecular Genetics, 16* (7), 774-782.

Ostapchenko, V. G., Chen, M., Guzman, M. S., Xie, Y. F., Lavine, N., Fan, J., . . . Jackson, M. F. (2015). The Transient Receptor Potential Melastatin 2 (TRPM2) Channel Contributes to β-Amyloid Oligomer-Related Neurotoxicity and Memory Impairment. *The Journal of Neuroscience, 35* (45), 15157-15169.

Overman, W. H., Ormsby, G., & Mishkin, M. (1990). Picture recognition vs. picture discrimination learning in monkey with medial temporal removals. *Experimental Brain Research, 79* (1), 18-24.

Papavassiliou, P., Charalsawadi, C., Rafferty, K., & Jackson-Cook, C. (2015). Mosaicism for trisomy 21: a review. *American Journal of Medical Genetics Part A, 167A* (1), 26-39.

Pennington, B. F., Moon, J., Edgin, J., Stedron, J., & Nadel, L. (2003). The neuropsychology of Down syndrome: evidence for hippocampal dysfunction. *Child Development, 74* (1), 75-93.

Pereira, P. L., Magnol, L., Sahún, I., Brault, V., Duchon, A., Prandini, P., . . . Herault Y. (2009). A new mouse model for the trisomy of the Abcg1-U2af1 region reveals the complexity of the combinatorial genetic code of down syndrome. *Human Molecular Genetics, 18* (24), 4756-4769.

Petrovic, M. M., Viana da Silva, S., Clement, J. P., Vyklicky, L., Mulle, C., González-González, I. M., & Henley, J. M. (2017). Metabotropic action of postsynaptic kainate receptors triggers hippocampal long-term potentiation. *Nature Neuroscience, 20* (4), 529-539.

Pinter, J. D., Brown, W. E., Eliez, S., Schmitt, J. E., Capone, G. T., & Reiss, A. L. (2001a). Amygdala and hippocampal volumes in children with Down syndrome: a high-resolution MRI study. *Neurology, 56* (7), 972-974.

Pinter, J. D., Eliez, S., Schmitt, J. E., Capone, G. T., & Reiss, A. L. (2001b). Neuroanatomy of Down's syndrome: a high resolution MRI study. *American Journal of Psychiatry, 158* (10), 1659-1665.

Plant, K., Pelkey, K. A., Bortolotto, Z. A., Morita, D., Terashima, A., McBain, C. J., . . . Isaac, J. T. (2006). Transient incorporation of native GluR2-lacking AMPA receptors during hippocampal long-term potentiation. *Nature Neuroscience, 9* (5), 602-604.

Plassman, B. L., Langa, K. M., Fisher, G. G., Heeringa, S. G., Weir, D. R., Ofstedal, M. B., . . . Wallace, R. B. (2007). Prevalence of Dementia in the United States: The Aging, Demographics, and Memory Study. *Neuroepidemiology, 29* (1-2), 125-132.

Powell, N. M., Modat, M., Cardoso, M. J., Ma, D., Holmes, H. E., Yu, Y., . . . Ourselin, S. (2016). Fully-automated μMRI morphometric phenotyping of the Tc1 mouse model of Down syndrome. *PLOS One, 11* (9), e0162974.

Presson, A. P., Partyka, G., Jensen, K.M, Devine, O. J., Rasmussen, S. A., McCabe, L. L., & McCabe, E. R. (2013). Current estimate of Down Syndrome population prevalence in the United States. *The Journal of Pediatrics, 163* (4), 1163-1168.

Proctor, D. T., Coulson, E. J., & Dodd, P. R. (2011). Post-synaptic scaffolding protein interactions with glutamate receptors in synaptic dysfunction and Alzheimer's disease. *Progress in Neurobiology, 93* (4), 509-521.

Purser, H. R., Farran, E. K., Courbois, Y., Lemahieu, A., Sockeel, P., Mellier, D., & Blades, M. (2015). The development of route learning in Down syndrome, Williams syndrome and typical development: investigations with virtual environments. *Developmental Science, 18* (4), 599-613.

Purves, D., Augustine, G. J., Fitzpatrick, D., Hall, W. C., LaMantia, A. S., & White, L. E. (2012). *Neuroscience* (5th ed.). Sunderland, MA: Sinauer Associates, Inc.

Raitano Lee, N., Pennington, B. F., & Keenan, J. M. (2010). Verbal short-term memory deficits in Down syndrome: phonological, semantic, or both? *Journal of Neurodevelopmental Disorders, 2* (1), 9-25.

Ranganath, C., & D'Esposito, M. (2001). Medial temporal lobe activity associated with active maintenance of novel information. *Neuron, 31* (5), 865-873.

Reeves, R. H., Irving, N. G., Moran, T. H., Wohn, A., Kitt, C., Sisodia, S. S., . . . Davisson, M. T. (1995). A mouse model for Down syndrome exhibits learning and behaviour deficits. *Nature Genetics, 11* (2), 177-184.

Régnier, V., Billard, J. M., Gupta, S., Potier, B., Woerner, S., Paly, E., . . . London, J. Brain phenotype of transgenic mice overexpressing cystathionine β-synthase. *PLOS One, 7* (1), e29056.

Riches, I. P., Wilson, F. A., & Brown, M. W. (1991). The effects of visual stimulation and memory on neurons of the hippocampal formation and the neighboring parahippocampal gyrus and inferior temporal cortex of the primate. *The Journal of Neuroscience, 11* (6), 1763-1779.

Richtsmeier, J. T., Baxter, L. L., & Reeves, R. H. (2000). Parallels of craniofacial maldevelopment in Down syndrome and Ts65Dn mice. *Developmental Dynamics, 217* (2), 137-145.

Richtsmeier, J. T., Zumwalt, A., Carlson, E. J., Epstein, C. J., & Reeves, R. H. (2002). Craniofacial phenotypes in segmentally trisomic mouse models for Down syndrome. *American Journal of Medical Genetics, 107* (4), 317-324.

Risser, D., Lubec, G., Cairns, N., & Herrera-Marschitz, M. (1997). Excitatory amino acids and monoamines in parahippocampal gyrus and frontal cortical pole of adults with Down syndrome. *Life Sciences, 60* (15), 1231-1237.

Robinson, W. P., Bernasconi, F., Basaran, S., Yüksel-Apak, M., Neri, G., Serville, F., . . . Schinzel, A. A. (1994). A Somatic Origin of Homologous Robertsonian Translocations and Isochromosomes. *American Journal of Human Genetics, 54* (2), 290-302.

Rolls, E. T., Miyashita, Y., Cahusac, P. M., Kesner, R. P., Niki, H., Feigenbaum, J. C., & Bach, L. (1989). Hippocampal neurons in the monkey with activity related to the place in which a stimulus is shown. *The Journal of Neuroscience, 9* (6), 1835-1845.

Roltsch, E., Holcomb, L., Young, K. A., Marks, A., & Zimmer, D. B. (2010). PSAPP mice exhibit regionally selective reductions in gliosis and plaque deposition in response to S100B ablation. *Journal of Neuroinflammation, 7*, 78.

Rosenmund, C., Stern-Bach, Y., & Stevens, C. F. (1998). The tetrameric structure of a glutamate receptor channel. *Science, 280* (5369), 1596-1599.

Royston, M. C., McKenzie, J. E., Gentleman, S. M., Sheng, J. G., Mann, D. M., Griffin, W. S., & Mrak, R. E. (1999). Overexpression of s100beta in Down's syndrome: correlation with patient age and with beta-amyloid deposition. *Neuropathology and Applied Neurobiology, 25* (5), 387-393.

Sago, H., Carlson, E. J., Smith, D. J., Killbridge, J., Rubin, E. M., Mobley, W. C., . . . Huang, T. T. (1998). Ts1Cje, a partial trisomy 16 mouse model for Down syndrome, exhibits learning and behavioral abnormalities. *Proceedings of the National Academy of Sciences, 95* (11), 6256-6261.

Sago, H., Carlson, E. J., Smith, D. J., Rubin, E. M., Crnic, L. S., Huang, T. T., & Epstein, C. J. (2000). Genetic dissection of region associated with behavioral abnormalities in mouse models for Down syndrome. *Pediatric Research, 48* (5), 606-613.

Sahún, I., Marechal, D., Pereira, P. L., Nalesso, V., Gruart, A., Garcia, J. M., . . . Herault, Y. (2014). Cognition and hippocampal plasticity in the mouse is altered by monosomy of a genomic region implicated in Down syndrome. *Genetics, 197* (3), 899-912.

Sanderson, D. J., & Bannerman, D. M. (2012). The role of habituation in hippocampus-dependent spatial working memory tasks: evidence from GluA1 AMPA receptor subunit knockout mice. *Hippocampus, 22* (5), 981-994.

Sanderson, D. J., Good, M. A., Skelton, K., Sprengel, R., Seeburg, P. H., Rawlins, J. N., & Bannerman, D. M. (2009). Enhanced long-term and impaired short-term spatial memory in GluA1 AMPA receptor subunit knockout mice: evidence for a dual-process memory model. *Learning & Memory, 16* (6), 379-386.

Sanderson, D. J., Hindley, E., Smeaton, E., Denny, N., Taylor, A., Barkus, C., . . . Bannerman, D. M. (2011). Deletion of the GluA1 AMPA receptor subunit impairs recency-dependent object recognition memory. *Learning & Memory, 18* (3), 181-190.

Sanz-Clemente, A., Nicoll, R. A., & Roche, K. W. (2013). Diversity in NMDA receptor composition: many regulators, many consequences. *Neuroscientist, 19* (1), 62-75.

Savioz, A., Leuba, G., & Vallet, P. G. (2014). A framework to understand the variations of PSD-95 expression in brain aging and in Alzheimer's disease. *Ageing Research Reviews, 18*, 86-94.

Scoville, W. B., & Milner, B. (1957). Loss of recent memory after bilateral hippocampal lesions. *Journal of Neurology, Neurosurgery and Psychiatry, 20* (1), 11-21.

Selvaraj, B. T., Livesey, M. R., Zhao, C., Gregory, J. M., James, O. T., Cleary, E. M., . . . Chandran, S. (2018). C9ORF72 repeat expansion causes vulnerability of motor neurons to Ca2+-permeable AMPA receptor-mediated excitotoxicity. *Nature Communications, 9* (1), 347.

Shallice, T., & Warrington, E. K. (1970). Independent functioning of verbal memory stores: a neuropsychological study. *The Quarterly Journal of Experimental Psychology, 22* (2), 261-273.

Shao, C. Y., Mirra, S. S., Sait, H. B., Sacktor, T. C., & Sigurdsson, E. M. (2011). Postsynaptic degeneration as revealed by PSD-95 reduction occurs after advanced Aβ and tau pathology in transgenic mouse models of Alzheimer's disease. *Acta Neuropathologica, 122* (3), 285-292.

Shi, S., Hayashi, Y., Esteban, J. A., & Malinow, R. (2001). Subunit-specific rules governing AMPA receptor trafficking to synapses in hippocampal pyramidal neurons. *Cell, 105* (3), 331-343.

Siarey, R. J., Carlson, E. J., Epstein, C. J., Balbo, A., Rapoport, S. I., & Galdzicki, Z. (1999). Increased synaptic depression in the Ts65Dn mouse, a model for mental retardation in Down syndrome. *Neuropharmacology, 38* (12), 1917-1920.

Siarey R. J., Kline-Burgess, A., Cho, M., Balbo, A., Best, T. K., Harashima, C., . . .Galdzicki, Z. (2006). Altered signaling pathways underlying abnormal hippocampal synaptic plasticity in the Ts65Dn mouse model of Down syndrome. *Journal of Neurochemistry, 98* (4), 1266-1277.

Siarey, R. J., Villar, A. J., Epstein, C. J., & Galdzicki, Z. (2005). Abnormal synaptic plasticity in the Ts1Cje segmental trisomy 16 mouse model of Down syndrome*. Neuropharmacology, 49* (1), 122-128.

Simón, A. M., Schiapparelli, L., Salazar-Colocho, P., Cuadrado-Tejedor, M., Escribano, L., López de Maturana, R., . . . Frechilla, D. (2009). Overexpression of wild-type human APP in mice causes cognitive deficits and pathological features unrelated to Aβ levels. *Neurobiology of Disease, 33* (3), 369-378.

Sita, G., Hrelia, P., Graziosi, A., Ravegnini, G., & Morroni, F. (2018). TRPM2 in the Brain: Role in Health and Disease. *Cells, 7* (7), E82.

Smith, G. K., Kesner, R. P., & Korenberg, J. R. (2014). Dentate gyrus mediates cognitive function in the Ts65Dn/DnJ mouse model of Down syndrome. *Hippocampus, 24* (3), 354-362.

Snyder, E. M., Nong, Y., Almeida, C. G., Paul, S., Moran, T., Choi, E. Y., . . . Greengard, P. (2005). Regulation of NMDA receptor trafficking by amyloid-β. *Nature Neuroscience, 8* (8), 1051-1058.

Sorrells, S. F., Paredes, M. F., Cebrian-Silla, A., Sandoval, K., Qi, D., Kelley, K. W., . . . Alvarez-Buylla, A. (2018). Human hippocampal neurogenesis drops sharply in children to undetectable levels in adults. *Nature, 555* (7696), 377-381.

Souchet, B., Duchon, A., Gu, Y., Dairou, J., Chevalier, C., Daubigney, F., . . . Delabar, J. M. (2019). Prenatal treatment with EGCG enriched green tea extract rescues GAD67 related developmental and cognitive defects in Down syndrome mouse models. *Scientific Reports, 9* (1), 3914.

Souchet, B., Guedj, F., Sahún, I., Duchon, A., Daubigney, F., Badel, A., . . . Delabar, J. M. (2014). Excitation/inhibition balance and learning are modified by Dyrk1A gene dosage. *Neurobiology of Disease, 69*, 65-75.

Squire, L. R., & Zola-Morgan, S. (1991). The medial temporal lobe memory system. *Science, 253* (5026), 1380-1386.

Stagni, F., Giacomini, A., Emili, M., Guidi, S., & Bartesaghi, R. (2018). Neurogenesis impairment: An early developmental defect in Down syndrome. *Free Radical Biology & Medicine, 114*, 15-32.

Starbuck, J. M., Dutka, T., Ratliff, T. S., Reeves, R. H., & Richtsmeier, J. T. (2014). Overlapping trisomies for human chromosome 21 orthologs produce similar effects on skull and brain morphology of Dp(16)1Yey and Ts65Dn mice. *American Journal of Medical Genetics Part A, 164A* (8), 1981-1990.

Sun, X., Wu, Y., Herculano, B., & Song, W. (2014). RCAN1 overexpression exacerbates calcium overloading-induced neuronal apoptosis*. PLOS One, 9* (4), e95471.

Suzuki, W. A., & Amaral, D. G. (1994). Topographic organization of the reciprocal connections between the monkey entorhinal cortex and the perirhinal and parahippocampal cortices. *The Journal of Neuroscience, 14* (3), 1856-1877.

Suzuki, E., & Kamiya, H. (2016). PSD-95 regulates synaptic kainate receptors at mouse hippocampal mossy fiber-CA3 synapses. *Neuroscience Research, 107*, 14-19.

Takashima, S., Iida, K., Mito, T., & Arima, M. (1994). Dendritic and histochemical development and ageing in patients with Down's syndrome. *Journal of Intellectual Disability Research, 38*, 265-273.

Tononi, G., & Cirelli, C. (2014). Sleep and the price of plasticity: from synaptic and cellular homeostasis to memory consolidation and integration. *Neuron, 81* (1), 12-34.

Tulving, E. (1985). How many memory systems are there? *American Psychologist, 40* (4), 385-398.

Tulving, E. (2002). Episodic memory: from mind to brain. *Annual Review of Psychology, 53*, 1-25.

Valenti, D., Braidy, N., De Rasmo, D., Signorile, A., Rossi, L., Atanasov, A. G., . . . Vacca, R. A. (2018). Mitochondria as pharmacological targets in Down syndrome. *Free Radical Biology and Medicine, 114*, 69-83.

Vann, S. D., & Aggleton, J. P. (2002). Extensive cytotoxic lesions of the rat retrosplenial cortex reveal consistent deficits on tasks that tax allocentric spatial memory. *Behavioral Neuroscience, 116* (1), 85-94.

Vicari, S., Bellucci, S., & Carlesimo, G. A. (2000). Implicit and explicit memory: a functional dissociation in persons with Down syndrome*. Neuropsychologia, 38* (3), 240-251.

Vicari, S., Bellucci, S., & Carlesimo, G. A. (2005). Visual and spatial long-term memory: differential pattern of impairments in Williams and Down syndromes. *Developmental Medicine & Child Neurology, 47* (5), 305-311.

Vicari, S., Marotta, L., & Carlesimo, G. A. (2004). Verbal short-term memory in Down's syndrome: an articulatory loop deficit? *Journal of Intellectual Disability Research, 48* (2), 80-92.

Vicari, S., Verucci, L., & Carlesimo, G. A. (2007). Implicit memory is independent from IQ and age but not from etiology: evidence from Down and Williams syndromes. *Journal of Intellectual Disability Research, 51*, 932-941.

Viggiano, D. (2008). The hyperactive syndrome: metanalysis of genetic alterations, pharmacological treatments and brain lesions which increase locomotor activity. *Behavioural Brain Research, 194* (1), 1-14.

Vuksić, M., Petanjek, Z., Rasin, M. R., & Kostović, I. (2002). Perinatal growth of prefrontal layer III pyramids in Down syndrome. *Pediatric Neurology, 27* (1), 36-38.

Vyazovskiy, V., Cirelli, C., Pfister-Genskow, M., Faraguna, U., & Tononi, G. (2008). Molecular and electrophysiological evidence for net synaptic potentiation in wake and depression in sleep. *Nature Neuroscience, 11* (2), 200-208.

Wagner, A. R. (1981). SOP: A model of automatic memory processing in animal behavior. In N. E. Spear & R. R. Miller (Eds.), *Information processing in animals: Memory mechanisms* (pp. 5-47). Hillsdale, NJ: Erlbaum.

Wakabayashi, K., Narisawa-Saito, M., Iwakura, Y., Arai, T., Ikeda, K., Takahashi, H., & Nawa, H. (1999). Phenotypic down-regulation of glutamate receptor subunit GluR1 in Alzheimer's disease. *Neurobiology of Aging, 20* (3), 287-295.

Wan, H., Aggleton, J. P., & Brown, M. W. (1999). Different contributions of the hippocampus and perirhinal cortex to recognition memory. *The Journal of Neuroscience, 19* (3), 1142-1148.

Warburton, E. C., & Brown, M. W. (2015). Neural circuitry for rat recognition memory. *Behavioural Brain Research, 285*, 131-139.

Watson-Scales, S., Kalmar, B., Lana-Elola E., Gibbins, D., La Russa, F., Wiseman, F., . . . Tybulewicz, V. L. J. (2018). Analysis of motor dysfunction in Down Syndrome reveals motor neuron degeneration. *PLOS Genetics, 14* (5), e1007383.

Webster, S. J., Bachstetter, A. D., Nelson, P. T., Schmitt, F. A., & Van Eldik, L. J. (2014). Using mice to model Alzheimer's dementia: an overview of the clinical disease and the preclinical behavioral changes in 10 mouse models. *Frontiers in Genetics, 5*, 88.

Weijerman, M. E., & de Winter, J. P. (2010). Clinical practice. The care of children with Down syndrome. *European Journal of Pediatrics, 169* (12), 1445-1452.

Wenthold, R. J., Petralia, R. S., Blahos, J. II, & Niedzielski, A. S. (1996). Evidence for multiple AMPA receptor complexes in hippocampal CA1/CA2 neurons. *The Journal of Neuroscience, 16* (6), 1982-1989.

Whitaker-Azmitia, P. M., Wingate, M., Borella, A., Gerlai, R., Roder, J., & Azmitia, E. C. (1997). Transgenic mice overexpressing the neurotrophic factor S-100 beta show neuronal cytoskeletal and behavioral signs of altered aging processes: implications for Alzheimer's disease and Down's syndrome. *Brain Research, 776* (1-2), 51-60.

Whitlock, J. R., Heynen, A. J., Shuler, M. G., & Bear, M. F. (2006). Learning induces long-term potentiation in the hippocampus. *Science, 313* (5790), 1093-1097.

Wilcock, D. M., & Griffin, W. S. (2013). Down's syndrome, neuroinflammation, and Alzheimer neuropathogenesis. *Journal of Neuroinflammation, 10*, 84.

Winters, B. D., & Bussey, T. J. (2005). Transient inactivation of perirhinal cortex disrupts encoding, retrieval, and consolidation of object recognition memory. *The Journal of Neuroscience, 25* (1), 52-61.

Wiseman, F. K., Pulford, L. J., Barkus, C., Liao, F., Portelius, E., Webb, R., . . . Fisher, E. M. C. (2018). Trisomy of human chromosome 21 enhances amyloid-β deposition independently of an extra copy of APP. *Brain, 141* (8), 2457-2474.

Wisniewski, K. E., Wisniewski, H. M., & Wen, G. Y. (1985). Occurrence of neuropathological changes and dementia of Alzheimer’s disease in Down’s syndrome. *Annals of Neurology, 17* (3), 278-282.

Witton, J., Padmashri, R., Zinyuk, L. E., Popov, V. I., Kraev, I., Line, S. J., . . . Jones, M. W. (2015). Hippocampal circuit dysfunction in the Tc1 mouse model of Down syndrome. *Nature Neuroscience, 18* (9), 1291-1298.

Won, S., Levy, J. M., Nicoll, R. A., & Roche, K. W. (2017). MAGUKs: multifaceted synaptic organizers. *Current Opinion in Neurobiology, 43*, 94-101.

Wu, J., & Morris, J. K. (2013). The population prevalence of Down’s syndrome in England and Wales in 2011. *European Journal of Human Genetics, 21* (9), 1016-1019.

Xiang, J. Z., & Brown, M. W. (1998). Differential neuronal encoding of novelty, familiarity and recency in regions of the anterior temporal lobe. *Neuropharmacology, 37* (4-5), 657-676.

Xie, Y. F., Belrose, J. C., Lei, G., Tymianski, M., Mori, Y., Macdonald, J. F., & Jackson, M. F. (2011). Dependence of NMDA/GSK-3β mediated metaplasticity on TRPM2 channels at hippocampal CA3-CA1 synapses. *Molecular Brain, 4*, 44.

Yeh, C. W., Yeh, S. H., Shie, F. S., Lai, W. S., Liu, H. K., Tzeng, T. T., . . . Shiao, Y. J. (2015). Impaired cognition and cerebral glucose regulation are associated with astrocyte activation in the parenchyma of metabolically stressed APPswe/PS1dE9 mice. *Neurobiology of Aging, 36* (11), 2984-2994.

Yin, X., Jin, N., Shi, J., Zhang, Y., Wu, Y., Gong, C. X., . . . Liu, F. (2017). Dyrk1A overexpression leads to increase of 3R-tau expression and cognitive deficits in Ts65Dn Down syndrome mice. *Scientific Reports, 7* (1), 619.

Yu, T., Li, Z., Jia, Z., Clapcote, S. J., Liu, C., Li, S., . . . Yu, Y. E. (2010a). A mouse model of Down syndrome trisomic for all human chromosome 21 syntenic regions. *Human Molecular Genetics, 19* (14), 2780-2791.

Yu, T., Liu, C., Belichenko, P., Clapcote, S. J., Li, S., Pao, A., . . . Yu, Y. E. (2010b). Effects of individual segmental trisomies of human chromosome 21 syntenic regions on hippocampal long-term potentiation and cognitive behaviors in mice. *Brain Research, 1366*, 162-171.

Zeng, H., Chattarji, S., Barbarosie, M., Rondi-Reig, L., Philpot, B. D., Miyakawa, T., . . . Tonegawa, S. (2001). Forebrain-specific calcineurin knockout selectively impairs bidirectional synaptic plasticity and working/episodic-like memory. *Cell, 107* (5), 617-629.

Zhang, L., Meng, K., Jiang, X., Liu, C., Pao, A., Belichenko, P. V., . . . Yu, Y. E. (2014). Human chromosome 21 orthologous region on mouse chromosome 17 is a major determinant of Down syndrome-related developmental cognitive deficits. *Human Molecular Genetics, 23* (3), 578-589.

Zhou, Q., Homma, K. J., & Poo, M. M. (2004). Shrinkage of dendritic spines associated with long-term depression of hippocampal synapses. *Neuron, 44* (5), 749-757.

Zhu, X. O., Brown, M. W., & Aggleton, J. P. (1995). Neuronal signalling of information important to visual recognition memory in rat rhinal and neighbouring cortices. *European Journal of Neuroscience, 7* (4), 753-765.